Phospholamban and Sarcolipin Oligomers Directly Modulate Ca²⁺-ATPase Activity

by

Joseph O. Primeau

A thesis submitted in partial fulfillment of the requirements for the degree of

Doctor of Philosophy

Department of Biochemistry

University of Alberta

Abstract

Oscillating cytosolic calcium concentrations dictate the contraction-relaxation cycles of muscle cells. Calcium release from the sarcoplasmic reticulum (SR) to the cytosol stimulates muscle contraction, while active transport of calcium back into the SR triggers muscle relaxation. Calcium reuptake involves the transport of calcium against its concentration gradient, which is facilitated by the sarcoendoplasmic reticulum calcium ATPase, or SERCA. SERCA has been traditionally described as an E1-E2 enzyme that follows the Post-Albers scheme for metal ion transport. SERCA undergoes substantial structural changes from a high-affinity state (E1) to a low-affinity state (E2) to facilitate calcium transport. SERCA's calcium transport properties are regulated by small, tissue-specific, transmembrane protein subunits; the most notable include phospholamban (PLN) and sarcolipin (SLN). PLN and SLN alter SERCA's calcium transport properties by reversibly interacting with the transmembrane domain of SERCA, allowing for dynamic control of muscle contractility. Crystal structures have revealed that PLN and SLN were both found to stabilize a calcium-free E1-like intermediate by interacting with an inhibitory groove formed by M2, M6, and M9 of SERCA. This interaction is involved in altering SERCA's calcium affinity and was canonically thought to be the primary mode of SERCA inhibition. We have identified through two-dimensional electron crystallography (2D crystals) of SERCA and PLN/SLN in a lipid membrane that PLN/SLN interacts with SERCA at a site distinct from the inhibitory groove, transmembrane segment M3. Both PLN and SLN 2D crystals reveal that this interaction is mediated by an oligomer consistent with a homopentamer.

Here, we functionally characterize the oligomeric interaction with SERCA for wild-type PLN, wild-type SLN and determined that this interaction alters SERCA's maximum turnover rate, with PLN eliciting a stimulatory effect and SLN eliciting an inhibitory effect. Protein docking and molecular dynamics simulations provided a model for this novel interaction, revealing a potential mechanism for the distinct regulatory roles of the PLN and SLN interaction with M3. In addition, we identified that SLN's regulatory function is dependent on the E1-E2 conformation of SERCA, suggesting that there are multiple modes of SERCA-SLN interaction that can persist throughout SERCA's calcium transport pathway and multiple turnover events. Based on our results, we have concluded that the PLN pentamer naturally associates with SERCA, the SLN pentamer naturally and persistently associates with SERCA, and the regulatory nature of these interactions with M3 is dependent on local micro-environment perturbations.

Acknowledgements

It is difficult to express the emotional journey undertaken over seven years of research and training. Flasks, grids, gloves, copper, glass, plastic, these become an integral part of your life. The daily foray into the curious unknown shapes you in ways you could not have predicted over half a decade ago. Your research becomes a part of you, and you become a part of it. There is a sort of melancholic satisfaction in assembling a document that consolidates your life's work into a 300 page, double spaced thesis. You go through a retrospective analysis of the last seven years of your life, where it started and what you have accomplished and, in the end, you feel a sense of finality to your work. Despite these feelings, this is inherently untrue, as scientific endeavours are never final. The scientific contribution of this thesis encapsulates the sum of the knowledge at this particular moment. The humbling reality of research is that it continually marches on; however, there is a contented feeling knowing that your contribution to science will further the understanding of the natural world, and that makes it all worth it.

I want to acknowledge the outstanding mentorship I have received from Dr. Howard Young. I entered his lab as a bright-eyed, bushy-tailed undergraduate researcher, only to return years later in a technician role. Following this experience, Howard offered to mentor me as a graduate student. Over the years, Howard has demonstrated immense support (and patience) as I bumbled my way from a fledgling graduate student to a competent researcher. From the lowest lows to the highest highs, Howard has always been in my corner. I cannot thank him enough for letting me a part of this.

I want to acknowledge the support, guidance, and friendship of my labmates, past and present, over the years. John Paul, Przemek, Delaine, Ludo, Paramita, Cathy, thank you for showing me the ropes in my early years. Grant, thanks for (continued) guidance, friendship, and Skype beers. Gareth, thanks for being my partner in crime and my number one resource, I am proud to have called you a colleague and friend. Bashir, Jessica, Jessi, M'lynn, Nish, Vinh, Mary, Steph, Graeden. I would also like to acknowledge the help you guys have given me over the years, in addition to tolerating my humour and music choices. Over the years, I had the pleasure of supervising some exceptionally gifted undergraduate and highschool students. Shauna, Tiffany, Madeleine, Sarah, Kerry, Rith, Alicia, Maggie, I learned much from each of you and enjoyed every minute of it, thank you. Craig, thanks for the continuous support and friendship over the years. Over the many beers and tears, sports and weights, I had a pretty good time. Ply, thanks for always whoopin' my butt in squash or whatever sport you play; I had a pretty good time. Cameron, thanks for always come to annoy me in the lab, it

has always been a pleasure to have you come in and cause mayhem in the lab. To the rest of my colleagues I have had the pleasure of working with, you made the hardest times a little easier.

I want to acknowledge the support of my family and friends. You always kept me grounded and pulled me away when I was a little too deep into research, reminding me that life is a balance.

And finally, I could not have gone through this crazy journey without the love and support of my darling wife Julie, daughter Gennalyn, and Einstein. You were (and still are) the rock that pushed me to finish this Ph.D. Whenever I wanted to quit, you kept me going. Through the darkest hours, you kept me going. I love you and thank you for seeing this to the end. To Gennalyn, you may not have been here for the first part of this journey, but you were here for the conclusion. The world is yours to discover and you will learn more than we will ever know.

To intrepid young researchers embarking on this journey, know this: You may feel like you are helplessly screaming into the void, but it is not hopeless, your perseverance will pay off. I am sure of it.

Preface

This thesis represents the culmination of my work performed in the lab of Dr. Howard Young. As such, published work represents the collaborative efforts of the Young lab and other research groups. All unpublished experiments (unless denoted otherwise) in the remaining chapters were performed by myself under the supervision of Dr. Howard Young. The published works utilized in chapters 1, 2, and 3 are detailed below.

Chapter 1

This introductory chapter contains excerpts from Primeau J.O., Armanious G.P., Fisher M.E., Young H.S. (2018) *The SarcoEndoplasmic Reticulum Calcium ATPase.* In: Harris J., Boekema E. (eds) Membrane Protein Complexes: Structure and Function. *Subcellular Biochemistry, vol 87.* Springer, Singapore. This chapter has been modified for relevancy and thesis rationale.

Chapter 2

This chapter represents the culmination of the work published in Biophysical Journal on February 19, 2019 (Glaves, J. P., Primeau, J. O., Espinoza-Fonseca, L. M., Lemieux, M. J., and Young, H. S. (2019) The Phospholamban Pentamer Alters Function of the Sarcoplasmic Reticulum Calcium Pump SERCA. *Biophys. J.* **116**, 633–647). JPG and JOP performed the research, analyzed data, and contributed to the writing and editing of the manuscript. MJL contributed to the design and analysis of the data and editing of the manuscript. LMEF performed and analyzed the protein-protein docking and MD simulations. HSY designed the research, analyzed the data and wrote the manuscript. This manuscript has been adapted and edited from its original state to fit the format of the thesis presented.

Chapter 3

This chapter represents the culmination of the work published in the Biophysical Journal on Jan 22, 2020 (Glaves, J. P., Primeau, J. O., Gorski, P. A., Espinoza-Fonseca, L. M., Lemieux, M. J., and Young, H. S. (2019) Interaction of a sarcolipin pentamer and monomer with the sarcoplasmic reticulum calcium pump, SERCA. *Biophysj.* **118**, 518–531). JPG, JOP, and PAG performed the research, analyzed data, and contributed to the writing and editing of the manuscript; MJL contributed to the design and analysis of the data, and editing of the manuscript; LMEF performed and analyzed the protein-protein docking and molecular dynamics simulations; HSY designed the research, analyzed the data, and wrote the manuscript. This manuscript has been adapted and edited from its original state to fit the format of the thesis presented.

Dedicated to my loving wife, Julie
None of this could have happened if not for you
I love you

And

My beautiful daughter, Gennalyn
None of this would be worth it if not for you
I love you

Table of Contents

List of Tables

List of Figures

Keywords

Sarcoplasmic reticulum

Calcium ATPase

Phospholamban

Sarcolipin

Pentamer

Abbreviations

2D crystal	Two-Dimensional Crystal
Å	Angstrom
ADP	Adenosine Diphosphate
A-domain	Actuator Domain of SERCA
AKAP	A Kinase Anchoring Protein
Akt	Protein Kinase B
AlF$_4$	Aluminum Tetrafluoride
ALN	Another-Regulin
AMP	Adenosine Monophosphate
AMPPCP	Phosphomethylphosphonic Acid Adenylate Ester
atm	atmosphere (pressure)
ATP	Adenosine triphosphate
C$_{12}$E$_8$	Octaethylene glycol monododecyl ether
C-Termin(us/al/i)	Carboxy termin(us/al/i)
CAMKII	Calcium/Calmodulin Dependent Protein Kinase II
cAMP	cyclic AMP
Co-IP	Coimmunoprecipitation
CPA	Cyclopiazonic Acid
CryoEM	Electron Cryomicroscopy
CTF	Contrast Transfer Function
Da	Dalton
DCM	Dilate Cardiomyopathy
DWORF	Dwarf Open Reading Frame

DTT	Dithiolthreitol
EGTA	Ethylene Glycol-bis(β-aminoethyl ether)-N,N,N',N'-tetraacetic acid
ELN	Endoregulin
EM	Electron Microscopy
ER	Endoplasmic Reticulum
EYPA	Egg Yolk Phosphatidic acid
EYPC	Egg Yolk Phosphatidylcholine
EYPE	Egg Yolk Phosphatidylethanolamine
fs	femtosecond
HAX1	HS-1 Associated Protein
Hsp20	Small Heat Shock Protein 20
Gdn	Guanadinium
I-1	Inhibitor-1
K	Kelvin
K_{Ca}	Apparent Calcium Affinity
kcal	kilocalorie
LDH	Lactate Dehydrogenase
M(#)	Transmembrane Domain of SERCA
MD	Molecular Dynamics
MLN	Myoregulin
MOPS	3-(*N*-morpholino)propanesulfonate
ms	millisecond
µs	microsecond
NADH	Nicotinamide Adenine Dinucleotide
N-Domain	Nucleotide-binding Domain of SERCA
nH	Cooperativity
NMR	Nuclear Magnetic Resonance
ns	Nanosecond
N-Termin(us/al/i)	Amino Termin(us/al/i)
P-Domain	Phosphorylation Domain of SERCA
PACL	P-type ATPase Calcium Transporter *L*
PAGE	Polyacrylamide Gel Electrophoresis

PA	Phosphatidic acid
PC	Phosphatidylcholine
PE	Phosphatidylethanolamine
PEP	Phosphoenolpyruvate
PDB	Protein Data Bank
PDE4D	Phosphodiesterase
Pi	Inorganic Phosphate
PK	Pyruvate Kinase
PKA	Protein Kinase A
PLN	Phospholamban
PMCA	Plasma Membrane Calcium ATPase
POPA	1-Palmitoyl-2-oleoyl Phosphatidic acid
POPC	1-Palmitoyl-2-oleoyl Phosphatidylcholine
POPE	1-Palmitoyl-2-oleoyl Phosphatidylethanolamine
PP-1	Protein Phosphatase 1
PP-2	Protein Phosphatase 2
ps	picosecond
RCF	Relative Centrifugal Force
RMSD	Root-Mean-Square Deviation
RNA	Ribonucleic Acid
RyR	Ryanodine Receptor
SDS	Sodium Dodecylsulfate
SERCA	Sarco/Endoplasmic Reticulum Calcium ATPase
SEM	Standard Error of the Mean
SLN	Sarcolipin
SmORF	Small Open Reading Frame
SPCA	Secretory Pathway Calcium ATPase
SR	Sarcoplasmic Reticulum
SUMO	Small Ubiqutin-related Modifier
TEM	Transmission Electron Microscopy
TG	Thapsigargin
TM	Transmembrane

UCP-1	Uncoupling Protein 1
V_{max}	Maximum Velocity
W/V	Weight per Volume ratio
W/W	Weight per Weight ratio

Amino Acid Abbreviations

Ala, A	Alanine
Arg, R	Arginine
Asn, N	Asparagine
Asp, D	Aspartate
Cys, C	Cysteine
Gln, Q	Glutamine
Glu, E	Glutamate
Gly, G	Glycine
His, H	Histidine
Ile, I	Isoleucine
Leu, L	Leucine
Lys, K	Lysine
Met, M	Methionine
Phe, F	Phenylalanine
Pro, P	Proline
Ser, S	Serine
Thr, T	Threonine
Trp, W	Tryptophan
Tyr, Y	Tyrosine
Val, V	Valine

"Walkin' in my old man shoes, with my scientist heart
I got a fever and a beaker and a shot in the dark
I need a Cadillac; I need a soft summer night
Say a prayer for my soul, Señorita."

B. Fallon – 2012

Chapter 1

The SarcoEndoplasmic Reticulum Calcium ATPase
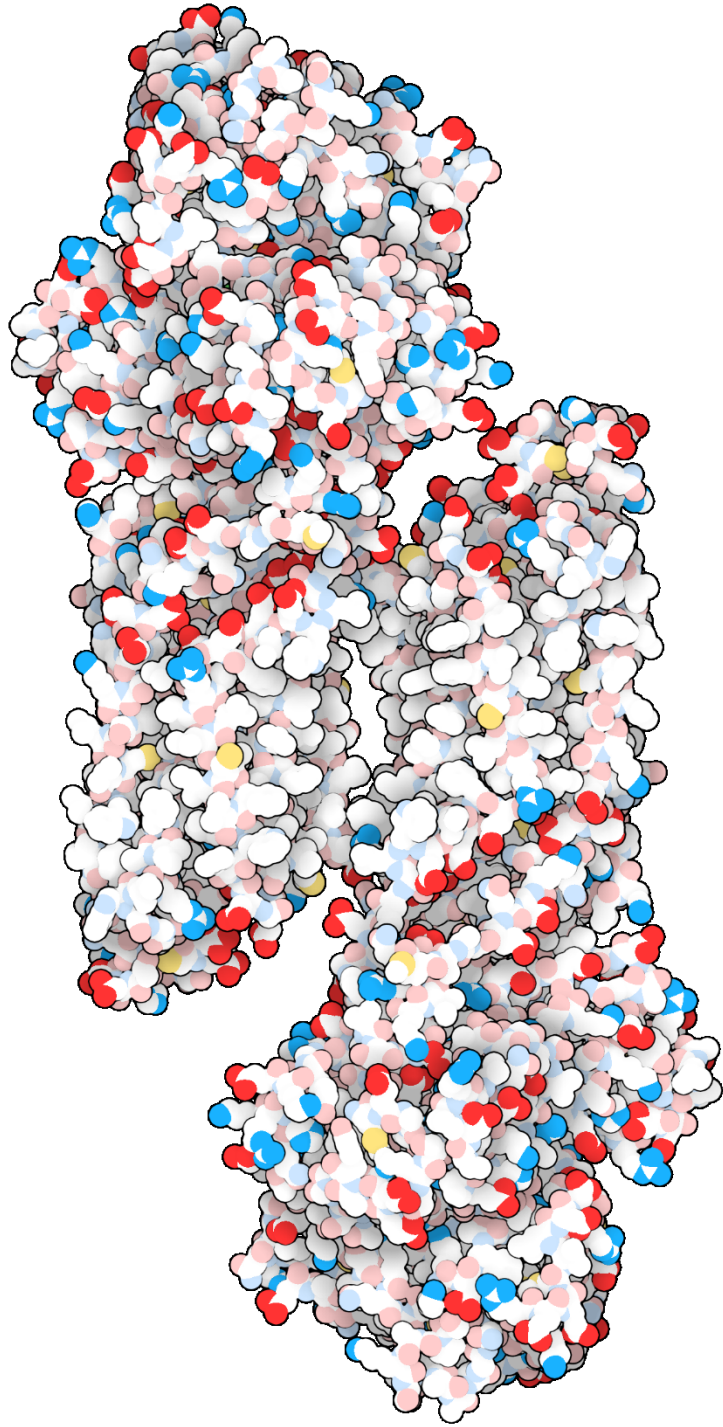
SERCA 1A (PDB:1VFP) in the E1•Ca•ATP conformation

Preface:

This introductory chapter contains excerpts from *Primeau J.O., Armanious G.P., Fisher M.E., Young H.S. (2018) The SarcoEndoplasmic Reticulum Calcium ATPase. In: Harris J., Boekema E. (eds) Membrane Protein Complexes: Structure and Function. Subcellular Biochemistry, vol 87. Springer, Singapore.* **The chapter has been modified for relevancy and thesis rationale. Title page figure generated using *Illustrate: Non-photorealistic Biomolecular Illustration*** (1)**.**

1.1 – Calcium drives the formation of early life

1.1.1 – Straining the primordial soup

Calcium is the paramount element in biology. From providing mechanical strength to chordate skeletons to acting as a signalling molecule for wildly complex cellular processes, calcium is essential to life on earth. The primordial oceans that served as the cradle for the beginnings of life contained the ions utilized by our cells, setting in motion Life's journey to contain and utilize the oceanic ionic composition. Archaean oceans were likely more saline than present-day oceans (2), full of sodium, magnesium, chloride, potassium, and calcium. However, evidence suggests that calcium was initially in relatively low abundance (3) (as the fifth most abundant element in the earth's crust, this is a surprise) and was injected into the sea in concentrated pockets from groundwater seepage, continental runoff, and ancient hydrothermal vents. Acidification of the early oceans liberated calcium sequestered in minerals, causing an enormous increase in oceanic calcium concentrations. The specific presence of these soluble inorganic ions dictated the biochemistry of early life and, as such, the primordial membrane-bound early organisms needed to modulate the access of these ions, as early ocean ion concentrations would prove fatal to early life.

Homeostasis of ion-flux is a mechanism required by early life to monitor and adapt to its environment. Maintaining a safe, low concentration of oceanic ions, such as calcium, became critical for survival. Calcium is an interesting element, and it is not surprising that early life utilized ionic free-calcium in the water for cellular processes. Calcium exists as a highly hydrated (6-8 H_2O) divalent cation with a propensity to interact with biological molecules. Due to its flexible electron-shell coordination, fast binding kinetics (due to quick release of bound H_2O), and high affinity for carboxylate oxygens and phosphates (precursors for the formation of amino and nucleotides), the early biochemistry of primitive organisms made use of calcium. The fundamental problem with utilizing calcium in a biological system is that at high concentrations, it is inherently toxic and incompatible with early life. Calcium can interact with and form an insoluble precipitate with proteins and nucleic acids, placing a considerable strain on early cellular processes, energy metabolism, and information storage. As such, it was critical for ancient organisms to develop a way to maintain low intracellular levels of calcium. Maintaining a low level of calcium (~ 100 nmol/L) despite an extracellular concentration in the mmol/L range placed evolutionary pressure on early organisms to develop a strategy to maintain calcium homeostasis. Indeed, early organisms adapted by utilizing two major approaches to preserve a low intracellular calcium concentration: exporting the calcium from the intracellular milieu or sequestering the calcium away from essential biomolecules.

The formation of calcium exporters was likely the first approach early life took (as calcium channels are phylogenetically older than the onset of eukaryogenesis (4)). Large concentration gradients between primitive intracellular milieu and the ion-rich seawater pressured early organisms to find ways to export or contain the toxic material to a manageable level. Development of calcium-binding proteins could serve this purpose; however, upon saturation, other methods of calcium removal would be required. Active transport became the next viable solution to maintaining calcium homeostasis. Rudimentary calcium pumps developed, with structural similarity to modern eukaryotic and prokaryotic P-type ATPases (5) (**Figure 1.1**) for active transport of calcium against its concentration gradient. Early organisms developed other methods in exporting calcium, such as early co-transporters, voltage-gated calcium channels, linking calcium movement with other ion transfer (such as potassium and sodium), leading to the development of calcium-dependent channels (6, 7). Thus, primitive calcium signalling was becoming established as a viable biochemical process.

PMCA   **PACL***   **SERCA2A**
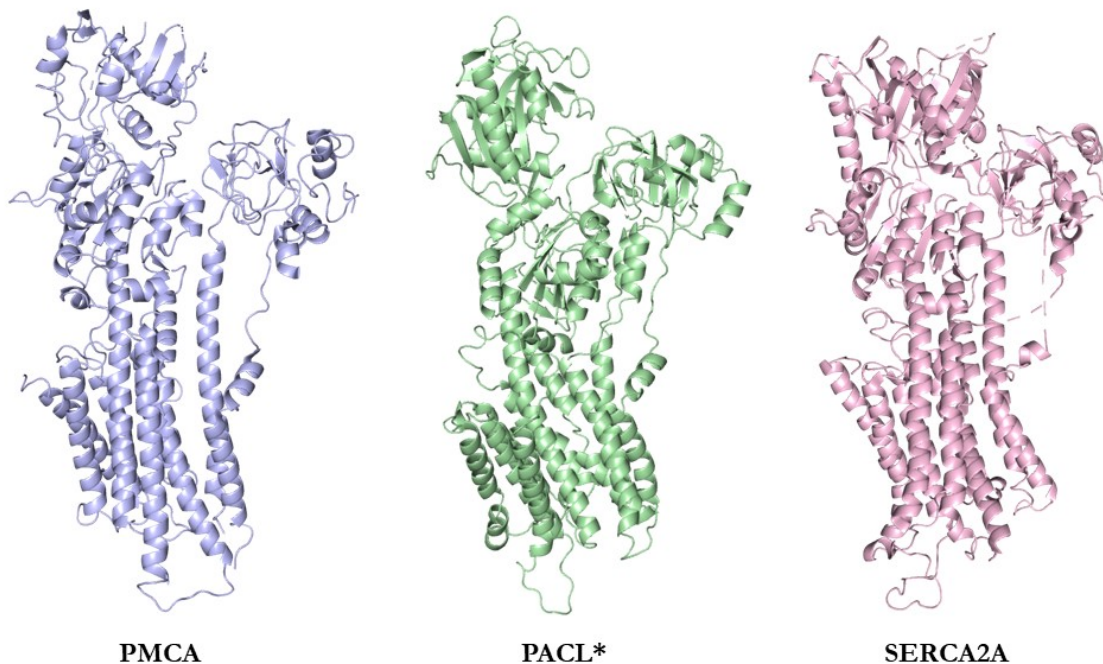
Figure 1.1: Members of the P-type ATPase family share similar structural motifs. Above are ribbon-structures of representative members of different P-type ATPases: PMCA (blue; PDB: 6A69) Plasma Membrane Calcium ATPase. PACL (green; model based on PDB: 5A3Q) bacterial P-Type ATPase. SERCA2a(pink; PDB: 6HXB) Sarco/Endoplasmic Reticulum Calcium ATPase. Note the shared structural features between these eukaryotic and prokaryotic calcium-handling proteins.

1.1.2 – Onset of eukaryogenesis and multicellular organisms

The next major leap for both early life and calcium homeostasis involves the establishment of endosymbiotic eukaryotic organisms (8). Evidence suggesting the acquisition of primitive prokaryotes/archaea and the establishment of subcellular organelles prompted the development of more complex cellular processes and a greater need for finely-tuned regulation of intracellular ionic concentrations. Primitive calcium handling proteins inherited from the "acquiring of kernel" (9) event prompted a more sophisticated, organelle-dependent control over local calcium concentrations. Plasmalemma imbedded calcium pumps became established within subcellular compartments (10, 11), allowing for a fine-tuning of calcium and many other ions. Intracellular signalling became more complex, and calcium began to have a prominent role in intracellular signalling systems, as well as being implemented into early cellular processes such as motor-function for motion, secretion systems, cell-division and mitosis, metabolism, and contraction. Several calcium transport proteins were inherited and evolved during the onset of eukaryogenesis (10, 12) that achieved the goal of pumping ions across a membrane. Of the newly evolved calcium transporters, P-type ATPases are of particular interest due to the transport of a broad range of ions (13), transition/heavy metals(14), lipids (15), *et cetera*.

1.1.3 – P-type ATPase superfamily

The P-type ATPases are a class of integral membrane transport proteins that undergo a phosphoenzyme intermediate during their catalytic transport cycle. The Na^+/K^+ pump was first identified in nerve membranes of crustaceans (16), which required phosphorylation to facilitate the transport of Na^+ across a membrane. We now know that P-type ATPases are a large family of evolutionarily related membrane proteins that span bacteria, archaea, and eukaryotes. These integral membrane "pumps" perform active transport of a diverse array of ions and lipids across biological membranes. Ligand transport and regulation divide the P-type ATPase superfamily into five subfamilies, titled *P1* through *P5*. The *P2* subfamily is of particular interest, as it includes the most well studied P-type ATPases, the Na^+/K^+ ATPase and the sarcoplasmic reticulum calcium pump, SERCA. The sodium pump is found in all eukaryotic cells where it maintains the cellular membrane potential by transporting sodium and potassium across the plasma membrane and against their concentration gradients. SERCA is also found in all eukaryotic cells where it maintains the low cytosolic calcium concentration by transporting calcium ions across the endoplasmic reticulum (ER) and sarcoplasmic reticulum (SR) membranes. In the case of SERCA, the hydrolysis of ATP is coupled

to the translocation of two calcium ions across the SR membrane and against their concentration gradient. SERCA counter-transports two-to-three protons out of the SR, though a proton gradient is not maintained across the SR membrane. Indeed, the generalized reaction scheme for P-type ATPases involves the exchange (active transport) of two different metal ions across a membrane at the expense of ATP (**Figure 1.2**). The Post-Albers scheme, proposed almost 50 years ago, is a simplistic but relevant description of calcium transport by SERCA and the high (E1) and low (E2) affinity state that SERCA populates during the reaction cycle and vectorial ion transport.
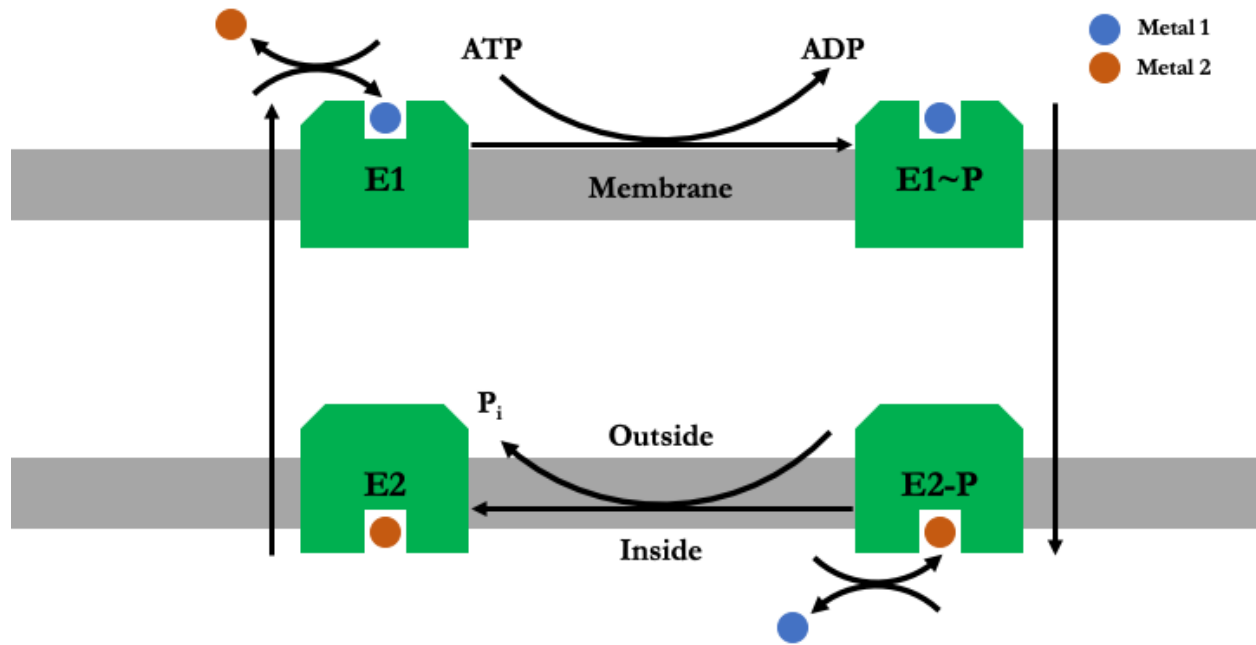
Figure 1.2: General Post-Post-Albers scheme of metal transport for P-type ATPases. A generalized schematic for vectorial transport of metal ions across a membrane at the expense of ATP, highlighting the transition from the high-affinity state (E1) to the low-affinity state (E2). In the E1 state, high affinity binding sites for metal ion 1 face the one side of the membrane. This E1 state corresponds to high affinity calcium binding sites that face the cytosol for SERCA. Upon ATP binding, the γ-phosphate is passed from ATP to the enzyme as a high energy aspartylphosphate intermediate. A major conformational change promotes the E2-P state, which results in low affinity binding sites for metal 1 facing the other side of the membrane. The phosphate and metal ion 1 are released and the enzyme ends in the E2 state with bound metal ion 2. This E2 state corresponds to SERCA with bound protons.

1.1.4 – From single-cell to multicellular organisms

Calcium-dependent cellular systems became critical during the establishment of multicellular organisms. Intercellular signalling became prominent, allowing communication between cells in the organism as a whole. Cellular specialization begat the formation of more complex organisms, with the ability to manipulate and navigate its environment. Subcellular compartmentalization and

functionally specialized aqueous environments distinct from the cytosol allowed for increased control over intracellular calcium concentrations. These intricate intracellular membrane systems include the ER, nucleus, Golgi apparatus, endosomes and lysosomes, and mitochondria, amongst others. These organelles perform distinct, essential physiological functions within the cell, and in many instances, these functions require signal transduction pathways involving calcium as a second messenger (17). For the signalling pathways to work, spatial and temporal calcium levels are tightly controlled and highly regulated. The cytosolic calcium concentration is necessarily maintained at low resting levels (<100 nmol/L, while the concentration of calcium within organelles can be much higher ($\sim$mmol/L). The signalling pathways then rely on a rapid rise in cytosolic calcium to initiate a signal, and a rapid decrease in cytosolic calcium to terminate the signal (18). Organelles such as the ER and mitochondria contain specialized calcium handling systems for the release and recovery of intracellular calcium stores. Specialized muscle cells have further specialized ER, the sarcoplasmic reticulum, that serves as a large intracellular calcium storage organelle. Locomotive organisms with specialized tissues for movement utilized calcium as in intracellular signal to shorten the tissues, or, *contract* them. In mammals, collections of these cells form the musculature utilized for a variety of tasks, like locomotor activities or pumping activities. Myocytes, the single functional unit of the cell, are also specialized depending on their tissue and function. Skeletal muscles, mostly used for locomotion and environmental manipulation, voluntarily undergo contraction and relaxation cycles over time to achieve a locomotor goal. Involuntary pumping organs, such as the heart, have a slightly more specialized myocyte, a cardiomyocyte, that has the same function (to contract and relax) but has specialized regulation and signalling to ensure involuntary contraction/relaxation cycles are smooth. Muscle contraction is achieved by calcium release from the SR in muscles, crosslinking actin and myosin filaments. The *sliding filament theory* (19) dictates that the presence of calcium shortens the contractile apparatus and contracts the cell. Calcium reuptake in the SR removes the cytosolic calcium and initiates relaxation of the contractile elements. Both skeletal and cardiac myocytes utilize this same contractile mechanism but have slightly different regulation of the calcium waves needed for contraction and relaxation cycles. Comparing fast-twitch skeletal and cardiac muscle provides insight into the diversity of cellular calcium signalling and how it enables vital physiological processes. Fast-twitch skeletal muscle contracts quickly and powerfully in response to a "voluntary" impulse, and it is the primary source of sudden, powerful bursts of movement (e.g., sprinting). In contrast, cardiac muscle contracts more slowly, with variable force, and in a continuous "involuntary" and rhythmic fashion (heartbeat). Similarities in the contractile machinery for these functionally different organs

requires an elaborate level of tissue-specific control that ultimately boils down to regulating the most critical element in life, calcium.

1.2 – SERCA

1.2.1 – Isoforms and tissue distribution

A signature example of organellar calcium storage and intracellular signalling is the sarcoplasmic reticulum (SR). In addition to carrying out functions normally associated with the ER, the SR is the primary storage site for the calcium used to trigger muscle contraction (20). On the one hand, the SR must provide an environment for the proper enzymatic function of proteins involved in protein folding, lipid biosynthesis, and the control of cell fate via apoptosis and cell growth. On the other hand, calcium release channels mobilize calcium stored in the SR for the activation of the contractile machinery within the cytosol. Following muscle contraction (systole), most of the cytosolic calcium is then recovered into the SR to initiate muscle relaxation (diastole). The release and recovery of calcium into the SR lumen ensures that the cell can begin the contraction-relaxation cycle anew. Importantly, the luminal storage of calcium is essential for a diverse array of functions, as well as the contractile role of the SR (21). An essential element of calcium reuptake in the SR is achieved by a member of the *P2A-ATPase* subfamily of P-type ATPases: The **S**arco/**E**ndoplasmic **R**eticulum **C**alcium **A**TPase, also known as **SERCA**, the calcium pump, or Ca^{2+}-ATPase.

Our detailed understanding of the structure and function of P-type ATPases is attributable to SERCA1a, the isoform present in and readily isolated from rabbit fast-twitch skeletal muscle. It is presumed that the structure and function of SERCA1a is generally reflective of the entire family of P-type ATPases (22). As noted above, calcium pumps appear to be present in all living organisms from prokaryotes to mammals, though our understanding of prokaryotic calcium pumps remains rudimentary. Of the eukaryotic calcium pumps, three multigene families and nine members are currently known. Three genes encode SERCA pumps (SERCA1-3 or ATP2A1-3), four that encode plasma membrane calcium pumps (PMCA1-4 or ATP2B1-4), and two that encode secretory pathway calcium pumps (SPCA1-2 or ATPC2A1-2). These genes give rise to more than 40 different splice variants, which result in an impressive diversification of form, function, regulation, and physiological role(23).

In vertebrates, a family of three genes encodes SERCA paralogues – SERCA1, SERCA2, and SERCA3 – located on three different chromosomes. This family is highly conserved, with SERCA1 and SERCA2 being ~84% identical and SERCA3 being ~75% identical to either of the other paralogues (**Figure 1.3**). The isoform diversity of SERCA is amplified by alternative splicing of transcripts, which occur mainly in the C-terminus of the protein. These splicing variations give rise to thirteen currently known isoforms (SERCA1a-b, SERCA2a-d, and SERCA3a-f) (24, 25). These

SERCA isoforms exhibit both tissue and developmental specificity, reflecting their diversified functionality. The SERCA1 gene encodes two spliced variants primarily expressed in adult (SERCA1a; 994 residues) and fetal-neonatal (SERCA1b; 1001 residues) fast-twitch skeletal muscle. The SERCA1a and SERCA1b isoforms are functionally equivalent and differ by only seven additional residues at the C-terminus. While there is no specific structure or function associated with the extended C-terminus of SERCA1b, it is highly charged and may play a role in skeletal muscle development (26). It is also interesting to consider that the C-terminus of the related sodium pump inserts into the membrane domain and modulates sodium affinity (27). Thus, the short extension found in SERCA1b may modulate function during the developmental switch from fetal to adult skeletal muscle.

Figure 1.3: **SERCA alignments of major isoforms show high identity.** A representative image of aligned identical residues (Blue) between respective canonical representatives of the three major isoforms of SERCA (SERCA1a, SERCA2a, SERCA2b, and SERCA3b).

11

The SERCA2 gene is best known for encoding both the ubiquitous and cardiac-specific isoforms of SERCA (28). In all, alternative splicing of the SERCA2 gene transcript generates four isoforms of SERCA (SERCA2a-d). SERCA2b is a ubiquitous isoform expressed in all cell types, whereas SERCA2a is restricted to cardiac muscle, slow-twitch skeletal muscle, and smooth muscle cells. In humans, SERCA2a encodes for a 997 amino acid protein and SERCA2b for a 1042 amino acid protein. These two isoforms differ by an unusual addition of 45 amino acids at the C-terminus, which gives SERCA2b an 11th transmembrane helix and places the C-terminus on the opposite side of the membrane in the lumen of the SR. The luminal tail and 11th transmembrane helix of SERCA2b imbue the highest calcium affinity amongst the SERCA isoforms (29, 30). A relatively new SERCA2c isoform has been shown to encode a functional form of SERCA2 expressed in cardiac muscle (31). This isoform is partially encoded by a short intronic sequence that results in a novel, truncated C-terminus. It is tempting to speculate that in line with the logic of the luminal SERCA2b tail having a regulatory capacity, this truncated version allows for alternative mechanisms of regulatory control. Along with SERCA2a and SERCA2b, ventricular muscle appears to contain a total of three SERCA isoforms. Finally, a novel SERCA2 variant (SERC2d) has been identified in skeletal muscle, though the significance and functionality of this isoform remain unknown (32).

The third SERCA gene, SERCA3, encodes the most splice variants with six known isoforms (SERCA3a-f). SERCA3 isoforms are expressed in non-muscle tissues including hematopoietic cells, platelets, epithelial cells, endothelial cells, and fibroblasts; however, it has also been found in cardiomyocytes (25). All SERCA3 isoforms are functional, though they appear to modulate cytosolic calcium and ER calcium load differently. Compared to the high prevalence of the muscle and ubiquitous SERCA isoforms (SERCA1 & SERCA2), SERCA3 is a more divergent, specialized isoform with the functional characteristics of a rapid, low-affinity calcium pump. That said, most cells likely contain multiple isoforms and splice variants as a means of diversifying intracellular calcium signalling on both global cellular and localized subcellular scales.

1.2.2 – SERCA structure, function, and physiology

1.2.2.1 – Function and physiology

SERCA isoforms are highly conserved and predicted to share the same general fold, transmembrane topology, and tertiary structure. Indeed, the highly conserved nature of SERCAs underlies the sensitivity of all isoforms to sub-nanomolar inhibition by the plant-derived sesquiterpene thapsigargin (**Figure 1.4**) (33). In contrast, other P-type ATPases such as the sodium pump are

relatively insensitive to thapsigargin. The sequence differences between SERCA1, SERCA2, SERCA3, and their splice variants are thought to involve relatively minor alterations in structure, which impart small variations to the calcium affinity and turnover rate of the different isoforms. For instance, the SERCA3 isoforms are faster, lower-affinity calcium pumps, while the SERCA2b isoform is a slower, higher-affinity calcium pump. Similarly, the small structural differences inherent in the many SERCA isoforms account for cell-specific functional and development differences at the level of ER and SR calcium handling. The one exception to this is the novel splice variation and sequence difference that occurs in the ubiquitous SERCA2b isoform. An extra, 11th transmembrane helix in SERCA2b imparts a higher calcium affinity and creates a luminal C-terminus that may sense and respond to the environment in the ER (30).
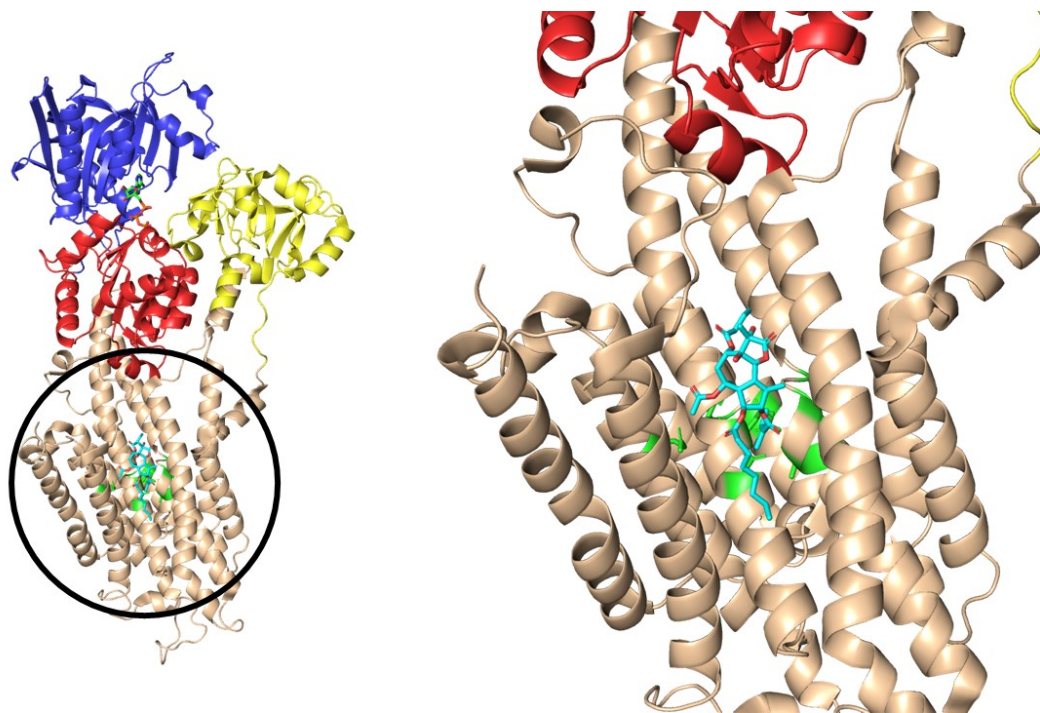
Figure 1.4: Structure of SERCA bound to thapsigargin. The overall structure of SERCA in the E2•ATP conformation (PDB: 3AR4) highlighting SERCA's structural domains. The actuator (A, yellow), nucleotide binding (N, blue), phosphorylation (P, red), and transmembrane (TM, cream) domain are indicated. SERCA contains two calcium-binding sites (green, Site I: Asn^{768}, Glu^{771}, Thr^{799}, Asp^{800}, Glu^{908}. Site II: Glu^{309}, Asn^{796}, Asp^{800}, backbone carbonyl oxygens contributed from Val^{304}, Ala^{305}, and Ile^{307}) that act to coordinate two calcium ions. This structure contains the potent non-competitive inhibitor thapsigargin (stick model, cyan) binding within the TM domain of SERCA, stabilizing the E2 conformation.

As stated above, the primary SERCA isoform in fast-twitch skeletal muscle is SERCA1a, and the isoform in cardiac muscle is SERCA2a. Studies exploring the differences between SERCA1a and SERCA2a have demonstrated that SERCA1a has a comparable calcium affinity to SERCA2a and a maximal activity that is approximately double that of SERCA2a (SERCA1a is a faster pump) (34). In addition, the density of SERCA1a is higher in skeletal muscle SR than SERCA2a is in cardiac muscle SR. Of course, there are many other protein and metabolic factors that contribute to the delineation between fast-twitch skeletal and cardiac muscle. However, these tissue-specific differences in SERCA function and distribution allow skeletal muscle fibres to achieve a faster rate of calcium uptake, more significant calcium load, and more forceful contractile function. It is also important to remember that skeletal and cardiac muscle cells contain multiple SERCA isoforms, which likely contribute to additional diversification of function depending on the compliment and abundance of isoforms present in a particular cell type. For instance, cardiomyocytes appear to contain at least four isoforms – SERCA2a, SERCA2b, SERCA2c and SERCA3b (35).

1.2.2.2 – Function and structure

The sodium pump was the first P-type ATPase identified in 1957 (16), and this seminal observation earned Jens Christian Skou the 1997 Nobel Prize in Chemistry. Since this discovery, the P-type ATPase superfamily of membrane-embedded pumps has been found to span all kingdoms of life and transport monovalent and divalent cations, heavy metals, and lipids. For the majority of these pumps, the mechanism of transport and physiological role remain unknown. Nonetheless, the SERCA calcium pump – specifically SERCA1a from rabbit skeletal muscle – has become a paradigm for the P-type ATPase family thanks to another breakthrough in the field. In the year 2000, Chikashi Toyoshima and colleagues reported the first crystal structure of SERCA with bound calcium ions (36). For those working in the field, it was a stunning revelation of the architectural complexity and molecular structure of a P-type ATPase. Since then, more than 70 structures of SERCA have been deposited in the Protein Data Bank (PDB), effectively mapping out the entire calcium transport reaction cycle. The myriad of SERCA structures have provided insight into the mechanism by which these P-type pumps use ATP to move ions across the membrane. The vast majority of these structures have come from the Toyoshima and Nissen laboratories, though our laboratory has also contributed novel insights into the structure of SERCA (37, 38). SERCA is a 110 kDa protein consisting of ten transmembrane helices that coordinate two calcium ions for transport into the SR lumen and two-to-three protons for counter-transport into the cytoplasm. While the SR membrane sequesters the

transported calcium against a concentration gradient, the SR membrane does not maintain a proton gradient. Four of the ten transmembrane helices (M4, M5, M6 & M8) form side-by-side calcium-binding sites with two partially unwound transmembrane helices (M4 & M6) in the middle of the membrane. The helix unwinding allows for the placement of the two calcium-binding sites at the same height in the membrane and coordination of the two ions by both side-chain and backbone carbonyl interactions. The first calcium ion (Site I) is coordinated by side-chain interactions with Asn^{768} and Glu^{771} from M5, Thr^{799}, and Asp^{800} from M6; and Glu^{908} from M8. Binding of the first calcium ion and E1 state transition is thought to induce a conformational change in M4 and M6 to allow binding of the second calcium ion (site II). The second calcium ion binds along the path of M4 in the gap created by the unwound helix, allowing both side-chain (Glu^{309} from M4; Asn^{796} and Asp^{800} from M6) and backbone carbonyl oxygens (Val^{304}, Ala^{305}, and Ile^{307} from M4) to contribute to ion coordination.

Of the four transmembrane helices that coordinate calcium ions, two are very long (M4 & M5; ~60Å) and extend into the cytoplasmic domain of the protein. Technically speaking, M4 is not a continuous helix because it is found to be unwound in the center of the membrane; however, it is part of a structural core that links the transmembrane and cytoplasmic domains of SERCA (22). SERCA possesses three cytoplasmic domains that sit atop the transmembrane domain 'impaled' on M4 and M5 – the nucleotide binding (N), phosphorylation (P), and actuator (A) domains. The heart of the protein is the P domain, which contains the conserved aspartate residue (Asp^{351}) that is the target of phosphoryl-transfer from ATP. The γ-phosphate of ATP is covalently passed with the retention of energy to this catalytic aspartate residue. The N domain, with its high-affinity binding site for ATP, emerges from the P domain. The N domain undergoes significant movement as the bound ATP must travel over 25 Å to reach its target catalytic Asp^{351} in the P domain to facilitate phosphoryl-transfer. In the primary structure, M4 is sequentially followed by the first half of the P domain, the N domain, the second half of the P domain, and then M5. The N domain sits atop the protein furthest from the membrane, and it is connected to the P domain by a narrow hinge region (Thr^{358}-Asn-Gln^{360} and the signature Asp^{601}-Pro-Pro-Arg^{604} motif). The N domain contains conserved residues required for nucleotide recognition, such as Phe^{487} and Lys^{515}, and the hinge region allows an extensive range of domain motion for catalytic activation once nucleotide is bound. The two halves of the P domain come together to form a Rossman fold, where the N-terminal portion packs against M4 and the C-terminal portion packs against M5. Asp^{351} lies atop the central β-strand that joins the two halves of the P domain. The N domain caps this intriguing split topology of M4-M5 and the P domain, thereby

linking calcium-binding in the membrane, nucleotide-binding in the N domain, and catalytic activation of Asp[351] in the P domain. Finally, the A domain is the most N-terminal domain and sits atop transmembrane segments M1, M2, and M3. This domain consists of a 'jelly roll' β-rich region between M2 and M3 and an N-terminal α-helical region that precedes M1 and packs against the β-rich region. As a result, the A domain is connected to M1, M2, and M3 by flexible linkers that allow large-range motions that accompany ATP utilization and ion movement. The A domain contains a signature sequence of the P-type ATPases, Thr[181]-Gly-Glu-Ser[184] (TGES), which is essential for dephosphorylation of Asp[351] in the later stages of the transport cycle. From a historical perspective, it is interesting to recall that several residues on the A domain were the targets of early proteolysis experiments that defined the E1 and E2 conformational states. The large movements of the A domain and the associated linkers in the absence and presence of calcium alternately exposed and buried residues such as Arg[198] (39).

With this domain architecture, SERCA uses the energy of ATP to move ions through the membrane. In the process, it passes through several major reaction intermediates typically denoted E1, E1P, E2P, and E2 (**Figure 1.5**), where E1 refers to a high-affinity state and E2 a low-affinity state for calcium-binding (40). The progression through the cycle involves rigid-body movements of the cytoplasmic domains and complex deformations of the transmembrane helices. The structures of the intermediates are wildly different from one another, and it is fascinating to see how they combine to animate the ion transport cycle. The P domain, containing the conserved Asp[351], is locked against M4 and M5 of the membrane domain. A central feature of the calcium transport cycle is that the P domain adopts a distinct orientation in each of the reaction intermediates, moving in a concerted way with M4 and M5. Additionally, the N and A domains adopt remarkably distinct orientations in each reaction intermediate, due to their flexible connections to the rest of the protein. In contrast to the rigid-body movements of the cytoplasmic domains, the membrane domain undergoes plastic deformations of helices M1-M6. The rearrangements in the transmembrane domain cause the calcium-binding sites to alternate their access to the cytosolic and luminal sides of the membrane. Upon phosphoryl-transfer from ATP to Asp[351], the A domain undergoes a significant rotation (41) that allows the conserved TGES motif to displace ADP, now occupying the ATP binding site in the N domain. Because the A domain links directly to M2 and M3, it serves to transduce movement in the cytoplasmic domain to conformational changes in the transmembrane domain (calcium ion occlusion). The A domain ultimately makes contact with both the P and N domains, such that the TGES motif can initiate the dephosphorylation event and continue the cycle. This association causes significant movement in M2

to M5, thereby exposing the calcium-binding sites to the SR lumen and allowing calcium release. The direct connections between the ion-binding sites in the membrane and the cytoplasmic domains provide a plausible mechanism for calcium transport, H^+ counter-transport, and phosphorylation and dephosphorylation of Asp^{351}. For a more detailed description of the structure and function of SERCA, there are many excellent reviews available (*see* (22, 42, 43)).
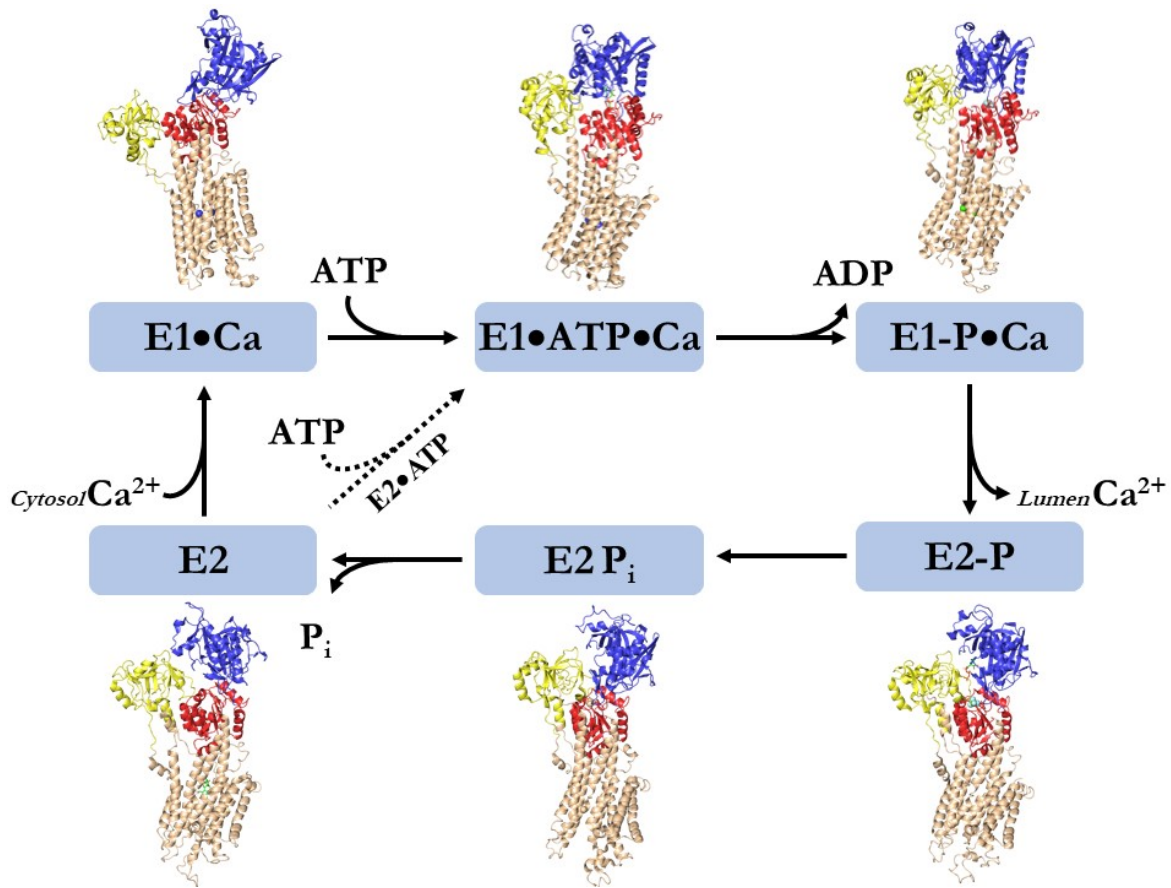
Figure 1.5: SERCA catalytic cycle of ATP mediated calcium transport. SERCA undergoes enormous structural changes during calcium transport. Major reaction intermediates are represented by SERCA crystal structures with major domains highlighted (Cytoplasmic domain: Blue – nucleotide binding domain, N domain. Yellow – actuator domain, A domain. Red – phosphorylation domain, P domain. Transmembrane domain, TM domain: Cream). Note significant conformation shifts in the cytoplasmic and TM domain. **E2** – Low-affinity state with no bound calcium and 2-3 bound protons (PDB: 1IWO). **E1•Ca** – Two cytosolic calcium ions are bound to SERCA's calcium-binding sites, and bound protons are released into the cytosol. Note that the calcium-binding event poises SERCA in a high-affinity state, this movement translated into a sizeable conformational shift in the cytoplasmic domain, allowing for easier nucleotide access to the N domain (blue) as well as a rearrangement in the TM domain (cream) allowing for calcium entry (PDB: 1SU4). **E2•ATP**- SERCA remains in a low-affinity state with ATP bound to the N domain (blue), note the stark contrast in the cytoplasmic domain between E1•Ca and E2•ATP. Despite SERCA being in a low-affinity state, there is evidence that nucleotide binding to the N domain leads to a disordering event in the cytoplasmic domain that lowers the energy barrier for a conformational shift to the next high-affinity reaction intermediate. It is important to note that both E1•Ca and E2•ATP effectively fit the same 'spot' during the calcium transport reaction in that they are loading SERCA with calcium or ATP, preparing for nucleotide hydrolysis, phosphoenzyme formation, and calcium transfer. **E1• ATP•Ca –** With ATP and calcium bound, SERCA undergoes a conformational shift in the cytoplasmic domain where the N and P domains become physically closer in space, ready for a phosphorylation event. More subtle movements occur in the core of the TM domain, preparing for calcium release into the sarcoplasmic reticulum (SR) lumen (PDB: 1VFP). **E1-P•Ca –** Phosphoenzyme formation induces a conformational change in the TM domain to a calcium-occluded state, further preparing for calcium release (PDB: 5XA8). **E2-P** – Calcium is released into the SR lumen, and ADP is released from the N domain, bringing the enzyme back to a low-affinity state (PDB: 3FPB). **E2 Pi** – SERCA binds 2-3 protons and forms a proton occluded state with the release of inorganic phosphate, returning the enzyme to the low-affinity E2 state (PDB: 3B9B).

With the many structures of SERCA available in the Protein Data Bank, one might assume that we understand everything there is to know about the calcium transport cycle. Sadly, or perhaps interestingly, this is not true. First, the structures provide snapshots of the stable intermediates SERCA adopts as it progresses through the reaction cycle, and it gives us an impressive vision of the mechanics of calcium transport. However, the molecular and energetic constraints that drive each step in the reaction cycle from ATP hydrolysis to calcium transport against a concentration gradient remain challenging to delineate. As an example, consider the transition from the E1•ATP•Ca state to the E1~P•Ca•ADP state following the transfer of the γ-phosphate to Asp[351] with nearly complete conservation of energy. The structures of these two intermediates are known and represented by E1•Ca•AMPPCP and E1~AlF₄•Ca•ADP complexes, respectively (44). These structures are identical, yet they possess distinct biochemical characteristics – in particular, only the E1~AlF₄•Ca•ADP complex adopts a stable occluded state, a pre-requisite for progression to the next intermediate in the transport cycle. Second, while such details may be of particular interest in the P-type ATPase field, the large number of structures available for SERCA does not mean that we have mapped the entire structural landscape of SERCA intermediates (there continue to be surprises in the field!). As an example, recent structures of SERCA in complex with the regulatory subunits phospholamban (PLN) and sarcolipin (SLN) revealed an unanticipated conformation of SERCA (45–47). In the complexes, SERCA adopts a previously undescribed E1-like state with formed calcium-binding sites that are open to the cytosol. In the two crystal structures of the SERCA-SLN complex, magnesium ions sit adjacent to the two calcium-binding sites (sites I & II). In one of the structures (45), two magnesium ions were found (adjacent to Asp[800] and Glu[309]), and in the other structure (46), one magnesium ion was found (adjacent to Ala[305]). At physiological concentrations, magnesium is expected to interact with the calcium-binding sites and modulate the transport cycle (48, 49), though the reaction cycle cannot progress without both calcium and ATP binding. In this E1-like state, the E2-to-E1 transition has begun, and the calcium sites are formed, though the magnesium ions must be displaced for calcium to bind. It is interesting to note that the SERCA-PLN complex is remarkably similar but does not appear to have a bound magnesium ions (47).

1.3 – SERCA rcgulator Complexes

Historically, PLN and SLN were the only known regulators of SERCA (50–53). PLN is a 52 amino acid integral membrane protein found in cardiac and smooth muscle (54), and SLN is a homologous 31 amino acid integral membrane protein found in skeletal and atrial muscle (52). The

canonical model for SERCA regulation by PLN and SLN involved a reversible one-to-one association that lowers the apparent calcium affinity of SERCA (55), and this has classically been termed SERCA inhibition. The inhibition is maximal at low physiological calcium concentrations (~0.1 μmol/L cytosolic calcium) and reversed at higher calcium concentrations (>1 μmol/L). However, PLN has also been reported to have a stimulatory effect on calcium reuptake (56), contrary to the classic 'inhibitor' designation, so perhaps the term 'regulator' would be a more suitable descriptor. The complex regulatory axis involved in PLN and SLN mediated SERCA regulation has expanded to include novel PLN and SLN functions and the discovery of additional regulatory peptides.
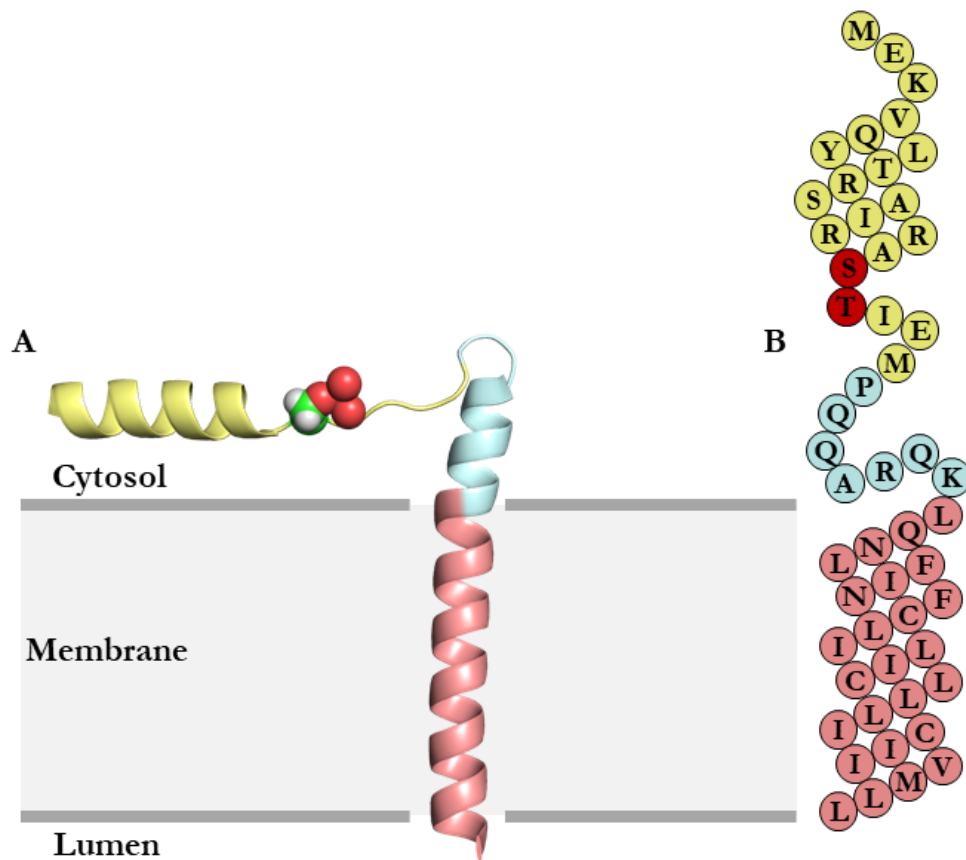
Figure 1.6: Phospholamban structure and topology. (A) A solution and solid-state NMR ensemble structure of Ser[16] phosphorylated PLN (PDB: 2M3B) and a topology diagram (B) indicating the primary sequence as well as the domain architecture of PLN. PLN cytoplasmic domain (yellow) is a highly dynamic helical structure containing two phosphorylation sites (crimson). A short linker (cyan) region connects the cytoplasmic from the transmembrane (red) domains.

1.3.1 – Phospholamban

PLN is a 52 amino acid, single-pass, transmembrane protein that is best known for its regulatory role in the heart. PLN is found predominantly in ventricular cardiac muscle and, to a lesser extent, in slow-twitch skeletal muscle, smooth muscle, and atrial muscle. PLN contains three domains (**Figure 1.6**) – a transmembrane helix responsible for most of its inhibitory properties (residues ~31–52), a small, unstructured linker region (residues ~21–30), and a soluble cytoplasmic helix that is thought to be more dynamic (residues ~1–20). PLN was discovered as the principal target of phosphorylation in isolated SR membranes, and was named accordingly (phospholamban was derived from *phosphate* and the Greek word '*to receive*') (50, 57). The name reflects the observation that protein kinase A (PKA) regulates cardiac contractility by phosphorylating Ser^{16} in the N-terminal domain of PLN. In cardiac and smooth muscle, PLN is a reversible, calcium-dependent regulator of SERCA, which modulates cardiac contractility in response to physiological cues (54, 58, 59). SERCA regulation by PLN is a dynamic process that depends on the cytosolic calcium concentration, the phosphorylation state of PLN, and the oligomeric state of PLN (54). First, PLN physically interacts with and lowers the calcium-affinity of SERCA at sub-micromolar calcium concentrations, and this is reversed by micromolar calcium concentrations (60). Maximal SERCA inhibition occurs within the physiological window of cytosolic calcium (0.1–1.0 μmol/l). Second, the inhibition is relieved by phosphorylation of PLN in a mechanism that is linked to β-adrenergic stimulation and PKA (61, 62). Third, PLN forms a homopentamer which is in dynamic equilibrium with the inhibitory monomer (63). The pentamer has been described as an inactive storage form of PLN, though it is required for physiological function (64), and it also interacts with SERCA (65, 66). The synergistic effect of these various regulatory mechanisms is a modulation of SR calcium stores and cardiac contractility that can be finely tuned in response to activity, stress, or disease.
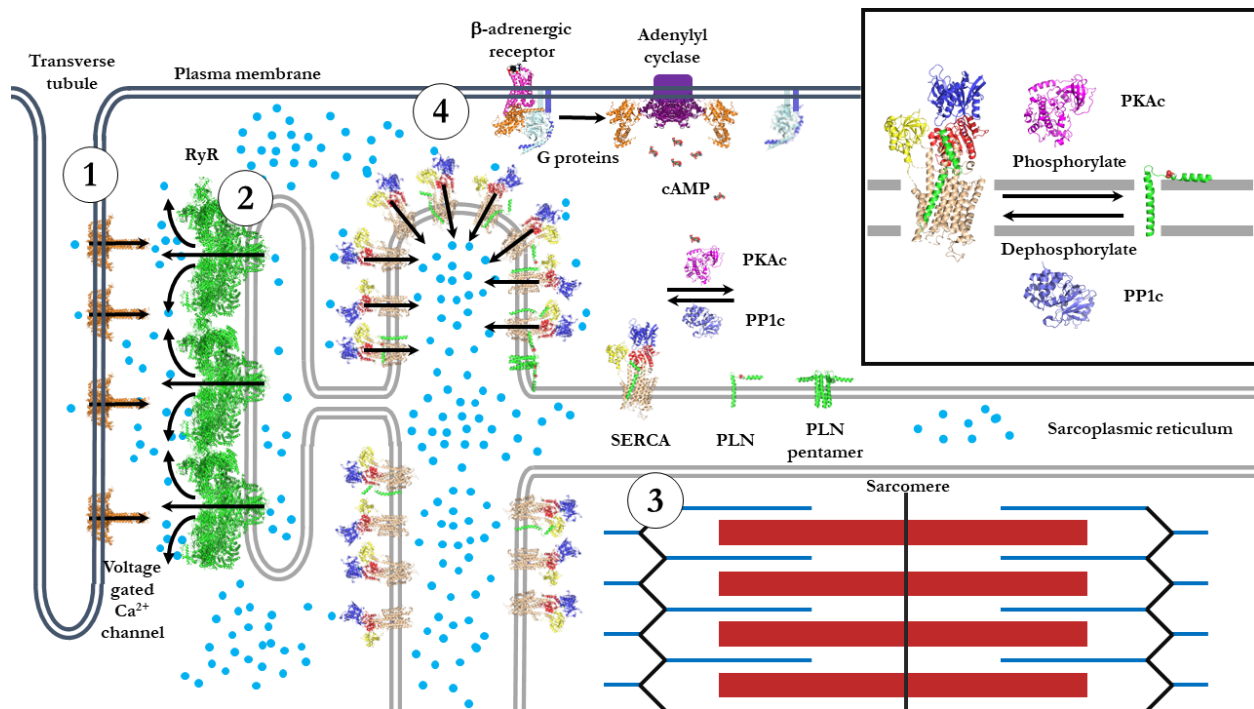
Figure 1.7: Schematic of calcium homeostasis in a generalized cardiomyocyte. 1 – To initiate muscle contraction, an action potential propagates into plasma membrane invaginations, known as transverse tubules, activating voltage-gated calcium channels (orange, PDB: 2KLB), causing a small trickle of calcium (blue sphere) into the cytosol. 2 – This low concentration of calcium activates calcium release channels (ryanodine receptor, RyR, green, PDB:3J8H) localized in the nearby localized sarcoplasmic reticulum (SR) (dyad) to release calcium, flooding the cytosol with calcium ions. 3 – increased cytosolic calcium concentrations go on to activate the contractile machinery in the cell and shorten the sarcomere. 4 – Calcium reuptake by SERCA (blue, red, yellow, cream PDB: E2 - 3AR4, E1 - 1SU4) into the SR lumen removes cytosolic calcium and engenders sarcomere relaxation, returning the cardiomyocyte to a state poised for subsequent contraction. This mechanism of calcium homeostasis can be modulated by catecholamines such as adrenaline, acting through the β-adrenergic signalling pathway. β-adrenergic receptor (purple, PDB:3SN6) stimulation liberates attached G-proteins (orange, cyan, blue, PDB 3SN6) which go on to modulate the activity of sarcolemma bound membrane proteins such as adenylyl cyclase (dark purple, PDB 3MAA) (a more in-depth analysis of this process can be found in (67, 68)). G-protein mediated activation of adenylyl cyclase increases cytosolic cAMP levels, which can then bind to the regulatory subunit of protein kinase A (PKA) and activate the catalytic subunit (PKAc, light purple, PDB:2PCK). PKAc phosphorylates PLN (green, PDB: monomer - 1ZLL, pentamer - 2KYL, phosphorylated - 2M3B) and modulates PLN's regulatory capabilities. Protein phosphatases (PP1c, blue, PDB: 4MOV) are responsible for dephosphorylation of PLN, restoring PLN's former regulatory capabilities. A large pool of SERCA and PLN monomers/pentamers allows for dynamic modulation of cardiac muscle relaxation and SR calcium refilling for subsequent contractions. The SERCA-PLN pool facilitates dynamic contractility in response to a swathe of environmental stimuli, dictating how the heart responds to different cardiac needs.

1.3.1.1 – Phospholamban structure and function

A primary mechanism for modulating SR calcium stores is through catecholamines, which act through the β-adrenergic pathway to activate PKA and phosphorylate several cardiac proteins (**Figure 1.7**). The goal of this pathway is to modulate cardiac output by targeting the contractile apparatus and calcium-handling proteins. Phosphorylation of PLN by PKA has a significant impact on cardiac contractility via a mechanism that reverses the inhibitory properties of PLN and increases the apparent calcium affinity of SERCA (61). Monomeric PLN inhibits SERCA, and phosphorylation of PLN is believed to cause dissociation from SERCA and oligomerization of PLN into storage pentamers (55, 63, 69). PLN has two adjacent phosphorylation sites – it is phosphorylated at Ser^{16} by PKA (58) and at Thr^{17} by calcium/calmodulin-dependent protein kinase II (CAMKII) (62) and Akt (70). Separately, or in combination, phosphorylation at these sites is essential for proper cardiac function (71). It is not well defined as to whether these sites are phosphorylated independently and have separate effects on the inhibition of SERCA or are phosphorylated concurrently and have a synergistic effect on inhibition. There is some consensus that the primary mode of regulation is through PKA and Ser^{16}, while Thr^{17} provides a means for tuning or terminating the response depending on physiological or pathophysiological conditions (72). Nonetheless, the intricacies of PLN inhibition of SERCA are of high clinical relevance in terms of cardiac health, where disruptions to the calcium cycle in the heart lead to contractile dysfunction, cardiac hypertrophy, and dilated cardiomyopathy (73–78).

Functionally, PLN inhibition is measured as an effect on the apparent calcium affinity of SERCA, with the main target being the SERCA2a isoform. However, PLN also inhibits SERCA1a and SERCA2b, but not SERCA3 (79, 80). SERCA inhibition is primarily encoded by the transmembrane domain of PLN (~80% of inhibition; (81)), while the linker region mitigates the inhibitory interaction, and the N-terminal helix allows for reversibility of inhibition via phosphorylation (and ~20% of the inhibitory activity). The transmembrane domain of PLN contains the structural determinants for SERCA inhibition (e.g., Leu^{31} & Asn^{34}) and structural determinants that are responsible for homopentamer formation (**Figure 1.8**) (Leu-Ile zipper motif; e.g. Leu^{37} & Ile^{40}) (63, 69, 82, 83). The monomeric form of PLN is sufficient for SERCA inhibition, though the recent crystal structures demonstrate that the interaction site could also accommodate an oligomeric form of PLN (47). By default, the PLN pentamer has been described as an inactive storage form, though there has been no direct demonstration of the functional capacity of oligomeric forms of PLN.
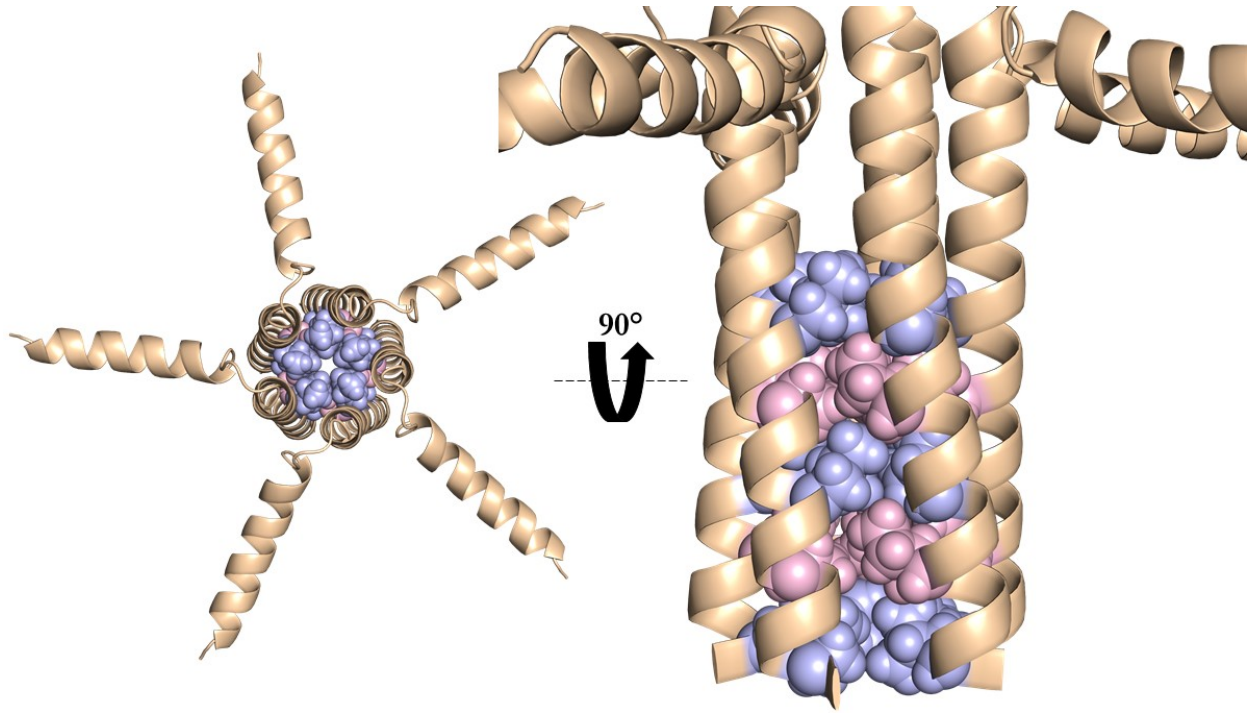
Figure 1.8: Phospholamban spontaneously forms homopentamers stabilized by an Ile/Leu zipper motif. PLN monomers (cream) arranged as a pentamer (PDB: 2KYV) with Ile in pink (Ile[40] and Ile[47]) and Leu residues in blue (Leu[37], Leu[44], and Leu[51]) indicated to display the Ile/Leu zipper motif stabilizing the oligomer.

The linker region of PLN (residues ~21–30) modulates the interaction of PLN's transmembrane domain with SERCA through charge repulsion. Residues such as Arg[25] and Lys[27] of PLN are proximal to residues such as Arg[324] and Lys[328] of SERCA. These adjacent charges are thought to "tune" the interaction of the transmembrane domain to achieve modest SERCA inhibition over a precise, physiological range of calcium concentrations. Furthermore, this linker region must transmit the reversal of inhibition from the N-terminal domain (Ser[16] & Thr[17]) to the transmembrane domain (residues ~31–52). As stated above, PLN is phosphorylated at Ser[16] via the β-adrenergic pathway as a direct result of sympathetic nervous system activation. PKA targets Ser[16] through the consensus recognition motif of Arg[13]-Arg-Ala-Ser[16] (54). Once phosphorylated, Ser[16] may form salt bridges with Arg[13] and/or Arg[14], thereby distorting the N-terminal helix of PLN and relieving SERCA inhibition (84). Phosphorylation alters the conformational dynamics of PLN's cytoplasmic domain and the interaction with SERCA (85, 86). PKA can target and phosphorylate PLN monomers bound to SERCA. In this context, PKA recognition of PLN is the first step in the reversal of SERCA inhibition and phosphorylation of Ser[16] serves to maintain the non-inhibitory state. PKA can also target PLN

monomers in the context of the PLN pentamer (87, 88) and shift the dynamic monomer-pentamer equilibrium toward the PLN pentamer (63). The PKA recognition motif is absolutely required for this to occur, though there are additional, unique structural determinants that allow PKA to recognize SERCA-bound PLN (Arg[9] & Ser[10]) and the PLN pentamer (Arg[9]) (87). There is an ongoing debate whether phosphorylation causes the PLN monomer to dissociate from SERCA following phosphorylation, though we consider PLN to be a subunit of SERCA. Instead, conformational changes in the N-terminal domain of PLN transmit to the transmembrane domain, allowing calcium translocation to occur without PLN dissociation from SERCA. We acknowledge that it may be advantageous, under physiological conditions such as exercise or stress, to fully dissociate the SERCA-PLN complex for maximal SERCA turnover.

1.3.1.2 – PLN phosphorylation state

The residues of PLN that directly associate with the catalytic subunit of PKA span from approximately Lys[3] to Ile[18]. In addition to the canonical recognition motif, PKA has a preference for upstream positively-charged residues and downstream hydrophobic residues. Arg[9] and Ile[18] of PLN fit these criteria, though Ile[18] has not been the focus of much attention. Extensive mutagenesis of Arg[9] in PLN revealed that PKA has a strong preference for this residue, particularly in the pentameric state. In the peptide-binding groove of PKA, Arg[9] of PLN packs against Glu[203] and Asp[241] of PKA, eliciting a strong influence on substrate recognition. PKA recognizes substrates by conformational selection (89), and the most efficient substrates are peptides in solution because of their conformational dynamics (90). Indeed, PKA-mediated phosphorylation is most efficient for a peptide corresponding to the cytoplasmic domain of PLN. By comparison, phosphorylation is less efficient for monomeric, full-length PLN, and far less efficient for the PLN pentamer or the SERCA-PLN complex. Arg[9], as well as Ser[10], and Ile[18] assist in recognition of PLN when its conformational dynamics are more constrained (i.e., PLN pentamer or SERCA-PLN complex). Arg[9] is so vital for PLN function and β-adrenergic signalling that human mutations at this locus (Arg[9]-to-Cys & Arg[9]-to-Leu) give rise to lethal, hereditary dilated cardiomyopathy. These mutations abrogate PLN function and create a kinetic trap for PKA, sequestering it from phosphorylating other cellular targets (75, 87). Perhaps equally important to phosphorylation of PLN by PKA is the dephosphorylation by Protein Phosphatase-1 (PP-1), which reactivates PLN for SERCA inhibition (91, 92). However, very little is known about the sequence determinants of PLN that govern its dephosphorylation. In addition, it remains uncertain as to which isoform of PP-1 dephosphorylates PLN in the myocardium. PP-1β is

the major isoform that co-localizes with the SERCA-PLN complex in cardiomyocytes, though PP-1α and PP-1γ can also dephosphorylate PLN. PP-2 has also been reported to dephosphorylate PLN (91). Regardless of which isoform is responsible for dephosphorylation of PLN in human myocardium, it is well-known that PP-1 activity has significant control over SERCA-PLN function and cardiac contractility. As another layer of complexity, these proteins form a regulatory complex at the level of the SR that includes SERCA, PLN, A kinase anchoring protein (AKAP18δ & γ), PKA (catalytic & regulatory subunits), PP-1, inhibitor-1 (I-1), small heat shock protein 20 (Hsp20), the HS-1 associated protein X-1 (HAX1), small ubiquitin-related modifier (SUMO-1), and phosphodiesterase (PDE4D, 3A). Furthermore, these interactions may involve oligomeric assemblies of both SERCA (93) and PLN (65, 88, 94). Finally, one must keep in mind that the copy number of SERCA and PLN molecules far exceeds the calcium release channel. Thus, compared to calcium release, calcium recovery involves a large "pool" of SERCA pumps that can be differentially and dynamically activated or suppressed depending on cardiac output.

1.3.1.3 – PLN oligomeric state

As stated earlier, PLN exists in a dynamic equilibrium between monomeric and oligomeric states. Canonically, PLN homopentamers have been described as an inactive store of inhibitory monomers, despite the absence of direct experimental evidence. Initial studies attempting to elucidate the function of the pentamers revealed that the pentameric form of PLN is essential for myocardial relaxation and contractility (64). Transgenic mice expressing Cys[41]-to-Phe monomeric PLN exhibit reduced muscle relaxation when compared to wild-type pentameric PLN. In contrast, PLN knockout mice in this study were reported to have peak contraction and relaxation cycles in the heart. Efforts by Chu et al. determined that the wild-type, pentameric PLN was more effective in reversing the PLN knockout phenotype in mice than its Cys[41]-to-Phe monomeric counterpart. *In vitro* studies suggested that, biochemically, both the mutant and wildtype PLN appeared to inhibit SERCA equally, but the *in vivo* studies paint a different picture. Wild-type PLN pentamers were found to depress cardiac relaxation to a greater extent than the monomeric mutant PLN, effectively reversing the phenotype and restoring cardiac contractility. The authors tried to rectify the discrepancy between biochemical and physiological data by suggesting that the ratios of PLN to SERCA appear to play a significant role in effective regulation, as well that PLN pentamers behave differently in a membrane, and, most interestingly, that PLN pentamers may cause a calcium leak in the membrane. Other groups, following

this study, have concluded that PLN pentamers may form a cation-selective channel in a membrane (95–97) as an explanation for an observed calcium leak.

These previous observations are consistent with direct experimental evidence that the PLN pentamer interacts with SERCA at a site distinct from the inhibitory groove (M2, M6, & M9) (65, 66). Two-dimensional cocrystals of SERCA and PLN revealed that PLN pentamers interact with SERCA at a non-inhibitory secondary site consistent with the transmembrane region around M3. When phosphorylated, the PLN pentamers were found to remain associated with SERCA and still form two-dimensional crystals. The fact that PLN pentamers were found to remain associated with SERCA is bolstered by observations of phosphorylated PLN pentamers continuing to modulate SERCA maximal activity (V_{max}) (98). Trieber et al. observed that, *apropos to* PLN pentamers, phosphorylation of PLN reversed the effect on the apparent calcium affinity of SERCA (K_{Ca}) but did not affect the stimulation of SERCA's maximal activity. This suggests that PLN remains associated with SERCA because it is still modulating SERCA activity, though the association must be distinct from the inhibitory interaction. Evidence from two-dimensional cocrystals also suggests that PLN remains associated with SERCA in a functional state that is distinct from the inhibitory interaction.

Additionally, PLN pentamers appear to modulate the PKA mediated phosphorylation of PLN monomers. Wittman et al. 2015 (88) revealed that pentameric PLN is the preferred substrate of PKA. The presence of pentameric PLN delayed the phosphorylation of monomeric PLN, and conversely, the absence of pentameric PLN resulted in phosphorylation of monomeric PLN at the same rate as if PLN were pentameric. Additionally, co-IPs of PLN pentamers and PKA revealed that more PKA precipitated with pentameric PLN over monomeric mutants. These same co-IP experiments indicated that phosphorylated PLN pentamers are proximal to SERCA2a, with the conclusion that phosphorylated PLN pentamers naturally associate with SERCA. These experiments contradict the canonical model where PLN dissociates from SERCA after phosphorylation AND PLN pentamers exist as a non-functional storage bundle. It is clear that PLN pentamers are of critical importance for SERCA-mediated calcium homeostasis in cardiomyocytes and smooth muscle. However, a fundamental question remains: What is the function of the PLN pentamer? Investigating this phenomenon demands an explanation for the exact function of the PLN pentamer and how it is involved in differential regulation of SERCA under multiple stimuli. This thesis hopes to answer these questions by showing that PLN can regulate SERCA through a natural association with a site independent of the inhibitory groove.

1.3.2 – Sarcolipin

Historically, the SERCA regulator PLN received much attention because of its role in cardiac muscle and the potential link to human heart disease (73, 75). Comparatively, SLN received less attention because it was assumed to mirror PLN function in skeletal muscle, and the potential human health implications were not obvious. However, with the recent identification of novel functions for SLN, attention has refocused on this important SERCA regulator. SLN is a 31 residue, mostly α-helical, integral membrane protein (**Figure 1.9**) that is the principal regulator of SERCA in skeletal and atrial muscle.
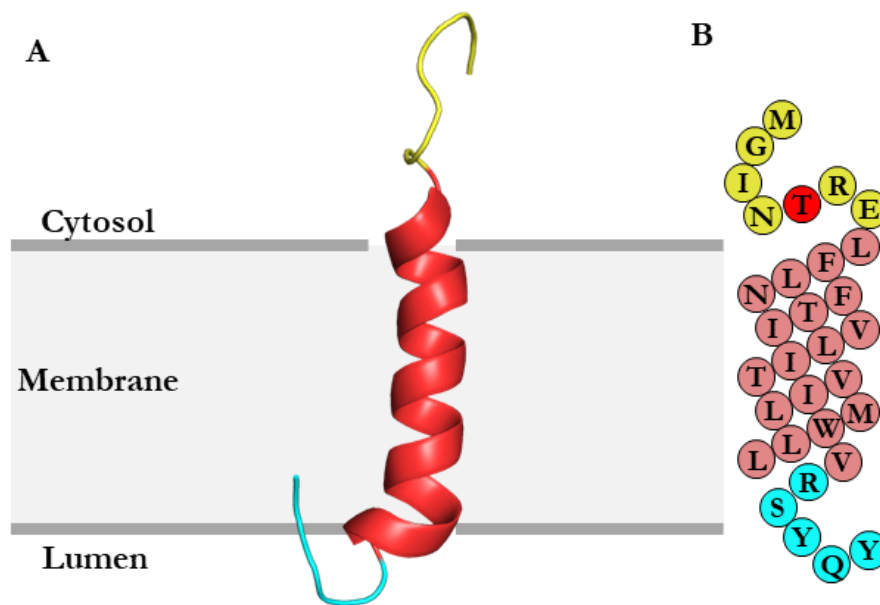
Figure 1.9: **Sarcolipin structure and topology**. (A) A solution and solid-state NMR structure of synthetic SLN in a lipid environment (PDB: 1JDM) and a topology diagram (B) indicating the primary amino acid sequence as well as the domain architecture of SLN. SLN contains a short, N-terminal, cytoplasmic domain (yellow) that is thought to contain a potential CAMKII phosphorylation site (crimson) and be involved in uncoupling SERCA ATPase activity from calcium transport (99). A transmembrane domain that interacts with the inhibitory groove of SERCA (red) spans the membrane and a highly conserved C-terminal tail (cyan) that is responsible for the bulk of SLN's inhibitory properties(100).

1.3.2.1 – SLN structure and function

First described as a proteo-lipid associated with SERCA1a (53), SLN is structurally and functionally homologous to PLN (with ~80% sequence homology between SLN and PLN TM domains), and it is postulated to regulate SERCA in a similar manner (52). SLN contains a short,

variable cytoplasmic domain (residues ~1–7), a transmembrane α-helix (residues ~8–26), and a short, highly-conserved luminal tail (residues 27–31). Like PLN, SLN alters the apparent calcium affinity of SERCA by binding in a groove formed by transmembrane helices M2, M6, and M9 (**Figure 1.10**). Crystal structures of a SERCA-SLN complex reveal that PLN and SLN use overlapping binding sites to interact with an E1-like state of SERCA (46, 101). However, despite the homology to PLN, there are substantial differences in the way that SLN regulates SERCA. SLN's unique and highly conserved C-terminal tail (Arg[27]-Ser-Tyr-Gln-Tyr[31]) encodes most of its inhibitory properties (100). Indeed, this C-terminal RSYQY sequence can be transferred to the C-terminus of a generic transmembrane helix, turning it into a SERCA inhibitor with SLN-like properties. Additionally, the transfer of SLN's C-terminus to PLN results in a chimeric protein with enhanced inhibitory and oligomeric properties (102). In the SERCA-SLN crystal structures, the RSYQY sequence is helical and not in direct contact with SERCA, suggesting that it serves to position SLN in the inhibitory groove of SERCA for optimal inhibition. For instance, the arginine and tyrosine residues could sit at the hydrocarbon core-water interface of the lipid bilayer, thereby positioning the transmembrane helix relative to SERCA. The RSYQY luminal tail is a distinct, essential and transferrable domain that contributes directly to SERCA inhibition (100). Thus, it seems likely that the SERCA-SLN inhibitory complex involves contacts between the RSYQY luminal tail of SLN and the luminal loops and calcium-exit channel of SERCA, though the structure of this inhibitory state remains unknown.
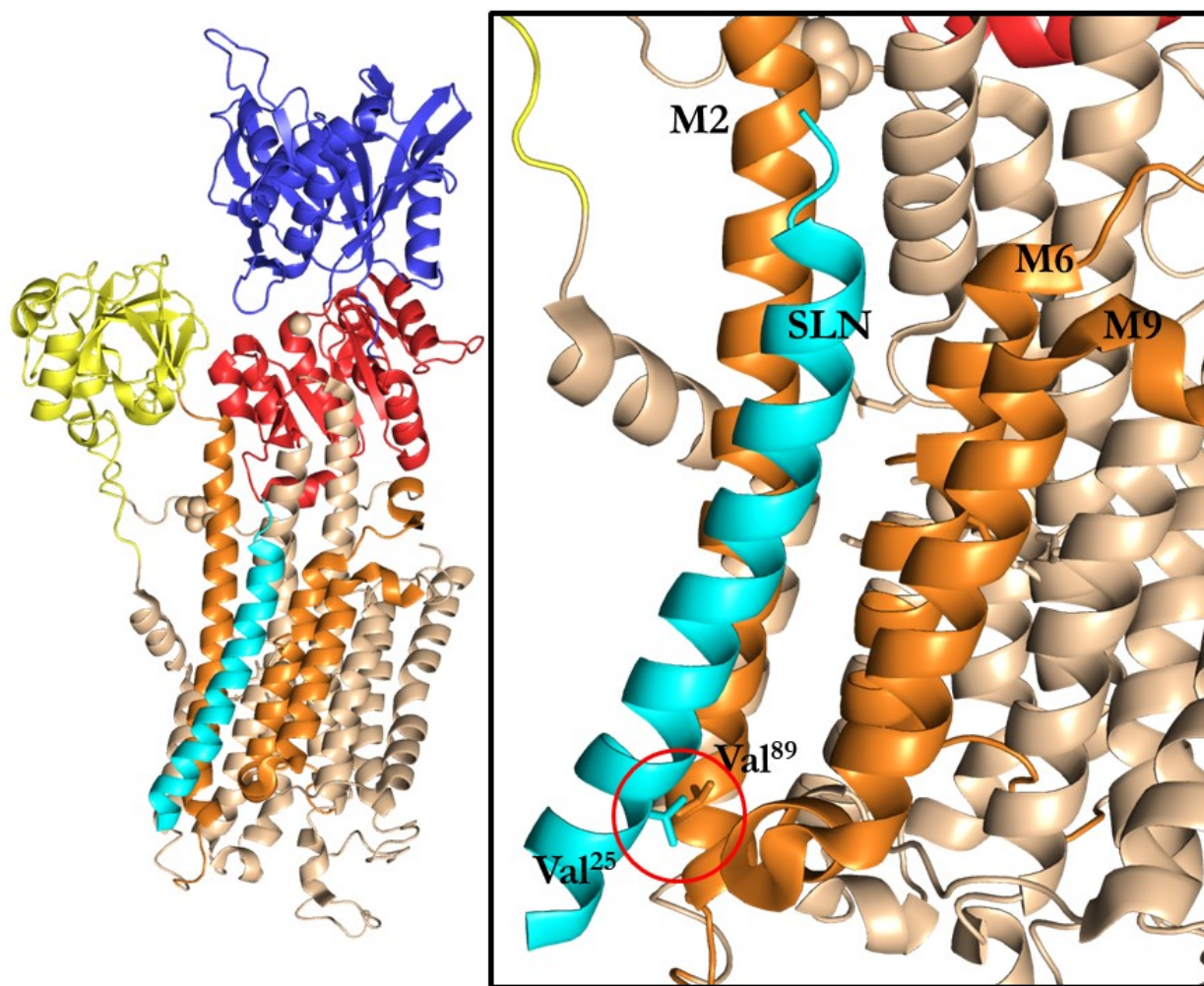
Figure 1.10: SLN occupies the same canonical inhibitory groove as PLN. Crystal structures of SLN with SERCA, shown with the A-domain (yellow), P-domain (red), N-domain (blue), TM domain (cream), and SLN (cyan), (PDB: 3W5A) reveals that SLN binds to SERCA's inhibitory groove (orange, TM segments M2, M6, and M9), stabilizing an E1-like state. Hydrophobic sidechains of SLN contribute to the binding interface formed by M2, M6, and M9 and overlap with residues contributing to PLN binding to the inhibitory groove. Val[25] of SLN was found to closely interact with Val[89] of M2, which lines up with Val[49] of PLN interacting with Val[89] of SERCA, confirming that SLN and PLN exhibit very similar binding characteristics.

In addition to altering the apparent calcium affinity of SERCA (K_{Ca}), one of the signatures of SLN inhibition is a decrease in the maximal activity of SERCA (V_{max}) (100, 103). This V_{max} depression is opposite to the trend observed for PLN, which increases the maximal activity of SERCA at saturating calcium concentrations (81, 87, 98, 104). These trends have been consistently observed using a highly purified membrane reconstitution system (co-reconstituted proteoliposomes), though other reports in the literature suggest that SLN could either decrease (105–107) or increase (52) the V_{max} of SERCA. Nonetheless, it is clear that SLN is a distinct regulatory subunit of the SERCA

calcium pump, and this has culminated in the observation that SLN may also possess a unique physiological role in skeletal muscle.

1.3.2.2 – Non-shivering thermogenesis

It has been reported that SLN promotes futile cycling of SERCA and increases the net balance of ATP consumption to calcium transport (a process termed uncoupling). The excess ATP hydrolysis contributes to heat production. Considering that skeletal muscle makes up ~40% of body mass, SERCA and SLN may be significant contributors to non-shivering, muscle-based thermogenesis (108). Also, the abundance of skeletal muscle and the role of SLN make it a potential contributor to metabolic demand and human disorders such as obesity, diabetes, and metabolic syndrome.

The idea of uncoupling ATP hydrolysis from calcium transport was first postulated by Lee et al. (109), wherein they suggest SLN association with SERCA promotes more ATP hydrolysis than calcium transport. They postulated that the observed uncoupling effects could be simulated by 'slippage' of calcium from SERCA's calcium-binding sites back to the cytosol. Based on these observations, they speculated on the role of SLN-mediated ATPase uncoupling as a mechanism for heat-generation in mammals. Since then, several groups have investigated this phenomenon to determine SLN's role in thermogenesis.

Speculation as to the mechanism by which SLN uncouples SERCA is a controversial research topic. As previously mentioned, SLN's C-terminal tail is highly conserved and critical for SLN's regulatory properties but appears not to affect ATPase uncoupling (102). An important detail to note is that SLN has been reported to depress the V_{max} of SERCA calcium uptake, but not the consumption of ATP (103). Recent research indicates that the N-terminal domain of SLN is essential for its uncoupling function (99, 102), in addition to its regulatory function (110). It has been posited that this region can induce structural rearrangement in SERCA's 'energy-transduction domain' (99) causing the region to become more plastic. In particular, charged glutamate residues in the N-terminus of SLN appear to be essential to uncoupling function, and removal of the N-terminus results in a truncated SLN that can still bind to SERCA's inhibitory groove. This indicates that SLN binding to SERCA's inhibitory groove is independent of its uncoupling effects on SERCA. SLN's N-terminus is variable in mammals and it is unclear how this variability contributes to SLN-mediated ATPase uncoupling in thermogenesis.

SLN's contribution to physiological thermogenesis continues to be a controversial topic. A number of research groups postulate that SLN is involved in adaptive thermogenesis (111–113), while

other groups reluctantly admit it may be involved in thermogenesis, but not in an adaptive capcity (114). These conflicting reports indicate a gap in the understanding of SLN mediated uncoupling of SERCA and its physiological relevance that, if resolved, provides an alluring explanation for cold adaptation (108, 115), and non-shivering heat generation in brown adipose tissue-deficient animals (99, 102).

1.3.2.3 – SLN regulation

The elaborate regulatory axis that targets SERCA-SLN is similar to that described above for SERCA-PLN. This is of particular importance in atrial muscle, where SLN and PLN are both present in a potential ternary, super-inhibitory complex with SERCA (116). The presence of SLN and PLN in the same tissue presents a unique challenge for both peptide and SERCA regulation. Given that there are also reports of SLN and PLN expression in diseased ventricles of patients with chronic isolated mitral regurgitation (117) and reports of SLN regulating cardiac SERCA2a (and conversely, PLN regulating SERCA1a (80)), it seems likely that the combination of PLN and SLN represents a unique signalling pathway dependent on the distinct regulatory capabilities of PLN and SLN. Despite the evident structural homology between SLN and PLN, relatively little is known about SLN regulation (perhaps the lack of disease association has failed to motivate a robust investigation). The N-terminus of SLN has a conserved threonine residue (Thr^5) that appears to be a target for phosphorylation. Two kinases have been reported to target SLN, CAMKII (110) and serine/threonine kinase 16 (118). It is also clear that Thr^5 is essential for normal SLN function and that phospho-mimetic mutations disrupt function (110), though the physiological mechanisms and consequences remain unknown. The cytoplasmic domain of SLN is the likely site for binding scaffolding proteins (AKAPs) and regulatory complex formation (kinases, phosphatases, oligomers, *et cetera*). However, this concept is obfuscated by the fact that the cytoplasmic domain of SLN is the most variable region and unique in humans. This sequence is MGINTRE in humans and MERSTQE in mice and many other mammals, and this contrasts sharply with the highly conserved cytoplasmic domain of SLN. Perhaps this variability reflects the relative role of SLN in different organisms and the requirement for thermogenesis, as well as skeletal and atrial muscle calcium homeostasis and contractility.

1.3.2.4 – SLN oligomers

SLN is considered a functional homologue of PLN, it occupies the same inhibitory groove as PLN (45–47) and it alters SERCA's apparent calcium affinity in the same manner as PLN. As a functional homologue of PLN, it would not be surprising if SLN could also form higher-order oligomers. Previous work indicates that much of the stability of the PLN pentamer stems from an Ile-Leu zipper motif (119), wherein successive Ile and Leu residues lie on the same 'face' of the PLN TM domain and interact with neighbouring PLN molecules to form a stable pentamer. The Ile-Lue residues inSLN's TM domain are not completely conserved but they align on the same TM domain face as PLN. Helical-wheel diagrams of SLN indicate that SLN may also form a pentamer, albeit perhaps less stable than PLN (**Figure 1.11**). Additionally, SLN dimers have been observed in MD simulations of mutated SLN (120), indicating that the molecular interactions in SLN multimers can be energetically favourable, but low-affinity.
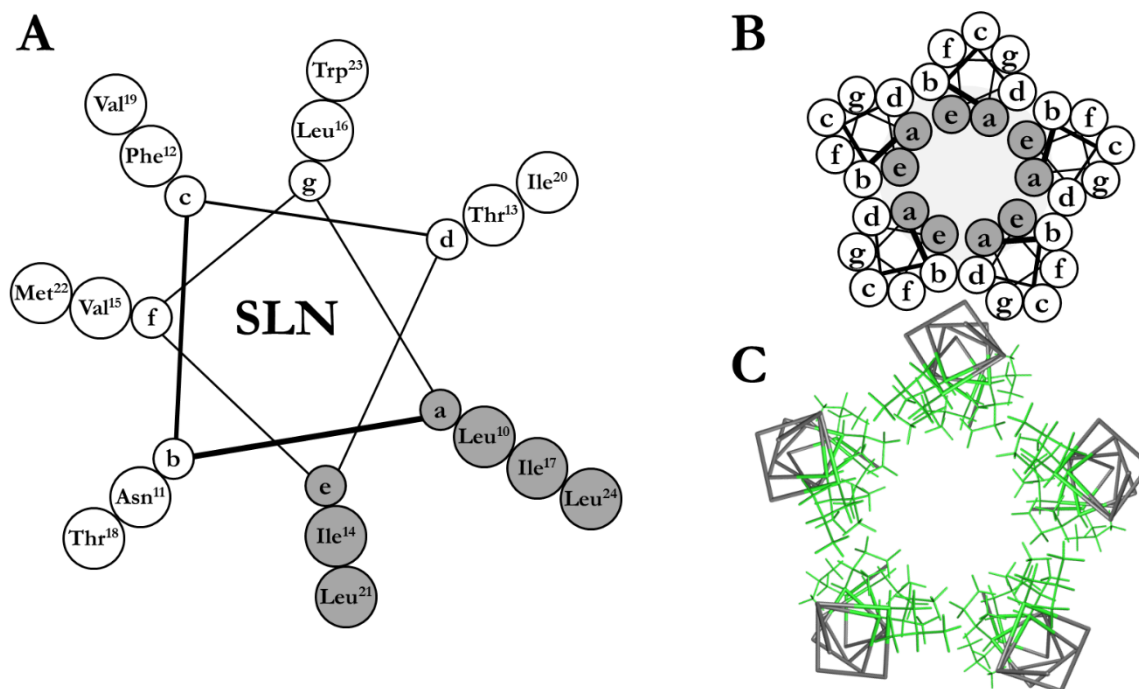
Figure 1.11: **An SLN Ile/Leu Zipper motif.** (A) Helical wheel schematic of SLN TM residues Leu[10] – Leu[24], highlighted residues indicate successive Ile/Leu residues on the same face of the helix (focusing on residues 10-24). (B) A representative schematic of multiple helical wheel SLN schematics indicating the Ile/Leu zipper interactions between SLN monomers. (C) A pseudo-atomic model of SLN TM residues Leu[10] – Leu[24] from the NMR structure of SLN (PDB: 1JDM) showing the interaction of Leu/Ile sidechains in a potential SLN pentamer.

Thus far, there is little direct experimental evidence of SLN forming higher-order oligomers in atrial and skeletal muscle to the same degree as PLN. The PLN pentamer is readily observable by SDS-PAGE; however, there is evidence showing that SLN can form dimers by SDS-PAGE. In addition, crosslinking and FRET spectroscopy have indirectly provided evidence of SLN oligomers (121, 122). Considering that SLN works as a homologue of PLN, it would be not surprising if SLN forms a pentamer that interacts with SERCA in a similar manner as PLN, but perhaps with lower stability of the pentamer and lower affinity for SERCA. As described above, previous work hints towards the existence of an SLN pentamer as a functional unit, not unlike PLN. This thesis hopes to prove that SLN oligomers are both present and naturally associate with SERCA throughout the transport cycle and have a measurable effect on SERCA regulation independent of the canonical inhibitory association.

1.4 – New regulatory peptides

The convergence of techniques such as bioinformatics, transcriptomics, and proteomics has recently led to the identification of hundreds of putative coding smORFs in vertebrate long noncoding RNAs. Since these smORFs encode theoretical peptides of less than ~100 amino acids, they have been described as micropeptides within the microproteome. However, these peptides have been overlooked because of the large number of potential smORFs and the difficulty in validating their expression and physiological roles.

Careful bioinformatic analysis of long noncoding RNAs has yielded the discovery of several new regulatory peptides. This discovery included the identification of two new muscle-specific peptides myoregulin (MLN) and DWORF (123, 124), and two non-muscle specific peptides endoregulin (ELN) and another-regulin (ALN). There is an overlap in the tissue-specific expression of SERCA isoforms and these newly identified regulators (125), which hints at their regulatory targets and properties. The SERCA1a isoform and MLN appear to be co-expressed in skeletal muscles and absent in most other tissues. Similarly, the ubiquitous expression pattern of the SERCA2b isoform is mirrored by ALN expression, and ELN mirrors the endothelial and epithelial expression pattern of SERCA3 isoforms. By comparison, the expression patterns of SERCA2a, PLN, and SLN are much more restricted to cardiac muscle (PLN in ventricular and atrial muscle; SLN in atrial muscle). This overlap in expression is not surprising as it is not unreasonable to assume that the complexity of calcium homeostasis in muscle cells is also reflected in all other cell types. As stated earlier, calcium

homeostasis is of the utmost importance and stands to require careful attention to avoid potentially fatal fluxes in calcium concentrations. Multiple SERCA isoforms in multiple cells and tissue types play a role in a vast array of signalling pathways and physiological processes. It stands to reason that tissue specific modulators of SERCA activity could fulfill the unique calcium regulatory needs found in other cell types that the SERCA2b isoform cannot accommodate.

Preliminary research has determined that these novel regulators share secondary structural characteristics with PLN and SLN and likely occupy the same inhibitory groove formed by M2, M6, and M9 of SERCA. This is not an unreasonable assumption, as SERCA has been found to interact with a wide range of hydrophobic peptides in its inhibitory cleft (100, 126–128). Functional homology of the newly discovered regulatory peptides with PLN and SLN begets speculation that these peptides could also share PLN and SLN's propensity to form oligomers. The proposal of a universal oligomeric association of regulatory peptides with SERCA is tantalizing as it brings to light an exciting new regulatory avenue for SERCA-mediated calcium homeostasis. How these new peptides fit into the extensive microproteome involved in calcium homeostasis remains an active area of research with a very bright future.

1.5 – The big picture

Our current understanding of SERCA, PLN, and SLN structure and function has evolved over the last 50 years as an immensely complicated regulatory network that controls SERCA-dependent calcium homeostasis. Considering that there are multiple SERCA isoforms in most cell types, and now multiple SERCA regulatory subunits in some tissues, there must be an elaborate regulatory network and spatio-temporal control mechanism for fine-tuning calcium handling. A gap remains in the understanding of PLN and SLN oligomers association with SERCA. This thesis aims to fill this gap by determining the function of PLN and SLN oligomers as a regulatory unit of SERCA. The understanding of this arm of the calcium regulatory network is of critical importance because the dysfunction of calcium homeostasis is a significant feature of human heart failure.

1.6 – Thesis outline

1.6.1 – Chapter 2: The phospholamban pentamer alters function of the sarcoplasmic reticulum calcium pump

In Chapter 2, we intended to challenge the current paradigm of PLN pentamer function. In this study, we demonstrate that PLN pentamers naturally associate with SERCA, which offers an

explanation for why they are required for the regulation of SERCA's calcium transport properties The evidence supporting this hypothesis was attained through a comparative analysis of different classes of two-dimensional co-crystals of SERCA in the presence and absence of PLN. MD simulations of PLN oligomers associated with SERCA and functional analysis of differing PLN to SERCA molar ratios further verified our assertion that the PLN pentamer is a functional regulatory subunit that acts to stimulate the V_{max} of SERCA.

1.6.2 – Chapter 3: Interaction of a sarcolipin pentamer and monomer with the sarcoplasmic reticulum calcium pump, SERCA

In chapter 3, we investigate the existence of an SLN pentamer and its function as a SERCA regulatory unit. Analysis of two-dimensional crystals of SLN and SERCA revealed that SLN oligomers interact with SERCA in a similar way to that identified in PLN previously, but have a unique arrangement and an additional caveat of the presence of an interacting monomer. These observations suggest that not only does SLN form regulatory oligomers that naturally associate with SERCA, but they remain associated with SERCA even when an inhibitory monomer is present in complex with SERCA. This research was further bolstered by MD simulations and functional analysis of differing SLN to SERCA molar ratios. This work verified our assertions that SLN forms a pentamer and that it functionally regulates SERCA's by depression V_{max} at elevated calcium concentrations.

1.6.3 – Chapter 4: Conformational diversity and memory in the interaction of sarcolipin with the sarcoplasmic reticulum calcium pump SERCA.

In chapter 4, we demonstrate that SLN continuously associates with SERCA throughout its catalytic cycle (E1-E2 transition). ATPase activity of proteoliposomes co-reconstituted with SERCA was measured under different starting conditions in the presence or absence of SLN. The starting conditions poise SERCA in different conformational states from which the catalytic cycle and SLN interaction can be initiated. The presence of SLN in co-reconstituted proteoliposomes appears to regulate SERCA throughout its catalytic cycle, suggesting that SLN does not dissociate entirely from SERCA as SERCA undergoes E2-E1 conformational transitions. SLN has differential inhibitory effects dependent on the starting conformation of SERCA, and this "conformational memory" persists during calcium transport and multiple turnover events, suggesting that there are multiple modes of interaction between SERCA and SLN. This work demonstrates that SLN remains

associated with SERCA and the interaction depends on the conformational state of SERCA, consistent with evidence that both the SLN monomer and pentamer act as regulatory units of SERCA.

1.6.4 – Chapter 5: Cryo-EM of two-dimensional crystals of SERCA and PLN

In chapter 5, we initiate structural studies of a unique variant of PLN. A human mutation in PLN (Pro[21]-to-Thr) renders PLN entirely alpha-helical. We combine this human mutation with a 'super-inhibitory' mutation (Lys[27]-to-Ala) creating a double mutant Pro[21]-to-Thr & Lys[27]-to-Ala.

1.6.5 – Chapter 6: Conclusions

In chapter 6, we state the major conclusions of this thesis and explore future directions for the field of SERCA-regulin interactions.

1.7 – References

1. Goodsell, D. S., Autin, L., and Olson, A. J. (2019) Illustrate: Software for Biomolecular Illustration. *Structure*. 10.1016/j.str.2019.08.011

2. Izawa, M. R. M., Nesbitt, H. W., MacRae, N. D., and Hoffman, E. L. (2010) Composition and evolution of the early oceans: Evidence from the Tagish Lake meteorite. *Earth Planet. Sci. Lett.* **298**, 443–449

3. Kazmierczak, J., and Kempe, S. (2004) Calcium build-up in the Precambrian Sea: A major promoter in the evolution of eukaryotic life, pp. 329–345

4. Plattner, H., and Verkhratsky, A. (2013) Ca2+ signalling early in evolution – all but primitive. *J. Cell Sci.* **126**, 2141 LP – 2150

5. Berkelman, T., Garret-Engele, P., and Hoffman, N. E. (1994) The pacL gene of Synechococcus sp. strain PCC 7942 encodes a Ca2+- transporting ATPase. *J. Bacteriol.* **176**, 4430–4436

6. Case, R. M., Eisner, D., Gurney, A., Jones, O., Muallem, S., and Verkhratsky, A. (2007) Evolution of calcium homeostasis: From birth of the first cell to an omnipresent signalling system. *Cell Calcium*. **42**, 345–350

7. Shemarova, I. V., and Nesterov, V. P. (2005) Evolution of mechanisms of Ca2+-signaling: Role of calcium ions in signal transduction in prokaryotes. *J. Evol. Biochem. Physiol.* **41**, 12–19

8. López-García, P., and Moreira, D. (2019) Eukaryogenesis, a syntrophy affair. *Nat. Microbiol.* **4**, 1068–1070

9. Plattner, H., and Verkhratsky, A. (2015) Evolution of calcium signalling. *Cell Calcium*. **57**, 121–

122

10. Verkhratsky, A., and Parpura, V. (2014) Calcium signalling and calcium channels: Evolution and general principles. *Eur. J. Pharmacol.* **739**, 1–3

11. Cai, X., Wang, X., Patel, S., and Clapham, D. E. (2015) Insights into the early evolution of animal calcium signaling machinery: A unicellular point of view. *Cell Calcium.* **57**, 166–173

12. Blackstone, N. W. (2015) The impact of mitochondrial endosymbiosis on the evolution of calcium signaling. *Cell Calcium.* **57**, 133–139

13. Snavely, M. D., Florer, J. B., Miller, C. G., and Maguire, M. E. (1989) Magnesium transport in Salmonella typhimurium: Expression of cloned genes for three distinct Mg2+ transport systems. *J. Bacteriol.* **171**, 4752–4760

14. Argüello, J. M., González-Guerrero, M., and Raimunda, D. (2011) Bacterial transition metal P 1B-ATPases: Transport mechanism and roles in virulence. *Biochemistry.* **50**, 9940–9949

15. Timcenko, M., Lyons, J. A., Januliene, D., Ulstrup, J. J., Dieudonné, T., Montigny, C., Ash, M.-R., Karlsen, J. L., Boesen, T., Kühlbrandt, W., Lenoir, G., Moeller, A., and Nissen, P. (2019) Structure and autoregulation of a P4-ATPase lipid flippase. *Nature.* 10.1038/s41586-019-1344-7

16. Skou, J. C. (1957) The influence of some cations on an adenosine triphosphatase from peripheral nerves. *Biochim. Biophys. Acta.* **23**, 394–401

17. Berridge, M. J., Bootman, M. D., and Roderick, H. L. (2003) Calcium signalling: dynamics, homeostasis and remodelling. *Nat. Rev. Mol. Cell Biol.* **4**, 517–529

18. Carafoli, E., and Krebs, J. (2016) Why Calcium? How Calcium Became the Best Communicator. *J. Biol. Chem. .* **291**, 20849–20857

19. Lieber, R. L., Roberts, T. J., Blemker, S. S., Lee, S. S. M., and Herzog, W. (2017) Skeletal muscle mechanics, energetics and plasticity. *J. Neuroeng. Rehabil.* **14**, 1–16

20. Doroudgar, S., and Glembotski, C. C. (2013) New concepts of endoplasmic reticulum function in the heart: Programmed to conserve. *J. Mol. Cell. Cardiol.* **55**, 85–91

21. Bers, D. M. (2008) Calcium Cycling and Signaling in Cardiac Myocytes. *Annu. Rev. Physiol.* **70**, 23–49

22. Møller, J. V., Olesen, C., Winther, A.-M. L., and Nissen, P. (2010) The sarcoplasmic Ca2+-ATPase: design of a perfect chemi-osmotic pump. *Q. Rev. Biophys.* **43**, 501–566

23. Brini, M., Calì, T., Ottolini, D., and Carafoli, E. (2012) Calcium Pumps: Why So Many? *Compr. Physiol.* doi:10.1002/cphy.c110034

24. Wuytack, F., Raeymaekers, L., and Missiaen, L. (2002) Molecular physiology of the SERCA and SPCA pumps. *Cell Calcium*. **32**, 279–305

25. Dally, S., Corvazier, E., Bredoux, R., Bobe, R., and Enouf, J. (2010) Multiple and diverse coexpression, location, and regulation of additional SERCA2 and SERCA3 isoforms in nonfailing and failing human heart. *J. Mol. Cell. Cardiol.* **48**, 633–644

26. Kósa, M., Brinyiczki, K., van Damme, P., Goemans, N., Hancsák, K., Mendler, L., and Zádor, E. (2015) The neonatal sarcoplasmic reticulum Ca2+-ATPase gives a clue to development and pathology in human muscles. *J. Muscle Res. Cell Motil.* **36**, 195–203

27. Toustrup-Jensen, M. S., Holm, R., Einholm, A. P., Schack, V. R., Morth, J. P., Nissen, P., Andersen, J. P., and Vilsen, B. (2009) The C Terminus of Na+,K+-ATPase Controls Na+ Affinity on Both Sides of the Membrane through Arg935. *J. Biol. Chem. .* **284**, 18715–18725

28. Vangheluwe, P., Raeymaekers, L., Dode, L., and Wuytack, F. (2005) Modulating sarco(endo)plasmic reticulum Ca2+ ATPase 2 (SERCA2) activity: Cell biological implications. *Cell Calcium*. **38**, 291–302

29. Gorski, P. a., Trieber, C. a., Larivière, E., Schuermans, M., Wuytack, F., Young, H. S., and Vangheluwe, P. (2012) Transmembrane helix 11 is a genuine regulator of the endoplasmic reticulum Ca2+ pump and acts as a functional parallel of β-subunit on α-Na+,K+-ATPase. *J. Biol. Chem.* **287**, 19876–19885

30. Vandecaetsbeek, I., Trekels, M., De Maeyer, M., Ceulemans, H., Lescrinier, E., Raeymaekers, L., Wuytack, F., and Vangheluwe, P. (2009) Structural basis for the high Ca2+ affinity of the ubiquitous SERCA2b Ca2+ pump. *Proc. Natl. Acad. Sci. U. S. A.* **106**, 18533–18538

31. Gélébart, P., Martin, V., Enouf, J., and Papp, B. (2003) Identification of a new SERCA2 splice variant regulated during monocytic differentiation. *Biochem. Biophys. Res. Commun.* **303**, 676–684

32. Regis Bobe, E. R. C. (2013) Sarco (Endo) Plasmic Reticulum Calcium Atpases (SERCA) Isoforms in the Normal and Diseased Cardiac, Vascular and Skeletal Muscle. *J. Cardiovasc. Dis. Diagnosis*. **01**, 1–6

33. Sagara, Y., Fernandez-Belda, F., de Meis, L., and Inesi, G. (1992) Characterization of the inhibition of intracellular Ca2+ transport ATPases by thapsigargin. *J. Biol. Chem. .* **267**, 12606–12613

34. Reddy, L. G., Jones, L. R., Pace, R. C., and Stokes, D. L. (1996) Purified, Reconstituted Cardiac Ca2+-ATPase Is Regulated by Phospholamban but Not by Direct Phosphorylation with Ca2+/Calmodulin-dependent Protein Kinase. *J. Biol. Chem. .* **271**, 14964–14970

35. Lipskaia, L., Keuylian, Z., Blirando, K., Mougenot, N., Jacquet, A., Rouxel, C., Sghairi, H., Elaib, Z., Blaise, R., Adnot, S., Hajjar, R. J., Chemaly, E. R., Limon, I., and Bobe, R. (2014) Expression of sarco (endo) plasmic reticulum calcium ATPase (SERCA) system in normal mouse cardiovascular tissues, heart failure and atherosclerosis. *Biochim. Biophys. Acta - Mol. Cell Res.* **1843**, 2705–2718

36. Toyoshima, C., Nakasako, M., Nomura, H., and Ogawa, H. (2000) Crystal structure of the calcium pump of sarcoplasmic reticulum at 2.6 A resolution. *Nature.* **405**, 647–655

37. Laursen, M., Bublitz, M., Moncoq, K., Olesen, C., Møller, J. V., Young, H. S., Nissen, P., and Morth, J. P. (2009) Cyclopiazonic Acid Is Complexed to a Divalent Metal Ion When Bound to the Sarcoplasmic Reticulum Ca2+-ATPase. *J. Biol. Chem. .* **284**, 13513–13518

38. Moncoq, K., Trieber, C. A., and Young, H. S. (2007) The Molecular Basis for Cyclopiazonic Acid Inhibition of the Sarcoplasmic Reticulum Calcium Pump. *J. Biol. Chem. .* **282**, 9748–9757

39. MacLennan, D. H., Brandl, C. J., Korczak, B., and Green, N. M. (1985) Amino-acid sequence of a Ca2+ + Mg2+ -dependent ATPase from rabbit muscle sarcoplasmic reticulum, deduced from its complementary DNA sequence. *Nature.* **316**, 696–700

40. de Meis, L., and Vianna, A. L. (1979) Energy interconversion by the Ca2+-dependent ATPase of the sarcoplasmic reticulum. *Annu. Rev. Biochem.* **48**, 275–292

41. Yokokawa, M., and Takeyasu, K. (2011) Motion of the Ca2+-pump captured. *FEBS J.* **278**, 3025–3031

42. Toyoshima, C. (2008) Structural aspects of ion pumping by Ca2+-ATPase of sarcoplasmic reticulum. *Arch. Biochem. Biophys.* **476**, 3–11

43. Toyoshima, C. (2009) How Ca2+-ATPase pumps ions across the sarcoplasmic reticulum membrane. *Biochim. Biophys. Acta - Mol. Cell Res.* **1793**, 941–946

44. Sørensen, T. L.-M., Møller, J. V., and Nissen, P. (2004) Phosphoryl Transfer and Calcium Ion Occlusion in the Calcium Pump. *Science (80-.).* **304**, 1672 LP – 1675

45. Winther, A.-M. L., Bublitz, M., Karlsen, J. L., Møller, J. V, Hansen, J. B., Nissen, P., and Buch-Pedersen, M. J. (2013) The sarcolipin-bound calcium pump stabilizes calcium sites exposed to the cytoplasm. *Nature.* **495**, 265

46. Toyoshima, C., Iwasawa, S., Ogawa, H., Hirata, A., Tsueda, J., and Inesi, G. (2013) Crystal structures of the calcium pump and sarcolipin in the Mg2+-bound E1 state. *Nature.* **495**, 260

47. Akin, B. L., Hurley, T. D., Chen, Z., and Jones, L. R. (2013) The Structural Basis for Phospholamban Inhibition of the Calcium Pump in Sarcoplasmic Reticulum. *J. Biol. Chem. .*

288, 30181–30191

48.   Henderson, I. M., Starling, A. P., Wictome, M., East, J. M., and Lee, A. G. (1994) Binding of Ca2+ to the Ca2+-ATPase of sarcoplasmic reticulum: kinetic studies. *Biochem. J.* **297**, 625 LP – 636

49.   Peinelt, C., and Apell, H.-J. (2002) Kinetics of the Ca2+, H+, and Mg2+ Interaction with the Ion-Binding Sites of the SR Ca-ATPase. *Biophys. J.* **82**, 170–181

50.   Kirchberber, M. A., Tada, M., and Katz, A. M. (1975) Phospholamban: a regulatory protein of the cardiac sarcoplasmic reticulum. *Recent Adv. Stud. Cardiac Struct. Metab.* **5**, 103–115

51.   Wawrzynow, A., Theibert, J. L., Murphy, C., Jona, I., Martonosi, A., and Collins, J. H. (1992) Sarcolipin, the "proteolipid" of skeletal muscle sarcoplasmic reticulum, is a unique, amphipathic, 31-residue peptide. *Arch. Biochem. Biophys.* **298**, 620–623

52.   Odermatt, A, Becker, S., Khanna, V. K., Kurzydlowski, K., Leisner, E., Pette, D., and MacLennan, D. H. (1998) Sarcolipin regulates the activity of SERCA1, the fast-twitch skeletal muscle sarcoplasmic reticulum Ca2+-ATPase. *J. Biol. Chem.* **273**, 12360–12369

53.   Odermatt, A, Taschner, P. E., Scherer, S. W., Beatty, B., Khanna, V. K., Cornblath, D. R., Chaudhry, V., Yee, W. C., Schrank, B., Karpati, G., Breuning, M. H., Knoers, N., and MacLennan, D. H. (1997) Characterization of the gene encoding human sarcolipin (SLN), a proteolipid associated with SERCA1: absence of structural mutations in five patients with Brody disease. *Genomics.* **45**, 541–553

54.   Simmerman, H. K. B., Collins, J. H., Theibert, J. L., Wegener, a. D., and Jones, L. R. (1986) Sequence analysis of phospholamban. Identification of phosphorylation sites and two major structural domains. *J. Biol. Chem.* **261**, 13333–13341

55.   Stokes, D. L. (1997) Keeping Calcium in its Place: Ca2+ ATPase and Phospholamban. *Curr. Opin. Struct. Biol.* **7**, 550–556

56.   Glaves, J. P., Primeau, J. O., Espinoza-Fonseca, L. M., Lemieux, M. J., and Young, H. S. (2019) The Phospholamban Pentamer Alters Function of the Sarcoplasmic Reticulum Calcium Pump SERCA. *Biophys. J.* **116**, 633–647

57.   KATZ, A. M. (1998) Discovery of Phospholamban: A Personal History. *Ann. N. Y. Acad. Sci.* **853**, 9–19

58.   Tada, M., Kirchberger, M. A., Repke, D. I., and Katz, A. M. (1974) The Stimulation of Calcium Transport in Cardiac Sarcoplasmic Reticulum by Adenosine 3':5'-Monophosphate-dependent Protein Kinase. *J. Biol. Chem. .* **249**, 6174–6180

59. MacLennan, D. H., and Kranias, E. G. (2003) Phospholamban: a crucial regulator of cardiac contractility. *Nat. Rev. Mol. Cell Biol.* **4**, 566–577

60. Asahi, M., Mckenna, E., Kurzydlowski, K., Tada, M., and Maclennan, D. H. (2000) Physical Interactions between Phospholamban and Sarco (endo) plasmic Reticulum Ca 2+-ATPases Are Dissociated by Elevated Ca 2+, but Not by Phospholamban Phosphorylation, Vanadate, or Thapsigargin, and Are Enhanced by ATP *. **275**, 15034–15038

61. Tada, M., Kirchberger, M. A., and Katz, A. M. (1976) Regulation of calcium transport in cardiac sarcoplasmic reticulum by cyclic AMP-dependent protein kinase. *Recent Adv. Stud. Cardiac Struct. Metab.* **9**, 225–239

62. Tada, M., Inui, M., Yamada, M., Kadoma, M., Kuzuya, T., Abe, H., and Kakiuchi, S. (1983) Effects of phospholamban phosphorylation catalyzed by adenosine 3':5'-monophosphate- and calmodulin-dependent protein kinases on calcium transport ATPase of cardiac sarcoplasmic reticulum. *J. Mol. Cell. Cardiol.* **15**, 335–346

63. Cornea, R. L., Jones, L. R., Autry, J. M., and Thomas, D. D. (1997) Mutation and Phosphorylation Change the Oligomeric Structure of Phospholamban in Lipid Bilayers. *Biochemistry.* **36**, 2960–2967

64. Chu, G., Li, L., Sato, Y., Harrer, J. M., Kadambi, V. J., Hoit, B. D., Bers, D. M., and Kranias, E. G. (1998) Pentameric Assembly of Phospholamban Facilitates Inhibition of Cardiac Function in Vivo . *J. Biol. Chem.* . **273**, 33674–33680

65. Glaves, J. P., Trieber, C. a., Ceholski, D. K., Stokes, D. L., and Young, H. S. (2011) Phosphorylation and mutation of phospholamban alter physical interactions with the sarcoplasmic reticulum calcium pump. *J. Mol. Biol.* **405**, 707–723

66. Stokes, D. L., Pomfret, A. J., Rice, W. J., Glaves, J. P., and Young, H. S. (2006) Interactions between Ca2+-ATPase and the Pentameric Form of Phospholamban in Two-Dimensional Co-Crystals. *Biophys. J.* **90**, 4213–4223

67. Rasmussen, S. G. F., Devree, B. T., Zou, Y., Kruse, A. C., Chung, K. Y., Kobilka, T. S., Thian, F. S., Chae, P. S., Pardon, E., Calinski, D., Mathiesen, J. M., Shah, S. T. A., Lyons, J. A., Caffrey, M., Gellman, S. H., Steyaert, J., Skiniotis, G., Weis, W. I., Sunahara, R. K., and Kobilka, B. K. (2011) Crystal structure of the β 2 adrenergic receptor-Gs protein complex. *Nature.* **477**, 549–557

68. Hilger, D., Masureel, M., and Kobilka, B. K. (2018) Structure and dynamics of GPCR signaling complexes. *Nat. Struct. Mol. Biol.* **25**, 4–12

69. Kimura, Y., Kurzydlowski, K., Tada, M., and MacLennan, D. H. (1997) Phospholamban Inhibitory Function Is Activated by Depolymerization. *J. Biol. Chem.* . **272**, 15061–15064

70. Catalucci, D., Latronico, M. V. G., Ceci, M., Rusconi, F., Young, H. S., Gallo, P., Santonastasi, M., Bellacosa, A., Brown, J. H., and Condorelli, G. (2009) Akt Increases Sarcoplasmic Reticulum Ca2+ Cycling by Direct Phosphorylation of Phospholamban at Thr17. *J. Biol. Chem.* . **284**, 28180–28187

71. Bartel, S., Vetter, D., Schlegel, W.-P., Wallukat, G., Krause, E.-G., and Karczewski, P. (2000) Phosphorylation of Phospholamban at Threonine-17 in the Absence and Presence of β - Adrenergic Stimulation in Neonatal Rat Cardiomyocytes. *J. Mol. Cell. Cardiol.* **32**, 2173–2185

72. Mattiazzi, A., and Kranias, E. (2014) The role of CaMKII regulation of phospholamban activity in heart disease. *Front. Pharmacol.* . **5**, 5

73. Haghighi, K., Kolokathis, F., Pater, L., Lynch, R. A., Asahi, M., Gramolini, A. O., Fan, G.-C., Tsiapras, D., Hahn, H. S., Adamopoulos, S., Liggett, S. B., Dorn II, G. W., MacLennan, D. H., Kremastinos, D. T., and Kranias, E. G. (2003) Human phospholamban null results in lethal dilated cardiomyopathy revealing a critical difference between mouse and human. *J. Clin. Invest.* **111**, 869–876

74. Landstrom, A. P., Adekola, B. A., Bos, J. M., Ommen, S. R., and Ackerman, M. J. (2011) PLN-encoded phospholamban mutation in a large cohort of hypertrophic cardiomyopathy cases: Summary of the literature and implications for genetic testing. *Am. Heart J.* **161**, 165–171

75. Schmitt, J. P., Kamisago, M., Asahi, M., Li, G. H., Ahmad, F., Mende, U., Kranias, E. G., MacLennan, D. H., Seidman, J. G., and Seidman, C. E. (2003) Dilated cardiomyopathy and heart failure caused by a mutation in phospholamban. *Science.* **299**, 1410–1413

76. P., S. J., Ferhaan, A., Kristina, L., Lutz, H., Stefan, S., Michio, A., H., M. D., E., S. C., J.G., S., and J., L. M. (2009) Alterations of Phospholamban Function Can Exhibit Cardiotoxic Effects Independent of Excessive Sarcoplasmic Reticulum Ca2+-ATPase Inhibition. *Circulation.* **119**, 436–444

77. DeWitt, M. M., MacLeod, H. M., Soliven, B., and McNally, E. M. (2006) Phospholamban R14 Deletion Results in Late-Onset, Mild, Hereditary Dilated Cardiomyopathy. *J. Am. Coll. Cardiol.* **48**, 1396–1398

78. Haghighi, K., Kolokathis, F., Gramolini, A. O., Waggoner, J. R., Pater, L., Lynch, R. A., Fan, G.-C., Tsiapras, D., Parekh, R. R., Dorn, G. W., MacLennan, D. H., Kremastinos, D. T., and Kranias, E. G. (2006) A mutation in the human phospholamban gene, deleting arginine 14,

results in lethal, hereditary cardiomyopathy. *Proc. Natl. Acad. Sci.* **103**, 1388 LP – 1393

79. Toyofuku, T., Kurzydlowski, K., Tada, M., and MacLennan, D. H. (1994) Amino acids Glu2 to Ile18 in the cytoplasmic domain of phospholamban are essential for functional association with the Ca(2+)-ATPase of sarcoplasmic reticulum. *J. Biol. Chem. .* **269**, 3088–3094

80. Fajardo, V. a., Bombardier, E., Vigna, C., Devji, T., Bloemberg, D., Gamu, D., Gramolini, A. O., Quadrilatero, J., and Tupling, a. R. (2013) Co-Expression of SERCA isoforms, phospholamban and sarcolipin in human skeletal muscle fibers. *PLoS One.* **8**, 1–13

81. Trieber, C. A., Afara, M., and Young, H. S. (2009) Effects of Phospholamban Transmembrane Mutants on the Calcium Affinity, Maximal Activity, and Cooperativity of the Sarcoplasmic Reticulum Calcium Pump. *Biochemistry.* **48**, 9287–9296

82. Autry, J. M., and Jones, L. R. (1997) Functional Co-expression of the Canine Cardiac Ca2+Pump and Phospholamban in Spodoptera frugiperda (Sf21) Cells Reveals New Insights on ATPase Regulation . *J. Biol. Chem. .* **272**, 15872–15880

83. Simmerman, H. K. B., Kobayashi, Y. M., Autry, J. M., and Jones, L. R. (1996) A leucine zipper stabilizes the pentameric membrane domain of phospholamban and forms a coiled-coil pore structure. *J. Biol. Chem.* **271**, 5941–5946

84. Sugita, Y., Miyashita, N., Yoda, T., Ikeguchi, M., and Toyoshima, C. (2006) Structural Changes in the Cytoplasmic Domain of Phospholamban by Phosphorylation at Ser16: A Molecular Dynamics Study. *Biochemistry.* **45**, 11752–11761

85. Gustavsson, M., Verardi, R., Mullen, D. G., Mote, K. R., Traaseth, N. J., Gopinath, T., and Veglia, G. (2013) Allosteric regulation of SERCA by phosphorylation-mediated conformational shift of phospholamban. *Proc. Natl. Acad. Sci. U. S. A.* **110**, 17338–43

86. Karim, C. B., Zhang, Z., Howard, E. C., Torgersen, K. D., and Thomas, D. D. (2006) Phosphorylation-dependent conformational switch in spin-labeled phospholamban bound to SERCA. *J. Mol. Biol.* **358**, 1032–40

87. Ceholski, D. K., Trieber, C. A., Holmes, C. F. B., and Young, H. S. (2012) Lethal, Hereditary Mutants of Phospholamban Elude Phosphorylation by Protein Kinase A. *J. Biol. Chem. .* **287**, 26596–26605

88. Wittmann, T., Lohse, M. J., and Schmitt, J. P. (2015) Phospholamban pentamers attenuate PKA-dependent phosphorylation of monomers. *J. Mol. Cell. Cardiol.* **80C**, 90–97

89. Masterson, L. R., Cheng, C., Yu, T., Tonelli, M., Kornev, A., Taylor, S. S., and Veglia, G. (2010) Dynamics connect substrate recognition to catalysis in protein kinase A. *Nat. Chem. Biol.* **6**, 821

90.   Kemp, B. E., Bylund, D. B., Huang, T. S., and Krebs, E. G. (1975) Substrate specificity of the cyclic AMP-dependent protein kinase. *Proc. Natl. Acad. Sci. U. S. A.* **72**, 3448–3452

91.   MacDougall, L. K., Jones, L. R., and Cohen, P. (1991) Identification of the major protein phosphatases in mammalian cardiac muscle which dephosphorylate phospholamban. *Eur. J. Biochem.* **196**, 725–734

92.   Steenaart, N. A. E., Ganim, J. R., Di Salvo, J., and Kranias, E. G. (1992) The phospholamban phosphatase associated with cardiac sarcoplasmic reticulum is a type 1 enzyme. *Arch. Biochem. Biophys.* **293**, 17–24

93.   Blackwell, D. J., Zak, T. J., and Robia, S. L. (2016) Cardiac Calcium ATPase Dimerization Measured by Cross-Linking and Fluorescence Energy Transfer. *Biophys. J.* **111**, 1192–1202

94.   Haghighi, K., Bidwell, P., and Kranias, E. G. (2014) Phospholamban interactome in cardiac contractility and survival: A new vision of an old friend. *J. Mol. Cell. Cardiol.* **77**, 160–167

95.   Kovacs, R. J., Nelson, M. T., Simmerman, H. K., and Jones, L. R. (1988) Phospholamban forms Ca2+-selective channels in lipid bilayers. *J. Biol. Chem.* . **263**, 18364–18368

96.   Smeazzetto, S., Schröder, I., Thiel, G., and Moncelli, M. R. (2011) Phospholamban generates cation selective ion channels. *Phys. Chem. Chem. Phys.* **13**, 12935–12939

97.   Smeazzetto, S., Saponaro, A., Young, H. S., Moncelli, M. R., and Thiel, G. (2013) Structure-Function Relation of Phospholamban: Modulation of Channel Activity as a Potential Regulator of SERCA Activity. *PLoS One.* **8**, e52744

98.   Trieber, C. A., Douglas, J. L., Afara, M., and Young, H. S. (2005) The Effects of Mutation on the Regulatory Properties of Phospholamban in Co-Reconstituted Membranes†. *Biochemistry.* **44**, 3289–3297

99.   Autry, J. M., Thomas, D. D., and Espinoza-Fonseca, L. M. (2016) Sarcolipin Promotes Uncoupling of the SERCA Ca2+ Pump by Inducing a Structural Rearrangement in the Energy-Transduction Domain. *Biochemistry.* **55**, 6083–6086

100.   Gorski, P. A., Glaves, J. P., Vangheluwe, P., and Young, H. S. (2013) Sarco(endo)plasmic Reticulum Calcium ATPase (SERCA) Inhibition by Sarcolipin Is Encoded in Its Luminal Tail. *J. Biol. Chem.* . **288**, 8456–8467

101.   Winther, A.-M. L., Bublitz, M., Karlsen, J. L., Møller, J. V, Hansen, J. B., Nissen, P., and Buch-Pedersen, M. J. (2013) The sarcolipin-bound calcium pump stabilizes calcium sites exposed to the cytoplasm. *Nature.* **495**, 265–9

102.   Sahoo, S. K., Shaikh, S. A., Sopariwala, D. H., Bal, N. C., Bruhn, D. S., Kopec, W., Khandelia,

H., and Periasamy, M. (2015) The N Terminus of Sarcolipin Plays an Important Role in Uncoupling Sarco-endoplasmic Reticulum Ca2+-ATPase (SERCA) ATP Hydrolysis from Ca2+ Transport. *J. Biol. Chem.* **290**, 14057–14067

103. Sahoo, S. K., Shaikh, S. A., Sopariwala, D. H., Bal, N. C., and Periasamy, M. (2013) Sarcolipin protein interaction with sarco(endo)plasmic reticulum Ca2+ ATPase (SERCA) is distinct from phospholamban protein, and only sarcolipin can promote uncoupling of the SERCA pump. *J. Biol. Chem.* **288**, 6881–6889

104. Reddy, L. G., Cornea, R. L., Winters, D. L., McKenna, E., and Thomas, D. D. (2003) Defining the Molecular Components of Calcium Transport Regulation in a Reconstituted Membrane System. *Biochemistry.* **42**, 4585–4592

105. Hughes, E., Clayton, J. C., Kitmitto, A., Esmann, M., and Middleton, D. A. (2007) Solid-state NMR and functional measurements indicate that the conserved tyrosine residues of sarcolipin are involved directly in the inhibition of SERCA1. *J. Biol. Chem.* **282**, 26603–26613

106. Tupling, A. R., Asahi, M., and MacLennan, D. H. (2002) Sarcolipin Overexpression in Rat Slow Twitch Muscle Inhibits Sarcoplasmic Reticulum Ca2+ Uptake and Impairs Contractile Function . *J. Biol. Chem. .* **277**, 44740–44746

107. Babu, G. J., Bhupathy, P., Petrashevskaya, N. N., Wang, H., Raman, S., Wheeler, D., Jagatheesan, G., Wieczorek, D., Schwartz, A., Janssen, P. M. L., Ziolo, M. T., and Periasamy, M. (2006) Targeted Overexpression of Sarcolipin in the Mouse Heart Decreases Sarcoplasmic Reticulum Calcium Transport and Cardiac Contractility. *J. Biol. Chem. .* **281**, 3972–3979

108. Bal, N. C., Maurya, S. K., Sopariwala, D. H., Sahoo, S. K., Gupta, S. C., Shaikh, S. a, Pant, M., Rowland, L. a, Goonasekera, S. a, Molkentin, J. D., and Periasamy, M. (2012) Sarcolipin is a newly identified regulator of muscle-based thermogenesis in mammals. *Nat. Med.* **18**, 1575–1579

109. Smith, W. S., Broadbridge, R., East, J. M., and Lee, A. G. (2002) Sarcolipin uncouples hydrolysis of ATP from accumulation of Ca2+ by the Ca2+-ATPase of skeletal-muscle sarcoplasmic reticulum. *Biochem. J.* **361**, 277–286

110. Bhupathy, P., Babu, G. J., Ito, M., and Periasamy, M. (2009) Threonine-5 at the N-terminus can modulate sarcolipin function in cardiac myocytes. *J. Mol. Cell. Cardiol.* **47**, 723–729

111. Gamu, D., Bombardier, E., Smith, I. C., Fajardo, V. A., and Tupling, A. R. (2014) Sarcolipin Provides a Novel Muscle-Based Mechanism for Adaptive Thermogenesis. *Exerc. Sport Sci. Rev.* **42**, 136–142

112. Pant, M., Bal, N. C., and Periasamy, M. (2016) Sarcolipin: A Key Thermogenic and Metabolic Regulator in Skeletal Muscle. *Trends Endocrinol. Metab.* 10.1016/j.tem.2016.08.006

113. Bal, N. C., Singh, S., Reis, F. C. G., Maurya, S. K., Pani, S., Rowland, L. A., and Periasamy, M. (2017) Both brown adipose tissue and skeletal muscle thermogenesis processes are activated during mild to severe cold adaptation in mice. *J. Biol. Chem.* **292**, 16616–16625

114. Campbell, K. L., and Dicke, A. A. (2018) Sarcolipin Makes Heat, but Is It Adaptive Thermogenesis? *Front. Physiol.* **9**, 714

115. Rowland, L. A., Bal, N. C., Kozak, L. P., and Periasamy, M. (2015) Uncoupling protein 1 and sarcolipin are required to maintain optimal thermogenesis, and loss of both systems compromises survival of mice under cold stress. *J. Biol. Chem.* **290**, 12282–12289

116. MacLennan, D. H., Asahi, M., and Tupling, A. R. (2003) The regulation of SERCA-type pumps by phospholamban and sarcolipin. *Ann. N. Y. Acad. Sci.* **986**, 472–480

117. Zheng, J., Yancey, D. M., Ahmed, M. I., Wei, C. C., Powell, P. C., Shanmugam, M., Gupta, H., Lloyd, S. G., McGiffin, D. C., Schiros, C. G., Denney, T. S., Babu, G. J., and Dell'Italia, L. J. (2014) Increased sarcolipin expression and adrenergic drive in humans with preserved left ventricular ejection fraction and chronic isolated mitral regurgitation. *Circ. Hear. Fail.* **7**, 194–202

118. Gramolini, A. O., Trivieri, M. G., Oudit, G. Y., Kislinger, T., Li, W., Patel, M. M., Emili, A., Kranias, E. G., Backx, P. H., and MacLennan, D. H. (2006) Cardiac-specific overexpression of sarcolipin in phospholamban null mice impairs myocyte function that is restored by phosphorylation. *Proc. Natl. Acad. Sci.* **103**, 2446 LP – 2451

119. Cornea, R. L., Autry, J. M., Jones, L. R., and Chen, Z. (2000) MEMBRANE TRANSPORT STRUCTURE FUNCTION AND BIOGENESIS : Reexamination of the Role of the Leucine / Isoleucine Zipper Residues of Phospholamban in Inhibition of the Ca 2 + Pump of Cardiac Sarcoplasmic Reticulum Reexamination of the Role of the Leucine / Iso. *J. Biol. Chem.* **275**, 41487–41494

120. Cao, Y., Wu, X., Yang, R., Wang, X., Sun, H., and Lee, I. (2017) Self-assembling study of sarcolipin and its mutants in multiple molecular dynamic simulations. *Proteins Struct. Funct. Bioinforma.* **85**, 1065–1077

121. Hellstern, S., Pegoraro, S., Karim, C. B., Lustig, A., Thomas, D. D., Moroder, L., and Engel, J. (2001) Sarcolipin, the Shorter Homologue of Phospholamban, Forms Oligomeric Structures in Detergent Micelles and in Liposomes. *J. Biol. Chem.* **276**, 30845–30852

122.	Autry, J. M., Rubin, J. E., Pietrini, S. D., Winters, D. L., Robia, S. L., and Thomas, D. D. (2011) Oligomeric interactions of sarcolipin and the Ca-ATPase. *J. Biol. Chem.* **286**, 31697–31706

123.	Anderson, D. M., Anderson, K. M., Chang, C.-L., Makarewich, C. A., Nelson, B. R., McAnally, J. R., Kasaragod, P., Shelton, J. M., Liou, J., Bassel-Duby, R., and Olson, E. N. (2015) A Micropeptide Encoded by a Putative Long Noncoding RNA Regulates Muscle Performance. *Cell.* **160**, 595–606

124.	Nelson, B. R., Catherine A. Makarewich, Douglas M. Anderson, Benjamin R. Winders, Constantine D. Troupes, F. W., Reese, A. L., McAnally, J. R., Chen, X., Kavalali, E. T., Cannon, S. C., Houser, S. R., Bassel-Duby, R., and Olson, E. N. (2016) A peptide encoded by a transcript annotated as long noncoding RNA enhances SERCA activity in muscle. *Science (80-.).*

125.	Anderson, D. M., Makarewich, C. A., Anderson, K. M., Shelton, J. M., Bezprozvannaya, S., Bassel-Duby, R., and Olson, E. N. (2016) Widespread control of calcium signaling by a family of SERCA-inhibiting micropeptides. *Sci. Signal.* **9**, ra119 LP-ra119

126.	Afara, M. R., Trieber, C. A., Glaves, J. P., and Young, H. S. (2006) Rational Design of Peptide Inhibitors of the Sarcoplasmic Reticulum Calcium Pump. *Biochemistry.* **45**, 8617–8627

127.	Afara, M. R., Trieber, C. a., Ceholski, D. K., and Young, H. S. (2008) Peptide inhibitors use two related mechanisms to alter the apparent calcium affinity of the sarcoplasmic reticulum calcium pump. *Biochemistry.* **47**, 9522–9530

128.	Desmond, P. F., Muriel, J., Markwardt, M. L., Rizzo, M. A., and Bloch, R. J. (2015) Identification of small ankyrin 1 as a novel sarco(endo)plasmic reticulum Ca2+-ATPase 1 (SERCA1) regulatory protein in skeletal muscle. *J. Biol. Chem.* **290**, 27854–27867

";p0l;=9l00kkkkkkk c   cvtbhbv77n v"

G.A. Primeau – 2019

-musings of an infant-

Chapter 2 – The phospholamban pentamer alters function of the sarcoplasmic reticulum calcium pump SERCA

J. P. Glaves[1], J. O. Primeau[1], L. M. Espinoza-Fonseca[2], M. J. Lemieux[1], and H. S. Young[1]

Running Title: PLN Pentamers Stimulate SERCA Function

[1]Department of Biochemistry, University of Alberta, Edmonton, Alberta, Canada and [2]Center for Arrhythmia Research, Division of Cardiovascular Medicine, Department of Internal Medicine, University of Michigan, Ann Arbor, Michigan
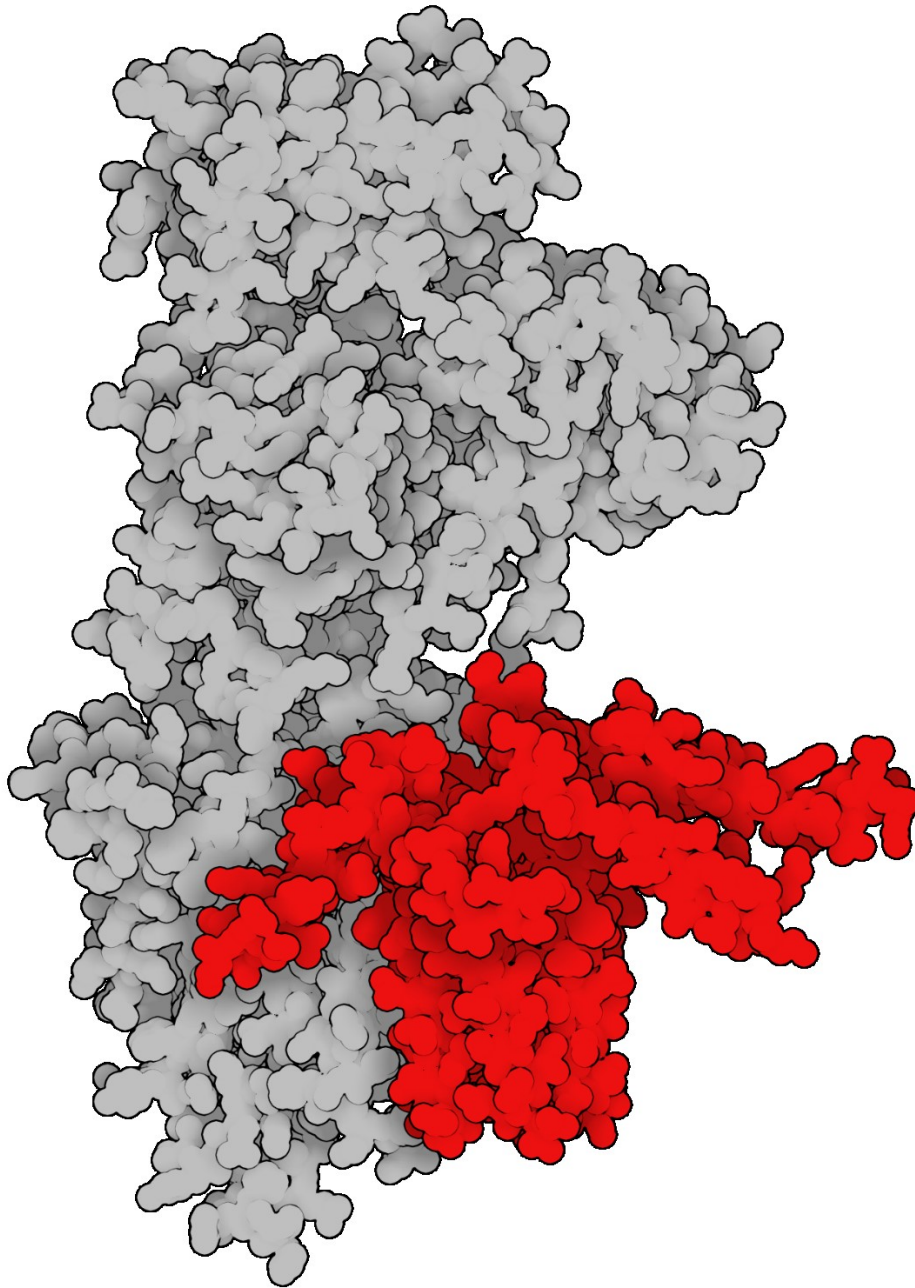
Stylized model of PLN interacting with M3 of SERCA

See Figure 2.7 and section 2.5.6

Preface

This chapter represents the culmination of the work published in Biophysical Journal on February 19, 2019 (Glaves, J. P., Primeau, J. O., Espinoza-Fonseca, L. M., Lemieux, M. J., and Young, H. S. (2019) The Phospholamban Pentamer Alters Function of the Sarcoplasmic Reticulum Calcium Pump SERCA. *Biophys. J.* **116**, 633–647**.**) J.P.G. and J.O.P. performed the research, analyzed data, and contributed to the writing and editing of the manuscript. M.J.L. contributed to the design and analysis of the data and editing of the manuscript. L.M.E.-F. performed and analyzed the protein-protein docking and MD simulations. H.S.Y. designed the research, analyzed the data, and wrote the manuscript. **This manuscript has been adapted and edited from its original state to fit the format of the thesis presented. Title page figure generated using** *Illustrate: Non-photorealistic Biomolecular Illustration* (1)**.**

2.1 – Summary

The interaction of phospholamban (PLN) with the sarco-endoplasmic reticulum Ca^{2+}-ATPase (SERCA) pump is a significant regulatory axis in cardiac muscle contractility. The prevailing model involves reversible inhibition of SERCA by monomeric PLN and storage of PLN as an inactive pentamer. However, this paradigm has been challenged by studies demonstrating that PLN remains associated with SERCA and that the PLN pentamer is required for the regulation of cardiac contractility. We have previously used two-dimensional (2D) crystallization and electron microscopy to study the interaction between SERCA and PLN. To further understand this interaction, we compared small helical crystals and large 2D crystals of SERCA in the absence and presence of PLN. In both crystal forms, SERCA molecules are organized into identical antiparallel dimer ribbons. The dimer ribbons pack together with distinct crystal contacts in the helical versus large 2D crystals, which allow PLN differential access to potential sites of interaction with SERCA. Nonetheless, we show that a PLN oligomer interacts with SERCA in a similar manner in both crystal forms. In the 2D crystals, a PLN pentamer interacts with transmembrane segments M3 of SERCA and participates in a crystal contact that bridges neighbouring SERCA dimer ribbons. In the helical crystals, an oligomeric form of PLN also interacts with M3 of SERCA, though the PLN oligomer straddles a SERCA-SERCA crystal contact. We conclude that the pentameric form of PLN interacts with M3 of SERCA and that it plays a distinct structural and functional role in SERCA regulation. The interaction of the pentamer places the cytoplasmic domains of PLN at the membrane surface proximal to the calcium entry funnel of SERCA. This interaction may cause localized perturbation of the membrane bilayer as a mechanism for increasing the turnover rate of SERCA.

2.2 – Introduction

Membrane transport by the sarco-endoplasmic reticulum Ca^{2+}-ATPase (SERCA) is central to restoring cytosolic calcium levels after intracellular calcium release. In muscle, calcium release from the sarcoplasmic reticulum (SR) leads to contraction. During the subsequent relaxation phase, SERCA transports two cytoplasmic calcium ions into the SR in exchange for two to three luminal protons and at the expense of one molecule of ATP. We currently have an excellent understanding of the SERCA transport cycle from crystallographic studies (reviewed in (2–4)). SERCA consists of three cytoplasmic domains (nucleotide-binding, phosphorylation, and actuator domains) connected to a 10-helix transmembrane domain. SERCA's cytoplasmic domains mediate the ATP binding and phosphoryl transfer, and the associated conformational changes are coupled to changes in the calcium-binding sites located in the transmembrane domain.

Physiologically, SERCA function depends on the differential expression of SERCA isoforms and splice variants as well as the differential co-expression of small regulatory transmembrane proteins. The SERCA2a isoform is predominantly expressed in cardiac muscle and is regulated by the co-expression of phospholamban (PLN), a 52 amino acid integral membrane protein that binds to and lowers the apparent calcium affinity (K_{Ca}) of SERCA. In fast-twitch skeletal muscle, SERCA1a is predominantly expressed and is regulated by the co-expression of sarcolipin (SLN), a 31- amino-acid integral membrane protein homologous to PLN. Although this regulatory pattern is representative of cardiac and skeletal muscle, respectively, SLN and PLN are co-expressed in some human skeletal muscle fibres (5). Thus, PLN is also a physiological regulator of SERCA1a. The prevailing model for PLN inhibition of SERCA involves the reversible association of a PLN monomer (6), which binds to the calcium-free state of SERCA and dissociates under conditions of elevated cytosolic calcium or PLN phosphorylation. This model originated with the observation that monomeric forms of PLN (i.e., mutants that disrupt the pentameric assembly of PLN) were better inhibitors of SERCA (7, 8). Later, cross-linking (9) and coimmunoprecipitation (10) studies suggested that relief of SERCA inhibition was accompanied by the dissociation of PLN. Monomeric and pentameric forms of PLN were said to be in dynamic equilibrium in the membrane, with the pool of monomers and pentamers influenced by the phosphorylation status of PLN (11). Finally, the PLN pentamer was described as an inactive storage form (6, 12) despite the absence of direct experimental evidence.

This paradigm for SERCA inhibition by PLN has been challenged by discrepant results as well as recent studies that show a persistent association between SERCA and PLN. Initial indications were from coimmunoprecipitation studies (10) and electron paramagnetic resonance spectroscopy (13),

which demonstrated that phosphorylated PLN did not dissociate from SERCA as expected. Since then, many studies using Förster resonance energy transfer (14–16), electron paramagnetic resonance (17, 18), and NMR (19) have reinforced the concept that PLN appears to be a constitutive regulatory subunit of SERCA. In addition, the PLN pentamer is required for normal cardiac development and function (20) despite being described as an inactive storage form. The active roles proposed for the PLN pentamer include a cation-selective channel (21, 22), modulation of PLN phosphorylation (23, 24), and direct interaction with SERCA (25, 26). Regarding this latter point, it is interesting to note that the crystal structure of the SERCA-PLN complex contains two PLN molecules in complex with a single SERCA molecule (27). Although only one PLN molecule directly interacts with SERCA, the structure reveals that an oligomeric form of PLN interacts with SERCA. Recall that PLN is proposed to exist as a dynamic equilibrium of oligomeric states ranging from pentamer to monomer (11). The crystal structures of the SERCA-PLN and SERCA-SLN complexes revealed a novel calcium-free E1-like state of SERCA (27–29). In these structures, the binding groove for PLN and SLN formed by transmembrane helices M2, M6, and M9 of SERCA is shallow enough to accommodate oligomeric forms of PLN. Thus, the interaction potential of PLN oligomers with SERCA remains an outstanding question in the field.

Toward this goal, our laboratory previously showed that PLN pentamers interacted with SERCA in two-dimensional (2D) co-crystals in a manner dependent on the functional state of PLN (25, 26). The physical interaction in these crystals occurred at an accessory site on SERCA (transmembrane segment M3), yet it bore all the hallmarks normally associated with SERCA inhibition by the PLN monomer in that crystal formation depended on the functional, oligomeric, and phosphorylation states of PLN. Although this suggested that PLN pentamers contribute to SERCA regulation in some unappreciated fashion, uncertainty remained because PLN participates in a crystal contact with SERCA in the large 2D co-crystals. To further examine this SERCA-PLN interaction, we undertook a comparison with helical crystals of the SERCA-PLN complex by electron cryo-microscopy. The site of interaction between SERCA and PLN in the large 2D crystals (i.e., transmembrane segment M3 of SERCA) is involved in a SERCA-SERCA crystal contact in the helical crystals. Because the SERCA-SERCA contact facilitates helical crystal formation, a PLN interaction at this site is not required for crystal formation. Nonetheless, we found transmembrane densities in the helical crystals that were attributable to PLN and associated with M3 of SERCA. We also demonstrated that the functional effects of PLN on SERCA depend on the stoichiometry, suggesting that PLN oligomers have a unique functional effect on SERCA. Combined, the results support

54

evidence of an association between PLN pentamers and SERCA, with structural and functional consequences that are distinct from the inhibitory interaction. A molecular model of this SERCA-PLN pentamer complex was generated using protein docking and molecular dynamics (MD) simulations.

2.3 – Results

The regulatory target of PLN in cardiac muscle is the SERCA2a isoform, which is 85% identical in primary structure to the skeletal muscle SERCA1a isoform used in this study. PLN has been shown to regulate both SERCA isoforms in a similar manner (30, 31). Perhaps more important, the physiological relevance of PLN regulation of SERCA1a has been demonstrated by the finding that PLN and SERCA1a are both present in human skeletal muscle (5).

2.3.1 – Functional differences between the PLN monomer and pentamer

The PLN-SERCA molar ratio reported for cardiac SR membranes varies from 1:1 (32) to 4:1 (33–35), suggesting that modulation of PLN content in the SR membranes may play a role in the regulation of SERCA and cardiac contractility. Yet the effect of PLN on the apparent K_{Ca} of SERCA saturates at a molar ratio of approximately one PLN monomer per SERCA (33, 36). These observations raise the question, "what are the consequences of excess PLN in cardiac SR membranes?" To investigate this, we measured the calcium-dependent ATPase activity of SERCA alone and in the presence of two molar ratios of SERCA-PLN (1:2.5 and 1:5; **Figure 2.1**). These SERCA-PLN ratios were chosen to saturate the effect of the PLN monomer (1:2.5 ratio) and reveal any effects of the PLN pentamer at a higher ratio (1:5). Whereas the effect of PLN on the K_{Ca} of SERCA remained unchanged under these conditions, there was a statistically significant increase in the maximal activity (V_{max}) of SERCA at the 1:5 molar ratio of SERCA-PLN. The V_{max} values for SERCA alone (4.10 ± 0.05 μmol/min/mg), SERCA with 2.5 mol of PLN (4.95 ± 0.08 μmol/min/mg), and SERCA with 5 mol of PLN (6.10 ± 0.20 μmol/min/mg) were all statistically significant from one another ($p < 0.01$). This result supports the notion that the membrane concentration of PLN influences SERCA activity (37–39). The dependence of V_{max}, but not K_{Ca}, on the SERCA-PLN membrane concentration, suggests that there are multiple modes of interaction between PLN and SERCA involving more than a simple one-to-one inhibitory interaction between these proteins.

	SERCA	PLN 2.5:1	PLN 5:1
K_{Ca}	0.46 ± 0.01	$0.86 \pm 0.06^*$	$0.89 \pm 0.03^*$
V_{max}	4.10 ± 0.05	$4.95 \pm 0.08^*$	$6.10 \pm 0.20^*$
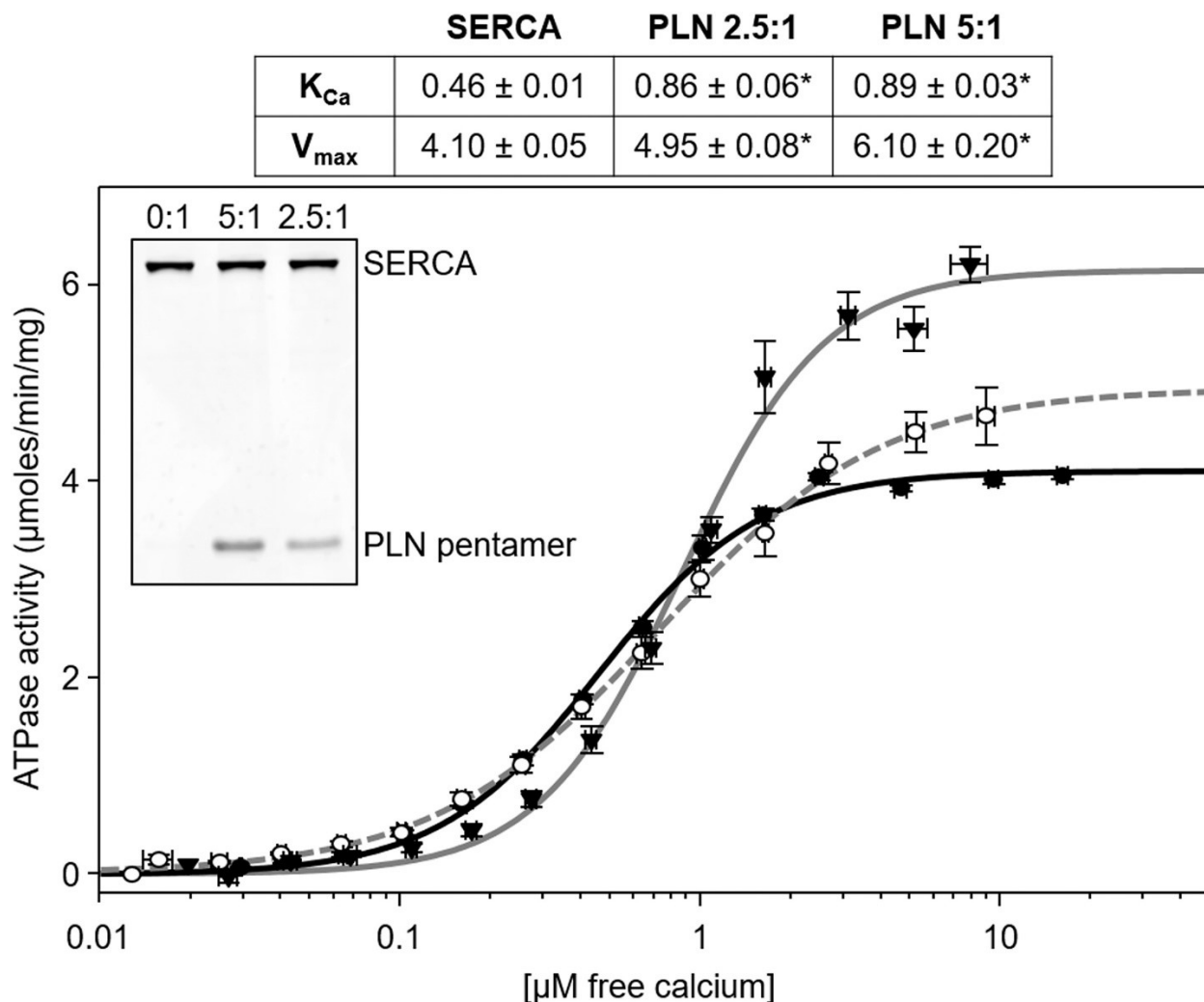
Figure 2.1: ATPase activity as a function of calcium concentration for SERCA proteoliposomes in the absence and presence of PLN. Proteoliposomes containing SERCA alone (filled circles, black line), proteoliposomes containing SERCA and a 2.5:1 molar ratio of PLN (open circles, gray dashed line), and proteoliposomes containing SERCA and a 5:1 molar ratio of PLN (filled triangles, gray line) are shown. The lines represent the curve fitting of the experimental data using the Hill equation, and the V_{max} (maximal activity) and K_{Ca} (apparent calcium affinity) are indicated in the inset table. The asterisk (*) indicates statistical significance ($p < 0.01$) compared to SERCA alone. The V_{max} values in the presence of PLN are also statistically significant from one another ($p < 0.01$). Each data point is the mean $\pm$ standard error (n≥4). The inset shows 10% sodium dodecyl sulfate polyacrylamide gel electrophoresis gel of the reconstituted proteoliposomes of SERCA in the absence and presence of PLN. The bands corresponding to SERCA and the PLN pentamer are indicated. The molar ratio of PLN to SERCA is indicated for each lane (0:1, 5:1, and 2.5:1). *ATPase activity measurements and inset gel collected by J.O.P.

2.3.2 – Crystallization

Our previous studies of large 2D crystals of the SERCA-PLN complex identified an M3 accessory site with characteristics consistent with a functional interaction (25, 26). However, these observations contradicted the central dogma that the pentamer is an inactive storage form of PLN.

Because PLN also participated in a crystal contact in the 2D crystals, the relevance of this interaction remained ambiguous. Thus, it became essential to determine if the interaction between SERCA and the PLN pentamer is a crystal contact or a natural association. To address this issue, we re-examined helical crystals of the SERCA-PLN complex (40–42) and compared them to the large 2D crystals (25, 26) (**Figure 2.2**). Helical crystals and large 2D crystals are grown from reconstituted proteoliposomes containing either SERCA alone or SERCA in the presence of PLN. The proteoliposomes readily form crystals when incubated in decavanadate and EGTA buffer (20 mmol/L imidazole (pH 7.4), 100 mmol/L KCl, 5 or 35 mmol/L $MgCl_2$, 0.5 mmol/L EGTA, and 0.25 mmol/L Na_3VO_4 converted to decavanadate), followed by several freeze-thaw cycles to promote proteoliposome fusion and the growth of large crystals. Incubation at 4°C produces optimal crystal formation within 3–5 days. Importantly, these experimental conditions are identical for the formation of helical and large 2D crystals except for the concentration of magnesium; 5 mmol/L $MgCl_2$ promoted the formation of helical crystals, and 35 mmol/L $MgCl_2$ promoted the formation of large 2D crystals. The fundamental units of both crystal forms are the well-characterized antiparallel dimer ribbons of SERCA molecules (25, 41), which are known to be a stable structural element induced by decavanadate in the absence of calcium (43, 44). However, the SERCA dimer ribbons are organized differently in the helical and large 2D crystals (**Figure 2.3**). Important for this study, the organization of the SERCA dimer ribbons in the helical crystals had a significant impact on the pentamer interaction site observed in the large 2D crystals.
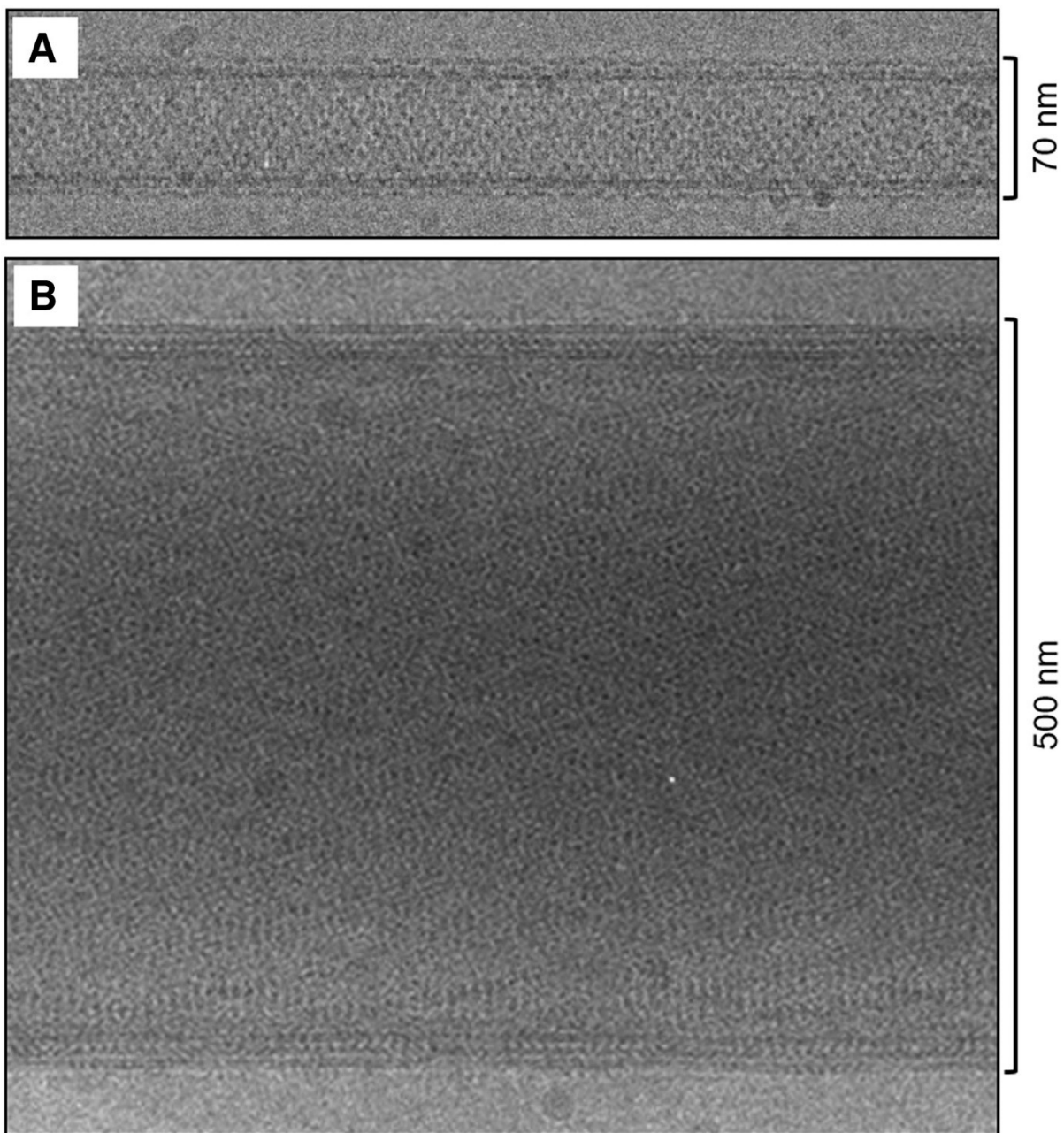
Figure 2.2: Representative examples of frozen-hydrated SERCA – PLN co-crystals. Helical crystals (A) and large 2D crystals (B) of SERCA and PLN.

2.3.3 – Helical versus large 2D crystals

In both crystal forms, the native-like membrane environment is well suited for structural studies of SERCA regulatory complexes (25, 26, 45). The helical crystals are membrane cylinders with relatively narrow diameter (~70 nm) in which the SERCA dimer ribbons are arranged with p2 symmetry (**Figure 2.3**). All SERCA molecules are oriented with their large cytoplasmic domains on the exterior of the membrane cylinder, and there is no gap between neighbouring SERCA dimer ribbons. The important point is that the inhibitory binding site for PLN (M2, M6, and M9 of SERCA) is unobstructed, whereas the accessory site (M3) is involved in a SERCA-SERCA crystal contact that brings together neighbouring dimer ribbons in the helical lattice (**Figure 2.3**). The crystal contact occurs between the M3 and M4 loops of neighbouring SERCA molecules, thus limiting access of the PLN pentamer to M3 of SERCA. The large 2D crystals form as single- or double-layered membrane tubes with a relatively large diameter (0.5–3 μm). The large 2D crystals are composed of the same SERCA dimer ribbons that make up the helical crystals, yet they are arranged differently in a $p22_12_1$ lattice (**Figure 2.3**; (25)). The SERCA molecules are oriented with their cytoplasmic domains alternately extending from both sides of the membrane, and there is a large gap between neighbouring SERCA dimer ribbons. Thus, both the inhibitory binding site for PLN (M2, M6, and M9 of SERCA) and the accessory site (M3) are open and unobstructed (**Figure 2.3**). In comparing the two crystals forms, the inhibitory site on SERCA is accessible in both helical and large 2D crystals, whereas a SERCA-SERCA crystal contact limits access to the M3 accessory site in the helical crystals.
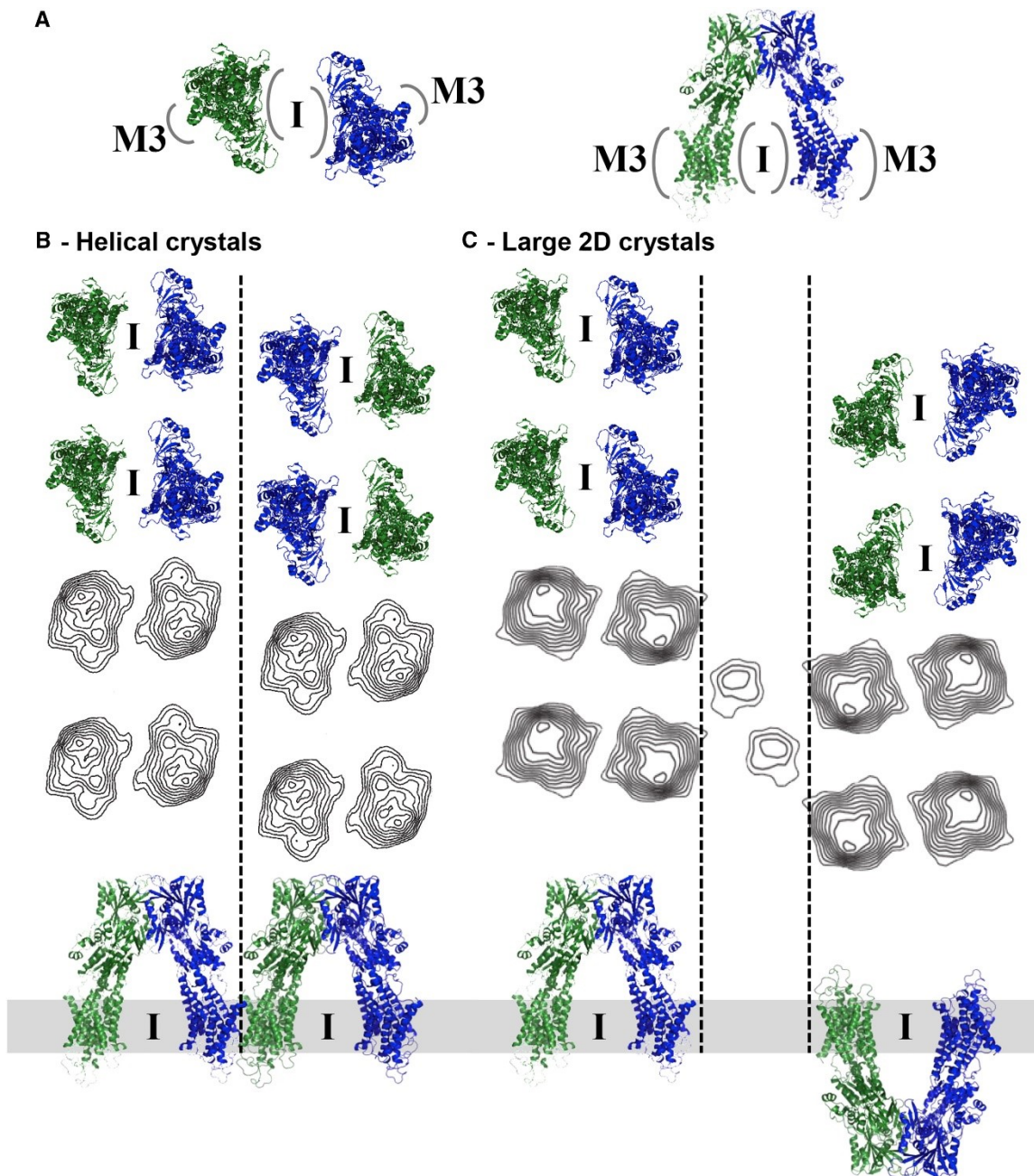
Figure 2.3: Arrangement of SERCA molecules in the helical and large 2D crystals. (A) Two orthogonal views of the antiparallel SERCA dimer that is a fundamental repeating unit of the helical and large 2D crystals are shown. Relative positions of the PLN inhibitory site (I; M2, M4, M6, and M9 of SERCA) and the M3 accessory site in the SERCA dimer are indicated. Pseudo-atomic models and projection contour maps for the helical crystals (B) and large 2D crystals (C) of SERCA and PLN are shown. The SERCA molecules are arranged in antiparallel dimer ribbons in both lattices. Top panels are the view orthogonal to the membrane bilayer (PDB: **1IWO**); bottom panels are the view normal to the membrane bilayer. The locations of the inhibitory binding sites for PLN (I; M2, M4, M6, and M9 of SERCA) are open in both crystal forms. The dashed line indicates the location of the accessory site for PLN binding (M3 of SERCA), which is limited in the helical crystals and open in the large 2D crystals. Middle panels are the projection contour maps for helical crystals (B) and large 2D crystals (C) The additional densities in the projection map of the large 2D crystals correspond to PLN pentamers (between the dashed lines; the density for two pentamers is shown).

2.3.4 – Helical crystals

In this study, we reanalyzed the helical crystals of SERCA and PLN (45) to identify densities associated with the transmembrane domain of PLN. Recall that our previous studies of the regulatory SERCA-PLN complex using helical crystals at 10 Å resolution provided a well-defined three-dimensional structure for SERCA and weak, discontinuous densities attributable to the cytoplasmic domain of PLN (45). To observe these PLN densities, it was necessary to calculate difference maps between helical reconstructions of SERCA in the absence and presence of PLN. Nonetheless, a model was proposed in which the cytoplasmic domain of PLN interacted with two SERCA molecules, though no difference densities were observed for the transmembrane helix of PLN (45).

To improve upon our previous analyses, we hypothesized that a higher-resolution control would facilitate comparison with our SERCA-PLN data sets and lead to the identification of transmembrane densities. A 6 Å resolution structure of SERCA by electron cryo-microscopy was reported, which improved upon our previous control data set by increasing the number of helical crystals included in the analysis (**Table 2.1**; (41)). The quality of the resultant density map was sufficient for fitting of SERCA atomic coordinates, which required rigid-body docking of SERCA domains into corresponding regions of the map. This higher-resolution control data set (SERCA in the absence of PLN) was necessary for the visualization of PLN densities. Second, to identify transmembrane densities, we focused on the highest resolution data set for SERCA in the presence of PLN (25). This higher-resolution data set of SERCA-PLN helical crystals was satisfied by 1) the super-inhibitory pentameric form of PLN (Asn^{27}-to-Ala mutant; canine PLN sequence), 2) a 1:3.5 molar ratio of SERCA to PLN, and 3) the absence of thapsigargin, which has traditionally been used to promote helical crystals.

	SERCA[a]	SERCA-PLN[b]
Number of crystals	58	32
Helical symmetries	5	2
Reference symmetry	-22,6	-27,9
Twofold phase statistics (Å)[c]		
40	1.1°	0.7°
30	1.7°	1.7°
20	4.0°	3.8°
14	15.2°	12.5°
10	27.5°	23.8°
8	37.2°	38.8°

[a]Previously described in (34).
[b]Previously described in (33).
[c]Amplitude-weighted phase resiudals for twofold symmetry, including 100% of the off-equatorial data for the indicated resolution ranges. Random phases produce a phase residual of 45°.

Table 2.1: **Crystallographic data for frozen-hydrated helical crystals of SERCA in the absence and presence of PLN is summarized**

To determine structural differences in the presence of PLN, we focused on helical crystals of the super-inhibitory pentameric form of PLN (Asn[27]-to-Ala mutant). The crystallographic data for the control and Asn[27]-to-Ala data sets have similar twofold phase statistics as a function of resolution to 8 Å (**Table 2.1**). The helical reconstructions for SERCA in the absence and presence of PLN at 8 Å resolution were subjected to two rounds of density scaling and real space alignment, followed by density subtraction to produce a difference map (**Figures 2.4 and 2.5**). This comparison finally revealed densities attributable to the transmembrane domain of PLN, which could be interpreted in terms of a pseudoatomic model for SERCA in the helical crystals (41). A set of densities was found at the M3 accessory site, along a twofold axis that relates a pair of SERCA molecules from neighbouring dimer ribbons. The twofold axis corresponds to a crystal contact between SERCA molecules involving M3 and M4 loop in which four PLN densities traverse the membrane and straddle a pair of M3 segments (**Figure 2.4**). Similarly, a series of densities were observed at the surface of the membrane, directly above the transmembrane densities (**Figure 2.5**). Although the densities were

consistent with a PLN tetramer, the observed oligomeric state is likely influenced by the twofold axis formed by the SERCA-SERCA crystal contact. An additional weak density was observed adjacent to the PLN tetramer, suggesting partial occupancy of a fifth PLN molecule (i.e., a PLN pentamer; **Figure 2.4**, arrow). Nonetheless, an oligomeric form of PLN was found associating with M3 of SERCA in the helical crystals, which is precisely what was observed in large 2D co-crystals of the SERCA-PLN complex (25, 26).
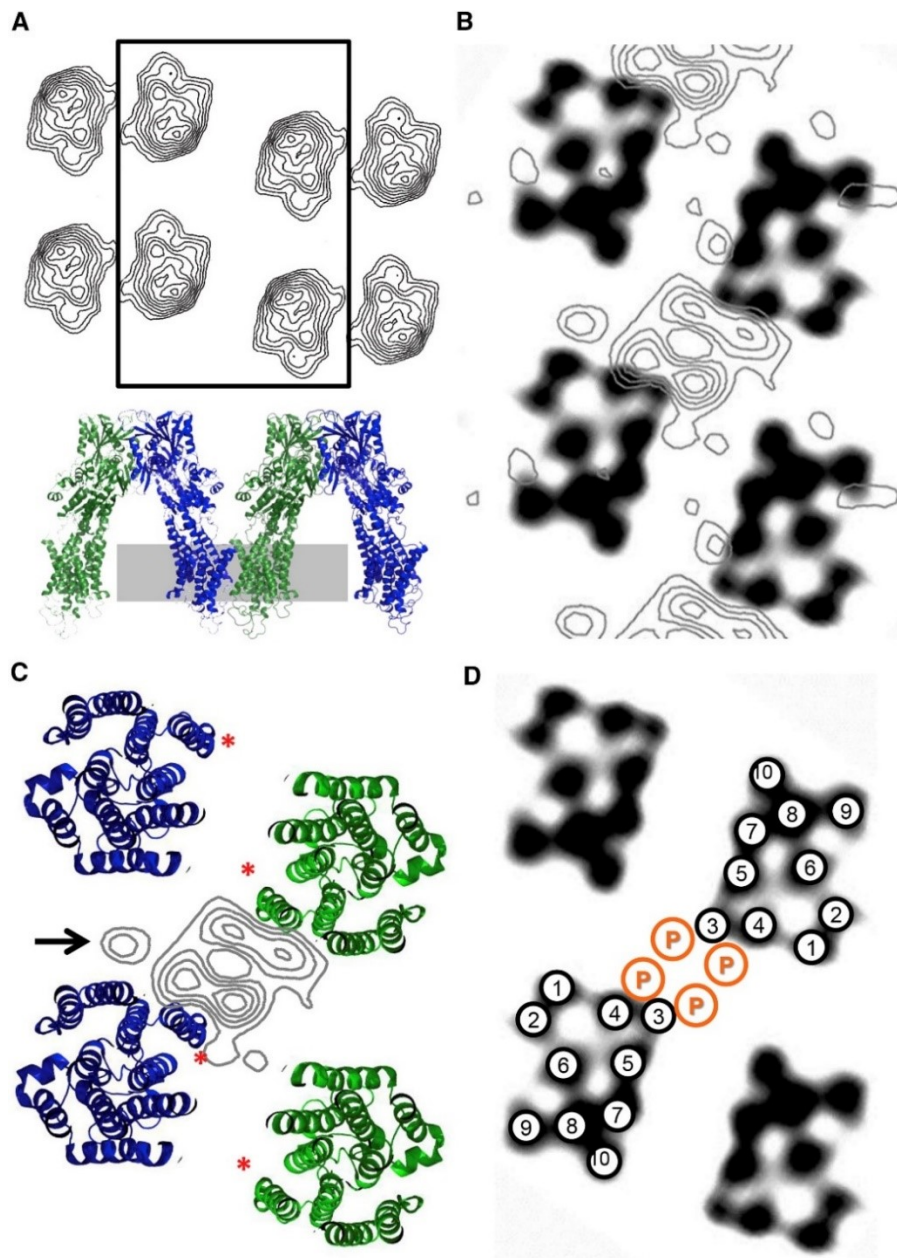
Figure 2.4: Transmembrane difference density map from helical crystals of SERCA in the absence and presence of PLN. (A) A projection map for the helical crystals with a box indicating the area of the helical lattice shown in the following panels and a pseudo-atomic model with a gray bar indicating the section of the map shown for the difference densities. (B) A difference density map at 8 Å resolution revealing transmembrane densities attributable to PLN (gray contours; 0.75 σ increment) is shown. The organization of SERCA's 10 transmembrane helices are shown as a black silhouette (four SERCA molecules are shown). (C) A pseudo-atomic model of the transmembrane domain, shown for four symmetry-related SERCA molecules in the helical crystals (viewed normal to the membrane bilayer). The difference density map (gray contours) is overlaid on the transmembrane helices of SERCA. Four discrete densities are observed for PLN; there is a weak fifth density adjacent to these densities (arrow). The transmembrane helix M3 is indicated by an asterisk in the four symmetry-related SERCA molecules. (D) The positions of the 10 transmembrane segments of SERCA and the PLN transmembrane helices (orange circles), as indicated by the difference density map shown in (B) and (C), are shown.

64
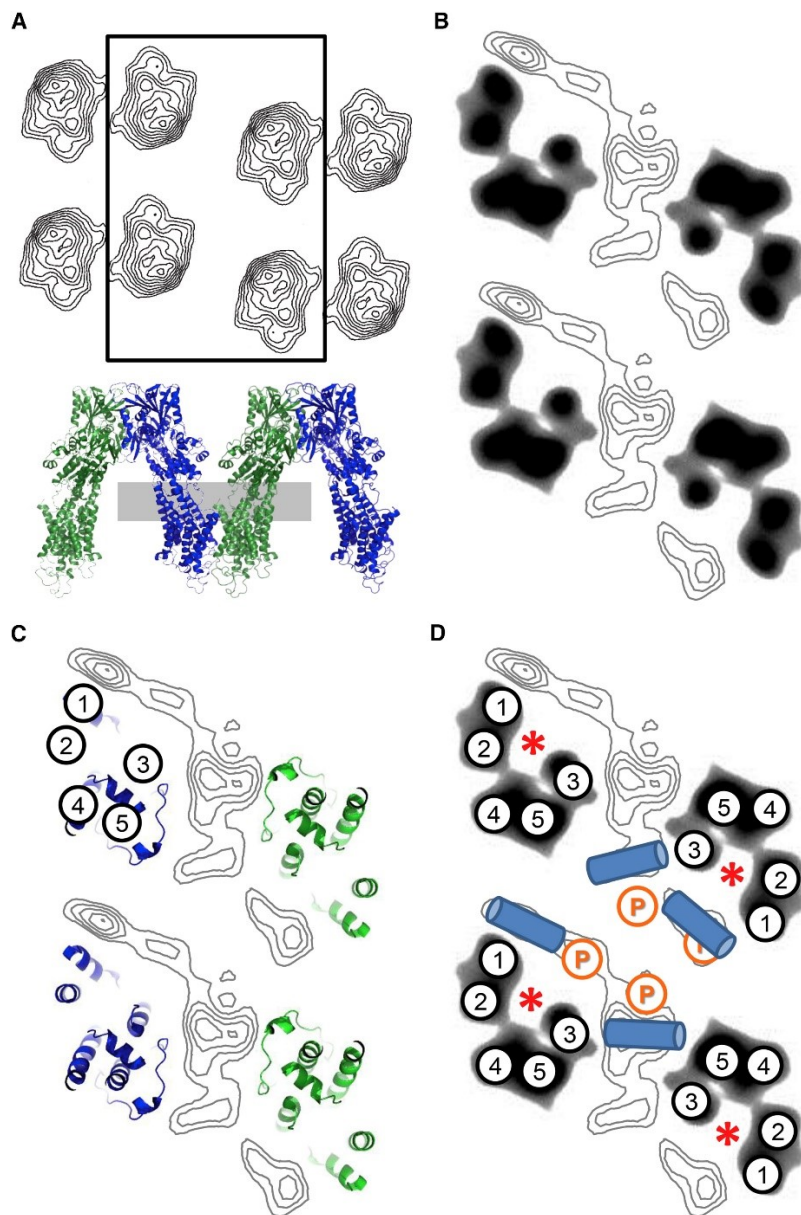
Figure 2.5: A difference density map at the surface of the membrane from helical crystals of SERCA in the absence and presence of PLN. (A) Shown again for clarity is the projection map for the helical crystals with a rectangle indicating the area of the helical lattice shown in the following panels. The pseudo-atomic model is also shown with a gray bar indicating the section of the map corresponding to the difference densities. (B) A difference density map at 8 Å resolution revealing discrete densities attributable to the cytoplasmic domain of PLN (gray contours; 0.75 σ increment) is shown. The organization of SERCA's "stalk" region is shown as a black silhouette (four SERCA molecules are shown). (C) A pseudo-atomic model for this region of SERCA, showing four molecules in the helical lattice viewed normal to the membrane bilayer, is shown. The difference density map (gray contours) is overlaid for comparison. There are two sets of four discrete densities observed for PLN within this region of the map. The transmembrane helices M1–M5 are indicated in one of the four symmetry-related SERCA molecules. (D) The positions of the helical segments of SERCA and the PLN cytoplasmic domains (only the central four are shown as blue cylinders) as indicated by the difference density map shown in (B) and (C) are shown. The positions of the PLN transmembrane densities are also indicated (orange circles). Asterisks indicate the location of the calcium access funnel of SERCA.

65

2.3.5 – Molecular model of the SERCA-PLN pentamer complex

To generate a molecular model of the SERCA-PLN pentamer complex that was representative of the state found in the 2D crystals without the constraints of crystal contacts, we performed protein-protein docking and MD simulations. After the protein-protein docking, the SERCA-PLN complex that most closely matched the arrangement in the 2D crystals was selected. This complex was embedded in a lipid bilayer (consisting of POPC, POPE, and POPA), fully hydrated to mimic physiological conditions, and subjected to 500-ns MD simulations. This latter step was done to validate the stability of the complex and ensure appropriate packing constraints at the molecular interface between SERCA and the PLN pentamer (**Figure 2.6**). We found that transmembrane segment M3 of SERCA interacts with the PLN pentamer at the interface between two PLN molecules within the pentamer **(Figure 2.7)**. The interaction occurs along the entire length of the PLN transmembrane domains and M3 of SERCA (**Figure 2.8; Figure 2.9**). The N-terminus of one PLN transmembrane domain interacts with the N-terminus of transmembrane segment M3 of SERCA (Gln^{29} and Phe^{32} of PLN molecule 1 are proximal to Lys^{262} of SERCA). The C-terminus of a second PLN transmembrane domain interacts with the C-terminus of transmembrane segment M3 of SERCA (Ile^{45} of PLN molecule 2 is proximal to Trp^{272} of SERCA). Between these regions, a lipid acyl chain bridges the interface between the two PLN molecules and M3 of SERCA. The residues involved in the lipid interaction include Leu^{39} of PLN molecule 1, Ile^{38} and Cys^{41} of PLN molecule 2, and Ser^{265} and Val^{269} of SERCA. The cytoplasmic domain of PLN molecule 1 also interacts with M3 of SERCA, with Arg^{25} forming an electrostatic pair with Glu^{258} amid a cluster of acidic residues (including Asp^{254} and Glu^{255}).
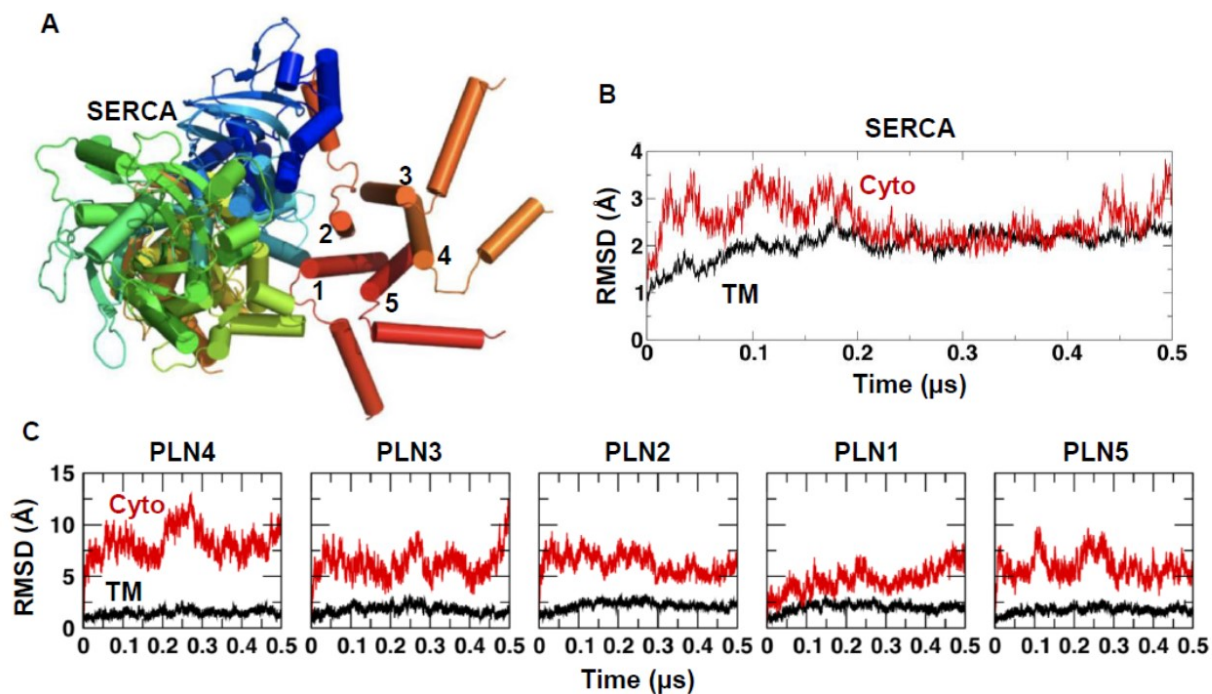
Figure 2.6: Time-dependent changes in the RMSD for the PLN pentamer and SERCA in MD simulations of the complex. (A) Structure of the complex showing the location of each PLN unit. (B) RMSD values calculated for the cytosolic (red line) and transmembrane (black line) domains of SERCA in the complex. (C) RMSD of the cytosolic and transmembrane domains of each unit of the PLN pentamer. The RMSD plots indicate that the time scale in this study is sufficiently long for convergence of the transmembrane regions of SERCA and the PLN pentamer in the modelled complex. In all cases, RMSD values were calculated using backbone alignment for transmembrane helices of the complex. Note that PLN1 and PLN2 are involved in the interaction with transmembrane segment M3 of SERCA (cyan).
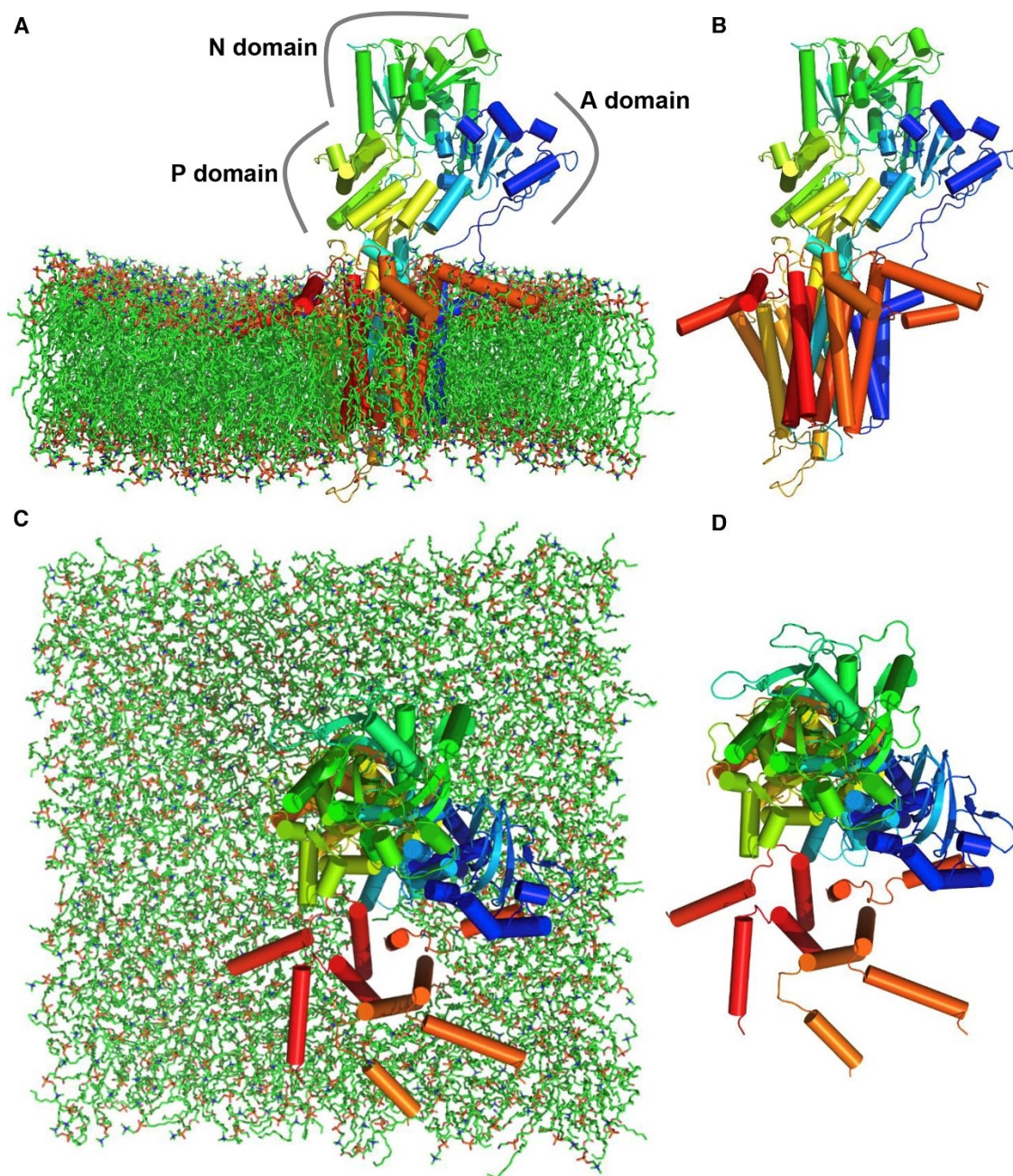
Figure 2.7: Molecular model for the interaction of SERCA with the pentameric form of PLN. Shown are the side view of the full atomistic model (A) and the SERCA-PLN complex (B) generated from protein-protein docking and MD simulations. The top views are shown in (C) and (D). SERCA and PLN are in cartoon cylinder representation, and the lipid bilayer is shown in stick representation. PLN is in orange and red, and SERCA is coloured in a spectrum from blue at the N-terminus to orange at the C-terminus. The locations of the A, N, and P domain are indicated in (A). Note that in the colour spectrum, the A domain is blue, the N domain is green, and the P domain is yellow. The transmembrane segment M3 of SERCA is visible as a cyan cylinder behind the PLN pentamer in (B).
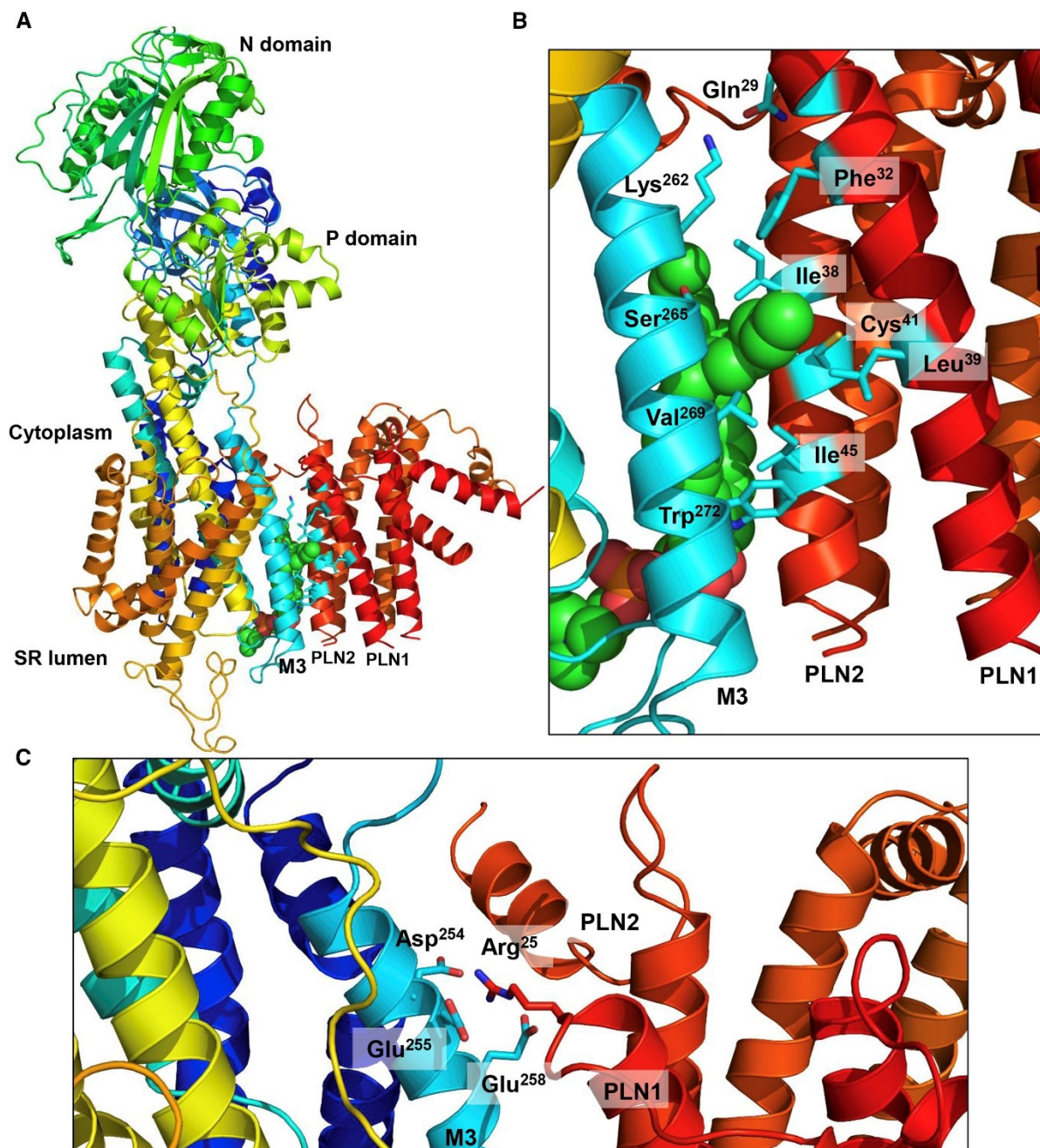
Figure 2.8: Interaction between SERCA and PLN oligomers. (A) Interaction interface between SERCA and the pentameric form of PLN. SERCA and PLN are shown in ribbon representation, with PLN in orange to red and SERCA in spectrum from blue at the N-terminus to orange at the C-terminus. (B) The interface between transmembrane segment M3 of SERCA (cyan) and two PLN molecules in the pentamer (red) is shown. The cytoplasmic end of M3 interacts with the transmembrane domain of one PLN molecule (PLN1), whereas the luminal end of M3 interacts with the transmembrane domain of a second PLN molecule (PLN2). Lys[262] of M3 interacts with Gln[29] and Phe[32] of PLN1, and Trp[262] of M3 interacts with Ile[45] of PLN2. In between these regions, a lipid acyl chain (green spheres) inserts into the SERCA-PLN interface and interacts with several residues from M3 (Ser[265] and Val[269]), PLN1 (Leu[39]), and PLN2 (Cys[41] and Ile[38]). (C) During the time course of the MD simulation, a stable salt bridge formed between Arg[25] of PLN1 and Glu[258] on M3 of SERCA. There are additional negatively charged residues in this region of M3 (Asp[254] and Glu[255]) that could interact with positively charged residues of PLN.
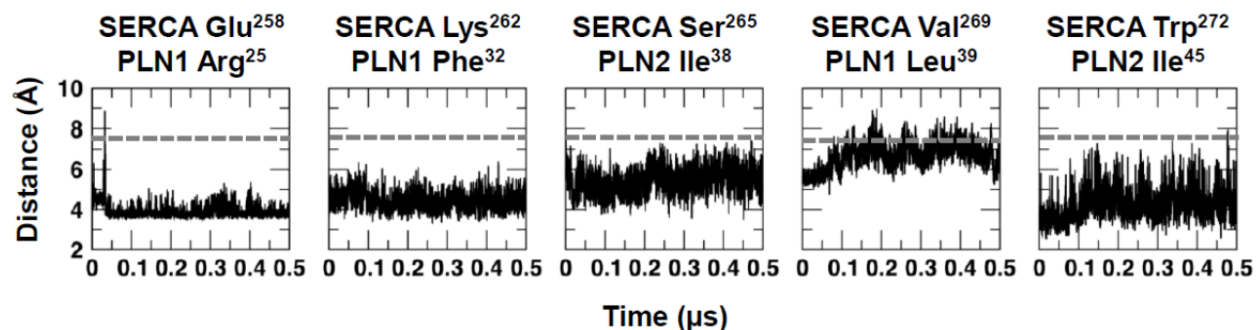
Figure 2.9: Distance evolution between residue pairs associated with binding of the PLN pentamer to SERCA. Distances between key contacts (**Figure 2.7**) involving PLN monomers PLN1 and PLN2 and SERCA were calculated by measuring the center-to-center distance of the sidechain of each residue. Intermolecular interactions are considered at center-to-center distance values <7.5 Å (dashed line).
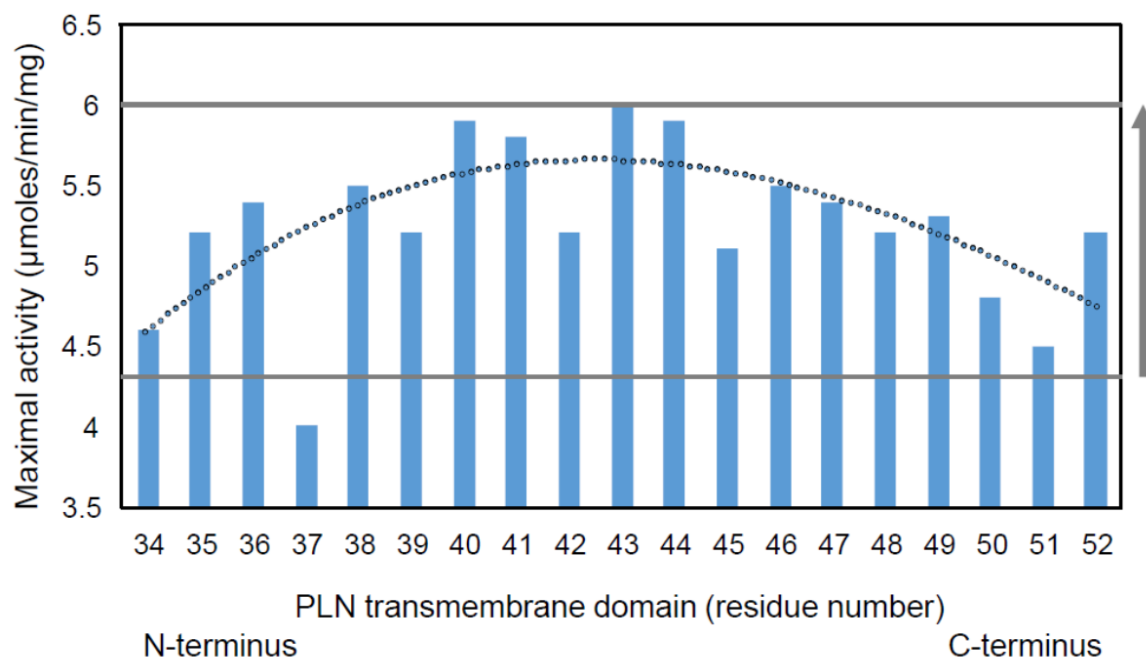
Figure 2.10: The maximal activity of SERCA is plotted for a series of alanine substitutions spanning the transmembrane domain of PLN. (data from Trieber, et at al., 2009(38)). The data is shown from residue 34 (Asn[34]-to-Ala) to the C-terminus of PLN (Leu[52]-to-Ala). The lower grey line is the maximal activity of SERCA in the absence of PLN, the upper grey line is the maximal activity of SERCA in the presence of PLN, and the grey arrow indicates the observed increase in the maximal activity of SERCA in the presence of PLN (at a molar ratio of 5 PLN to 1 SERCA). The dotted line is a trend curve indicating that the N- and C-termini of PLN's transmembrane domain have the largest impact on the ability of PLN to increase the maximal activity of SERCA. This is consistent with the structural model shown in **Figures 2.7 & 2.8**.

2.4 – Discussion

Early studies of PLN focused on the monomeric state as the species responsible for SERCA inhibition (7, 8), whereas the pentamer was assigned the default role of an inactive storage form. These conclusions were based on the observation that periodic mutations in the transmembrane domain of PLN disrupt the pentamer, enhance monomer formation, and increase SERCA inhibition. The consensus model that emerged included SERCA inhibition by monomeric PLN, a reversible association between PLN and SERCA (46), and the dissociation of PLN as the primary mechanism for relieving SERCA inhibition (i.e., after phosphorylation of PLN or elevated cytosolic calcium). Molecular models of the SERCA-PLN inhibitory complex, based on the calcium-free E2 state of SERCA, also appeared to support the monomer as the inhibitory form of PLN. In the E2 state, there is a deep groove formed by transmembrane segments M2, M4, M6, and M9 of SERCA. Modeling PLN's transmembrane helix into this groove provided a plausible mechanism for SERCA inhibition (47, 48). PLN would impede groove closure and the E2-E1 transition that accompanies calcium binding by SERCA. In these molecular models, the deep binding groove could not accommodate a PLN pentamer. However, recent crystal structures of the SERCA-PLN (27) and SERCA-SLN (28, 29) complexes have shed new light on the regulatory interaction. The structure of SERCA in these complexes is an E1-like, calcium-free state with PLN or SLN bound in a partially closed groove formed by M2, M6, and M9 of SERCA. In the structure of the SERCA-PLN complex, there are two PLN transmembrane helices associated with SERCA, and the shallow binding groove could accommodate a PLN pentamer (27). Thus, the consensus model no longer adequately describes all the available evidence regarding SERCA-PLN interactions.

2.4.1 – Functional consequences of PLN oligomers

In this study, the proteoliposomes containing SERCA and PLN provided a well-defined and well-characterized (25, 26, 37, 42, 45) starting material for functional analysis and crystal formation. Like cardiac and skeletal muscle SR membranes, the proteoliposomes are densely packed with SERCA molecules uniformly oriented with their cytoplasmic domains on the exterior side of the lipid membrane (molar ratio of ~120 lipids per SERCA (42)). The proteoliposomes also contain a molar excess of PLN (~2.5–5 molecules of PLN per SERCA) in which the majority of PLN is similarly oriented with the cytoplasmic domains on the exterior side of the membrane (38). These SERCA-PLN ratios are similar to cardiac SR membranes (33–35). PLN exists as both a monomer and a pentamer, with ~80% of PLN in the pentameric state (7, 11, 26, 38, 49, 50). Thus, the stoichiometry

71

in the proteoliposomes ranges from 0.4 to 0.8 PLN pentamers per SERCA, respectively. These proteoliposomes were used to measure SERCA ATPase activity in the absence and presence of PLN (**Figure 2.1**). Two molar ratios of PLN were chosen to demonstrate the dependence of SERCA function on increasing concentrations of the PLN pentamer. We observed an increase in the V_{max} of SERCA at the higher concentration of PLN pentamers. In contrast, the effect of PLN on the K_{Ca} of SERCA saturated at the lower concentration of PLN pentamers, as expected. Thus, the effect on the V_{max} of SERCA is dependent on the concentration of PLN pentamers and separate from the inhibitory interaction between PLN and SERCA.

2.4.2 – Structural consequences of PLN oligomers

The proteoliposomes used for functional assays were the same as those used to generate helical and large 2D crystals of SERCA in the absence and presence of PLN (25, 26, 45). These two crystal morphologies were formed under relatively similar and straightforward crystallization conditions. Besides the difference in magnesium concentration discussed above, the essential components included EGTA to remove calcium and decavanadate to induce the formation of the SERCA dimer ribbons. The removal of calcium promotes a calcium-free state of SERCA that is compatible with PLN binding. Decavanadate interacts with SERCA at two sites, one that encompasses the nucleotide-binding site and a second site that bridges the actuator domains of two SERCA molecules and thereby stabilizes the antiparallel dimer ribbons (51).

Our initial finding that PLN pentamers interacted with SERCA in large 2D crystals was a surprise (25). Nonetheless, this interaction was observed using wild-type PLN, Ile[40]-to-Ala PLN (previously thought to be a monomeric form of PLN (46)), Lys[27]-to-Ala PLN (a super-inhibitory mutant), and Arg[14]-to-Ala PLN (a partial loss of function mutant). In all cases, the oligomeric densities were observed proximal to M3 of SERCA. At the time, the simplest explanation was that the PLN pentamer makes a crystal contact with SERCA that is not relevant to the function of these two proteins. However, further studies revealed that the SERCA-PLN interaction in the crystals responded to physiological perturbations (26); namely, phosphorylation of PLN and mutations that impact PLN function also impeded crystal formation. These perturbations have been used as hallmarks for the functional interaction between SERCA and PLN. Thus, the PLN pentamer appeared to interact with SERCA in a functionally relevant, though unexpected manner. However, there were two SERCA interaction sites identified in the crystal lattice, one with M3 and one with M10 of SERCA, and the PLN pentamer clearly participates in a crystal contact. This ambiguity led us

72

to consider another crystal form capable of discriminating between a crystallographic and non-crystallographic interaction. The helical crystals of the SERCA-PLN complex satisfied this requirement. A simple change in the crystallization conditions (i.e., 5 vs. 35 mmol/L magnesium) dramatically altered the crystal packing and the relative accessibility of transmembrane segment M3 of SERCA. The helical crystals form at a lower magnesium concentration (5 mmol/L), and they transform into the large 2D crystals at a higher magnesium concentration (35 mmol/L).

With this small change in magnesium, a significant difference between the helical and large 2D crystals was the accessibility of transmembrane segment M3 of SERCA. In the helical crystals, M3 is involved in a SERCA-SERCA crystal contact, which is absent in the large 2D crystals. Thus, the helical crystals offer limited access to the M3 accessory site, whereas this site is accessible in the large 2D crystals. Despite the limited access to M3 in the helical crystals, an oligomeric form of PLN was found straddling the M3 transmembrane segments of adjacent SERCA molecules (**Figure 2.4**). Four discrete transmembrane densities were found, which correspond to the transmembrane helices of a PLN oligomer. The evidence for the densities corresponding to PLN include the following observations:

1) the size and density of each peak ($\sim$3.5 σ) are consistent with transmembrane helices;

2) besides SERCA, the only other protein present in the co-reconstituted proteoliposomes is PLN (at $\sim$1:3.5 SERCA/PLN molar ratio);

and

3) we know that PLN is present in the crystal lattice because an anti-PLN monoclonal antibody disrupts crystallization (45).

We observed four densities rather than the five expected for a PLN pentamer; however, the PLN oligomer sits across a twofold axis, and this must influence the interaction and the observed densities. There is an adjacent fifth density (**Figure 2.4**), though it is weak and may represent partial occupancy of an additional PLN molecule. We also observed four densities at the surface of the membrane (equivalent to the cytosolic side of the SR membrane), situated above the PLN transmembrane densities (**Figure 2.5**). These densities are consistent with the N-terminal α-helix of PLN and molecular models that place it at the membrane surface (19, 52). In this case, the PLN oligomer does not appear to interact with M10 of SERCA or another PLN oligomer, as was observed in the large 2D crystals. Thus, the data presented herein indicate that PLN associates with the M3 accessory site of SERCA independent of crystal contacts (**Figure 2.7**).

2.4.3 – The PLN pentamer and SERCA activity

The increased V_{max} of SERCA in the presence of PLN pentamers has been shown to be sensitive to mutation and the oligomeric state of PLN (37, 39). Here, we show that the increase in the V_{max} of SERCA depends on the abundance of PLN pentamers in the same proteoliposomes used for 2D crystallization (**Figure 2.1**). Thus, we can consider the interaction in the helical and large 2D crystals in the context of the effect on the V_{max} of SERCA. Based on the protein-protein docking and MD simulations, the SERCA-PLN interaction involves the transmembrane domains of two PLN molecules within the pentamer (**Figure 2.8**). The N-terminus of one PLN transmembrane domain interacts with the N-terminus of transmembrane segment M3 of SERCA, whereas the C-terminus of a second PLN transmembrane domain interacts with the C-terminus of M3. The main stabilizing interactions appear to be Arg[25] of PLN and Glu[258] of SERCA, Phe[32] of PLN and Lys[262] of SERCA, and Ile[45] of PLN and Trp[272] of SERCA. Between these regions, a lipid acyl chain lies at the interface between the two PLN molecules and M3, lined by a series of hydrophobic residues. The cytoplasmic domain of PLN molecule 2 (**Figure 2.8C**) lies closest to the calcium access funnel of SERCA. How does this interaction increase the turnover rate of SERCA?

There are two well-known mechanisms for increasing the V_{max} of SERCA. The first is to solubilize SERCA in the detergent $C_{12}E_8$ (53, 54), which frees SERCA from the lateral constraints of the lipid bilayer and increases its V_{max} approximately twofold. The second is to reconstitute SERCA in the presence of a mixture of lipids including PC, PE, and PA. The addition of lipids that mildly destabilize the bilayer (PE and PA) also increases SERCA's V_{max} (42, 55). With this context in mind, the observed physical interaction between the PLN pentamer and SERCA offers a plausible explanation for the stimulation of SERCA V_{max}. M3 acts as an activation site that lines the calcium entry funnel of SERCA formed by transmembrane segments M1 and M2. In particular, the transmembrane densities (**Figure 2.4**) and the membrane-surface densities flank the calcium access funnel (**Figure 2.5, asterisks**). The cytoplasmic domain of PLN is highly basic and lies along the membrane surface (19). As such, it would be expected to perturb lipid packing adjacent to the calcium access funnel and transmembrane segments M1 and M2 of SERCA. This region of SERCA is highly mobile in the SERCA transport cycle, and the membrane perturbation may facilitate the movement of transmembrane helices and thereby increase the turnover rate of SERCA.

As mentioned above, the effect of PLN on the V_{max} of SERCA is sensitive to PLN mutation, but not to PLN phosphorylation or anti-PLN antibodies (38). Merging our current findings with previous mutagenesis studies revealed that particular residues in the primary structure of PLN, when

mutated to alanine, failed to increase the V_{max} of SERCA (35, 37, 38). The residues found to have the largest loss of function included Val^4, Gln^5, Asn^{34}, Leu^{37}, Met^{50}, and Leu^{51}. The first two residues, Val^4 and Gln^5, have minimal impact on the ability of PLN to shift the K_{Ca} of SERCA, whereas the remaining residues are critical for PLN function (Asn^{34}) and pentamer formation (Leu^{37}, Met^{50}, and Leu^{51}). It is interesting that residues at the N-terminus (Val^4 and Gln^5) and C-terminus (Met^{50} and Leu^{51}) of PLN are critical for this effect, suggesting that coordinated positioning of the cytoplasmic and transmembrane domains may play a role (Asn^{34} and Leu^{37} may also contribute). Moreover, previous alanine-scanning mutagenesis of PLN (38) revealed that the N- and C-termini of the transmembrane domain were most important for influencing the V_{max} of SERCA, whereas residues in the central portion of the transmembrane domain had a lesser effect (**Figure 2.10**). At the time, we lacked an explanation for this effect, though we can now interpret these data in terms of the structural model for the interaction between SERCA and the PLN pentamer. The molecular interactions that appear to stabilize the pentamer interaction with SERCA are localized to the N- and C-termini of PLN's transmembrane domain (**Figure 2.8**), and this correlates with the functional consequences of alanine-scanning mutagenesis, which also localizes to these regions of PLN (**Figure 2.10**). It is important to note that there must be competing consequences of alanine-scanning mutagenesis of the transmembrane domain of PLN. A particular alanine substitution may directly influence the V_{max} of SERCA or indirectly influence the V_{max} of SERCA by disrupting the pentameric state of PLN. The pentamer stabilizing residues include Leu^{37}, Ile^{40}, Leu^{44}, Ile^{47}, and Leu^{51} (7, 8). Finally, residues were also found to increase the V_{max} of SERCA further when mutated to alanine, including Arg^9, Arg^{13}, and Arg^{14} in the cytoplasmic domain of PLN (35). The modulation of charged residues in the cytoplasmic domain would be expected to alter the amphipathic membrane interactions of PLN. Together with the coordinated positioning of the cytoplasmic and transmembrane domains of PLN, these observations are consistent with the hypothesis that membrane perturbation may facilitate a more rapid turnover rate for SERCA.

2.5 – Experimental procedures

2.5.1 – Materials

All reagents were of the highest purity available: octaethylene glycol monododecyl ether ($C_{12}E_8$; Barnet Products, Englewood Cliff, NJ); egg yolk phosphatidylcholine, egg yolk phosphatidylethanolamine (PE), and egg yolk phosphatidic acid (PA) (Avanti Polar Lipids, Alabaster, AL); all reagents used for crystallization and the coupled-enzyme assay including sodium

orthovanadate, NADH, ATP, phosphoenolpyruvate, lactate dehydrogenase, and pyruvate kinase (Sigma-Aldrich, Oakville, ON, Canada).

2.5.2 – Co-reconstitution of PLN and SERCA

Recombinant PLN was expressed and purified, as previously described (56). SERCA1a was purified from rabbit skeletal muscle SR (53, 57). Lyophilized PLN (100 or 50 μg) was suspended in a 100-μL mixture of chloroform-trifluoroethanol (2:1) and mixed with lipids (400 μg egg yolk phosphatidylcholine (PC), 50 μg egg yolk PE, and 50 μg egg yolk PA) from stock chloroform solutions. The peptide-lipid mixture was dried to a thin film under nitrogen gas and desiccated under vacuum overnight. The peptide-lipid mixture was hydrated in buffer (20 mmol/L imidazole (pH 7.0); 100 mmol/L KCl; 0.02% NaN_3) at 37°C for 10 min, cooled to room temperature, and detergent solubilized by the addition of $C_{12}E_8$ (0.2% final concentration) with vigorous vortexing. Detergent-solubilized SERCA1a was added (500 μg in a total volume of 500 μL), and the reconstitution was stirred gently at room temperature. Detergent was slowly removed by the addition of SM-2 Bio-Beads (Bio-Rad, Hercules, CA) over a 4-h time course (final weight ratio of 25 Bio-Beads to 1 detergent). After detergent removal, the reconstitution was centrifuged over a sucrose gradient for 1 h at 100,000 x RCF. The resultant layer of reconstituted proteoliposomes was removed, flash frozen in liquid N_2, and stored at -80°C. The final approximate molar ratios were 120 lipids to 3.5 PLN to 1 SERCA (45).

2.5.3 – Crystallization conditions

The helical and large 2D crystal data sets used in this study have been previously published (26, 41, 45). The methods used to generate these crystals are reiterated here. Co-reconstituted proteoliposomes were collected by centrifugation in crystallization buffer (20 mmol/L imidazole (pH 7.4), 100 mmol/L KCl, 5 or 35 mmol/L $MgCl_2$, 0.5 mmol/L EGTA, and 0.25 mmol/L Na_3VO_4, with or without 30 mmol/L thapsigargin). The 0.25 mmol/L Na_3VO_4 was converted to decavanadate form by lowering the pH to 2 on ice, then slowly raising the pH to ~7 and immediately using the solution for crystallization. The pellet was subjected to two freeze-thaw cycles, resuspended with a micropipette, followed by two additional freeze-thaw cycles. The samples were incubated at 4°C for several days to 1 week. The use of 5 mmol/L $MgCl_2$ in the crystallization buffer promoted the formation of helical crystals, whereas the use of 35 mmol/L $MgCl_2$ promoted the formation of large 2D crystals. The large 2D crystals were formed from SERCA in the presence of a Lys[27]-to-Ala PLN mutant (human PLN sequence (26)), whereas the helical crystals were formed from SERCA in the

presence of an Asn^{27}-to-Ala PLN mutant (canine PLN sequence (45)). Note that these two sequences are nearly identical, with two minor sequence variations (Glu^2 and Lys^{27} in human PLN are Asp^2 and Asn^{27} in canine PLN). Thus, the PLN variants in the crystals differ only by having Glu^2 or Asp^2, and they are both super-inhibitory pentameric forms of PLN.

2.5.4 – ATPase activity assays of SERCA reconstitutions

A coupled-enzyme assay measured ATPase activity of the co-reconstituted proteoliposomes over a range of calcium concentrations from 0.1 to 10 µmol/L (38, 58, 59). The assay has been adapted to a 96-well format utilizing Synergy 4 (BioTek Instruments, Winooski, VT) or SpectraMax M3 (Molecular Devices, San Jose, CA) microplate readers. Data points were collected at 340 nm wavelength, with a well volume of 150 mL containing 10–20 nmol/L SERCA at 30°C (data points were collected every 28–39 s for one hour). The reactions were initiated by the addition of proteoliposomes to the assay solution, which corresponds to the simultaneous addition of calcium and ATP condition reported previously (59). The V_{max} (maximal activity) and K_{Ca} (apparent calcium affinity) were determined based on nonlinear least-squares fitting of the activity data to the Hill equation (Sigma Plot software; SPSS, Chicago, IL). Errors were calculated as the standard error of the mean for a minimum of four independent reconstitutions.

2.5.5 – Data processing

The helical crystals data sets have been previously published (**Table 1**; (41, 45)). The structure from helical crystals of SERCA alone was an average generated from five helical symmetry groups (-22, 6 reference symmetry). The structure from helical crystals of SERCA in the presence of PLN (Asn^{27}-to-Ala mutant; canine sequence) was an average generated from two helical symmetry groups (-27, 9 reference symmetry). Density maps were calculated for the SERCA-PLN helical crystals without enforcing twofold symmetry. The two molecules composing the unit cell for the control structure (SERCA alone) were masked and aligned by cross-correlation with the corresponding molecules from the SERCA-PLN map. After alignment, the two molecules composing the unit cell for the control structure were summed to generate a single map and back-transformed to Fourier space to generate layer-line data with the SERCA-PLN helical symmetry (-27, 9 reference symmetry). Density maps were then calculated from the control and PLN layer-line data with and without twofold symmetry enforced. Because the control and PLN layer-line data were now of the same helical

symmetry group, a difference map could be calculated by simple density scaling and pixel-by-pixel subtraction.

2.5.6 – Atomistic modelling of the PLN pentamer bound to SERCA

The crystal structure of SERCA1a in the E2•MgF$_4^{2-}$ state (Protein Data Bank (PDB): **1WPG**) and the NMR structure of the PLN pentamer (PDB: **2KYV**) were used as templates for the construction of an atomic model of the SERCA-PLN complex. The model of the SERCA-PLN complex was guided by the relative positions of SERCA and the PLN pentamer in projection maps of the large 2D crystals (**Figure 2.3**; (25, 26)). Protein-protein docking simulations identified an appropriate binding interface between the M3 helix of SERCA and the PLN pentamer. The program *ClusPro* (60) was used to dock the M3 helix (residues Pro^{248} to Phe^{279} were included) to the transmembrane helices of the PLN pentamer (residues Gln^{26} to Leu^{52} were included). We chose to dock the pentamer onto the isolated M3 helix of SERCA to avoid artifacts inherent to the hydrophobic nature of SERCA's transmembrane domain, which can result in many false positives during the protein-protein docking process. Only residues that do not participate in intramolecular SERCA contacts were considered as potential SERCA-PLN interaction sites (i.e., Glu^{258}, Gln^{259}, Lys^{262}, Leu^{266}, Val^{269}, Trp^{272}, Leu^{273}, Ile^{276}, and Phe^{279}). The resulting docked orientations were clustered and compared against the 2D crystallographic data to select the most appropriate M3-PLN pentamer complex. The SERCA-PLN pentamer complex was then constructed by superposing the coordinates of the M3 helix onto the crystal structure of the E2•MgF$_4^{2-}$ state of SERCA. This initial model was relaxed by performing a 0.2-ms MD simulation in the presence of ions, lipids, and water molecules. To obtain the full-length PLN pentamer in the SERCA-PLN complex, we inserted the cytosolic domain (residues 1–27) of each PLN unit into the relaxed model of SERCA bound to the transmembrane helices of the PLN pentamer; we used the approximate location of the cytosolic domains as found in the 2D crystals. The final full-length model of the SERCA-PLN complex was then subjected to 5000 steps of energy minimization.

2.5.7 – MD simulations of the SERCA-PLN pentamer complex

The atomistic SERCA-PLN pentamer complex served as a starting structure to obtain a structural model of the complex at physiologically relevant simulation conditions. Based on previous studies of the E2 state of SERCA (61), we modelled transport site residues Glu^{309}, Glu^{771}, and Glu^{908} as protonated and residue Asp^{800} as ionized. The complex was inserted in a pre-equilibrated 150 X

150 Å bilayer of POPC:POPE:POPA (1-palmitoyl-2-oleoyl-*sn*-glycero-3-phosphocholine:1-palmitoyl-2-oleoyl-*sn*-glycero-3-phosphoethanolamine:1-palmitoyl-2-oleoyl-*sn*-glycero-3-phosphate) lipids (8:1:1). This lipid-protein system was solvated using three-site transferrable intermolecular potential (TIP3P) water molecules with a minimal margin of 15 Å between the protein and the edges of the periodic box in the z-axis, and K^+ and Cl^- ions were added (KCl concentration of ~0.1 mmol/L). To generate a reliable model of the complex, we performed MD simulations of the fully solvated complex using NAMD 2.12 (62) with periodic boundary conditions (63), particle mesh Ewald (64, 65), a nonbonded cut-off of 9 Å, and a 2-fs time step. The CHARMM36 force field topologies and parameters were used for the proteins (66), lipids (67), water, and ions. The constant-temperature, constant-pressure ensemble was maintained with a Langevin thermostat (310 K) and an anisotropic Langevin piston barostat (1 atm). The system was first subjected to energy minimization, followed by gradually warming up of the system for 200 ps. This procedure was followed by 10 ns of equilibration with backbone atoms harmonically restrained using a force constant of 10 kcal mol^{-1} Å^{-2}. The MD simulation of the complex was continued without restraints for 500 ns.

2.6 – Acknowledgments

2.6.1 – Author contributions

J.P.G. and J.O.P. performed the research, analyzed data, and contributed to the writing and editing of the manuscript. M.J.L. contributed to the design and analysis of the data and editing of the manuscript. L.M.E.-F. performed and analyzed the protein-protein docking and MD simulations. H.S.Y. designed the research, analyzed the data and wrote the manuscript.

2.6.2 – Acknowledgments

2.7 – Conflict of interest

There is no conflict of interest in the work reported in this manuscript.

2.8 – References

1. Goodsell, D. S., Autin, L., and Olson, A. J. (2019) Illustrate: Software for Biomolecular Illustration. *Structure.* 10.1016/j.str.2019.08.011

2. Toyoshima, C. (2009) How Ca2+-ATPase pumps ions across the sarcoplasmic reticulum membrane. *Biochim. Biophys. Acta - Mol. Cell Res.* **1793**, 941–946

3. Toyoshima, C., and Cornelius, F. (2013) New crystal structures of PII-type ATPases: Excitement continues. *Curr. Opin. Struct. Biol.* **23**, 507–514

4. Møller, J. V., Olesen, C., Winther, A.-M. L., and Nissen, P. (2010) The sarcoplasmic Ca2+-ATPase: design of a perfect chemi-osmotic pump. *Q. Rev. Biophys.* **43**, 501–566

5. Fajardo, V. a., Bombardier, E., Vigna, C., Devji, T., Bloemberg, D., Gamu, D., Gramolini, A. O., Quadrilatero, J., and Tupling, a. R. (2013) Co-Expression of SERCA isoforms, phospholamban and sarcolipin in human skeletal muscle fibers. *PLoS One.* **8**, 1–13

6. Stokes, D. L. (1997) Keeping Calcium in its Place: Ca2+ ATPase and Phospholamban. *Curr. Opin. Struct. Biol.* **7**, 550–556

7. Kimura, Y., Kurzydlowski, K., Tada, M., and MacLennan, D. H. (1997) Phospholamban Inhibitory Function Is Activated by Depolymerization. *J. Biol. Chem. .* **272**, 15061–15064

8. Autry, J. M., and Jones, L. R. (1997) Functional Co-expression of the Canine Cardiac Ca2+Pump and Phospholamban in Spodoptera frugiperda (Sf21) Cells Reveals New Insights on ATPase Regulation . *J. Biol. Chem. .* **272**, 15872–15880

9. Jones, L. R., Cornea, R. L., and Chen, Z. (2002) Close proximity between residue 30 of phospholamban and cysteine 318 of the cardiac Ca2+ pump revealed by intermolecular thiol cross-linking. *J. Biol. Chem.* **277**, 28319–28329

10. Asahi, M., Mckenna, E., Kurzydlowski, K., Tada, M., and Maclennan, D. H. (2000) Physical Interactions between Phospholamban and Sarco (endo) plasmic Reticulum Ca 2+ -ATPases Are Dissociated by Elevated Ca 2+, but Not by Phospholamban Phosphorylation, Vanadate, or Thapsigargin, and Are Enhanced by ATP *. **275**, 15034–15038

11. Cornea, R. L., Jones, L. R., Autry, J. M., and Thomas, D. D. (1997) Mutation and Phosphorylation Change the Oligomeric Structure of Phospholamban in Lipid Bilayers. *Biochemistry.* **36**, 2960–2967

12. Becucci, L., Cembran, A., Karim, C. B., Thomas, D. D., Guidelli, R., Gao, J., and Veglia, G. (2009) On the Function of Pentameric Phospholamban: Ion Channel or Storage Form? *Biophys. J.* **96**, L60–L62

13. Negash, S., Yao, Q., Sun, H., Li, J., BigeloW, D. J., and Squier, T. C. (2000) Phospholamban remains associated with the Ca2+- and Mg2+-dependent ATPase following phosphorylation by cAMP-dependent protein kinase. *Biochem. J.* **351**, 195 LP – 205

14. Mueller, B., Karim, C. B., Negrashov, I. V, Kutchai, H., and Thomas, D. D. (2004) Direct Detection of Phospholamban and Sarcoplasmic Reticulum Ca-ATPase Interaction in Membranes Using Fluorescence Resonance Energy Transfer. *Biochemistry.* **43**, 8754–8765

15. Li, J., Bigelow, D. J., and Squier, T. C. (2004) Conformational Changes within the Cytosolic Portion of Phospholamban upon Release of Ca-ATPase Inhibition. *Biochemistry.* **43**, 3870–3879

16. Bidwell, P., Blackwell, D. J., Hou, Z., Zima, A. V, and Robia, S. L. (2011) Phospholamban Binds with Differential Affinity to Calcium Pump Conformers. *J. Biol. Chem.* . **286**, 35044–35050

17. James, Z. M., McCaffrey, J. E., Torgersen, K. D., Karim, C. B., and Thomas, D. D. (2012) Protein-Protein Interactions in Calcium Transport Regulation Probed by Saturation Transfer Electron Paramagnetic Resonance. *Biophys. J.* **103**, 1370–1378

18. Martin, P. D., James, Z. M., and Thomas, D. D. (2018) Effect of Phosphorylation on Interactions between Transmembrane Domains of SERCA and Phospholamban. *Biophys. J.* **114**, 2573–2583

19. Gustavsson, M., Verardi, R., Mullen, D. G., Mote, K. R., Traaseth, N. J., Gopinath, T., and Veglia, G. (2013) Allosteric regulation of SERCA by phosphorylation-mediated conformational shift of phospholamban. *Proc. Natl. Acad. Sci. U. S. A.* **110**, 17338–43

20. Chu, G., Li, L., Sato, Y., Harrer, J. M., Kadambi, V. J., Hoit, B. D., Bers, D. M., and Kranias, E. G. (1998) Pentameric assembly of phospholamban facilitates inhibition of cardiac function in vivo. *J. Biol. Chem.* **273**, 33674–33680

21. Kovacs, R. J., Nelson, M. T., Simmerman, H. K., and Jones, L. R. (1988) Phospholamban forms Ca2+-selective channels in lipid bilayers. *J. Biol. Chem.* . **263**, 18364–18368

22. Smeazzetto, S., Schröder, I., Thiel, G., and Moncelli, M. R. (2011) Phospholamban generates cation selective ion channels. *Phys. Chem. Chem. Phys.* **13**, 12935–12939

23. Wittmann, T., Lohse, M. J., and Schmitt, J. P. (2015) Phospholamban pentamers attenuate PKA-dependent phosphorylation of monomers. *J. Mol. Cell. Cardiol.* **80C**, 90–97

24. Ceholski, D. K., Trieber, C. A., Holmes, C. F. B., and Young, H. S. (2012) Lethal, Hereditary Mutants of Phospholamban Elude Phosphorylation by Protein Kinase A. *J. Biol. Chem.* . **287**, 26596–26605

25. Stokes, D. L., Pomfret, A. J., Rice, W. J., Glaves, J. P., and Young, H. S. (2006) Interactions between Ca2+-ATPase and the pentameric form of phospholamban in two-dimensional co-crystals. *Biophys. J.* **90**, 4213–4223

26. Glaves, J. P., Trieber, C. a., Ceholski, D. K., Stokes, D. L., and Young, H. S. (2011) Phosphorylation and mutation of phospholamban alter physical interactions with the sarcoplasmic reticulum calcium pump. *J. Mol. Biol.* **405**, 707–723

27. Akin, B. L., Hurley, T. D., Chen, Z., and Jones, L. R. (2013) The Structural Basis for Phospholamban Inhibition of the Calcium Pump in Sarcoplasmic Reticulum. *J. Biol. Chem.* . **288**, 30181–30191

28. Toyoshima, C., Iwasawa, S., Ogawa, H., Hirata, A., Tsueda, J., and Inesi, G. (2013) Crystal structures of the calcium pump and sarcolipin in the Mg2+-bound E1 state. *Nature.* **495**, 260

29. Winther, A.-M. L., Bublitz, M., Karlsen, J. L., Møller, J. V, Hansen, J. B., Nissen, P., and Buch-Pedersen, M. J. (2013) The sarcolipin-bound calcium pump stabilizes calcium sites exposed to the cytoplasm. *Nature.* **495**, 265

30. Gorski, P. A., Trieber, C. A., Ashrafi, G., and Young, H. S. (2015) Regulation of the Sarcoplasmic Reticulum Calcium Pump by Divergent Phospholamban Isoforms in Zebrafish. *J. Biol. Chem.* . **290**, 6777–6788

31. Verboomen, H., Wuytack, F., De Smedt, H., Himpens, B., and Casteels, R. (1992) Functional difference between SERCA2a and SERCA2b Ca$²⁺$ pumps and their modulation by phospholamban. *Biochem. J.* **286**, 591 LP – 595

32. Akin, B. L., and Jones, L. R. (2012) Characterizing Phospholamban to Sarco(endo)plasmic Reticulum Ca2+-ATPase 2a (SERCA2a) Protein Binding Interactions in Human Cardiac Sarcoplasmic Reticulum Vesicles Using Chemical Cross-linking. *J. Biol. Chem.* **287**, 7582–7593

33. Ferrington, D. A., Yao, Q., Squier, T. C., and Bigelow, D. J. (2002) Comparable Levels of Ca-ATPase Inhibition by Phospholamban in Slow-Twitch Skeletal and Cardiac Sarcoplasmic Reticulum. *Biochemistry.* **41**, 13289–13296

34. Negash, S., Chen, L. T., Bigelow, D. J., and Squier, T. C. (1996) Phosphorylation of Phospholamban by cAMP-Dependent Protein Kinase Enhances Interactions between Ca-ATPase Polypeptide Chains in Cardiac Sarcoplasmic Reticulum Membranes. *Biochemistry.* **35**, 11247–11259

35. Ceholski, D. K., Trieber, C. a., and Young, H. S. (2012) Hydrophobic imbalance in the cytoplasmic domain of phospholamban is a determinant for lethal dilated cardiomyopathy. *J.*

Biol. Chem. **287**, 16521–16529

36.   Waggoner, J. R., Huffman, J., Griffith, B. N., Jones, L. R., and Mahaney, J. E. (2004) Improved expression and characterization of Ca2+-ATPase and phospholamban in High-Five cells. *Protein Expr. Purif.* **34**, 56–67

37.   Trieber, C. A., Douglas, J. L., Afara, M., and Young, H. S. (2005) The Effects of Mutation on the Regulatory Properties of Phospholamban in Co-Reconstituted Membranes†. *Biochemistry.* **44**, 3289–3297

38.   Trieber, C. A., Afara, M., and Young, H. S. (2009) Effects of Phospholamban Transmembrane Mutants on the Calcium Affinity, Maximal Activity, and Cooperativity of the Sarcoplasmic Reticulum Calcium Pump. *Biochemistry.* **48**, 9287–9296

39.   Reddy, L. G., Cornea, R. L., Winters, D. L., McKenna, E., and Thomas, D. D. (2003) Defining the Molecular Components of Calcium Transport Regulation in a Reconstituted Membrane System. *Biochemistry.* **42**, 4585–4592

40.   Young, H. S., Xu, C., Zhang, P., and Stokes, D. L. (2001) Locating the thapsigargin-binding site on Ca(2+)-ATPase by cryoelectron microscopy. *J. Mol. Biol.* **308**, 231–240

41.   Xu, C., Rice, W. J., He, W., and Stokes, D. L. (2002) A structural model for the catalytic cycle of Ca2+-ATPase11Edited by W. Baumeister. *J. Mol. Biol.* **316**, 201–211

42.   Young, H. S., Rigaud, J. L., Lacapère, J. J., Reddy, L. G., and Stokes, D. L. (1997) How to make tubular crystals by reconstitution of detergent-solubilized Ca2(+)-ATPase. *Biophys. J.* **72**, 2545–2558

43.   Dux, L., and Martonosi, A. (1983) Two-dimensional arrays of proteins in sarcoplasmic reticulum and purified Ca2+-ATPase vesicles treated with vanadate. *J. Biol. Chem. .* **258**, 2599–2603

44.   Maurer, A., and Fleischer, S. (1984) Decavanadate is responsible for vanadate-induced two-dimensional crystals in sarcoplasmic reticulum. *J. Bioenerg. Biomembr.* **16**, 491–505

45.   Young, H. S., Jones, L. R., and Stokes, D. L. (2001) Locating phospholamban in co-crystals with Ca(2+)-ATPase by cryoelectron microscopy. *Biophys. J.* **81**, 884–894

46.   Robia, S. L., Campbell, K. S., Kelly, E. M., Hou, Z., Winters, D. L., and Thomas, D. D. (2007) Förster Transfer Recovery Reveals That Phospholamban Exchanges Slowly From Pentamers but Rapidly From the SERCA Regulatory Complex. *Circ. Res.* **101**, 1123–1129

47.   Toyoshima, C., Asahi, M., Sugita, Y., Khanna, R., Tsuda, T., and MacLennan, D. H. (2003) Modeling of the inhibitory interaction of phospholamban with the Ca2+ ATPase. *Proc. Natl.*

Acad. Sci. U. S. A. **100**, 467–472

48. Seidel, K., Andronesi, O. C., Krebs, J., Griesinger, C., Young, H. S., Becker, S., and Baldus, M. (2008) Structural Characterization of Ca2+-ATPase-Bound Phospholamban in Lipid Bilayers by Solid-State Nuclear Magnetic Resonance (NMR) Spectroscopy,. *Biochemistry.* **47**, 4369–4376

49. Li, M., Reddy, L. G., Bennett, R., Silva, N. D., Jones, L. R., and Thomas, D. D. (1999) A Fluorescence Energy Transfer Method for Analyzing Protein Oligomeric Structure: Application to Phospholamban. *Biophys. J.* **76**, 2587–2599

50. Reddy, L. G., Jones, L. R., and Thomas, D. D. (1999) Depolymerization of Phospholamban in the Presence of Calcium Pump: A Fluorescence Energy Transfer Study [†]. *Biochemistry.* **38**, 3954–3962

51. Stokes, D. L., Delavoie, F., Rice, W. J., Champeil, P., McIntosh, D. B., and Lacapère, J.-J. (2005) Structural Studies of a Stabilized Phosphoenzyme Intermediate of Ca2+-ATPase. *J. Biol. Chem.* . **280**, 18063–18072

52. Traaseth, N. J., Shi, L., Verardi, R., Mullen, D. G., Barany, G., and Veglia, G. (2009) Structure and topology of monomeric phospholamban in lipid membranes determined by a hybrid solution and solid-state NMR approach. *Proc. Natl. Acad. Sci. U. S. A.* **106**, 10165–10170

53. Stokes, D. L., and Green, N. M. (1990) Three-dimensional crystals of CaATPase from sarcoplasmic reticulum. Symmetry and molecular packing. *Biophys. J.* **57**, 1–14

54. Afara, M. R., Trieber, C. A., Glaves, J. P., and Young, H. S. (2006) Rational Design of Peptide Inhibitors of the Sarcoplasmic Reticulum Calcium Pump. *Biochemistry.* **45**, 8617–8627

55. Young, H. S., Reddy, L. G., Jones, L. R., and stokes, D. L. (1998) Co-reconstitution and Co-crystallization of Phospholamban and Ca2+-ATPase a. *Ann. N. Y. Acad. Sci.* **853**, 103–115

56. Douglas, J. L., Trieber, C. a., Afara, M., and Young, H. S. (2005) Rapid, high-yield expression and purification of Ca2+-ATPase regulatory proteins for high-resolution structural studies. *Protein Expr. Purif.* **40**, 118–125

57. Eletr, S., and Inesi, G. (1972) Phospholipid orientation in sacroplasmic membranes: Spin-label ESR and proton NMR studies. *Biochim. Biophys. Acta - Biomembr.* **282**, 174–179

58. Warren, G. B., Toon, P. A., Birdsall, N. J., Lee, A. G., and Metcalfe, J. C. (1974) Reconstitution of a calcium pump using defined membrane components. *Proc. Natl. Acad. Sci. U. S. A.* **71**, 622–626

59. Smeazzetto, S., Armanious, G. P., Moncelli, M. R., Bak, J. J., Lemieux, M. J., Young, H. S., and Tadini-Buoninsegni, F. (2017) Conformational memory in the association of the

transmembrane protein phospholamban with the sarcoplasmic reticulum calcium pump SERCA. *J. Biol. Chem.* **292**, 21330–21339

60. Kozakov, D., Hall, D. R., Xia, B., Porter, K. A., Padhorny, D., Yueh, C., Beglov, D., and Vajda, S. (2017) The ClusPro web server for protein–protein docking. *Nat. Protoc.* **12**, 255

61. Espinoza-Fonseca, L. M., Autry, J. M., Ramírez-Salinas, G. L., and Thomas, D. D. (2015) Atomic-Level Mechanisms for Phospholamban Regulation of the Calcium Pump. *Biophys. J.* **108**, 1697–1708

62. Phillips, J. C., Braun, R., Wang, W., Gumbart, J., Tajkhorshid, E., Villa, E., Chipot, C., Skeel, R. D., Kalé, L., and Schulten, K. (2005) Scalable molecular dynamics with NAMD. *J. Comput. Chem.* **26**, 1781–1802

63. Weber, W., Hünenberger, P. H., and McCammon, J. A. (2000) Molecular Dynamics Simulations of a Polyalanine Octapeptide under Ewald Boundary Conditions: Influence of Artificial Periodicity on Peptide Conformation. *J. Phys. Chem. B.* **104**, 3668–3675

64. Darden, T., York, D., and Pedersen, L. (1993) Particle mesh Ewald: An N·log(N) method for Ewald sums in large systems. *J. Chem. Phys.* **98**, 10089–10092

65. Essmann, U., Perera, L., Berkowitz, M. L., Darden, T., Lee, H., and Pedersen, L. G. (1995) A smooth particle mesh Ewald method. *J. Chem. Phys.* **103**, 8577–8593

66. Best, R. B., Zhu, X., Shim, J., Lopes, P. E. M., Mittal, J., Feig, M., and MacKerell, A. D. (2012) Optimization of the Additive CHARMM All-Atom Protein Force Field Targeting Improved Sampling of the Backbone ϕ, ψ and Side-Chain χ1 and χ2 Dihedral Angles. *J. Chem. Theory Comput.* **8**, 3257–3273

67. Klauda, J. B., Venable, R. M., Freites, J. A., O'Connor, J. W., Tobias, D. J., Mondragon-Ramirez, C., Vorobyov, I., MacKerell, A. D., and Pastor, R. W. (2010) Update of the CHARMM All-Atom Additive Force Field for Lipids: Validation on Six Lipid Types. *J. Phys. Chem. B.* **114**, 7830–7843

"Let me spin and excite you"

F. Starlite – 2016

-written about NMR, probably-

Chapter 3 – Interaction of a sarcolipin pentamer and monomer with the sarcoplasmic reticulum calcium pump, SERCA

J. P. Glaves[1], J. O. Primeau[1], P. A. Gorski[1], L. M. Espinoza-Fonseca[2], M. J. Lemieux[1], and H. S. Young[1]

Running Title: A novel complex of sarcolipin and SERCA.

[1]Department of Biochemistry, University of Alberta, Edmonton, Alberta, Canada and [2]Center for Arrhythmia Research, Division of Cardiovascular Medicine, Department of Internal Medicine, University of Michigan, Ann Arbor, Michigan
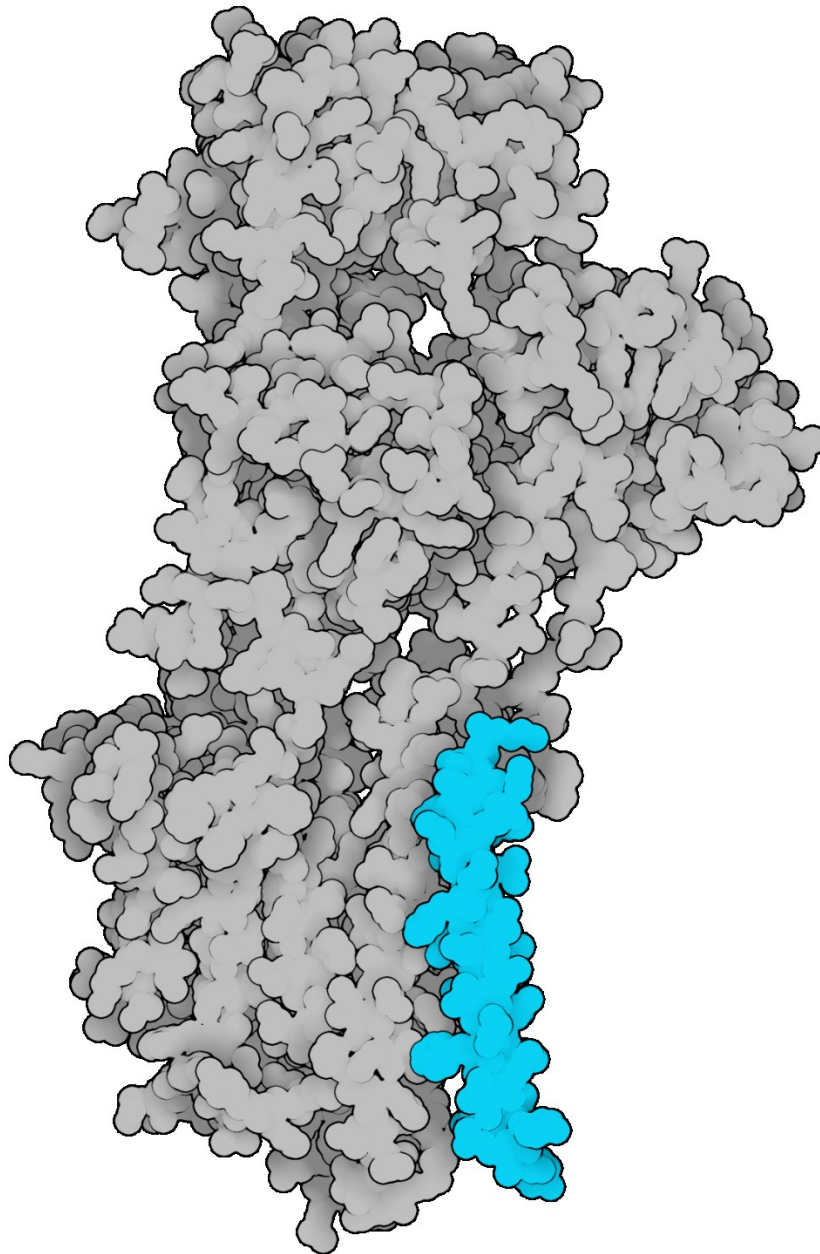
Stylized model of SLN interacting with M3 of SERCA

See **Figure 3.7 and section 3.5.8**

Preface

This chapter represents the culmination of the work published in the Biophysical Journal on January 22, 2020. (Glaves, J. P., Primeau, J. O., Gorski, P. A., Espinoza-Fonseca, L. M., Lemieux, M. J., and Young, H. S. (2019) Interaction of a sarcolipin pentamer and monomer with the sarcoplasmic reticulum calcium pump, SERCA. *Biophysj.* **118**, 518–531). JPG, JOP, and PAG performed the research, analyzed data, and contributed to the writing and editing of the manuscript; MJL contributed to the design and analysis of the data, and editing of the manuscript; LMEF performed and analyzed the protein-protein docking and molecular dynamics simulations; HSY designed the research, analyzed the data, and wrote the manuscript. **This manuscript has been adapted and edited from its original state to fit the format of the thesis presented. Title page figure generated using *Illustrate: Non-photorealistic Biomolecular Illustration*** (1)**.**

3.1 – Summary

The sequential rise and fall of cytosolic calcium underlie the contraction-relaxation cycle of muscle cells. While the initiation of contraction occurs by the release of calcium from the sarcoplasmic reticulum, muscle relaxation involves the active transport of calcium back into the sarcoplasmic reticulum. This re-uptake of calcium is catalyzed by the sarco-endoplasmic reticulum Ca^{2+}-ATPase (SERCA), which plays a lead role in muscle contractility. Small membrane protein subunits regulate the activity of SERCA, the most well-known being phospholamban (PLN) and sarcolipin (SLN). SLN physically interacts with SERCA and differentially regulates contractility in skeletal and atrial muscle. SLN has also been implicated in skeletal muscle thermogenesis. Despite these important roles, the structural mechanisms by which SLN modulates SERCA-dependent contractility and thermogenesis remain unclear. Here, we functionally characterized wild-type SLN and a pair of mutants, Asn^4-to-Ala and Thr^5-to-Ala, which yielded gain-of-function behaviour comparable to previous findings with PLN. Next, we analyzed two-dimensional crystals of SERCA in the presence of wild-type SLN by electron cryo-microscopy. The fundamental units of the crystals are anti-parallel dimer ribbons of SERCA, known for decades as an assembly of calcium-free SERCA molecules induced by the addition of decavanadate. A projection map of the SERCA-SLN complex was determined to a resolution of 8.5 Å, which allowed the direct visualization of an SLN pentamer. The SLN pentamer was found to interact with transmembrane segment M3 of SERCA, though the interaction appeared to be indirect and mediated by an additional density consistent with an SLN monomer. This SERCA-SLN complex correlated with the ability of SLN to decrease the maximal activity of SERCA, which is distinct from the ability of PLN to increase the maximal activity of SLN. Protein-protein docking and molecular dynamics simulations provided models for the SLN pentamer and the novel interaction between SERCA and an SLN monomer.

3.2 – Introduction

A major regulator of cellular calcium homeostasis in skeletal muscle is the sarcoendoplasmic reticulum Ca^{2+}-ATPase (SERCA). Calcium release channels trigger muscle contraction by releasing calcium stored in the sarcoplasmic reticulum (SR). In turn, the SERCA pump (SERCA1a isoform) triggers muscle relaxation by returning calcium from the cytosol to the lumen of the SR. In skeletal and atrial muscle, SERCA is regulated by sarcolipin (SLN), which allows for dynamic control of calcium homeostasis and the contraction-relaxation cycle in skeletal muscle and the atria of the heart. SLN is a 31-residue tail-anchored integral membrane protein that resides in the SR membrane and acts as an inhibitor of SERCA. SLN is homologous to phospholamban (PLN), a well-known regulatory subunit of SERCA in cardiac muscle (SERCA2a isoform). Both regulatory subunits inhibit SERCA by lowering its apparent affinity for calcium. The relief of inhibition and re-activation of SERCA is mediated by adrenergic signalling pathways and the reversible phosphorylation of PLN and SLN, which in turn has significant effects on calcium uptake in muscle tissues.

Over the last few years, studies have revealed that SLN belongs to a family of regulatory subunits that target SERCA in a tissue-specific manner, herein collectively described as the "regulins"(2–4). Prior to this, PLN and SLN were the only known SERCA regulatory subunits, with the importance of PLN in cardiac muscle overshadowing the role of SLN in skeletal muscle. However, SLN is also found in atrial muscle, alongside PLN, where it plays an important, albeit undefined, role in cardiac contractility. In addition, interest in SLN has intensified with the identification of a new physiological role – SLN appears to be involved in non-shivering, skeletal muscle-based thermogenesis (5). The current theory is that SLN promotes uncoupling of SERCA, where the net balance of ATP hydrolysis does not correlate with productive calcium transport. The excess ATP hydrolysis contributes to thermal energy in skeletal muscle, the largest tissue mass in the human body. Given the abundance of skeletal muscle and the role of SLN in thermogenesis and energy balance, SLN may also contribute to metabolic disorders such as obesity and diabetes. With this potential new functionality of SLN, a molecular understanding of the SERCA regulatory mechanism is imperative. The homology between SLN and PLN lies within their transmembrane domains, and this has long suggested commonality in function. However, the structure of SLN is quite distinct, with a short cytoplasmic domain (residues 1-7), a transmembrane α-helix (residues 8-26), and a unique luminal tail (residues 27-31). Like PLN, SLN alters the apparent calcium affinity of SERCA, yet there are substantial differences in the mechanism (6). The inhibitory properties of SLN are strongly dependent

on the highly conserved C-terminal tail (Arg[27]-Ser-Tyr-Gln-Tyr[31] or RSYQY sequence), whereas the inhibitory properties of PLN are encoded in its transmembrane domain. In addition, SLN appears to remain associated with SERCA throughout the calcium transport cycle (7). Recall that PLN is thought to interact with calcium-free forms of SERCA and dissociate from the enzyme under certain conditions (e.g., elevated calcium plus PLN phosphorylation). Crystal structures of a SERCA-SLN complex have been determined, revealing SLN binding to the inhibitory groove (M2, M6, & M9) in a novel E1-like state of SERCA (8, 9). This novel conformation of SERCA was not the anticipated calcium-free E2 state and the luminal RSYQY sequence of SLN was not in direct contact with SERCA. Thus, it seems likely that the crystal structures represent one intermediate as SERCA and SLN progress together through the calcium transport cycle, and that the SERCA-SLN complex involves multiple conformational states. How the regulatory RSYQY sequence of SLN interacts with SERCA remains elusive.

We have previously shown that PLN pentamers interact with SERCA in the membrane environment of large two-dimensional (2D) co-crystals and that the association is distinct from the inhibitory interaction and dependent on the functional state of PLN (10, 11). Our recent study compared helical crystals of the SERCA-PLN complex with the large 2D crystals, which allowed us to conclude that the PLN pentamer naturally associates with SERCA at a distinct site (12). This interaction correlated with the ability of PLN pentamers to increase the maximal activity of SERCA at high calcium concentrations, and a molecular model of the novel SERCA-PLN complex was presented. Given the similar functional properties of SLN and observations that SLN can form oligomers (13, 14), we set out to determine if SLN could co-crystallize with SERCA. Here, we functionally characterized wild-type SLN, as well as gain-of-function mutants Asn[4]-to-Ala and Thr[5]-to-Ala **(Figure 3.1)**. These mutants confirm structural and functional elements that are conserved in PLN and SLN. Additionally, we analyzed large 2D crystals of the SERCA-SLN complex by electron cryo-microscopy. Both wild-type SLN and a gain-of-function mutant (Asn[4]-to-Ala) were evaluated. We report the first direct observation of an SLN pentamer and we show that it interacts with SERCA in a manner similar, but distinct, to that previously observed for PLN. Instead of direct interaction between the SLN pentamer and transmembrane segment M3 of SERCA, this interaction is mediated by an additional density most consistent with an SLN monomer. The ability of SLN and PLN to interact with an accessory site of SERCA (M3) appears to contribute to the regulatory mechanism. However, the interactions of the PLN and SLN pentamers with SERCA are different, and the

functional effects on the maximal activity of SERCA are opposite; PLN increases while SLN decreases the maximal activity of SERCA.
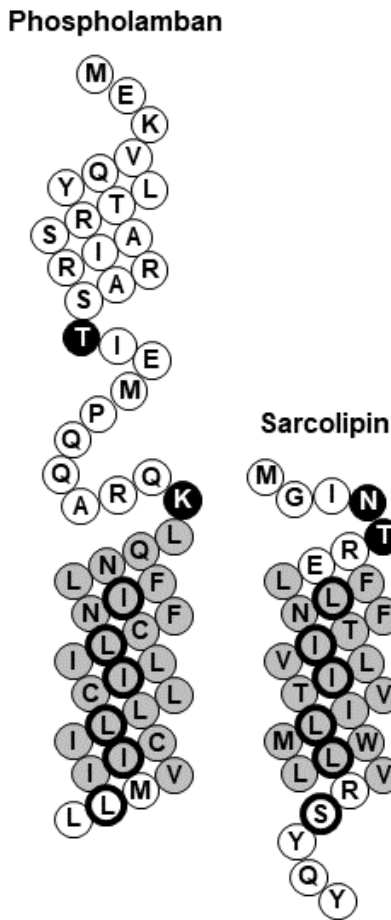
Figure 3.1: Topology diagrams for human phospholamban (PLN) and sarcolipin (SLN). The transmembrane domains are coloured grey and the cytoplasmic and luminal domains are coloured white. Asn^4 and Thr^5 are indicated in black, as are the comparative residues in PLN (Lys^{27} and Thr^{17}). The Leu-Ile residues of PLN that stabilize the pentameric state are outlined in black (Ile^{33}, Leu^{37}, Ile^{40}, Leu^{44}, Ile^{47}, and Leu^{51}), as are the comparative residues in SLN (Leu^{10}, Ile^{14}, Ile^{17}, Leu^{21}, Leu^{24}, and Ser^{28}).

3.3 – Results

Since SLN is a homolog of PLN found in skeletal muscle and the atria of the heart, it was reasonable to consider whether SLN can interact with transmembrane segment M3 of SERCA. While SLN and PLN have a similar inhibitory effect on SERCA, the molecular mechanisms by which they regulate SERCA are distinct. The inhibitory properties of PLN are encoded in the transmembrane domain, whereas the unique luminal domain of SLN strongly influences its inhibitory properties of SLN (6). The cytoplasmic domains of both PLN and SLN allow for the reversal of SERCA inhibition

by phosphorylation, though the signaling pathways and molecular mechanisms are different. In addition, PLN is known to form a pentamer that persists in SDS-PAGE analyses, whereas SLN has a reduced tendency to form higher-order oligomers with monomers and dimers being the prevalent species identified by SDS-PAGE (13). Thus, the interaction of an oligomeric species (e.g. pentamer) with SERCA may not occur or may be different for SLN. To investigate this, we co-reconstituted SERCA with wild-type and mutant forms of SLN. ATPase activity of the co-reconstituted proteoliposomes demonstrated a functional interaction between the proteins, and we correlated these data with structural analyses from 2D crystals and molecular dynamics (MD) simulations.

3.3.1 – Co-reconstitution of SERCA and SLN

In the present study, we produced proteoliposomes containing a high density of SERCA and SLN with a lipid-to-protein molar ratio of approximately 120-to-1 and a SERCA-SLN molar ratio of either 1:2 or 1:5 (10, 11, 15–17). The 1:5 SERCA-SLN ratio was used throughout, with the exception of the 1:2 ratio used for comparative activity assays (see below). Focusing on wildtype and two mutant forms of SLN, we measured the calcium-dependent ATPase activity of SERCA with or without SLN. The measurement of ATP hydrolysis rates by reconstituted SERCA proteoliposomes yielded an apparent calcium affinity (K_{Ca}) of 0.41 ± 0.02 µmol/L for SERCA alone and 0.76 ± 0.02 µmol/L for SERCA in the presence of wild-type SLN (**Figure 3.2A**). This level of inhibitory activity is consistent with earlier SLN and SERCA co-reconstitution (13, 15, 18) and heterologous co-expression studies (19). We also studied two mutants of SLN, a previously characterized gain-of-function mutant (Thr[5]-to-Ala; not shown) and an uncharacterized mutant (Asn[4]-to-Ala; **Figure 3.2A**) designed to mimic the Lys[27]-to-Ala gain-of-function mutant at the homologous position in human PLN (10). Asn[4]-to-Ala and Thr[5]-to-Ala were both gain-of-function mutants, further reducing the apparent calcium affinity of SERCA (K_{Ca} values were 1.27 ± 0.05 µmol/L and 0.95 ± 0.05 µmol/L, respectively). Thus, the potent gain of function observed for the Asn[4]-to-Ala mutant supported the notion that Asn[4] of human SLN and Lys[27] of human PLN (**Figure 3.1**) serve the analogous function of influencing the stability of the inhibitory complex (20). In addition, the gain of function observed for the Thr[5]-to-Ala mutant compares well with a similar mutation in PLN, Thr[17]-to-Ala, which has been reported to be a gain-of-function form of PLN (21).

A

	K_{Ca} (µM calcium)
SERCA	0.43 ± 0.02
SERCA + SLN	0.76 ± 0.02
SERCA + N4A	1.27 ± 0.05
SERCA + T5A (not shown)	0.95 ± 0.05

B

	K_{Ca} (µM calcium)	V_{max} (µmoles/min/mg)
SERCA	0.43 ± 0.02	4.10 ± 0.05
SERCA + SLN (1:2)	0.73 ± 0.06	4.12 ± 0.12
SERCA + SLN (1:5)	0.68 ± 0.04	3.06 ± 0.06
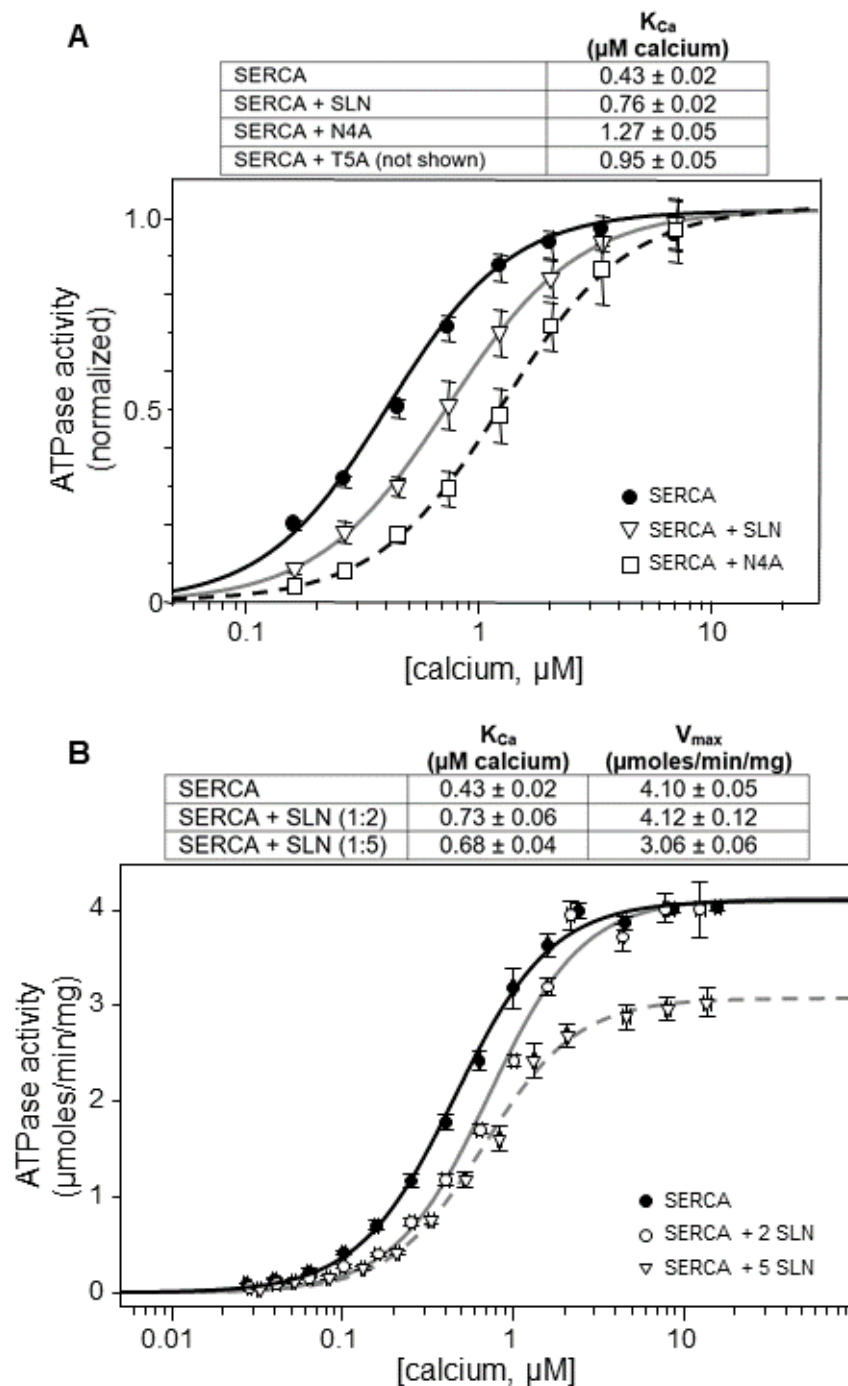
Figure 3.2: ATPase activity of co-reconstituted proteoliposomes containing SERCA and SLN. (A) ATPase activity of SERCA reconstituted in the absence (SERCA; circles) and in the presence of wild type SLN (SERCA + SLN; triangles) and Asn[4]-to-Ala SLN (SERCA + N4A; squares) at a 1:5 molar ratio. The calcium affinity values (K_{Ca}) are shown in the inset table, and all curves have been normalized to the maximal activity (V/V_{max}). Notice the gain-of-function behaviour observed for the Asn[4]-to-Ala mutant (larger rightward shift of the ATPase activity curve). (B) ATPase activity of SERCA reconstituted in the absence of SLN (black circles), in the presence of 1:2 molar ratio (white circles) and a 1:5 molar ratio (triangles) of SERCA to wild-type SLN. The calcium affinity (K_{Ca}) and maximal activity (V_{max}) values are shown in the inset table. Notice the decrease in the V_{max} of SERCA at the 1:5 molar ratio of SERCA-SLN. *ATPase activity measurements collected in (B) were collected by J.O.P.

The effect of PLN on the apparent calcium affinity of SERCA saturates at a molar ratio of approximately one PLN monomer per SERCA (22, 23) and it is assumed that SLN behaves in a similar manner. However, the PLN pentamer also affects the maximal activity of SERCA in a concentration-dependent manner (12). This raises the question what are the consequences of higher ratios of SLN on SERCA maximal activity? To address this, we measured the calcium-dependent ATPase activity of SERCA alone and in the presence of two molar ratios of SERCA-SLN (**Figure 3.2B**). The SERCA-SLN ratios were designed to saturate an effect on the apparent calcium affinity of SERCA (1:2 ratio) and uncover any effects on the maximal activity of SERCA (1:5 ratio). Similar to what was observed for PLN, the effect of SLN on the apparent calcium affinity (K_{Ca}) of SERCA remained unchanged for the two molar ratios. In contrast to what was observed for PLN, there was a statistically significant decrease in the maximal activity (V_{max}) of SERCA at the 1:5 molar ratio of SERCA-SLN. The V_{max} value for SERCA alone (4.10 ± 0.05 μmoles/min/mg) was similar to SERCA in the presence of the 1:2 ratio of SLN (4.12 ± 0.12 μmoles/min/mg). In contrast, the decreased V_{max} for SERCA in the presence of the 1:5 ratio of SLN (3.06 ± 0.06 μmoles/min/mg) was statistically significant from SERCA alone and SERCA in the presence of the 1:2 ratio of SLN ($p<0.01$). This result supports the notion that SERCA activity is influenced by the membrane concentration of SLN, though the effect is opposite to that seen for PLN. The decrease of SERCA's V_{max} occurs at the higher concentration of SLN in the membrane, suggesting that it may involve an oligomeric form of SLN and a distinct interaction between SLN and SERCA.

3.3.2 – Two-dimensional co-crystals of SERCA and SLN

Proteoliposomes containing SERCA in the presence of a 1:5 molar ratio of wild-type and mutants forms of SLN were capable of forming large 2D crystals (10, 11). Interestingly, wild-type SLN generally produced fewer co-crystals with SERCA than the Asn[4]-to-Ala gain-of-function mutant of SLN. A similar trend was observed for wild-type PLN and the Lys[27]-to-Ala gain-of-function mutant (10). Despite the differences in crystal frequency, the morphology and lattice parameters were comparable to one another and to those previously reported for SERCA-PLN crystals ($p22_12_1$ plane group symmetry; $a \sim 346$ Å and $b \sim 70$ Å (10, 11)). Given that the fundamental units of the crystals are SERCA dimer ribbons rigidly held together by decavanadate (24, 25), this was an indication that PLN and SLN may have a similar mode of interaction with SERCA. For wild-type SLN, a projection map of negatively stained 2D crystals was calculated after averaging Fourier data from at least five independent crystals (~20 Å resolution). We used standard methods for correcting lattice distortions,

and no CTF correction was applied. The projection map from negatively stained crystals revealed SERCA dimer ribbons as a fundamental feature of the crystals, with densities consistent with SLN oligomers interspersed between the SERCA dimer ribbons (**Figure 3.3**). The relative size and position of the SLN oligomer density was similar to PLN. We concluded that an oligomeric form of SLN could interact with SERCA in the 2D co-crystals, though the negative stain projection maps did not reveal the size and stoichiometry of the complex.
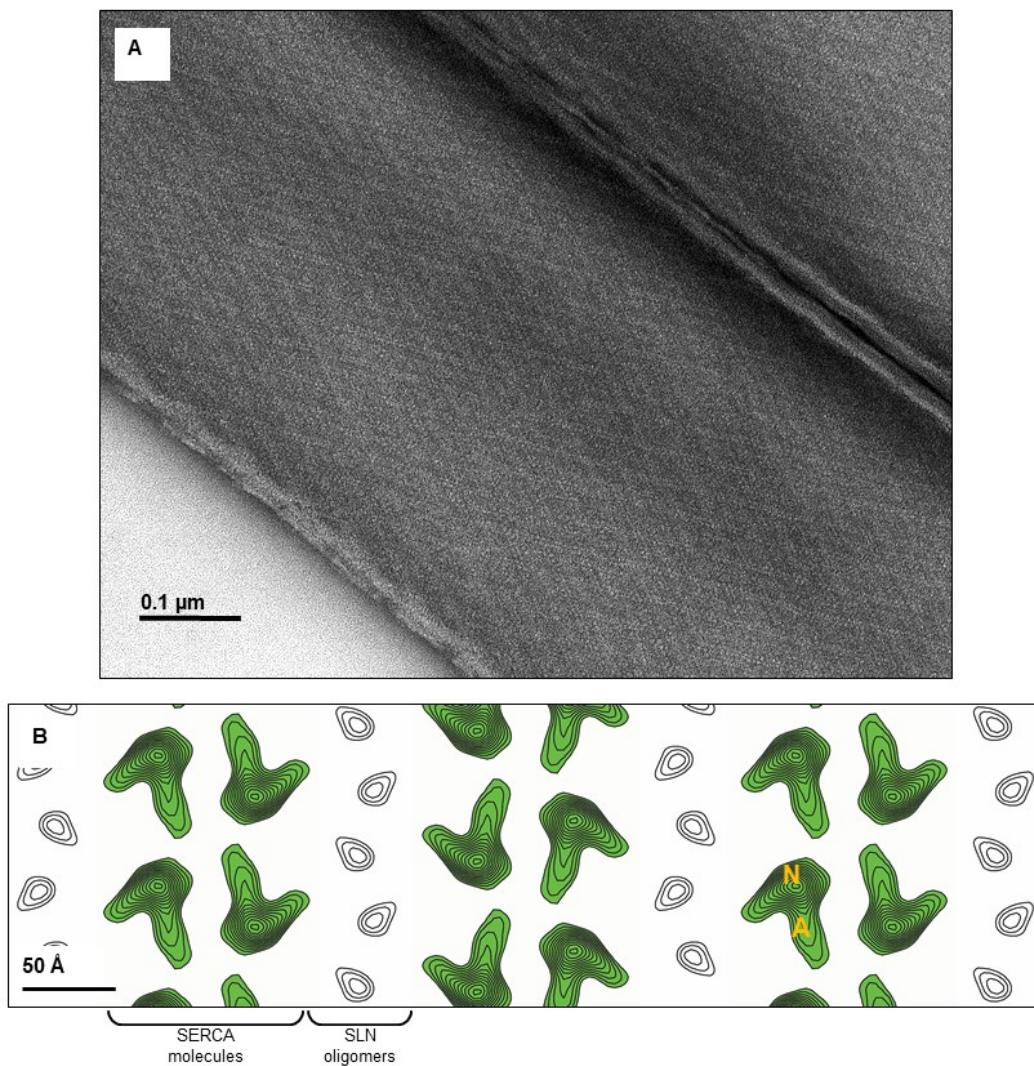
F**igure 3.3: Two-dimensional crystals of SERCA and wild-type SLN.** (A) Negatively stained image of two side-by-side crystals. The central crystal is a flattened cylinder approximately 0.5 μm wide, with the two independent lattices (one from each side of the crystal) appearing as diagonal arrays in the image. The scale bar is 0.1 μm. (B) Projection map from negatively stained 2D crystals of SERCA and wild-type SLN (SERCA density is highlighted in green; SLN density is white contours). The projection map is contoured, showing only positive (continuous lines) densities; each contour level corresponds to 0.25 σ. The relative positions of the nucleotide binding (N) and actuator (A) domains of SERCA are indicated.

The level of detail required for the structural characterization of a SERCA-SLN complex in a membrane environment demanded the use of frozen-hydrated specimens. In the case of PLN (10), we focused on SERCA co-crystals with the Lys^{27}-to-Ala gain-of-function mutant because the abundance of crystals facilitated data collection. Indeed, we initially pursued the Asn^{4}-to-Ala mutant of SLN for this same reason. However, the direct observation of an SLN oligomer required that we image co-crystals of wild-type SLN. Images from frozen-hydrated co-crystals displayed computed diffraction to 15 Å, which improved to approximately 8.5 Å with the averaging of multiple datasets in the $p22_12_1$ space group (**Table 3.1 & Figure 3.4A**). The projection map for wild-type SLN revealed an oligomeric density (**Figure 3.4B**) that was similar to previous observations for PLN (10, 11). However, despite the quality of the data, it was unclear how many SLN molecules were present in the oligomer density. A comparison of the frozen-hydrated projection maps for SERCA-PLN and SERCA-SLN crystals revealed a slightly more compact density for SLN. An interesting difference in the SERCA-SLN crystals was the presence of an additional density adjacent to transmembrane segment M3 of SERCA (**Figure 3.4C**). The additional density was well resolved in the projection map for wild-type SLN co-crystals, which included 34 images and an excellent overall phase residual (**Table 3.1**). Moreover, this feature was uniquely observed in wild-type SLN co-crystals and has not been observed in any co-crystals containing PLN, including wild-type and the Ile^{40}-to-Ala and Lys^{27}-to-Ala mutants of PLN (10, 11).

	wtSLN
Number of images	34
Cell parameters	a = 346.8Å
	b = 70.5 Å
	γ = 90.2 °
Weighted phase residual	14.8 °

Table 3.1: Summary of crystallographic data for frozen-hydrated two-dimensional co-crystals of SERCA and SLN.
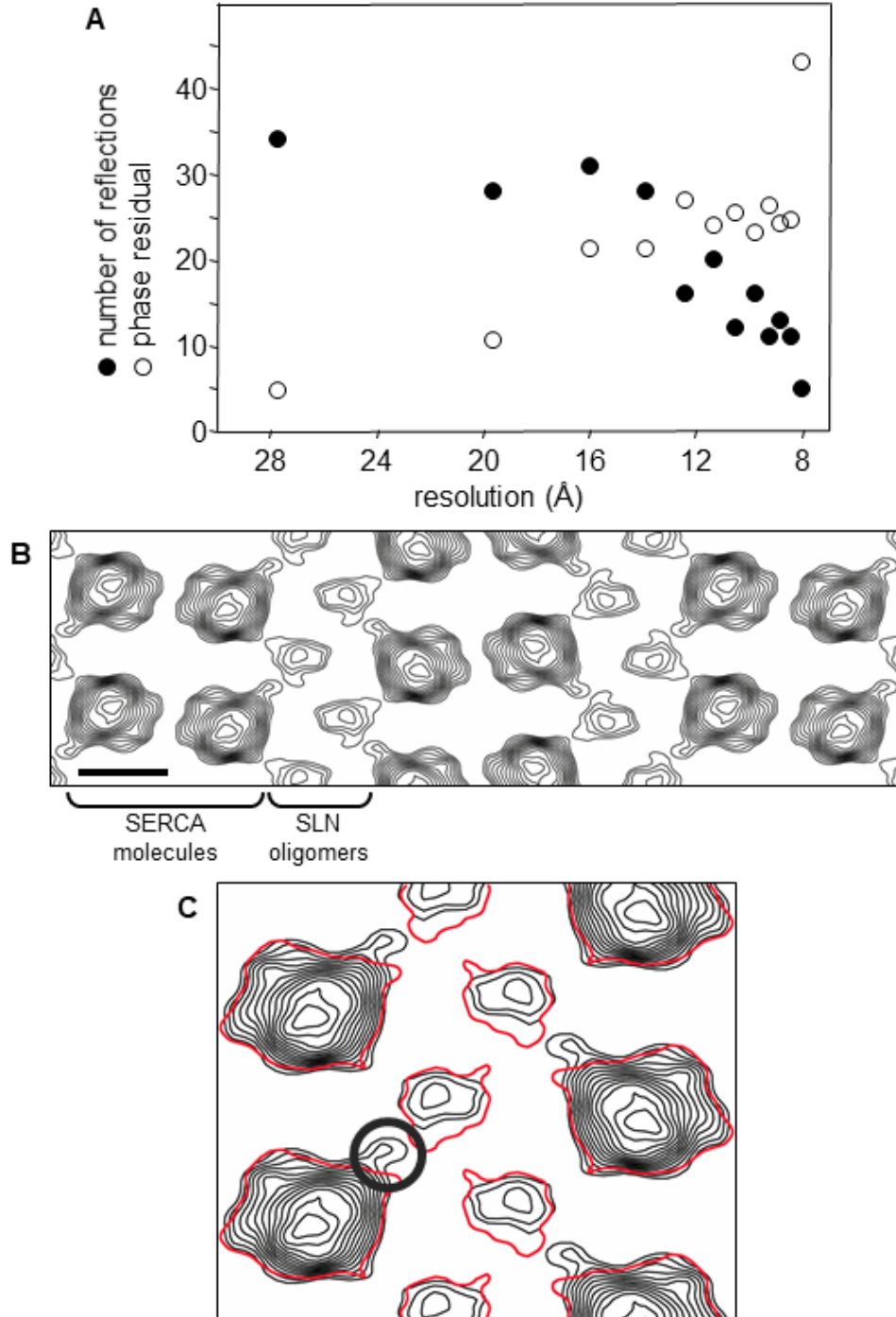
Figure 3.4: Two-dimensional crystals of SERCA and wild-type SLN. (A) Negatively stained image of two side-by-side crystals. The central crystal is a flattened cylinder approximately 0.5 μm wide, with the two independent lattices (one from each side of the crystal) appearing as diagonal arrays in the image. The scale bar is 0.1 μm. (B) Projection map from negatively stained 2D crystals of SERCA and wild-type SLN (SERCA density is highlighted in green; SLN density is white contours). The projection map is contoured, showing only positive (continuous lines) densities; each contour level corresponds to 0.25 σ. The relative positions of the nucleotide binding (N) and actuator (A) domains of SERCA are indicated.

98

We next sought a more definitive interpretation of the density associated with the SLN oligomer. As a first approach, we integrated and compared the densities corresponding to the PLN pentamers and SLN oligomers in their respective co-crystals. The total density in projection maps corresponding to the PLN pentamer (Figure 6 in (10)) and the SLN oligomer (**Figure 3.4**) was calculated (**Table 3.2**) and compared to the molecular weights for SLN and PLN. Since the density and molecular weight ratios were in excellent agreement and the PLN density is known to be a pentamer (10), we concluded that the oligomeric state of SLN was consistent with a pentamer. To better visualize the SLN pentamer, we enhanced the high-resolution terms of the cryo-EM density projection map by applying a negative *B*-factor (temperature factor) of 500 Å^2 during Fourier synthesis (**Figure 3.5**). The application of a negative *B*-factor is a standard approach for restoring high-resolution information in cryo-EM density maps. The SLN density resolved into a five-lobed pentamer following the truncation of Fourier data at 8.5 Å to minimize the contribution of noise in the map and temperature factor sharpening to improve the contrast and detail for the SLN density. Compared to PLN (10), there were shared and unique features of the SLN projection map. As shared features, both the PLN and SLN densities interacted with the same region of SERCA (transmembrane segment M3) and deviated from the expected five-fold symmetry of a pentamer. As unique features, the SLN density was clearly more pentameric in shape and had a central depression consistent with a central pore. There was an additional density that appeared to connect SERCA and the SLN pentamer, which was consistent with an SLN monomer bridging the interaction.

Projection Map	Integration of Oligomer density	Ratio[b]	Molecular weight	Ratio[c]
PLN[a]	41674 A.U		6108 Da	
wtSLN	25234 A.U	0.61	3761 Da	0.62
Asn[4]-Ala SLN	26929 A.U	0.65	3718 Da	0.61

[a] Projection map from glaves et al, 2011

[b] Ratio of the integradated density for SLN versus PLN for the projection maps indicated.

[c] Ratio of the molecular weights for SLN versus PLN

Table 2: Densities associated with PLN and SLN oligomers.
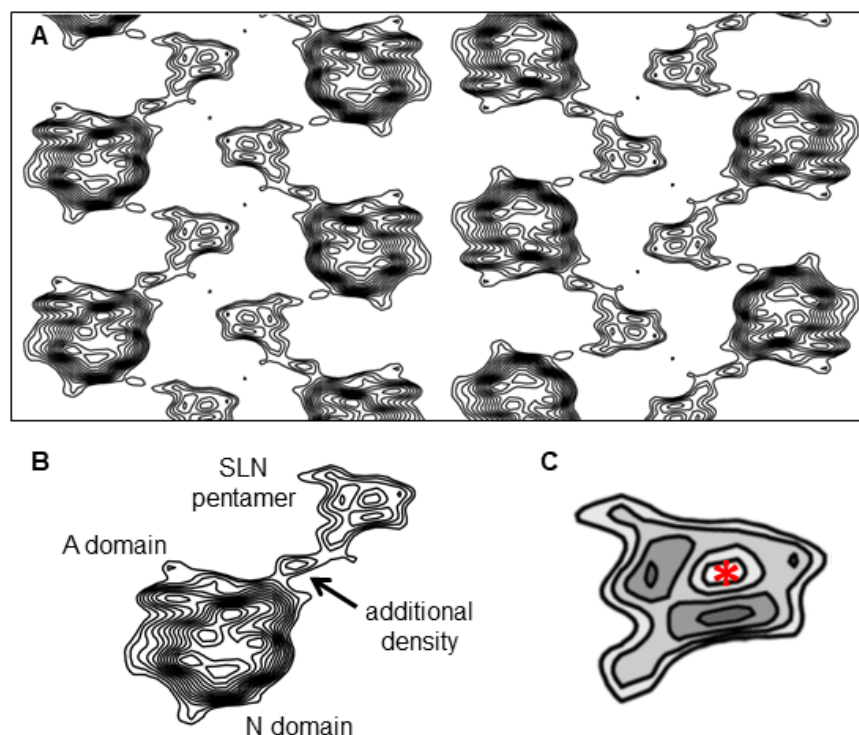
Figure 3.5: The projection map for SERCA in the presence of wild-type SLN recalculated with an applied negative *B*-factor. (A) In the sharpened projection map, the contrast and level of detail are enhanced for both SERCA and SLN. (B) A close-up view of the density associated with SLN. The size and shape of the SLN densities are now compatible with a pentamer, and there is an additional density adjacent to transmembrane segment 3 (M3) of SERCA. (C) The overall shape of the SLN density is consistent with a pentamer, though individual monomers are not resolved. There is a central depression in the SLN density (asterisk), further supporting pentameric architecture.

3.3.3 – Molecular model of the SERCA-SLN complex

Molecular models of the SLN pentamer and the SERCA-SLN heterodimeric complex were generated using protein-protein docking and MD simulations to examine these complexes without the constraints of crystal contacts. For the SLN pentamer, the initial model was constructed based on the symmetric structure of the PLN pentamer (PDB ascension code **2KYV** (26)); however, the relaxed structure following MD simulation deviated from the expected structure of a symmetric SLN pentamer (**Figure 3.6A**). The molecular model was elongated, asymmetric, and appeared to be a complex between an SLN dimer and an SLN trimer. Nonetheless, the *en face* view of the molecular model for the SLN pentamer (**Figure 3.6B**) closely matched the density for the SLN pentamer in the projection map from 2D crystals (**Figure 3.5C**). The Leu-Ile repeat that forms the core of the PLN pentameric assembly is relatively conserved between SLN and PLN (**Figure 3.1**). The SLN residues involved (Leu[10], Ile[14], Ile[17], Leu[21], Leu[24], and Ser[28]) compare favourably with the PLN resides implicated

in pentamer formation (Ile[33], Leu[37], Ile[40], Leu[44], Ile[47], and Leu[51]). However, the SLN residues formed complementary interfaces that separately stabilized an SLN dimer and trimer (**Figure 3.6C**), which together form the SLN pentamer. The model offers an explanation for the reduced stability of the SLN pentamer compared to PLN, and the observation of lower molecular weight species by SDS-PAGE (i.e., monomers & dimers rather than a pentamer). The arrangement of the complementary interfaces in the molecular model also suggests that SLN may be capable of forming an additional oligomeric assembly, such as a hexamer.
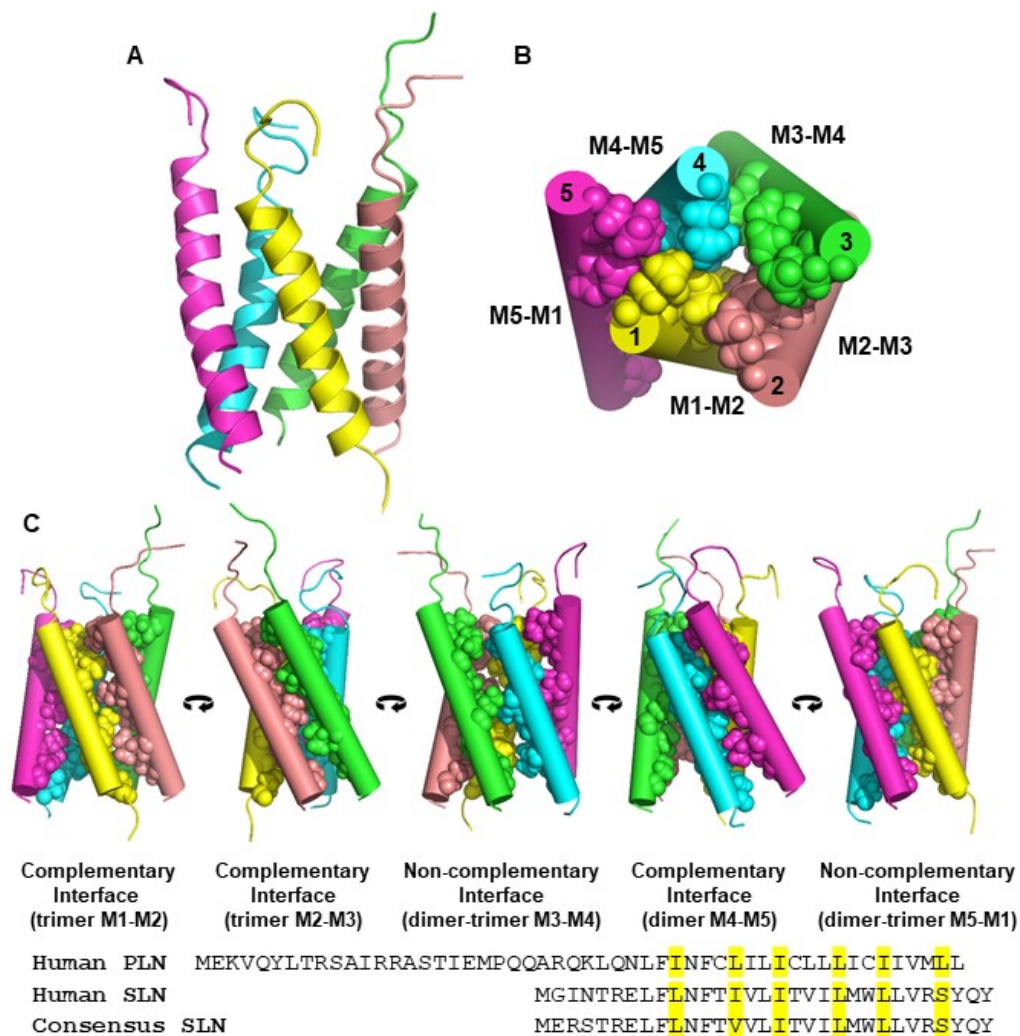
Figure 3.6: Molecular model for the SLN pentamer. (A) Side view of the model with the SLN monomers shown in cartoon format. (B) *En face* view of the SLN pentamer with the helices shown as cylinders and residues Leu[10], Ile[14], Ile[17], Leu[21], Leu[24], and Ser[28] shown as spheres and the SERCA-SLN complex (B) generated from protein-protein docking and MD simulations. M1, M2, and M3 appear to form a trimer, and M4 and M5 appear to form a dimer. (C) Side views of the SLN pentamer showing each of the monomer-monomer interfaces. M1-M2, M2-M3, and M4-M5 form complementary hydrophobic interfaces. The non-complementary interfaces between M3-M4 and M5-M1 delineate the SLN dimer and trimer that come together to form the pentamer. A sequence alignment is shown for human PLN, human SLN, and the consensus SLN sequence. The sequence of pentamer interface residues are highlighted in yellow.

The SERCA-SLN heterodimeric complex was constructed based on the interaction of an SLN monomer with transmembrane segment M3 of SERCA in the 2D crystals (**Figure 3.7**). Following protein-protein docking, the SERCA-SLN complex that most closely matched the arrangement in the 2D crystals was selected. This complex was embedded in a lipid bilayer, fully hydrated to mimic physiological conditions, and subjected to 400 ns MD simulations. These conditions allowed for the formation of a stable complex with appropriate packing constraints at the SERCA-SLN molecular interface (**Figure 3.8**). We found that transmembrane segment M3 of SERCA formed a complementary hydrophobic interface with an SLN monomer. The interaction involved the opposite face of SLN's transmembrane helix (residues Leu^8, Phe^{12}, Leu^{16}, & Ile^{20}) and the central region of transmembrane segment M3 of SERCA (Leu^{266}, Val^{269}, & Leu^{273}). In addition, Asn^4 and Arg^6 of SLN were positioned near a cluster of negatively charged residues on M3 of SERCA (Asp^{254}, Glu^{255}, & Glu^{258}), which is comparable to the interaction between Arg^{25} of PLN and Glu^{258} of SERCA (12). There is limited data on mutagenesis of these residues and the impact on SLN function, with the exceptions being Asn^4-to-Ala (**Figure 3.1**) and Leu^8-to-Ala (19). The Asn^4-to-Ala mutation results in a gain of function, while the Leu^8-to-Ala results in a loss of function. A lipid straddles the SERCA-SLN interaction on the luminal side of the membrane. Trp^{23} of SLN interacts with the glycerol backbone of the lipid, appearing to position the lipid headgroup toward the M3-M4 loop of SERCA (**Figure 3.8C**, arrow). This interaction could impact the movement of the M3-M4 loop during the calcium transport cycle, thereby decreasing the turnover rate of SERCA.
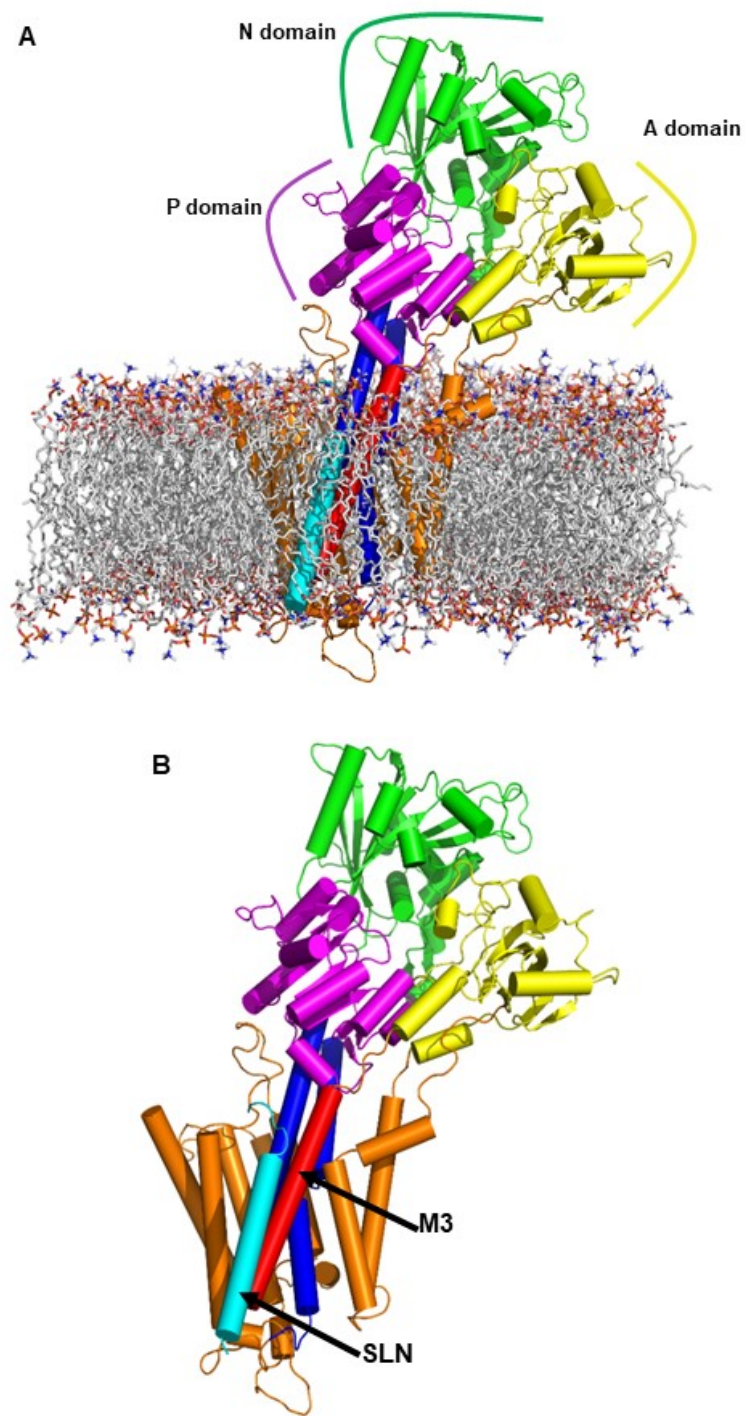
Figure 3.7: Molecular model for the interaction of SERCA with an SLN monomer. Shown are the side view of the full atomistic model (A) and the SERCA-SLN complex (B) generated from protein-protein docking and MD simulations. The lipids are shown in stick representation. SERCA and SLN are in cartoon cylinder representation. SLN is in the foreground (cyan) adjacent to transmembrane segment M3 of SERCA (red). SERCA is coloured according to the domain architecture. The nucleotide binding (N domain; green), actuator (A domain; yellow), and phosphorylation (P domain; magenta) domains are indicated. Also indicated are M3 (red), M4 and M5 (blue), and SLN (cyan).
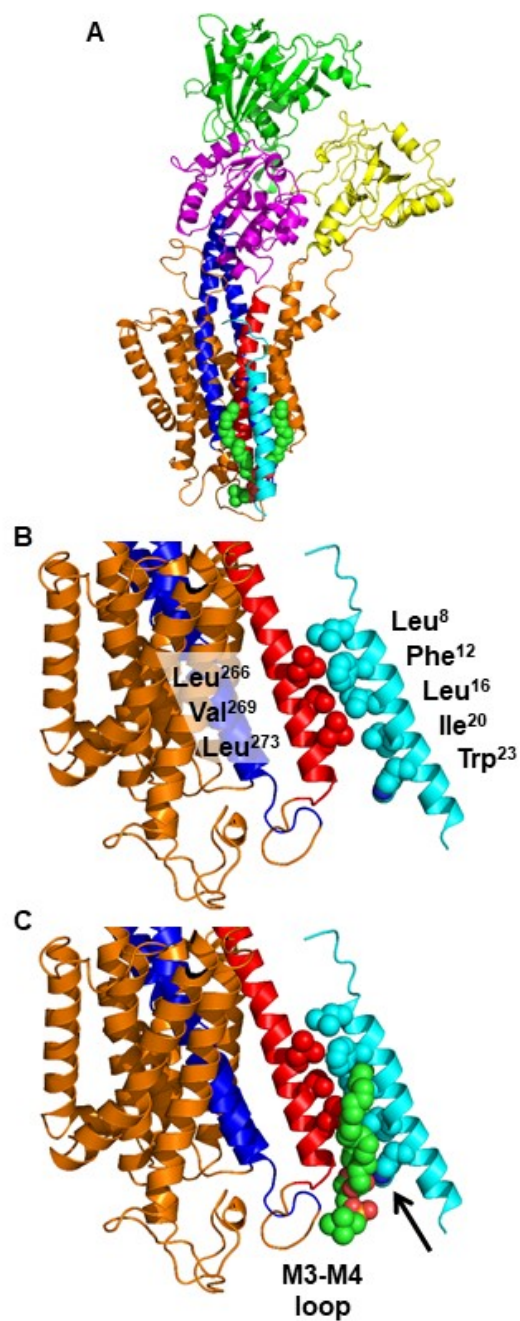
Figure 3.8: Interaction interface between transmembrane segment M3 of SERCA and an SLN monomer. (A) SERCA and SLN are shown in ribbon representation. SERCA is coloured according to the domain architecture, with the N domain (green), A domain (yellow), and P domain (magenta) indicated. Also indicated are M3 (red), M4 and M5 (blue), and SLN (cyan). Green spheres represent a lipid that straddles the interface. (B) The interface between transmembrane segment M3 of SERCA (red) and the SLN monomer (cyan) is shown. The residues involved in the interaction include Leu[266], Val[269], and Trp[272] of M3 and Leu[8], Phe[12], Leu[16], and Ile[20] of SLN. The same interface is shown in (C) with the lipid that straddles the interface on the luminal side of the membrane (spheres representation). The acyl chains straddle each side of the SERCA-SLN interface, and Trp[23] of SLN interacts with the glycerol backbone of the lipid and appears to cause the lipid headgroup to impinge on the M3-M4 loop.

3.4 – Discussion

3.4.1 – The PLN pentamer associates with SERCA

The initial model for SERCA inhibition involved reversible binding of monomeric PLN and the dynamic equilibrium of the monomer between the SERCA-bound and pentameric states (27). In this scenario, the pentamer was considered an inactive storage form of PLN. However, active roles have been proposed for the PLN pentamer, including the modulation of SR cation homeostasis (28) and PKA-mediated phosphorylation (29, 30). The PLN pentamer has also been found to stimulate the V_{max} of SERCA (12, 16, 17, 31–33), which depends on the SERCA-PLN molar ratio and density in the membrane (12, 31). Providing a context for this latter effect was the finding that PLN pentamers associate with SERCA (10–12). We concluded that the PLN pentamer spontaneously associates with SERCA at a site distinct from the inhibitory groove (M2, M6, & M9 of SERCA (8, 34)). The interaction provides an explanation for the stimulation of SERCA's maximal activity, and a molecular model of the complex has been presented (12).

3.4.2 – Functional comparison of SLN and PLN

Does SLN, a PLN homologue, interact with and similarly modulate SERCA maximal activity? To address this question, we focused on large 2D crystals of the SERCA-SLN complex. We characterized wild-type SLN, and a gain-of-function mutant deemed suitable for structure determination. Prior mutagenesis studies of SLN targeted select residues homologous to either the functional interface or the pentamer interface of PLN (19). Essential functional residues such as Leu[8] and Asn[11] (Leu[31] and Asn[34] of PLN) were found to cause loss of function when mutated to alanine, yet mutagenesis revealed little similarity to the pentamer interface of PLN. Nonetheless, SLN has since been shown to form a pentamer (13, 14). In the cytoplasmic domain of SLN, only Thr[5] was studied as a potential site of regulation by phosphorylation. Sequence comparison with PLN indicated that the cytoplasmic domain of SLN consists of the first seven residues (**Figure 3.1**; M[1]GINTRE[7] in humans; M[1]ERSTQE[7] consensus sequence), followed by the transmembrane domain (residues 8-26), and a luminal extension (residues 27-31).

In the present study, we mutated Asn[4] of human SLN to alanine (Asn[4]-to-Ala) and found it to result in a gain of function. Asn[4] of SLN is similar to Lys[27] of human PLN, and both residues deviate from the consensus sequence and are unique to humans (and primates). The gain-of-function behaviour observed for both residues suggests a commonality in function between the membrane-

proximal region of PLN and the N-terminus of SLN, despite low overall sequence conservation. The crystal structure of the SERCA-PLN complex (34) places this residue (Asn[27] in canine PLN; Lys[27] in human PLN) between Phe[809] and Trp[932] of SERCA, which draws this region of PLN closer to M6 and M9 of SERCA. The homologous consensus residue in the crystal structures of the SERCA-SLN complex (8, 9) is Ser[4] of rabbit SLN. This residue does not interact with Phe[809] and Trp[932] of SERCA, which allows a small rotation of the SLN helix in this region. However, this residue is Asn[4] in human SLN, and there is a functional similarity to Asn[27] in canine PLN and Lys[27] in human PLN. Thus, Asn[4] in human SLN may interact with Phe[809] and Trp[932] of SERCA, thereby playing a role in positioning the N-terminus of SLN. Moreover, Asn[4] in SLN and Lys[27] in PLN appear to be evolutionary sequence modifications unique to primates (35).

3.4.3 – SLN as a pentamer

The original mutagenesis studies of SLN did not reveal the expected gain-of-function pattern associated with PLN pentamer destabilization, supporting observations by SDS-PAGE that SLN did not appear to form an oligomeric structure (19). However, several studies have since shown that SLN can form a mixture of oligomeric species including a pentamer (13, 14) and that mutations can depolymerize SLN oligomers (14). Intriguingly, recent studies have reported chloride and phosphate transport properties for SLN (36, 37) and potassium transport properties for PLN (38), which would be consistent with a similar oligomeric architecture for the two proteins. Here, we report the first direct observation of an SLN pentamer in 2D crystals with SERCA. Both the PLN pentamer characterized previously (10), and the SLN density observed in this study (**Figure 3.5**) deviate from the five-fold symmetry expected for a pentamer, though the SLN density is more symmetric than the observed PLN density. The SLN density also displayed a distinct central depression (**Figure 3.5C**) consistent with a channel-like architecture, which was not as well defined for the PLN pentamer (10). The distortion of symmetry for both the PLN and SLN pentamers may be due to noise and the moderate resolution (8.5 Å) of the projection maps, or it may be a modulation of the PLN and SLN pentamers due to the physical interaction with SERCA. This latter point seems plausible, given that molecular dynamics simulations of the SERCA-PLN complex revealed that the symmetry of the PLN pentamer is altered in the interaction with SERCA (12).

Protein-protein docking and MD simulations generated a molecular model of the SLN pentamer. An initial symmetric model of the SLN pentamer was generated based on the docking of SLN monomers to the PLN pentamer (26). Following MD simulations, the final model of the SLN

pentamer was asymmetric and elongated (**Figure 3.6B**), which agreed well with the density map from 2D crystals (**Figure 3.5C**). Moreover, the SLN pentamer appeared to be a complex of a SLN dimer and an SLN trimer, with complementary hydrophobic interfaces that stabilize the dimer and trimer (**Figure 3.6C**).

3.4.4 – Interaction between SERCA and SLN

As with PLN, an interaction between an oligomeric form of SLN and transmembrane segment M3 of SERCA was observed in the 2D crystals. This interaction site does not correspond to the inhibitory groove of SERCA (M2, M6, & M9). This interaction only occurs at a high membrane density and molar excess of PLN relative to SERCA, similar to what is found in cardiac SR membranes (22, 33, 39–42). This packing density of SERCA and PLN is also similar to what is found in large 2D crystals (10, 11), albeit without the regular order induced by the crystal lattice. The molar ratio of SERCA-SLN in the reconstituted proteoliposomes, 1:5, is higher than that found in skeletal muscle SR membranes (19). At these ratios and membrane densities, SLN and PLN monomers and oligomers will be in close proximity to SERCA molecules in their respective SR membranes. Given their close proximity, it is not surprising that the oligomeric forms of these proteins are capable of a physical association with SERCA. In the case of PLN, we found that the interaction of the PLN pentamer with M3 of SERCA correlates with an increase in the V_{max} of SERCA (12). The proximity of this interaction to the calcium entry funnel of SERCA provided an explanation for the increased turnover rate of SERCA – namely, the cytoplasmic domains of PLN lie along the membrane surface and perturb lipid packing adjacent to the calcium access funnel.

The interaction of a pentamer with the M3 accessory site was also observed for 2D crystals of SLN and SERCA. The PLN and SLN pentamers occupy a similar position, though the SLN pentamer has a narrower density profile reflecting its smaller size (**Figure 3.4C**). While the PLN pentamer directly contacts M3 of SERCA, the SLN pentamer is more distant from M3, and an additional density bridges the interaction (**Figure 3.5B**). The additional density has the appearance of an α-helix oriented perpendicular to the membrane plane as visualized by cryo-electron crystallography (43), consistent with an SLN monomer lying adjacent to M3 of SERCA. The question then becomes, why do PLN and SLN interact with this region of SERCA? In the model of the SERCA-PLN pentamer complex, the interaction appears to be stabilized by electrostatic interactions between the cytoplasmic domain of PLN and transmembrane segment M3 of SERCA. Indeed, there is a cluster of negatively charged residues on M3 of SERCA at the cytoplasmic membrane surface (Asp^{254}, Glu^{255}, & Glu^{258}). The

cytoplasmic domain of PLN is highly basic and a stable electrostatic interaction forms between Arg[25] of PLN and Glu[258] of SERCA. There are additional negatively charged residues on M1 along the calcium access funnel of SERCA (Glu[51], Glu[55], Glu[58], & Asp[59]). Complementary to this, there are several positively charged residues in the cytoplasmic domain of PLN (Arg[9], Arg[13], Arg[14], & Lys[27]). Thus, the electrostatic attraction may drive the interaction between the PLN pentamer and SERCA. By comparison, Asn[4] and Arg[6] of human SLN are proximal to Glu[258] of SERCA in a similar manner as Arg[25] of PLN (the consensus SLN sequence includes Ser[4], which is Asn[4] in humans and primates (35)). Thus, SLN may be electrostatically drawn to M3 of SERCA, though this is likely reduced compared to PLN.

In the model of the SERCA-SLN complex, the monomer forms a complementary hydrophobic interface with a central region of transmembrane segment M3 of SERCA (**Figure 3.8**). This interface, combined with the reduced stability of the SLN pentamer, may explain why a SLN monomer was found associated with the M3 site. As stated above, the residues involved are on the opposite face of the SLN transmembrane helix (Leu[8], Phe[12], Leu[16], & Ile[20]) compared to the residues that stabilize the model of the SLN pentamer (Leu[10], Ile[14], Ile[17], Leu[21], Leu[24], & Ser[28]), and the SLN monomer appears to form a more direct interface with M3 of SERCA than the PLN pentamer. The different interactions between PLN and SLN and the M3 site of SERCA correlate with distinct functional effects on the V_{max} of SERCA. The PLN pentamer increases the V_{max} of SERCA, while SLN decreases the V_{max} of SERCA. In the model of the SERCA-PLN pentamer complex, a cluster of negatively charged residues on M3 of SERCA attracts the cluster of positively charged residues in the cytoplasmic domain of PLN. This draws the PLN pentamer toward M3, with an interaction-interface that involves two PLN monomers and a lipid acyl chain (12). This places the cytoplasmic domains of PLN proximal to the calcium access funnel of SERCA, without impeding the movement of M3 during the calcium transport cycle. The V_{max} stimulation by the PLN pentamer was attributed to membrane destabilization by the cytoplasmic domain of PLN near the calcium access funnel of SERCA, thereby allowing a more rapid turnover rate (12). This is absent in the SERCA-SLN complex, suggesting that the M3 interaction alone does not stimulate SERCA. Indeed, the model of the SERCA-SLN monomer complex involves a complementary hydrophobic interface, which would be expected to reduce the turnover rate of SERCA by impeding the movement of M3 during the calcium transport cycle. A lipid straddles the SERCA-SLN interface on the luminal side of the membrane and may play a role in mediating the functional effect of SLN. We have previously shown that the unique luminal tail at the C-terminus of SLN (R[27]SYQY[31] sequence) contributes to the decrease in the V_{max}

of SERCA (6). The crystal structures of the SERCA-SLN inhibitory complex (8, 9) and the model of the SERCA-SLN complex presented herein (**Figure 3.7 & 3.8**), suggest that the luminal tail serves to position the transmembrane helix of SLN in the membrane for optimal interaction with SERCA.

Finally, the full complex that interacts with M3 of SERCA involves an SLN monomer that mediates the interaction between the SLN pentamer and M3 of SERCA, though the role of the SLN pentamer in this complex remains unknown. However, compared to PLN, the lower stability of the SLN pentamer combined with the M3 interaction may select for an SLN monomer. Indeed, the molecular models for the SLN pentamer and the SERCA-SLN interaction raise the possibility that the full complex represents a transition state in which the interaction of M3 with an oligomeric form of SLN causes an SLN monomer to dissociate for optimal interaction with M3. Since both the SERCA-PLN (12) and SERCA-SLN (**Figure 3.8**) complexes appear to involve a lipid molecule at the interface, this may explain the dependence of the interaction on high membrane densities and low lipid-to-protein ratios.

3.5 – Experimental procedures

3.5.1 – Materials

The following reagents were of the highest purity available: octaethylene glycol monododecyl ether ($C_{12}E_8$; Barnet Products, Englewood Cliff, NJ); egg yolk phosphatidylcholine (EYPC), phosphatidylethanolamine (EYPE) and phosphatidic acid (EYPA) (Avanti Polar Lipids, Alabaster, AL); reagents used in the coupled enzyme assay (Sigma-Aldrich, Oakville, ON Canada).

3.5.2 – Expression and purification of recombinant SLN

Recombinant SLN was expressed and purified, as previously described (15), with an additional organic extraction step. Following protease digestion of a maltose-binding protein and SLN fusion protein, trichloroacetic acid was added to a final concentration of 6%. This mixture was incubated on ice for a minimum of 20 minutes. The resultant precipitate was collected by centrifugation at 4°C and subsequently homogenized in a mixture of chloroform-isopropanol-water (4:4:1) and incubated at room temperature for 3 hours. The organic phase, highly enriched in recombinant SLN, was removed, dried to a thin film under nitrogen gas and resuspended in 7 M GdnHCl. Reverse-phase HPLC was performed as described (15).

3.5.3 Co-reconstitution of SLN and SERCA

Lyophilized SLN (30 μg or 75 μg) was resuspended in a 75 μl mixture of chloroform : trifluroethanol (2:1) and mixed with lipids (400 μg EYPC, 50 μg EYPE, 50 μg EYPA) from stock chloroform solutions. The peptide-lipid mixture was dried to a thin film under nitrogen gas and desiccated under vacuum overnight. The peptide-lipid mixture was hydrated in buffer (20 mmol/L imidazole pH 7.0; 100 mmol/L KCl; 0.02% NaN$_3$) at 37 °C for 10 min, cooled to room temperature, and detergent-solubilized by the addition of C$_{12}$E$_8$ (0.2 % final concentration) with vigorous vortexing. Detergent-solubilized SERCA was added (500 μg in a total volume of 200 μl) and the reconstitution was stirred gently at room temperature. Detergent was slowly removed by the addition of SM-2 biobeads (Bio-Rad, Hercules, CA) over a 4-hour time course (final ratio of 25 biobeads: 1 detergent w/w). Following detergent removal, the reconstitution was centrifuged over a 20-50% sucrose step-gradient for one hour at 100,000 x g. The resultant layer of reconstituted proteoliposomes was removed, flash-frozen in liquid nitrogen and stored at -80 °C. The final approximate molar ratios were 120 lipid : 2 or 5 SLN: 1 SERCA (16).

3.5.4 – ATPase activity assays of SERCA reconstitutions

ATPase activity of the co-reconstituted proteoliposomes was measured by a coupled enzyme assay over a range of calcium concentrations from 0.1 μmol/L to 10 μmol/L (16, 44). The K$_{Ca}$ (apparent calcium affinity) and V$_{max}$ (maximal activity) were determined by fitting the data to the Hill equation (Sigma Plot software, SPSS Inc., Chicago, IL). Errors were calculated as the standard error of the mean for a minimum of three independent reconstitutions.

3.5.5 – Crystallization of SLN with SERCA

SLN and SERCA were co-reconstituted in the presence of a lipid mixture (final lipid ratio of 8 EYPC:1 EYPA:1 EYPE) that promoted vesicle fusion and crystallization (10, 17, 18). Co-reconstituted proteoliposomes were collected by centrifugation in crystallization buffer (20 mmol/L imidazole pH 7.0, 100 mmol/L KCl, 35 mmol/L MgCl$_2$, 0.5 mmol/L EGTA, 0.25 mmol/L Na$_3$VO$_4$, 30 μmol/L thapsigargin). Note that the sodium orthovanadate (Na$_3$VO$_4$) was converted to decavanadate and immediately added to the crystallization buffer (12). The samples were subjected to four freeze-thaw cycles, followed by incubation at 4°C for up to one week. Three to five days were optimal for the highest frequency and quality of two-dimensional crystals. For initial screening of crystals by negative stain, crystals were adsorbed to carbon-coated grids and stained with 2% uranyl

acetate. The grids were blotted with filter paper and air-dried. Crystals suitable for imaging were adsorbed to holey-carbon grids and plunge-frozen in liquid ethane.

3.5.6 – Electron microscopy of frozen-hydrated SERCA and SLN co-crystals

Crystals were imaged in a Tecnai F20 electron microscope (Thermo-Fisher Scientific, Eindhoven, Netherlands) in the Microscopy and Imaging Facility (University of Calgary) or a JEOL 2200FS electron microscope (JEOL Ltd., Tokyo, Japan) in the Electron Microscopy Facility (National Institute for Nanotechnology, University of Alberta and National Research Council of Canada). A standard room temperature holder was used for negatively stained samples, and a Gatan 626 cryoholder (Gatan Inc., Pleasanton, CA) was used for frozen-hydrated samples. The microscope was operated at 200 kV accelerating voltage, and low-dose images were recorded at a magnification of 50,000x. The best films were digitized at 6.35 μm/pixel with a Nikon Super Coolscan 9000 followed by pixel averaging to achieve a final resolution of 2.54 Å/pixel. All data were recorded with defocus levels of 0.5-2 μm with an emphasis on low-defocus images for frozen-hydrated samples (0.5 to 1.0 μm).

3.5.7 – Data processing

The MRC image processing suite was used for images of frozen-hydrated SERCA-SLN crystals (47). Two rounds of unbending were performed prior to extracting amplitudes and phases from each image. Data was then corrected for the contrast transfer function using the program PLTCTFX (48). Common phase origins for merging were determined in the $p22_12_1$ plane group using ORIGTILT with reflections of signal-to-noise ratio (IQ) <4. For averaging, data were weighted based on IQ including data with IQ <7, and the corresponding phase residuals represent the inverse cosine of the figure of merit from this averaging. Projection maps were calculated by Fourier synthesis from the averaged data using the CCP4 software suite (49).

3.5.8 – Molecular modelling of SLN pentamer and SLN bound to SERCA

The hybrid solution and solid-state NMR structure of the PLN pentamer (PDB accession code **2KYV**) and the structure of SLN (PDB accession code **3W5A**) were used as templates for the construction of an atomistic model of the SLN pentamer. SLN monomers were aligned to each PLN monomer position in the structure of the PLN pentamer. The resultant model of the SLN pentamer was subjected to 5,000 steps of energy minimization. The crystal structure of SERCA1a in the

E2•MgF$_4^{2-}$ state (PDB accession code **1WPG**) and the structure of SLN (PDB accession code **3W5A**) were used as templates for the construction of an atomistic model of the SERCA-SLN complex. The model of the SERCA-SLN complex was guided by the relative positions of SERCA and the SLN monomer in projection maps of the large 2D crystals (**Figure 3.5**). Protein-protein docking simulations identified an appropriate binding interface between the M3 helix of SERCA and the SLN monomer using ClusPro (50). The resulting docked orientations were clustered and compared against the 2D crystallographic data to select the most appropriate M3-SLN complex. The model of the SERCA-SLN complex was then subjected to 5,000 steps of energy minimization.

3.5.9 – Molecular dynamics simulations of the SLN pentamer and SERCA-SLN complex

The SLN pentamer and SERCA-SLN complex served as starting models to obtain structures of these complexes at physiologically relevant simulation conditions. Based on previous studies of the E2 state of SERCA (51), we modeled transport site residues Glu^{309}, Glu^{771} and Glu^{908} as protonated and residue Asp^{800} as ionized. Both complexes were inserted in a pre-equilibrated 150 Å x 150 Å bilayer of POPC:POPE:POPA lipids (8:1:1). This lipid-protein system was solvated using TIP3P water molecules with a minimum margin of 15 Å between the protein and the edges of the periodic box in the z-axis, and K+ and Cl- ions were added (KCl concentration of ~0.1 mmol/L). Molecular dynamics (MD) simulations of the fully solvated complexes were performed using NAMD 2.12 (52) with periodic boundary conditions (53), particle mesh Ewald (54, 55), a nonbonded cut-off of 9 Å, and a 2 fs time step. The CHARMM36 force field topologies and parameters were used for the proteins (56), lipids (57), waters, and ions. The NPT ensemble was maintained with a Langevin thermostat (310K) and an anisotropic Langevin piston barostat (1 atm). The systems were first subjected to energy minimization, followed by gradually warming up of the system for 200 ps. This procedure was followed by 10 ns of equilibration with backbone atoms harmonically restrained using a force constant of 10 kcal mol^{-1} Å^{-2}. The MD simulations of the complexes were continued without restraints for 400 ns (**Figure 3.9**).
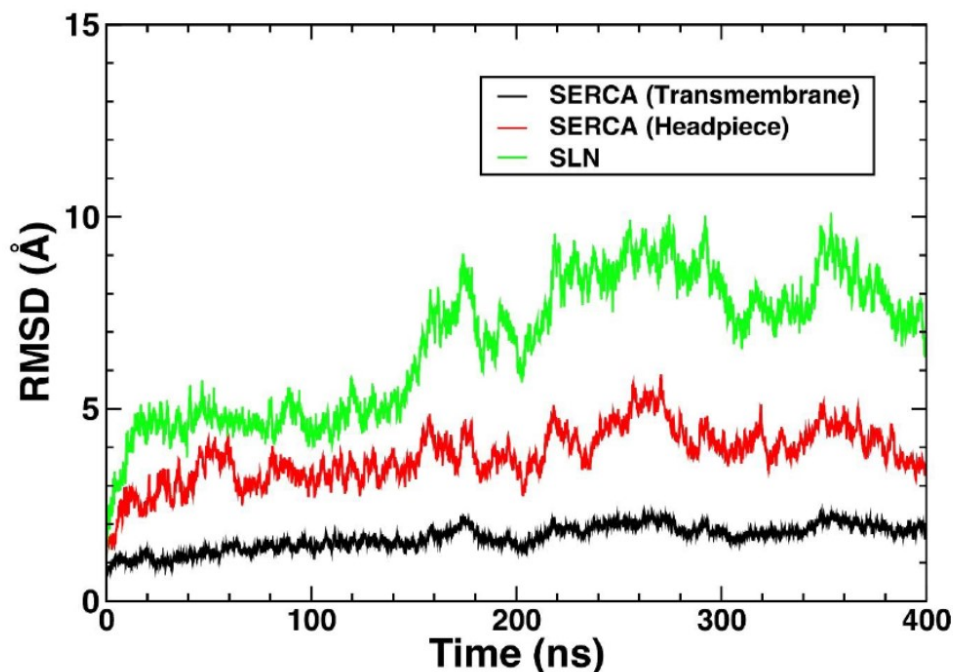
Figure 3.9: Time-dependent changes in the RMSD for the SLN monomer and SERCA in MD simulations of the heterodimeric complex.

3.6 – Acknowledgements

3.6.1 – Author contributions

JPG, JOP, and PAG performed the research, analyzed data, and contributed to the writing and editing of the manuscript; MJL contributed to the design and analysis of the data, and editing of the manuscript; LMEF performed and analyzed the protein-protein docking and molecular dynamics simulations; HSY designed the research, analyzed the data, and wrote the manuscript.

3.6.2 – Acknowledgements

3.7 – Conflict of interest

There is no conflict of interest in the work reported in this manuscript

3.8 – References

1.   Goodsell, D. S., Autin, L., and Olson, A. J. (2019) Illustrate: Software for Biomolecular Illustration. *Structure*. 10.1016/j.str.2019.08.011

2.   Anderson, D. M., Anderson, K. M., Chang, C.-L., Makarewich, C. A., Nelson, B. R., McAnally, J. R., Kasaragod, P., Shelton, J. M., Liou, J., Bassel-Duby, R., and Olson, E. N. (2015) A Micropeptide Encoded by a Putative Long Noncoding RNA Regulates Muscle Performance. *Cell*. **160**, 595–606

3.   Anderson, D. M., Makarewich, C. A., Anderson, K. M., Shelton, J. M., Bezprozvannaya, S., Bassel-Duby, R., and Olson, E. N. (2016) Widespread control of calcium signaling by a family of SERCA-inhibiting micropeptides. *Sci. Signal.* **9**, ra119 LP-ra119

4.   Nelson, B. R., Catherine A. Makarewich, Douglas M. Anderson, Benjamin R. Winders, Constantine D. Troupes, F. W., Reese, A. L., McAnally, J. R., Chen, X., Kavalali, E. T., Cannon, S. C., Houser, S. R., Bassel-Duby, R., and Olson, E. N. (2016) A peptide encoded by a transcript annotated as long noncoding RNA enhances SERCA activity in muscle. *Science (80-.).*

5.   Bal, N. C., Maurya, S. K., Sopariwala, D. H., Sahoo, S. K., Gupta, S. C., Shaikh, S. A., Pant, M., Rowland, L. A., Bombardier, E., Goonasekera, S. A., Tupling, A. R., Molkentin, J. D., and Periasamy, M. (2012) Sarcolipin is a newly identified regulator of muscle-based thermogenesis in mammals. *Nat. Med.* **18**, 1575

6.   Gorski, P. A., Glaves, J. P., Vangheluwe, P., and Young, H. S. (2013) Sarco(endo)plasmic Reticulum Calcium ATPase (SERCA) Inhibition by Sarcolipin Is Encoded in Its Luminal Tail. *J. Biol. Chem. .* **288**, 8456–8467

7.   Sahoo, S. K., Shaikh, S. a., Sopariwala, D. H., Bal, N. C., and Periasamy, M. (2013) Sarcolipin protein interaction with Sarco(endo)plasmic reticulum CA 2+ ATPase (SERCA) Is distinct from phospholamban protein,and only sarcolipin can promote uncoupling of the serca pump. *J. Biol. Chem.* **288**, 6881–6889

8.   Winther, A.-M. L., Bublitz, M., Karlsen, J. L., Møller, J. V, Hansen, J. B., Nissen, P., and Buch-Pedersen, M. J. (2013) The sarcolipin-bound calcium pump stabilizes calcium sites exposed to the cytoplasm. *Nature*. **495**, 265

9.   Toyoshima, C., Iwasawa, S., Ogawa, H., Hirata, A., Tsueda, J., and Inesi, G. (2013) Crystal

structures of the calcium pump and sarcolipin in the Mg2+-bound E1 state. *Nature.* **495**, 260

10.   Glaves, J. P., Trieber, C. a., Ceholski, D. K., Stokes, D. L., and Young, H. S. (2011) Phosphorylation and mutation of phospholamban alter physical interactions with the sarcoplasmic reticulum calcium pump. *J. Mol. Biol.* **405**, 707–723

11.   Stokes, D. L., Pomfret, A. J., Rice, W. J., Glaves, J. P., and Young, H. S. (2006) Interactions between Ca2+-ATPase and the Pentameric Form of Phospholamban in Two-Dimensional Co-Crystals. *Biophys. J.* **90**, 4213–4223

12.   Glaves, J. P., Primeau, J. O., Espinoza-Fonseca, L. M., Lemieux, M. J., and Young, H. S. (2019) The Phospholamban Pentamer Alters Function of the Sarcoplasmic Reticulum Calcium Pump SERCA. *Biophys. J.* **116**, 633–647

13.   Hellstern, S., Pegoraro, S., Karim, C. B., Lustig, A., Thomas, D. D., Moroder, L., and Engel, J. (2001) Sarcolipin, the Shorter Homologue of Phospholamban, Forms Oligomeric Structures in Detergent Micelles and in Liposomes. *J. Biol. Chem.* **276**, 30845–30852

14.   Autry, J. M., Rubin, J. E., Pietrini, S. D., Winters, D. L., Robia, S. L., and Thomas, D. D. (2011) Oligomeric interactions of sarcolipin and the Ca-ATPase. *J. Biol. Chem.* **286**, 31697–31706

15.   Douglas, J. L., Trieber, C. a., Afara, M., and Young, H. S. (2005) Rapid, high-yield expression and purification of Ca2+-ATPase regulatory proteins for high-resolution structural studies. *Protein Expr. Purif.* **40**, 118–125

16.   Trieber, C. A., Douglas, J. L., Afara, M., and Young, H. S. (2005) The Effects of Mutation on the Regulatory Properties of Phospholamban in Co-Reconstituted Membranes†. *Biochemistry.* **44**, 3289–3297

17.   Trieber, C. A., Afara, M., and Young, H. S. (2009) Effects of Phospholamban Transmembrane Mutants on the Calcium Affinity, Maximal Activity, and Cooperativity of the Sarcoplasmic Reticulum Calcium Pump. *Biochemistry.* **48**, 9287–9296

18.   Buck, B., Zamoon, J., Kirby, T. L., DeSilva, T. M., Karim, C., Thomas, D., and Veglia, G. (2003) Overexpression, purification, and characterization of recombinant Ca-ATPase regulators for high-resolution solution and solid-state NMR studies. *Protein Expr. Purif.* **30**, 253–261

19.   Odermatt, A., Becker, S., Khanna, V. K., Kurzydlowski, K., Leisner, E., Pette, D., and MacLennan, D. H. (1998) Sarcolipin Regulates the Activity of SERCA1, the Fast-twitch Skeletal Muscle Sarcoplasmic Reticulum Ca2+-ATPase . *J. Biol. Chem.* . **273**, 12360–12369

20.   Kimura, Y., Asahi, M., Kurzydlowski, K., Tada, M., and MacLennan, D. H. (1998)

Phospholamban Domain Ib Mutations Influence Functional Interactions with the Ca2+-ATPase Isoform of Cardiac Sarcoplasmic Reticulum . *J. Biol. Chem.* . **273**, 14238–14241

21. Toyofuku, T., Kurzydlowski, K., Tada, M., and MacLennan, D. H. (1994) Amino acids Glu2 to Ile18 in the cytoplasmic domain of phospholamban are essential for functional association with the Ca(2+)-ATPase of sarcoplasmic reticulum. *J. Biol. Chem.* . **269**, 3088–3094

22. Ferrington, D. A., Yao, Q., Squier, T. C., and Bigelow, D. J. (2002) Comparable Levels of Ca-ATPase Inhibition by Phospholamban in Slow-Twitch Skeletal and Cardiac Sarcoplasmic Reticulum. *Biochemistry*. **41**, 13289–13296

23. Waggoner, J. R., Huffman, J., Griffith, B. N., Jones, L. R., and Mahaney, J. E. (2004) Improved expression and characterization of Ca2+-ATPase and phospholamban in High-Five cells. *Protein Expr. Purif.* **34**, 56–67

24. Maurer, A., and Fleischer, S. (1984) Decavanadate is responsible for vanadate-induced two-dimensional crystals in sarcoplasmic reticulum. *J. Bioenerg. Biomembr.* **16**, 491–505

25. Dux, L., and Martonosi, A. (1983) Two-dimensional arrays of proteins in sarcoplasmic reticulum and purified Ca2+-ATPase vesicles treated with vanadate. *J. Biol. Chem.* . **258**, 2599–2603

26. Verardi, R., Shi, L., Traaseth, N. J., Walsh, N., and Veglia, G. (2011) Structural topology of phospholamban pentamer in lipid bilayers by a hybrid solution and solid-state NMR method. *Proc. Natl. Acad. Sci.* **108**, 9101 LP – 9106

27. Kimura, Y., Kurzydlowski, K., Tada, M., and MacLennan, D. H. (1997) Phospholamban Inhibitory Function Is Activated by Depolymerization. *J. Biol. Chem.* . **272**, 15061–15064

28. Smeazzetto, S., Tadini-Buoninsegni, F., Thiel, G., Berti, D., and Montis, C. (2016) Phospholamban spontaneously reconstitutes into giant unilamellar vesicles where it generates a cation selective channel. *Phys. Chem. Chem. Phys.* **18**, 1629–1636

29. Wittmann, T., Lohse, M. J., and Schmitt, J. P. (2015) Phospholamban pentamers attenuate PKA-dependent phosphorylation of monomers. *J. Mol. Cell. Cardiol.* **80C**, 90–97

30. Ceholski, D. K., Trieber, C. a., Holmes, C. F. B., and Young, H. S. (2012) Lethal, hereditary mutants of phospholamban elude phosphorylation by protein kinase A. *J. Biol. Chem.* **287**, 26596–26605

31. Reddy, L. G., Cornea, R. L., Winters, D. L., McKenna, E., and Thomas, D. D. (2003) Defining the Molecular Components of Calcium Transport Regulation in a Reconstituted Membrane System. *Biochemistry*. **42**, 4585–4592

32. Afara, M. R., Trieber, C. A., Glaves, J. P., and Young, H. S. (2006) Rational Design of Peptide Inhibitors of the Sarcoplasmic Reticulum Calcium Pump. *Biochemistry*. **45**, 8617–8627

33. Ceholski, D. K., Trieber, C. a., and Young, H. S. (2012) Hydrophobic imbalance in the cytoplasmic domain of phospholamban is a determinant for lethal dilated cardiomyopathy. *J. Biol. Chem.* **287**, 16521–16529

34. Akin, B. L., Hurley, T. D., Chen, Z., and Jones, L. R. (2013) The structural basis for phospholamban inhibition of the calcium pump in sarcoplasmic reticulum. *J. Biol. Chem.* **288**, 30181–30191

35. Gaudry, M. J., Jastroch, M., Treberg, J. R., Hofreiter, M., Paijmans, J. L. A., Starrett, J., Wales, N., Signore, A. V, Springer, M. S., and Campbell, K. L. (2017) Inactivation of thermogenic UCP1 as a historical contingency in multiple placental mammal clades. *Sci. Adv.* **3**, e1602878–e1602878

36. Becucci, L., Guidelli, R., Karim, C. B., Thomas, D. D., and Veglia, G. (2007) An Electrochemical Investigation of Sarcolipin Reconstituted into a Mercury-Supported Lipid Bilayer. *Biophys. J.* **93**, 2678–2687

37. Becucci, L., Guidelli, R., Karim, C. B., Thomas, D. D., and Veglia, G. (2009) The role of sarcolipin and ATP in the transport of phosphate ion into the sarcoplasmic reticulum. *Biophys. J.* **97**, 2693–2699

38. Smeazzetto, S., Schröder, I., Thiel, G., and Moncelli, M. R. (2011) Phospholamban generates cation selective ion channels. *Phys. Chem. Chem. Phys.* **13**, 12935–12939

39. Negash, S., Chen, L. T., Bigelow, D. J., and Squier, T. C. (1996) Phosphorylation of Phospholamban by cAMP-Dependent Protein Kinase Enhances Interactions between Ca-ATPase Polypeptide Chains in Cardiac Sarcoplasmic Reticulum Membranes. *Biochemistry*. **35**, 11247–11259

40. Colyer, J., and Wang, J. H. (1991) Dependence of cardiac sarcoplasmic reticulum calcium pump activity on the phosphorylation status of phospholamban. *J. Biol. Chem.* . **266**, 17486–17493

41. Brittsan, A. G., Carr, A. N., Schmidt, A. G., and Kranias, E. G. (2000) Maximal Inhibition of SERCA2 Ca2+ Affinity by Phospholamban in Transgenic Hearts Overexpressing a Non-phosphorylatable Form of Phospholamban . *J. Biol. Chem.* . **275**, 12129–12135

42. Mishra, S., Gupta, R. C., Tiwari, N., Sharov, V. G., and Sabbah, H. N. (2002) Molecular mechanisms of reduced sarcoplasmic reticulum Ca2+ uptake in human failing left ventricular myocardium. *J. Hear. Lung Transplant.* **21**, 366–373

43. Henderson, R., and Unwin, P. N. T. (1975) Three-dimensional model of purple membrane obtained by electron microscopy. *Nature.* **257**, 28–32

44. Warren, G. B., Toon, P. a, Birdsall, N. J., Lee, a G., and Metcalfe, J. C. (1974) Reconstitution of a calcium pump using defined membrane components. *Proc. Natl. Acad. Sci. U. S. A.* **71**, 622–626

45. Young, H. S., Jones, L. R., and Stokes, D. L. (2001) Locating Phospholamban in Co-Crystals with Ca2+-ATPase by Cryoelectron Microscopy. *Biophys. J.* **81**, 884–894

46. Young, H. S., Rigaud, J. L., Lacapère, J. J., Reddy, L. G., and Stokes, D. L. (1997) How to make tubular crystals by reconstitution of detergent-solubilized Ca2(+)-ATPase. *Biophys. J.* **72**, 2545–2558

47. Crowther, R. A., Henderson, R., and Smith, J. M. (1996) MRC Image Processing Programs. *J. Struct. Biol.* **116**, 9–16

48. Toyoshima, C., Yonekura, K., and Sasabe, H. (1993) Contrast transfer for frozen-hydrated specimens II. Amplitude contrast at very low frequencies. *Ultramicroscopy.* **48**, 165–176

49. Potterton, E., McNicholas, S., Krissinel, E., Cowtan, K., and Noble, M. (2002) The CCP4 molecular-graphics project. *Acta Crystallogr. Sect. D.* **58**, 1955–1957

50. Kozakov, D., Hall, D. R., Xia, B., Porter, K. A., Padhorny, D., Yueh, C., Beglov, D., and Vajda, S. (2017) The ClusPro web server for protein–protein docking. *Nat. Protoc.* **12**, 255

51. Espinoza-Fonseca, L. M., Autry, J. M., Ramírez-Salinas, G. L., and Thomas, D. D. (2015) Atomic-Level Mechanisms for Phospholamban Regulation of the Calcium Pump. *Biophys. J.* **108**, 1697–1708

52. Phillips, J. C., Braun, R., Wang, W., Gumbart, J., Tajkhorshid, E., Villa, E., Chipot, C., Skeel, R. D., Kalé, L., and Schulten, K. (2005) Scalable molecular dynamics with NAMD. *J. Comput. Chem.* **26**, 1781–1802

53. Weber, W., Hünenberger, P. H., and McCammon, J. A. (2000) Molecular Dynamics Simulations of a Polyalanine Octapeptide under Ewald Boundary Conditions: Influence of Artificial Periodicity on Peptide Conformation. *J. Phys. Chem. B.* **104**, 3668–3675

54. Darden, T., York, D., and Pedersen, L. (1993) Particle mesh Ewald: An N·log(N) method for Ewald sums in large systems. *J. Chem. Phys.* **98**, 10089–10092

55. Essmann, U., Perera, L., Berkowitz, M. L., Darden, T., Lee, H., and Pedersen, L. G. (1995) A smooth particle mesh Ewald method. *J. Chem. Phys.* **103**, 8577–8593

56. Best, R. B., Zhu, X., Shim, J., Lopes, P. E. M., Mittal, J., Feig, M., and MacKerell, A. D. (2012)

Optimization of the Additive CHARMM All-Atom Protein Force Field Targeting Improved Sampling of the Backbone ϕ, ψ and Side-Chain χ1 and χ2 Dihedral Angles. *J. Chem. Theory Comput.* **8**, 3257–3273

57. Klauda, J. B., Venable, R. M., Freites, J. A., O'Connor, J. W., Tobias, D. J., Mondragon-Ramirez, C., Vorobyov, I., MacKerell, A. D., and Pastor, R. W. (2010) Update of the CHARMM All-Atom Additive Force Field for Lipids: Validation on Six Lipid Types. *J. Phys. Chem. B.* **114**, 7830–7843

"Pages bleed forgiveness
Every word handwritten"

B. Fallon – 2008

Chapter 4 – Conformational diversity and memory in the interaction of sarcolipin with the sarcoplasmic reticulum calcium pump SERCA

J.O. Primeau[1] and Howard S. Young[1]

Running Title: SERCA conformation influences SLN interaction.

[1]Department of Biochemistry, University of Alberta, Edmonton, Alberta, Canada

Preface

This chapter represents the culmination of the work to be submitted for publication in Journal of Biological Chemistry. JOP performed the research, analyzed data, and wrote the manuscript. HSY advised the research, analyzed the data, and edited the manuscript**. This manuscript has been adapted and edited from its original state to fit the format of the thesis presented.**

4.1 – Summary

Calcium reuptake during muscle relaxation is carried out by the sarco(endo)plasmic reticulum Ca^{2+}- ATPase (SERCA), which transports calcium from the cytosol of myocytes into the lumen of the sarcoplasmic reticulum. SERCA is traditionally described as an E1-E2 enzyme that follows the Post-Albers scheme for metal ion transport. The E1-E2 conformational cycle includes a low-affinity E2 state and a metal-bound high-affinity E1 state, where metal transport is mediated through ATP hydrolysis and a phosphoenzyme intermediate. Following metal transport and phosphate release, the enzyme can enter its low-affinity state and begin the cycle anew. The regulation of this process is essential for normal muscle contraction/relaxation cycles. A family of tissue-specific transmembrane peptides regulate SERCA, collectively referred to as the "Regulins." Notable regulins that have been reported to regulate SERCA function include sarcolipin (SLN) in skeletal muscle and phospholamban (PLN) in ventricular muscle. SLN and PLN are most well known for altering the calcium transport properties of SERCA, but recent reports are beginning to elucidate a much more complex regulatory role for calcium transport. In particular, PLN is now understood to elicit both an inhibitory and a stimulatory effect on SERCA calcium transport, dependent on the calcium concentration and the oligomeric state of PLN. The revelation of conformational memory and multiple modes of interaction further complicates our understanding of PLN-SERCA regulation. Previous work concluded that substrate-dependent starting conditions 'lock' SERCA in particular conformational states from which the transport cycle can be initiated. This results in distinct changes in the kinetic properties of SERCA in the presence of PLN. In the present study, we investigate the effects of substrate-dependent starting conditions for SERCA in the presence and absence of SLN. We found that SLN's regulatory function is dependent on the initial conformational state of SERCA. We infer that SLN is capable of multiple modes of interaction with SERCA, depending on SERCA's conformational state, and that once a particular mode of interaction is engaged, it persists during multiple turnover events. These observations are consistent with conformational memory in the interaction between SERCA and SLN, thus providing insights into the physiological role of SLN and its regulatory effect on SERCA transport activity.

4.2 – Introduction

The sarco(endo)plasmic reticulum Ca^{2+}-ATPase (SERCA) is crucial for calcium-reuptake during the relaxation cycle following muscle contraction (1). SERCA utilizes the energy from ATP to refill the lumen of the sarcoplasmic reticulum (SR) with cytosolic calcium following muscle

contraction. The calcium transport mechanism of SERCA has been extensively studied (2–5) and can be approximated by the Post-Albers scheme of P-type ATPases. In the process of translocating calcium, SERCA undergoes substantial conformational changes that progress through a series of intermediate states (**Figure 4.1**) that alternate between a high-affinity E1 state and a low-affinity E2 state (6). Calcium transport requires the co-operative binding of two calcium ions (E1•Ca) and the hydrolysis of ATP (E1•Ca•ATP → E2-P) to generate the energy required for the large conformational changes that accompany calcium transport. The energy of ATP is captured in the form of a phospho-enzyme intermediate and released through a conformational change that facilitates calcium translocation. Following calcium release (E2P) into the SR lumen, the phosphate is hydrolyzed and released, returning SERCA to a low-affinity E2 state. From this point, SERCA is poised to begin the transport cycle anew. It is important to note that the presence or absence of substrates can be used to poise SERCA in different conformational states (e.g. E2, E2•ATP, E1•Ca) and that the crystal structures of these conformational states have been determined (7).
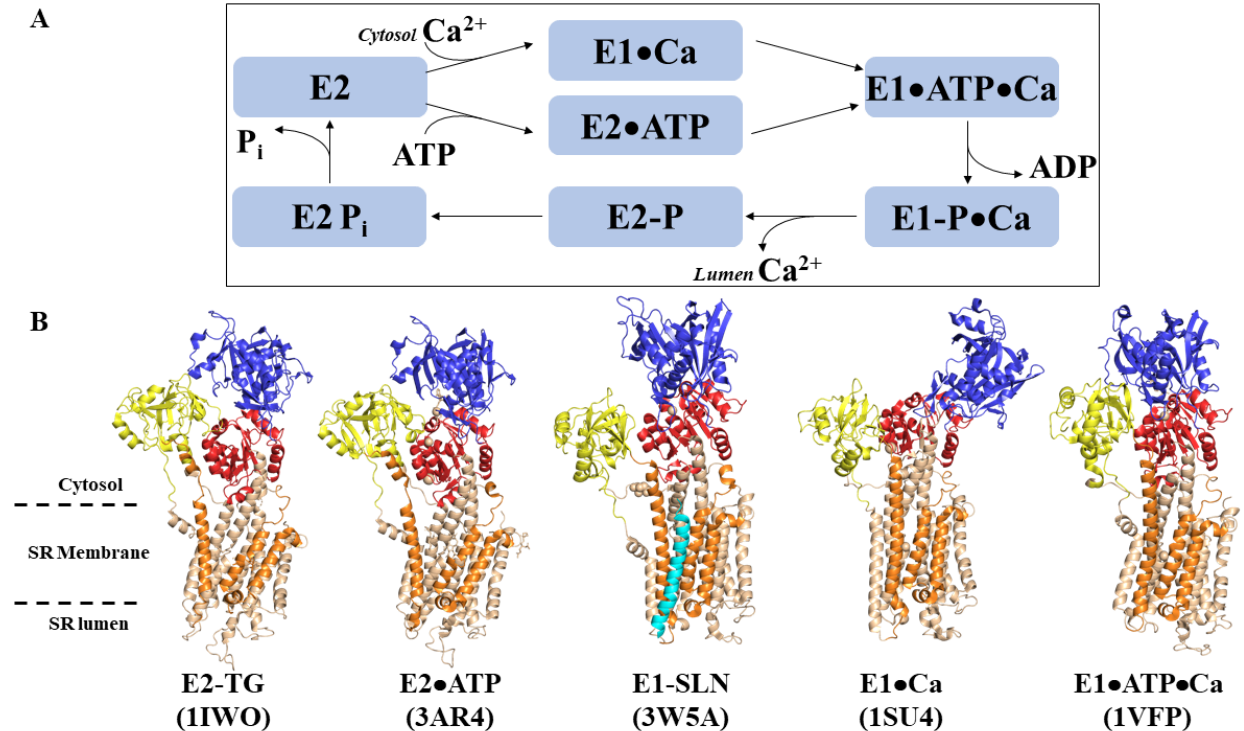
Figure 4.1: SERCA undergoes enormous conformational changes when transporting calcium from the myocyte cytosol to the lumen of the SR. (**A**) A simplified Post-Albers scheme describing E2-E1 conformational changes SERCA undergoes during metal ion translocation. Note there are two substrate-dependent 'pathways' SERCA can take when transitioning from E2 → E1•ATP•Ca. The transition from these states has a global effect on the remaining cycle for calcium transport. (**B**) Crystal structures of SERCA with different substrates bound and with SLN bound. These structures (PDB ascension numbers included) highlight important conformational states SERCA undergoes during calcium transport. Note the large cytoplasmic domain transitioning from an 'open' and 'closed' state and the inhibitory groove opening and forming. Cyan – SLN, blue – SERCA nucleotide binding domain, red – SERCA phosphorylation domain, yellow – SERCA actuator domain, orange – SERCA M2, M6, and M9 TM domains that form the inhibitory groove.

SERCA activity is regulated in muscle cells by a number of tissue-specific small transmembrane proteins (8) including phospholamban (PLN) (9) and DWORF (10) in cardiomyocytes and smooth muscle, and sarcolipin (SLN) (11–13) and myoregulin (MLN) (10) in skeletal fast-twitch muscle. SLN is a 31-residue, largely α-helical integral membrane protein, consisting of a short cytoplasmic domain that contains a purported CAMKII binding site, a transmembrane spanning domain, and a highly conserved luminal tail. SLN regulation of SERCA is inhibitory, acting to reduce the apparent calcium affinity and V_{max} of SERCA. SLN and PLN have been found to interact with SERCA in a groove formed by the transmembrane helices M2, M6, and M9 (14–17). SLN has been traditionally thought to be functionally homologous to PLN (13, 18); however, the mechanism by

which SLN regulates SERCA is distinct from PLN (19–21). The interaction of SERCA with SLN at the 'regulatory groove' stabilizes a novel, calcium-free intermediate E1•SLN (PDB: **3W5A**) that appears poised between the calcium-free E2 and calcium-bound E1 states. The transmembrane portion of SLN mediates this interaction; however, SLN regulation is strongly dependent on the unique, and highly conserved luminal Arg^{27}-Ser-Tyr-Gln-Tyr^{31} sequence of SLN (22).

In addition to SLN's roll in the regulation of calcium homeostasis in skeletal muscle, observations have been made that suggest that SLN also plays a unique role in thermogenesis and energy metabolism (23–26). SLN has been reported to uncouple SERCA ATPase activity from calcium transport by preventing calcium transport into the lumen and promoting a backflow of calcium back into the cytosol during ATP hydrolysis (27). Recent reports suggest that SLN promotes uncoupling through the interaction of SLN's N-terminus with SERCA (28). These uncoupling events are akin to heat-generation observed in the uncoupling event of UCP-1 in brown adipose tissue (29) but instead are located in skeletal muscle, which accounts for approximately 40% of adult body mass.

The crystal structures of SERCA in the presence of SLN revealed a surprising conformation of SERCA – an E1-like state without calcium bound that appeared poised between the E2 and E1 states. SLN stabilization of an E1-like conformation provides a structural mechanism for calcium-slippage. Exposed calcium-binding sites in the E1-like state stabilized by SLN provide a potential explanation for SLN inhibition and/or the uncoupling of calcium transport. Previous work has reported that the conformational state of SERCA influences the interaction with PLN, and this effect persists through the catalytic cycle and multiple turnover events – a process termed 'conformational memory' (30, 31). Pre-incubating SERCA with particular substrates (e.g. ATP or calcium) had a significant effect on the catalytic cycle of SERCA and the E2-E1 transition. Depending on the availability of substrates, SERCA could be poised in a conformation closer to the calcium-free E2 state (no substrates), the calcium-bound E1 state (pre-incubation with calcium), or in between these states (pre-incubation with ATP or ATP + low calcium). This influenced the conformational pathway through the E2-E1 transition of SERCA and moulded future catalytic cycles during continuous enzyme turnover. These differing conformational trajectories were recorded as changes to SERCA's kinetic parameters, with the most notable changes occurring in the co-operative binding of calcium. The next logical step was to determine if this phenomenon is unique to the SERCA-PLN interaction, or is it utilized by the other small regulatory proteins of SERCA (8, 32–34).

We investigated this phenomenon by preincubating co-reconstituted proteoliposomes containing SERCA and SERCA in the presence of SLN with different substrates and measuring the

resultant changes in ATPase activity. Based on previous results with PLN, we expected to see changes in SERCA calcium transport properties in the presence of SLN, depending on the starting conditions. These changes might shed light on the current hypothesis that SLN causes SERCA uncoupling as a mechanism for heat generation in non-shivering thermogenesis. In addition, the different modes of interaction between SERCA, PLN, and SLN may shed light on the ability of these complexes to exhibit conformational memory during multiple calcium transport cycles depending on how SERCA is poised to initiate turnover.
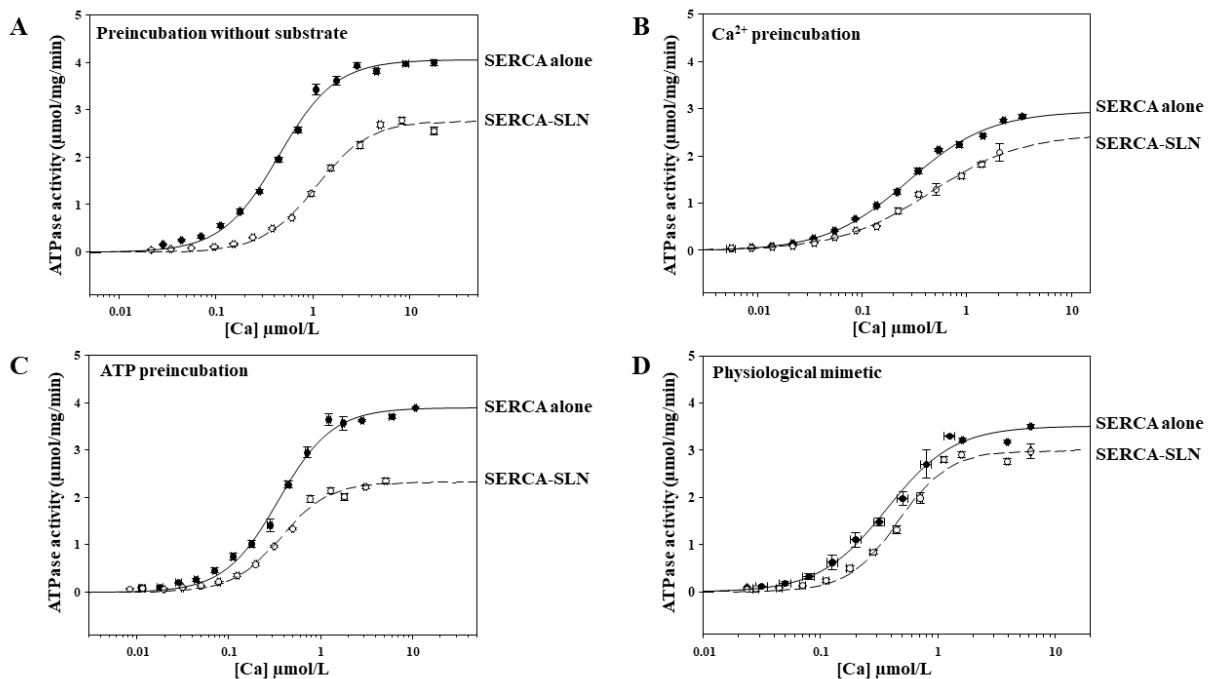
Figure 4.2: ATPase activity of SERCA containing proteoliposomes versus [Ca^{2+}] under different starting and pre-incubation conditions. ATPase activity of co-reconstituted proteoliposomes containing SERCA alone (black lines) or SERCA with SLN (dashed lines). (**A**) ATPase activity of SERCA upon simultaneous addition of ATP and calcium (pre-incubation in the absence of substrates) dubbed the 'traditional' ATPase assay. (**B**) ATPase activity of SERCA pre-incubated with calcium at concentrations ranging from ~0.005 – 10 μmol/L (concentration of calcium indicated on the graph represent the concentration of pre-incubated calcium) and initiated with 4mmol/L ATP. (**C**) ATPase activity of SERCA pre-incubated with 4 mmol/L ATP and initiated with calcium at concentrations ranging from ~0.005 – 10 μmol/L. (**D**) ATPase activity of SERCA preincubated under our emulated physiological conditions, 4mmol/L ATP and 0.1 μmol/L calcium and initiated with calcium at concentrations ranging from ~0.005 – 10 μmol/L. Curves were fitted to experimental data using the Hill equation (V$_{max}$, K$_{Ca}$, and nH values for each curve can be found in **Table 4.1**). Individual data point error bars indicate S.E.M. for a minimum of 3 independent reconstitutions and ATPase activity assays.

4.3 – Results

Human SLN and rabbit SERCA1a were used in these studies. SERCA1a from rabbit skeletal muscle is a facile substitute for human SERCA1a as it is nearly identical in sequence and readily available in large quantities (will be called SERCA from now on). SERCA resides in the SR of myocytes, where the normal substrate conditions include millimolar levels of ATP and nanomolar levels of calcium under resting conditions. Under pathological conditions, the levels of ATP and calcium can change dramatically, having an enormous impact on SERCA function and cellular calcium homeostasis. Thus, it is important to understand the effect of various substrate conditions on the ATPase activity of SERCA.

ATP hydrolysis by SERCA proteoliposomes in the absence and presence of SLN was measured as a function of calcium concentration (0.1μmol/L - 10μmol/L). The calcium concentration indicates [free Ca^{2+}] in solution based on the composition of the assay mix (calculated with CHELATOR (35)). The data were fit to the Hill equation and enzymatic parameters (V_{max}, K_{Ca}, and co-operativity (nH)) were determined based on the resultant curve fits (**Figure 4.2**). Based on previous work (36), the Hill coefficient reflects co-operativity of ion binding to SERCA and it has a theoretical maximum that indicates the number of ion-binding sites being utilized for metal-ion transport across the membrane. For SERCA, this value indicates a theoretical maximum of 2 calcium ions or 2-3 protons. ATP hydrolysis by proteoliposomes containing SERCA with or without SLN was measured and modulated by subjecting the proteoliposomes to differing preincubation conditions before measuring ATPase activity using a coupled-enzyme assay. Kinetic parameters obtained for these conditions have been tabulated in **Table 4.1** and represented graphically in **Figure 4.3**.

		K_{Ca} ($\mu mol/L$)	V_{max} ($\mu mol/min/mg$)	nH
SERCA	Preincubation without substrate	0.46 ± 0.02	4.09 ± 0.06	1.53 ± 0.07
SERCA + SLN		0.68 ± 0.04	3.06 ± 0.06	1.6 ± 0.1
SERCA	Ca^{2+} preincubation	0.27 ± 0.02	2.96 ± 0.07	1.11 ± 0.06
SERCA + SLN		0.45 ± 0.07	2.5 ± 0.1	0.99 ± 0.07
SERCA	ATP preincubation	0.35 ± 0.02	3.89 ± 0.06	1.5 ± 0.1
SERCA + SLN		0.37 ± 0.03	2.32 ± 0.07	1.6 ± 0.2
SERCA	Physiological mimetic	0.37 ± 0.01	3.5 ± 0.1	1.5 ± 0.1
SERCA + SLN		0.46 ± 0.03	3.0 ± 0.1	2.0 ± 0.2

Table 4.1: Kinetic parameters of SERCA and SERCA – SLN co-reconstituted proteoliposomes. Values derived from coupled enzyme assay measurements are tabulated based on substrate preincubation starting conditions. Error measurements are reported as S.E.M.

4.3.1 – Calcium-dependent ATPase activity when initiated with calcium and ATP simultaneously

Co-reconstituted SERCA proteoliposomes in the absence and presence of SLN were subjected to the simultaneous addition of calcium and ATP to initiate ATPase activity (**Figure 4.2A**). This method has been used in the past as the usual ("traditional") method of measuring ATPase activity (37), and it is useful for generating a baseline for comparison. Proteoliposomes containing SERCA alone were found to yield a V_{max} of 4.09 ± 0.06 $\mu mol/min/mg$ while proteoliposomes containing SERCA and SLN were found to yield a $V_{max} = 3.06 \pm 0.06$ $\mu mol/min/mg$. This V_{max} depression was expected based on previous observations (22) and indicated that our proteoliposomes are behaving as previously described. K_{Ca} was found to be 0.46 ± 0.02 $\mu mol/L$ and 0.68 ± 0.04 $\mu mol/L$ for SERCA alone and SERCA with SLN, respectively. The increase in K_{Ca} indicates a decrease in relative calcium affinity of SERCA in the presence of SLN, which is the characteristic feature of SERCA inhibition. The Hill coefficient (nH) for SERCA proteoliposomes in the absence or presence of SLN was 1.5 ± 0.1 and 1.6 ± 0.1, indicating little change to the co-operativity of calcium binding to the enzyme under these conditions.
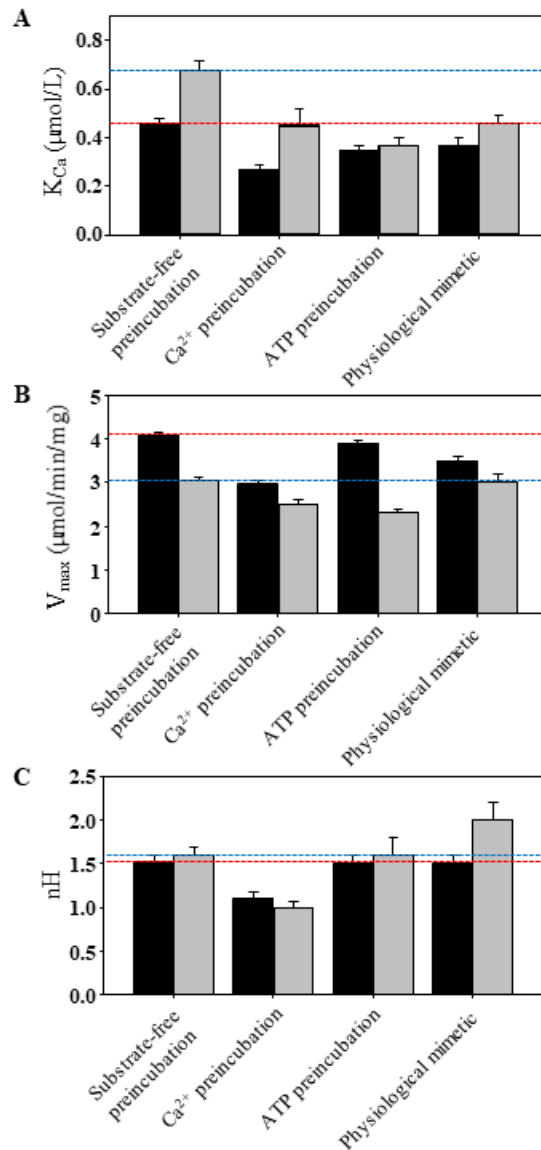
Figure 4.3: Graphical representation of SERCA kinetic parameters under differing starting conditions. Values determined from coupled enzyme assay measurements under differing starting conditions for SERCA alone (Black) and SERCA + SLN (Grey). (**A**) Apparent calcium affinity (K_{Ca}) values: red line represents the reported K_{Ca} for SERCA alone when preincubated in the absence of substrate, and blue line represents the reported K_{Ca} for SERCA + SLN when preincubated in the absence of substrate. Note the trend of SLN increasing the K_{Ca} when co-reconstituted with SERCA. However, under ATP preincubation conditions, we observe a general decrease in K_{Ca} (increase in calcium affinity), and we note that SLN's calcium affinity-altering effect on SERCA has been ablated. (**B**) V_{max} values: red line represents the reported V_{max} for SERCA alone when preincubated in the absence of substrate, and blue line represents the reported V_{max} for SERCA + SLN when preincubated in the absence of substrate. Note how V_{max} values are depressed by roughly the same amount when SERCA is co-reconstituted with SLN regardless of starting substrate. (**C**) Hill coefficient (nH) values: red line represents the reported nH for SERCA alone when preincubated in the absence of substrate, and blue line represents the reported nH for SERCA + SLN when preincubated in the absence of substrate. Note how nH values vary dependent on substrate preincubation, decreasing when preincubated with calcium and increasing when in the presence of SLN under physiological mimetic conditions. All conditions, other than SERCA preincubated in the absence of substrate, report a general increase in calcium affinity. Error bars generated by S.E.M.

4.3.2 – Calcium-dependent ATPase activity when preincubated with calcium

Co-reconstituted proteoliposomes of SERCA in the absence and presence of SLN were preincubated with calcium concentrations ranging from 0.1μmol/L to 10μmol/L before initiating SERCA ATPase activity **(Figure 4.2B)**. A more modest depression in V_{max} was observed between SERCA (2.96 ± 0.07 μmol/mg/min) and SERCA in the presence of SLN (2.5 ± 0.1 μmol/min/mg), compared to the V_{max} depression observed in SERCA when preincubated without substrate. The effect of SLN on the K_{Ca} of SERCA remained indicative of SERCA inhibition under the calcium pre-incubation conditions. However, the observed K_{Ca} values were shifted to higher affinity (0.27 ± 0.02 μmol/L for SERCA alone and 0.45 ± 0.07 μmol/L for SERCA-SLN. Overall, when compared to the SERCA activity when preincubated in the absence of substrate, the K_{Ca} for SERCA decreased by approximately 0.2 μmol/L when preincubated with calcium in the absence and presence of SLN. SERCA co-operativity remained virtually unchanged in the absence and presence of SLN, with an nH value of 1.11 ± 0.06 for SERCA alone and 0.99 ± 0.07 for SERCA in the presence of SLN. In comparison to the co-operativity exhibited by SERCA preincubated in the absence of substrate, we observed an overall decrease in SERCA co-operativity of ΔnH SERCA ($SERCA_{trad} - SERCA_{Ca}^{2+}$) = 0.4 ± 0.1 and ΔnH SERCA-SLN ($SERCA\text{-}SLN_{trad} - SERCA\text{-}SLN_{Ca}^{2+}$) = 0.6 ± 0.2. Consequentially, preincubating the SERCA proteoliposomes with calcium, whether in the absence or presence of SLN, caused an overall increase in the apparent calcium affinity for SERCA (decreased values for K_{Ca}) and a decrease in co-operativity (decreased values for nH), when compared to SERCA activity measurements when preincubated without substrate.

4.3.3 – Calcium-dependent ATPase activity when preincubated with ATP

Proteoliposomes containing SERCA with or without SLN were preincubated in assay buffer containing 4mmol/L ATP, and ATP hydrolysis was initiated with the addition of calcium **(Figure 4.2C)**. The V_{max} values were found to be 3.89 ± 0.09 μmol/min/mg and 2.32 ± 0.07 μmol/min/mg for proteoliposomes containing SERCA in the absence and presence of SLN, respectively. The V_{max} values observed for preincubation with ATP were diminished compared to when SERCA is preincubated in the absence of substrates. However, the depression of SERCA's V_{max} by SLN was preserved, albeit the magnitude was slightly reduced (~25% reduction in V_{max} when preincubated without substrate and ~16% reduction with ATP preincubation; **Table 4.1**). Similarly, the overall co-operativity of SERCA for calcium binding did not change in the absence or presence of SLN (nH

values of 1.5 ± 0.1 for SERCA alone and 1.6 ± 0.2 for SERCA-SLN). In contrast, the effect of SLN on the apparent calcium affinity of SERCA was completely eliminated with ATP preincubation (K_{Ca} of 0.35 ± 0.02 μmol/L for SERCA alone and 0.37 ± 0.03 μmol/L for SERCA-SLN). These measurements indicate that nucleotide preincubation had a small effect on V_{max} and did not significantly alter the co-operativity of SERCA. However, SLN's modulation of calcium-affinity with SERCA was lost as the apparent calcium affinity of SERCA was unaltered by SLN. Of note, this contrasts with the trend seen for PLN where ATP preincubation did not alter SERCA inhibition (30).

4.3.4 – Calcium-dependent ATPase activity with a physiological-mimetic calcium jump

The changes brought about by different preincubation conditions and their divergence from 'baseline' enzymatic parameters prompted further investigation into starting conditions using a more physiological condition. The resting-state condition of a cell includes millimolar concentrations of ATP and nanomolar concentrations of calcium. To mimic this, SERCA and SERCA-SLN proteoliposomes were preincubated with 4 mmol/L ATP and 0.1 μmol/L calcium, near the low end of the cytosolic calcium concentration gradient that myocytes experience ([Ca^{2+}] of 500nmol/L – 1μmol/L). ATPase activity measurements of SERCA and SERCA-SLN proteoliposomes under these conditions were compared to the other starting conditions tested (**Figure 4.2D**). The observed V_{max} depression remained between SERCA and SERCA-SLN proteoliposomes, though it was slightly reduced (V_{max} values of 3.5 ± 0.1 μmol/mg/min and 3.0 ± 0.1 μmol/mg/min, respectively; ~14% depression). The K_{Ca} shift observed between SERCA and SERCA-SLN proteoliposomes was found to be 0.37 ± 0.01 μmol/L and 0.46 ± 0.03 μmol/L, respectively. This small change in the apparent calcium affinity of SERCA was akin to the loss of SLN inhibition observed for the ATP preincubation condition. Under these preincubation conditions, the most significant change occurred in the co-operativity of SERCA. The Hill coefficient for proteoliposomes containing SERCA alone (1.5 ± 0.1) was similar to values for SERCA alone under substrate-free preincubation and ATP preincubation conditions. However, there was an increase in co-operativity (nH = 2.0 ± 0.2) for SERCA in the presence of SLN under the physiological-mimetic conditions. These latter trends (increased co-operativity and reduced SLN inhibition) were similar to previous observations with SERCA in the presence of PLN (30). That said, the regulation of SERCA by SLN seemed to be particularly sensitive to preincubation with ATP.

4.4 – Discussion

4.4.1 – Substrate-dependent conformational states of SERCA

Preincubation of SERCA with or without substrates stabilizes conformational states that span the substrate-free E2 state to the ATP- and calcium-bound E1 state of the calcium transport cycle. An atomic-level description is available for these conformational states, providing a snapshot of the complex conformational changes that SERCA undergoes during these stages of the transport cycle. Previous reports indicate that preincubation with calcium stabilizes a high-affinity E1•Ca conformation (38), preincubation with ATP likely favours a E2•ATP state (3), simultaneous pre-incubation with both ATP and calcium is reported to stabilize the E1•ATP•Ca conformational state (39), and the absence of substrate favours a low-affinity E2 state (40). Based on previous work (30), SERCA's conformational state, dictated by substrate binding, can be poised at different points in the calcium transport cycle. This initial conformational state influences subsequent calcium transport cycles as SERCA undergoes continuous turnover, a behaviour termed conformational memory (31). The conformational memory during SERCA turnover, dependent on the starting substrate conditions, manifests as changes in the kinetic parameters determined from ATPase activity measurements. These subtle differences in activity measurements reflect changes in the positions of the cytoplasmic and transmembrane domains of SERCA that alter calcium transport, ATP hydrolysis, and substrate binding-site dynamics.

The SERCA-SLN structure determined by X-ray crystallography revealed that SLN stabilizes an unexpected calcium-free E1-like state (14, 15) through an interaction with an inhibitory groove in the transmembrane domain of SERCA. A similar structure was also reported for the SERCA-PLN complex (17). In separate findings, our lab has shown that two-dimensional co-crystals of PLN and SERCA naturally associate at a site independent of the inhibitory groove under substrate-free conditions (19). Two-dimensional co-crystals of SERCA and SLN reveal that SLN can also interact with SERCA at a site independent of the inhibitory groove, termed the "accessory site" (41). These interactions are likely dependent on the conformation of SERCA, and the conformation of the transmembrane domain, thus changing the nature of the interaction between SERCA and SLN. These sites are not mutually exclusive and may be occupied at the same time, allowing for both PLN and SLN to persistently associate with SERCA throughout the reaction cycle. The sequential and cooperative binding of two calcium ions to SERCA, and the proximity of the SLN binding site to the

calcium sites, explains the effect of SLN on the apparent calcium affinity (K_{Ca}) and Hill coefficient (nH) measured for SERCA. Similarly, the interaction with the accessory site influences the V_{max} of SERCA (*see* (19) *and* (41)). The data presented here reveal that these SERCA-SLN interactions depend on the conformational state of SERCA and that the effect of SLN on the catalytic cycle of SERCA (V_{max}, K_{Ca}, and nH) must involve distinct binding modes. The effect of SLN and SERCA conformation on the E2-E1 transition may provide insight into the reported 'calcium-slippage' hypothesized for the uncoupling of SERCA by SLN (27).
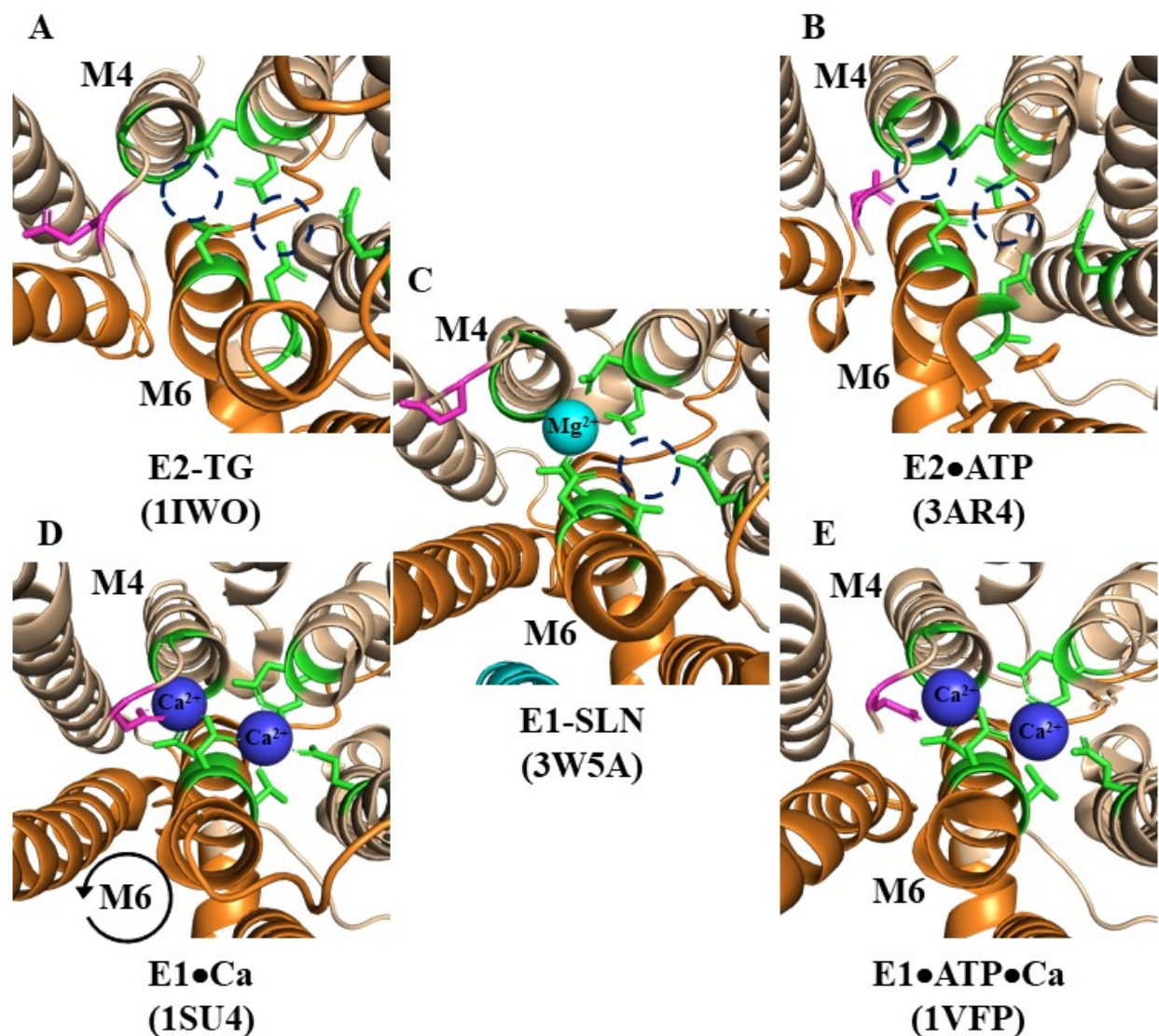
Figure 4.4: The calcium-binding sites in different conformational states of SERCA. SERCA's calcium-binding sites (highlighted by hashed circles) I (right) and II (left) are formed by residues: (I) Asn[768], Glu[771] (M5), Thr[799], Asp[800] (M6) and Glu[908] (M8). (II) Glu[309] (M4), Asn[796], Asp[800] (M6) and backbone carbonyls of Val[304], Ala[305], Ile[307] (M4). Relevant residues coloured green with exception to Glu[309] (purple) and the TM's of the inhibitory groove (orange). (**A**) Calcium-binding sites in the E2 conformation (**1IWO**), hashed circles represent where the placement of Ca^{2+} ions should be relative to E1. (**B**) Calcium-binding residues in the E2•ATP (**3AR4**) conformation. Note the similarity to the E2 conformation. Note Glu[309] is swung out, and M6 is unwound in this conformation. (**C**) Calcium-binding residues in the E1-like state with SLN (cyan α-helix) (**3W5A**). Note the presence of Mg^{2+}(Cyan) and the semi-formed calcium-binding site I formed by rotation of M6. (**D**) Calcium-binding residues in the E1•Ca conformation (**1SU4**). Note M6 rotated (arrow) into an amicable position to fully form the calcium-binding sites. Note the similarity to E1•SLN and Glu[309] contribution to calcium-binding site II (Blue – Ca^{2+}). (**E**) Calcium-binding residues in the E1•ATP•Ca conformation (**1VFP**). Note the structural similarities to E1•SLN and E1•Ca.

4.4.2 – Promoting E1 by preincubation with calcium

Relative to preincubation in the absence of substrates, all preincubation conditions resulted in changes to SERCA ATPase activity and catalytic parameters. Preincubation of SERCA-SLN proteoliposomes with calcium significantly deviated from the results of the other tested preincubation conditions in that all three kinetic parameters were altered (V_{max}, nH, and K_{Ca}). SERCA's overall maximal activity (V_{max}) and co-operativity (nH) were lower, though SERCA's sensitivity to V_{max} depression by SLN was preserved. The most significant effect was on the ability of SLN to alter the apparent calcium affinity (K_{Ca}) of SERCA. The overall affinity of SERCA for calcium was higher, though a change in K_{Ca} was still present indicative of SERCA inhibition by SLN. Interestingly, a previous study with PLN under calcium preincubation conditions observed the same overall effects on V_{max}, nH, and K_{Ca} (30), though SLN inhibition of SERCA is much lower.

Calcium preincubation gradually shifts SERCA equilibrium from predominantly an E2 conformation at low calcium to predominantly an E1 conformation at high calcium. Of course, this equilibrium also depends on the affinities of SLN and PLN for SERCA and their ability to stabilize the E2 state (i.e. inhibit SERCA). The simplest explanation for the observed results is that SLN has a lower affinity for SERCA than PLN and that the addition of calcium more easily overcomes SLN binding to SERCA. However, the results are from steady-state activity measurements where SERCA is continuously cycling. Thus, the persistence of this effect is surprising because SLN should be able to access the inhibitory site on SERCA as it passes through an appropriate conformational state during turnover (e.g. E2). The reduced inhibitory effect suggests that SLN remains associated with SERCA, though it may not fully access the inhibitory site. Both PLN and SLN stabilize a calcium-free E1-like state of SERCA, as evident in the X-ray crystal structures. Thus, the inhibition of SERCA involves the transition from this calcium-free state (E1-like) to the calcium bound state (E1), which is a considerably smaller conformational change compared to the expected E2-to-E1 transition thought to be associated with PLN and SLN inhibition of SERCA. SLN stabilizes SERCA in an E1-like state with a calcium-binding site that looks very similar to the E1•Ca conformation of site I and site II (**Figure 4.4B**). M4 and M6 are both extended, but Glu[309], a critical residue for both site formation and gating of the calcium access funnel, is swung out and restricting calcium access to the binding sites. The increase in calcium affinity and lack of co-operativity, even in the presence of SLN (lower nH near a value of 1), suggests that the binding sites are completely formed and functioning independently. The reduced SERCA inhibition and loss of co-operativity indicate that SERCA is

poised to bind calcium and that SLN and SERCA remain associated in a way that cannot access the full inhibitory complex.

4.4.3 – Promoting the E2•ATP state by preincubation with nucleotide

Canonically, SLN alters the calcium affinity of SERCA upon association with the inhibitory groove of SERCA and lowers the V_{max} possibly through lower affinity interactions with SERCA independent of the inhibitory groove (41). As described above, preincubation with calcium lowers the co-operativity of calcium binding to SERCA in the absence and presence of SLN. Conversely, preincubation with ATP yielded expected levels of SERCA co-operativity in the absence and presence of SLN, and the expected V_{max} depression in the presence of SLN. Preincubation with ATP increased the apparent calcium affinity of SERCA and eliminated inhibition in the presence of SLN (no K_{Ca} shift). ATP preincubation would stabilize SERCA in the E2•ATP **(3AR4)** (42) conformational state with structural highlights including closed calcium access (Glu^{309} swung in; **Figure 4.4B**), a compact cytoplasmic domain, and a deep inhibitory groove that could accommodate SLN (**Figure 4.1B**). ATP binding is expected to promote a more compact and less dynamic cytoplasmic domain (43), which ultimately lowers the activation energy for calcium binding and phosphoenzyme formation. This state may not be compatible with SLN inhibition (E1-like state), which persists during steady-state turnover of SERCA.

The inclusion of SLN under these conditions gave very perplexing results. With no shift in either co-operativity or calcium affinity, it appears that SLN cannot interact with the inhibitory groove and form the inhibitory complex with SERCA. However, the E2•ATP state is known to be accessible to PLN (16, 44–46), and presumably to SLN as well. Moreover, preincubating SERCA and SLN in the absence of substrates promotes the formation of the calcium-free E2 state of SERCA, which is thought to be structurally similar to E2•ATP but perhaps more dynamic. Under this latter condition, SLN can shift the apparent calcium affinity of SERCA characteristic of the inhibitory complex. How these states differ, and why one is amenable to SLN inhibition (E2) and the other (E2•ATP) is not, remains unknown. Despite the similar X-ray crystal structures for these two states (40, 42) our data suggest that they are distinct.

SERCA in the presence of SLN still exhibits a reduced V_{max}, indicating that SLN is still interacting with SERCA and influencing ATPase activity. Previous works in our lab showed that PLN and SLN can alter the maximal activity (V_{max}) of SERCA when interacting with an accessory site (19, 41). In this previous work, we determined that the V_{max} effects of PLN and SLN in association with

137

SERCA is linked to the interaction of oligomeric forms of PLN and SLN at a site independent of the inhibitory groove. The V_{max} depression demonstrated under the ATP preincubation conditions indicates that there is still an SLN association with SERCA, which is consistent with an association of oligomeric SLN with the accessory site, transmembrane segment M3 (41).

4.4.4 – Mimicking physiological conditions and promoting an E1-like state?

In the presence of ATP, the addition of calcium initiates phosphoenzyme formation in a concentration-dependent manner through the formation of an E1•ATP•Ca intermediate (47) with the catalytic complex being E1~P•ADP•Ca. To investigate the E2•ATP to E1•ATP•Ca transition, we chose conditions that mimic the physiological resting state by preincubating our proteoliposomes at saturating ATP [4mmol/L ATP] and resting cytosolic calcium [0.1 mmol/L Ca^{2+}]. Crystal structures of the E2•ATP and E1•ATP•Ca conformations indicate compact states that are quite different from one another (**Figure 4.1B and 4.4E**). The progression from E2•ATP → E1•ATP•Ca involves large movements of the cytoplasmic domains and rearrangement of the transmembrane helices to form the first calcium-binding site. Once the first site becomes occupied, the second site forms co-operatively and becomes occupied, followed by phosphoenzyme formation and calcium occlusion. The calcium-free E1-like state, identified in the SERCA-SLN crystal structures (14, 15), appears to lie along the trajectory from E2•ATP → E1•ATP•Ca. SLN inhibits SERCA by stabilizing this intermediate state between E2 and E1, and the physiological starting conditions should poise SERCA in a conformation suitable for the formation of the SERCA-SLN inhibitory complex.

Under these preincubation conditions, SERCA has a slower turnover rate (lower V_{max}) and a higher affinity for calcium (lower K_{Ca}). The presence of SLN had the expected effect on V_{max} and K_{Ca}, decreasing both the turnover rate (V_{max}) and calcium affinity (K_{Ca}), though these effects were diminished (**Figure 4.3**). Interestingly, our results indicated that the presence of SLN under these conditions increased the co-operativity of calcium-binding to SERCA (nH 1.5 → 2.0). Typically, the addition of SLN to SERCA is not associated with an increase in co-operativity, though the homologous regulatory peptide PLN does increase SERCA's co-operativity in (48). Also, a similar trend was observed for PLN, where preincubation under physiological conditions further increased co-operativity (30) (nH 1.6 → 3.0). Assuming SLN stabilizes SERCA in an E1-like state poised to bind calcium, this is the framework for considering the impact on the co-operativity of calcium binding to SERCA. The two conditions that alter co-operativity are calcium preincubation (loss of co-

operativity) and the more physiological ATP/calcium preincubation (enhanced co-operativity). The former condition likely promotes a SERCA-SLN complex that is closer to the fully formed calcium-binding sites found in the E1•Ca or E1•ATP•Ca state (**Figure 4.4**). The latter condition likely promotes a SERCA-SLN complex that is E1-like but further from the E1•ATP•Ca state, requiring binding of the first calcium ion before the second site can fully form. It is interesting to note that these conditions still possess some inhibitory capacity (ΔK_{Ca} in the presence of SLN) and that the preincubation with ATP has the largest impact on SLN inhibition of SERCA (no ΔK_{Ca}).

Ultimately, substrate-dependent initial conformations appear to dictate SLN's mode of interaction with SERCA. Substrate-dependent conformational dynamics influence the conformation of SERCA's TM domain, directly changing the inhibitory groove and/or accessory site of SERCA. The question becomes: can SLN interact with one or both sites and how does SERCA's substrate-dependent conformation influence this interaction. We observe that SLN can occupy both the inhibitory and accessory sites on SERCA (**Figure 4.5**) (indicating that the interactions between both sites are not mutually exclusive), as SERCA's V_{max} is a simple indicator for binding of SLN to the accessory site. The E2•ATP starting condition likely reflects SLN interaction at the accessory site, which influences the V_{max} of the enzyme. Following this line of reasoning, SLN was found to influence the stability and formation of the calcium-binding sites and ATP hydrolysis activity of SERCA, which likely involves binding the inhibitory groove of SERCA. The sensitivity of these latter parameters to the starting conformation of SERCA suggests that there are multiple modes of binding between SERCA and SLN and that once a mode of binding is engaged, it persists through steady-state SERCA turnover. This latter concept is consistent with conformational memory – the conformational dynamics that accompany transitions from one SERCA reaction intermediate to the next is not a stochastic process and can be influenced by the conformational states that precede it.
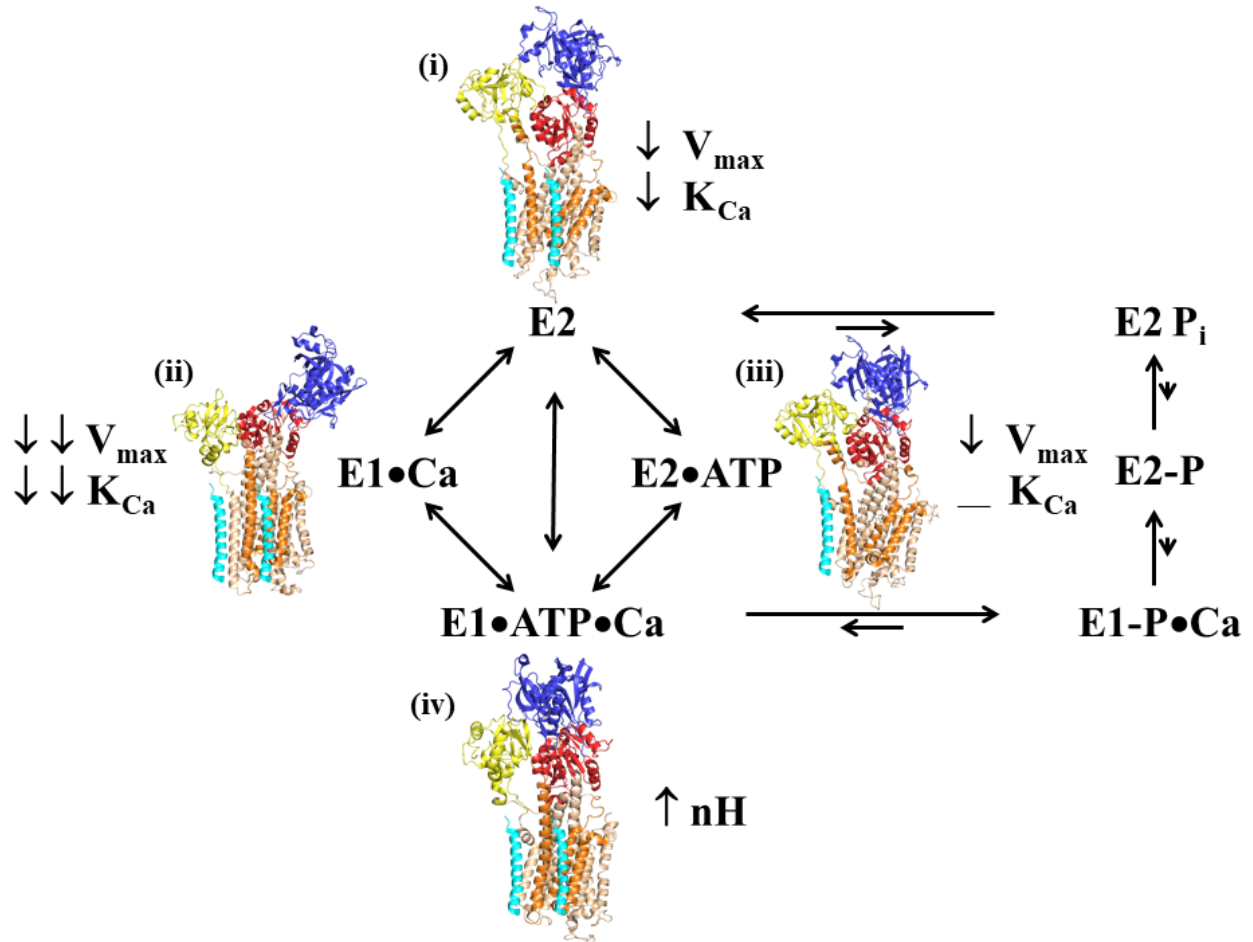
Figure 4.5: The effect of SERCA substrate preincubation on SERCA conformation and SLN regulatory properties. A modified model of E2→E1 conformational changes during calcium transport. Highlighted structures indicate the conformational states stabilized by preincubation with (i) no substrate (ii) calcium (iii) ATP and (iv) 'physiological' [ATP] and low [Ca^{2+}]. Cyan α-helix represents the estimated position of SLN with SERCA in its respective conformational state in either the inhibitory groove (orange) or an accessory site elsewhere. Note that starting conditions stabilize SERCA conformational states and reinforce the path to phosphoenzyme formation to be followed upon cycle completion. Substrate and SLN preincubation have some effect on the conformational dynamics of SERCA, affecting the SERCA calcium transport properties indicated above. The relative changes of V_{max}, K_{Ca}, and nH, to the SERCA-SLN conformation-dependent pathway, are found above (i-iv). SERCA cytoplasmic domain is represented by (red) phosphorylation domain (blue) nucleotide binding domain and (yellow) actuator domain.

4.5 – Experimental procedures

4.5.1 – Materials

All reagents used were of the highest purity available. Reagents used for proteoliposome reconstitution include egg yolk phosphatidylcholine (PC), egg yolk phosphatidic acid (PA) (Avanti Polar Lipids, Alabaster AL), and octaethylene glycol monododecyl ether ($C_{12}E_8$) (Barnet Products, Englewood Cliff, NJ). Reagents used for couple-enzyme ATPase measurements include ATP, NADH, phosphoenolpyruvate, pyruvate kinase, and lactate dehydrogenase (Sigma-Aldrich, Oakville, ON).

4.5.2 – SLN expression and purification

Recombinant SLN was expressed and purified, as previously described (22).

4.5.3 – Rabbit SR purification from white-muscle

Rabbit SR was purified from rabbit hind-leg muscle homogenized in medium 1 (50mmol/L MOPS pH 7.0, 10% sucrose, 10mmol/L EDTA). Homogenized tissue was centrifuged at 15 000 x RCF for 20 minutes, and supernatant was filtered through cheesecloth. The supernatant was then centrifuged at 40 000 x RCF for 90 minutes, and the resulting pellet was resuspended in medium 2 (25mmol/L MOPS pH 7.0, 600 mmol/L KCl). Following homogenization, the mixture was stirred slowly at 4°C for 50 minutes and subsequently centrifuged at 13 000 x RCF for 20 minutes. The mixture separated into three distinct zones, and the middle zone was collected and subsequently centrifuged at 120 000 x RCF for 60 minutes. The resultant pellet was resuspended in medium 3 (10mmol/L MOPS pH 7.0, 30% sucrose) and aliquoted for use.

4.5.4 – SERCA1a purification from rabbit SR

SERCA1a was purified from rabbit hind-leg muscle SR as previously described (49, 50) with the following alterations. 100mg rabbit SR was added to extraction buffer (10mg/mL $C_{12}E_8$, 8mmol/L $CaCl_2$, 50mmol/L MOPS pH 7.0, 5mmol/L DTT, 20% glycerol) and stirred for 15 minutes at 4°C. Extracted SR was centrifuged at 120 000 X RCF for 20 minutes and loaded onto a packed column containing Reactive Green Resin (Sigma-Aldrich, Oakville, ON) equilibrated with extraction buffer. Column was washed with two column volumes of wash buffer (1mg/mL $C_{12}E_8$, 1mmol/L $CaCl_2$, 20mmol/L MOPS pH 7.0, 1mmol/L DTT, 20% glycerol) and eluted with elution buffer (10mg/mL $C_{12}E_8$, 8mmol/L $CaCl_2$, 50mmol/L MOPS pH 7.0, 5mmol/L DTT, 20% glycerol, 10mmol/L ADP,

50mmol/L NaCl, 10mmol/L NaOH). Eluted fractions were collected based on separation by SDS-PAGE and coupled enzyme ATPase activity(51).

4.5.5 – SLN and SERCA co-reconstitution

Co-reconstitution of SLN and SERCA was performed as previously described (22, 52) with the following alterations. 75μg of lyophilized SLN was resuspended in 100μL trifluoroethanol: 2-propanol (5:1) and mixed with 360μg egg yolk PC and 40μg egg yolk PA. The mixture was then dried down under N_2(g) to form a thin film of lipid and protein and placed under vacuum overnight. 16 hours later, thin films were solubilized in buffer containing SERCA1a (3mg/mL $C_{12}E_8$, 33mmol/L MOPS pH 7.0, 5mmol/L $CaCl_2$, 3mmol/L DTT, 7mmol/L ADP, 36mmol/L NaCl, 7mmol/L NaOH, 7mmol/L imidazole pH 7.0, 0.07% NaN_3, 0.25 mg/mL egg yolk PC, 1mg/mL SERCA1a), achieving a final molar ratio of 1 SERCA1a: 6 SLN: 195 lipid (9:1 egg yolk PC to egg yolk PA). Membrane reconstitution was facilitated by the slow removal of detergent by the addition of SM-2 Biobeads (BioRad, Hercules, CA) at a mass ratio of 25:1 biobeads to detergent. Reconstituted proteoliposomes were then purified in a step gradient sucrose gradient (20% / 50% sucrose, 20mmol/L imidazole pH 7.0, 100 mmol/L KCl, 0.2% NaN_3) by centrifugation at 110 000 X RCF for 1.5 hours at 4°C. A punctate band formed at the 20% / 50% interface and was collected in 3 x 200μL aliquots. Purified co-reconstituted proteoliposomes yield an approximate final molar ratio of 1 SERCA1a:4.5 SLN: 120 lipid (confirmed on an assay to assay basis by protein quantitation).

4.5.6 – Calcium-dependent ATPase activity measurements

ATPase activity of co-reconstituted proteoliposomes was determined by a coupled-enzyme reaction over a calcium concentration range (0.1 – 10 μmol/L) (30, 37, 51). The assay used has been adjusted to fit a 96-well format for use in a Synergy 4 (Biotek Instruments, Winooski, VT) or SpectraMax M3 (Molecular Devices, San Jose, CA) microplate reader. Proteoliposomes containing SERCA1a alone (negative control) and SERCA1a with SLN (experimental) were utilized in the coupled-enzyme reaction (~10-20nmol/L SERCA1a at 30°C). Absorbance measurements at 340nm were collected every ~30 seconds for 30 minutes, and slopes were determined for each $[Ca^{2+}]$ interval. These slopes were then used to determine the specific ATPase activity as each respective $[Ca^{2+}]$ interval. Reactions were initiated under different conditions (i-iv). Assays were performed in assay mix buffer (50mmol/L imidazole pH 7.0, 100mmol/L KCl, 5mmol/L $MgCl_2$, 0.5mmol/L EGTA pH 8.0, 4mmol/L ATP, 0.18mmol/L NADH, 0.5mmol/L PEP, 9.6U/mL LDH, 9.6U/mL PK). (i) For

simultaneous calcium and ATP addition, reconstituted proteoliposomes containing SERCA1a (negative control) or SERCA1a with SLN (experimental) were introduced to wells containing 150μL assay buffer and calcium to initiate the reaction. (ii) For calcium preincubation conditions, reconstituted proteoliposomes were introduced to wells containing ATP-free assay buffer and calcium. ATP was then added to the wells to initiate the reaction. (iii) For ATP preincubation conditions, reconstituted proteoliposomes were introduced to wells containing assay buffer. Calcium was then added to the wells to initiate the reaction. (iv) For the physiological mimetic conditions, 0.1μmol/L calcium was added to each well that contained assay mix and reconstituted proteoliposomes. For all conditions, substrate was preincubated at 22°C for approximately 10 minutes. The remaining calcium required to meet the gradient criteria was then added to initiate the reaction. Enzymatic parameters V_{max} (maximal activity), K_{Ca} (apparent calcium affinity), and nH (co-operativity) were determined by nonlinear least-squares fitting of the activity data to the Hill equation (53) (Sigma Plot software, SPSS, Chicago, IL). Errors were determined using S.E.M for a minimum of three independent reconstitutions.

4.6 – Acknowledgments

I would like to acknowledge the contributions of Dr. Paul LaPointe (University of Alberta, Department of Cell Biology, Edmonton, Canada) and Dr. Sue-Ann Mok (University of Alberta, Department of Biochemistry, Edmonton, Canada) for the access to the Synergy 4 and SpectraMax M3 plate readers (respectively).

4.7 – Conflict of interest

There is no conflict of interest in the work reported in this manuscript

4.8 – References

1. Ebashi, S., and Lipmann, F. (1962) Adenosine Triphosphate-linked concentration of calcium ions in a particulate fraction of rabbit muscle. *J. Cell Biol.* **14**, 389–400

2. Kühlbrandt, W. (2004) Biology, structure and mechanism of P-type ATPases. *Nat. Rev. Mol. Cell Biol.* **5**, 282–295

3. Toyoshima, C., and Mizutani, T. (2004) Crystal structure of the calcium pump with a bound ATP analogue. *Nature.* **430**, 529–535

4. Toyoshima, C., and Cornelius, F. (2013) New crystal structures of PII-type ATPases: Excitement continues. *Curr. Opin. Struct. Biol.* **23**, 507–514

5. Drachmann, N. D., Olesen, C., Møller, J. V., Guo, Z., Nissen, P., and Bublitz, M. (2014) Comparing crystal structures of Ca(2+) -ATPase in the presence of different lipids. *FEBS J.* **281**, 4249–4262

6. Toyoshima, C. (2009) How Ca2+-ATPase pumps ions across the sarcoplasmic reticulum membrane. *Biochim. Biophys. Acta - Mol. Cell Res.* **1793**, 941–946

7. Primeau, J. O., Armanious, G. P., Fisher, M. E., and Young, H. S. (2018) The SarcoEndoplasmic Reticulum Calcium ATPase BT - Membrane Protein Complexes: Structure and Function (Harris, J. R., and Boekema, E. J. eds), pp. 229–258, Springer Singapore, Singapore, 10.1007/978-981-10-7757-9_8

8. Anderson, D. M., Makarewich, C. A., Anderson, K. M., Shelton, J. M., Bezprozvannaya, S., Bassel-Duby, R., and Olson, E. N. (2016) Widespread control of calcium signaling by a family of SERCA-inhibiting micropeptides. *Sci. Signal.* **9**, ra119 LP-ra119

9. Kirchberber, M. A., Tada, M., and Katz, A. M. (1975) Phospholamban: a regulatory protein of the cardiac sarcoplasmic reticulum. *Recent Adv. Stud. Cardiac Struct. Metab.* **5**, 103–115

10. Anderson, D. M., Anderson, K. M., Chang, C.-L., Makarewich, C. A., Nelson, B. R., McAnally, J. R., Kasaragod, P., Shelton, J. M., Liou, J., Bassel-Duby, R., and Olson, E. N. (2015) A Micropeptide Encoded by a Putative Long Noncoding RNA Regulates Muscle Performance. *Cell.* **160**, 595–606

11. Odermatt, A, Becker, S., Khanna, V. K., Kurzydlowski, K., Leisner, E., Pette, D., and MacLennan, D. H. (1998) Sarcolipin regulates the activity of SERCA1, the fast-twitch skeletal muscle sarcoplasmic reticulum Ca2+-ATPase. *J. Biol. Chem.* **273**, 12360–12369

12. Odermatt, A, Taschner, P. E., Scherer, S. W., Beatty, B., Khanna, V. K., Cornblath, D. R., Chaudhry, V., Yee, W. C., Schrank, B., Karpati, G., Breuning, M. H., Knoers, N., and

MacLennan, D. H. (1997) Characterization of the gene encoding human sarcolipin (SLN), a proteolipid associated with SERCA1: absence of structural mutations in five patients with Brody disease. *Genomics.* **45**, 541–553

13.   Asahi, M., Sugita, Y., Kurzydlowski, K., De Leon, S., Tada, M., Toyoshima, C., and MacLennan, D. H. (2003) Sarcolipin regulates sarco(endo)plasmic reticulum Ca2+-ATPase (SERCA) by binding to transmembrane helices alone or in association with phospholamban. *Proc. Natl. Acad. Sci. U. S. A.* **100**, 5040–5045

14.   Toyoshima, C., Iwasawa, S., Ogawa, H., Hirata, A., Tsueda, J., and Inesi, G. (2013) Crystal structures of the calcium pump and sarcolipin in the Mg2+-bound E1 state. *Nature.* **495**, 260

15.   Winther, A.-M. L., Bublitz, M., Karlsen, J. L., Møller, J. V, Hansen, J. B., Nissen, P., and Buch-Pedersen, M. J. (2013) The sarcolipin-bound calcium pump stabilizes calcium sites exposed to the cytoplasm. *Nature.* **495**, 265–9

16.   Chen, Z., Akin, B. L., Stokes, D. L., and Jones, L. R. (2006) Cross-linking of C-terminal residues of phospholamban to the Ca 2+ pump of cardiac sarcoplasmic reticulum to probe spatial and functional interactions within the transmembrane domain. *J. Biol. Chem.* **281**, 14163–14172

17.   Akin, B. L., Hurley, T. D., Chen, Z., and Jones, L. R. (2013) The structural basis for phospholamban inhibition of the calcium pump in sarcoplasmic reticulum. *J. Biol. Chem.* **288**, 30181–30191

18.   Stammers, A. N., Susser, S. E., Hamm, N. C., Hlynsky, M. W., Kimber, D. E., Kehler, D. S., and Duhamel, T. A. (2015) The regulation of sarco(endo)plasmic reticulum calcium-ATPases (SERCA). *Can. J. Physiol. Pharmacol.* **93**, 843–854

19.   Glaves, J. P., Primeau, J. O., Espinoza-Fonseca, L. M., Lemieux, M. J., and Young, H. S. (2019) The Phospholamban Pentamer Alters Function of the Sarcoplasmic Reticulum Calcium Pump SERCA. *Biophys. J.* **116**, 633–647

20.   Chen, Z., Akin, B. L., and Jones, L. R. (2007) Mechanism of reversal of phospholamban inhibition of the cardiac Ca 2+-ATPase by protein kinase A and by anti-phospholamban monoclonal antibody 2D12. *J. Biol. Chem.* **282**, 20968–20976

21.   Shaikh, S. A., Sahoo, S. K., and Periasamy, M. (2016) Phospholamban and sarcolipin: Are they functionally redundant or distinct regulators of the Sarco(Endo)Plasmic Reticulum Calcium ATPase? *J. Mol. Cell. Cardiol.* **91**, 81–91

22.   Gorski, P. A., Glaves, J. P., Vangheluwe, P., and Young, H. S. (2013) Sarco(endo)plasmic

Reticulum Calcium ATPase (SERCA) Inhibition by Sarcolipin Is Encoded in Its Luminal Tail. *J. Biol. Chem.* **288**, 8456–8467

23. Bal, N. C., Maurya, S. K., Sopariwala, D. H., Sahoo, S. K., Gupta, S. C., Shaikh, S. a, Pant, M., Rowland, L. a, Goonasekera, S. a, Molkentin, J. D., and Periasamy, M. (2012) Sarcolipin is a newly identified regulator of muscle-based thermogenesis in mammals. *Nat. Med.* **18**, 1575–1579

24. Sahoo, S. K., Shaikh, S. A., Sopariwala, D. H., Bal, N. C., and Periasamy, M. (2013) Sarcolipin protein interaction with sarco(endo)plasmic reticulum Ca2+ ATPase (SERCA) is distinct from phospholamban protein, and only sarcolipin can promote uncoupling of the SERCA pump. *J. Biol. Chem.* **288**, 6881–6889

25. Bal, N. C., Sahoo, S. K., Maurya, S. K., and Periasamy, M. (2018) The Role of Sarcolipin in Muscle Non-shivering Thermogenesis . *Front. Physiol.* . **9**, 1217

26. Pant, M., Bal, N. C., and Periasamy, M. (2016) Sarcolipin: A Key Thermogenic and Metabolic Regulator in Skeletal Muscle. *Trends Endocrinol. Metab.* **27**, 881–892

27. Smith, W. S., Broadbridge, R., East, J. M., and Lee, A. G. (2002) Sarcolipin uncouples hydrolysis of ATP from accumulation of Ca2+ by the Ca2+-ATPase of skeletal-muscle sarcoplasmic reticulum. *Biochem. J.* **361**, 277–286

28. Sahoo, S. K., Shaikh, S. a., Sopariwala, D. H., Bal, N. C., Bruhn, D. S., Kopec, W., Khandelia, H., and Periasamy, M. (2015) The N-Terminus of Sarcolipin plays an important role in uncoupling Sarco-endoplasmic Reticulum Ca 2+ ATPase (SERCA) ATP hydrolysis from Ca 2+transport. *J. Biol. Chem.* 10.1074/jbc.M115.636738

29. Cypess, A. M., Lehman, S., Williams, G., Tal, I., Rodman, D., Goldfine, A. B., Kuo, F. C., Palmer, E. L., Tseng, Y.-H., Doria, A., Kolodny, G. M., and Kahn, C. R. (2009) Identification and importance of brown adipose tissue in adult humans. *N. Engl. J. Med.* **360**, 1509–1517

30. Smeazzetto, S., Armanious, G. P., Moncelli, M. R., Bak, J. J., Lemieux, M. J., Young, H. S., and Tadini-Buoninsegni, F. (2017) Conformational memory in the association of the transmembrane protein phospholamban with the sarcoplasmic reticulum calcium pump SERCA. *J. Biol. Chem.* **292**, 21330–21339

31. Schörner, M., Beyer, S. R., Southall, J., Cogdell, R. J., and Köhler, J. (2015) Conformational Memory of a Protein Revealed by Single-Molecule Spectroscopy. *J. Phys. Chem. B.* **119**, 13964–13970

32. Anderson, D. M., Anderson, K. M., Bassel-duby, R., Olson, E. N., Mcanally, J. R., Kasaragod,

P., Shelton, J. M., Liou, J., Bassel-duby, R., and Olson, E. N. (2015) A Micropeptide Encoded by a Putative Long Noncoding RNA Regulates Muscle Performance Article A Micropeptide Encoded by a Putative Long Noncoding RNA Regulates Muscle Performance. *Cell.* **160**, 1–12

33. Tonkin, J., and Rosenthal, N. (2015) One small step for muscle: a new micropeptide regulates performance. *Cell Metab.* **21**, 515–6

34. Nelson, B. R., Catherine A. Makarewich, Douglas M. Anderson, Benjamin R. Winders, Constantine D. Troupes, F. W., Reese, A. L., McAnally, J. R., Chen, X., Kavalali, E. T., Cannon, S. C., Houser, S. R., Bassel-Duby, R., and Olson, E. N. (2016) A peptide encoded by a transcript annotated as long noncoding RNA enhances SERCA activity in muscle. *Science (80-.).*

35. Schoenmakers, T. J., Visser, G. J., Flik, G., and Theuvenet, A. P. (1992) CHELATOR: an improved method for computing metal ion concentrations in physiological solutions. *Biotechniques.* **12**, 870-874,876-879

36. Lolkema, J. S., and Slotboom, D.-J. (2015) The Hill analysis and co-ion-driven transporter kinetics. *J. Gen. Physiol.* **145**, 565–574

37. Trieber, C. A., Douglas, J. L., Afara, M., and Young, H. S. (2005) The Effects of Mutation on the Regulatory Properties of Phospholamban in Co-Reconstituted Membranes†. *Biochemistry.* **44**, 3289–3297

38. Toyoshima, C., Nakasako, M., Nomura, H., and Ogawa, H. (2000) Crystal structure of the calcium pump of sarcoplasmic reticulum at 2.6 A resolution. *Nature.* **405**, 647–655

39. Clausen, J. D., Bublitz, M., Arnou, B., Montigny, C., Jaxel, C., Møller, J. V., Nissen, P., Andersen, J. P., and le Maire, M. (2013) SERCA mutant E309Q binds two Ca(2+) ions but adopts a catalytically incompetent conformation. *EMBO J.* **32**, 3231–3243

40. Toyoshima, C., and Nomura, H. (2002) Structural changes in the calcium pump accompanying the dissociation of calcium. *Nature.* **418**, 605–611

41. Glaves, J. P., Primeau, J. O., Gorski, P. A., Espinoza-Fonseca, L. M., Lemieux, M. J., and Young, H. S. (2019) Interaction of a sarcolipin pentamer and monomer with the sarcoplasmic reticulum calcium pump, SERCA. Running Title: A novel complex of sarcolipin and SERCA. *Biophys J.* **118**, 518–531

42. Toyoshima, C., Yonekura, S.-I., Tsueda, J., and Iwasawa, S. (2011) Trinitrophenyl derivatives bind differently from parent adenine nucleotides to Ca2+-ATPase in the absence of Ca2+. *Proc. Natl. Acad. Sci. U. S. A.* **108**, 1833–1838

43. Autry, J. M., Rubin, J. E., Svensson, B., Li, J., and Thomas, D. D. (2012) Nucleotide activation of the Ca-ATPase. *J. Biol. Chem.* **287**, 39070–39082

44. Akin, B. L., and Jones, L. R. (2012) Characterizing Phospholamban to Sarco(endo)plasmic Reticulum Ca2+-ATPase 2a (SERCA2a) Protein Binding Interactions in Human Cardiac Sarcoplasmic Reticulum Vesicles Using Chemical Cross-linking. *J. Biol. Chem.* **287**, 7582–7593

45. James, P., Inui, M., Tada, M., Chiesi, M., and Carafoli, E. (1989) Nature and site of phospholamban regulation of the Ca2+ pump of sarcoplasmic reticulum. *Nature.* **342**, 90–92

46. Jones, L. R., Cornea, R. L., and Chen, Z. (2002) Close proximity between residue 30 of phospholamban and cysteine 318 of the cardiac Ca2+ pump revealed by intermolecular thiol cross-linking. *J. Biol. Chem.* **277**, 28319–28329

47. Campbell, K. L., and Dicke, A. A. (2018) Sarcolipin Makes Heat, but Is It Adaptive Thermogenesis? *Front. Physiol.* **9**, 714

48. Inesi, G., Kurzmack, M., Coan, C., and Lewis, D. E. (1980) Cooperative calcium binding and ATPase activation in sarcoplasmic reticulum vesicles. *J. Biol. Chem.* **255**, 3025–3031

49. Stokes, D. L., and Green, N. M. (1990) Three-dimensional crystals of CaATPase from sarcoplasmic reticulum. Symmetry and molecular packing. *Biophys. J.* **57**, 1–14

50. Eletr, S., and Inesi, G. (1972) Phospholipid orientation in sarcoplasmic membranes: spin-label ESR and proton MNR studies. *Biochim. Biophys. Acta.* **282**, 174–179

51. Warren, G. B., Toon, P. A., Birdsall, N. J., Lee, A. G., and Metcalfe, J. C. (1974) Reconstitution of a calcium pump using defined membrane components. *Proc. Natl. Acad. Sci. U. S. A.* **71**, 622–626

52. Young, H. S., Jones, L. R., and Stokes, D. L. (2001) Locating phospholamban in co-crystals with Ca(2+)-ATPase by cryoelectron microscopy. *Biophys. J.* **81**, 884–894

53. Weiss, J. N. (1997) The Hill equation revisited: uses and misuses. *FASEB J. Off. Publ. Fed. Am. Soc. Exp. Biol.* **11**, 835–841

"Don't panic."

D. Adams – 1979

Chapter 5

Cryo-EM of two-dimensional crystals of SERCA and PLN

J.O. Primeau[1], G.P. Armanious[1], and Howard S. Young[1]

[1]Department of Biochemistry, University of Alberta, Edmonton, Alberta, Canada
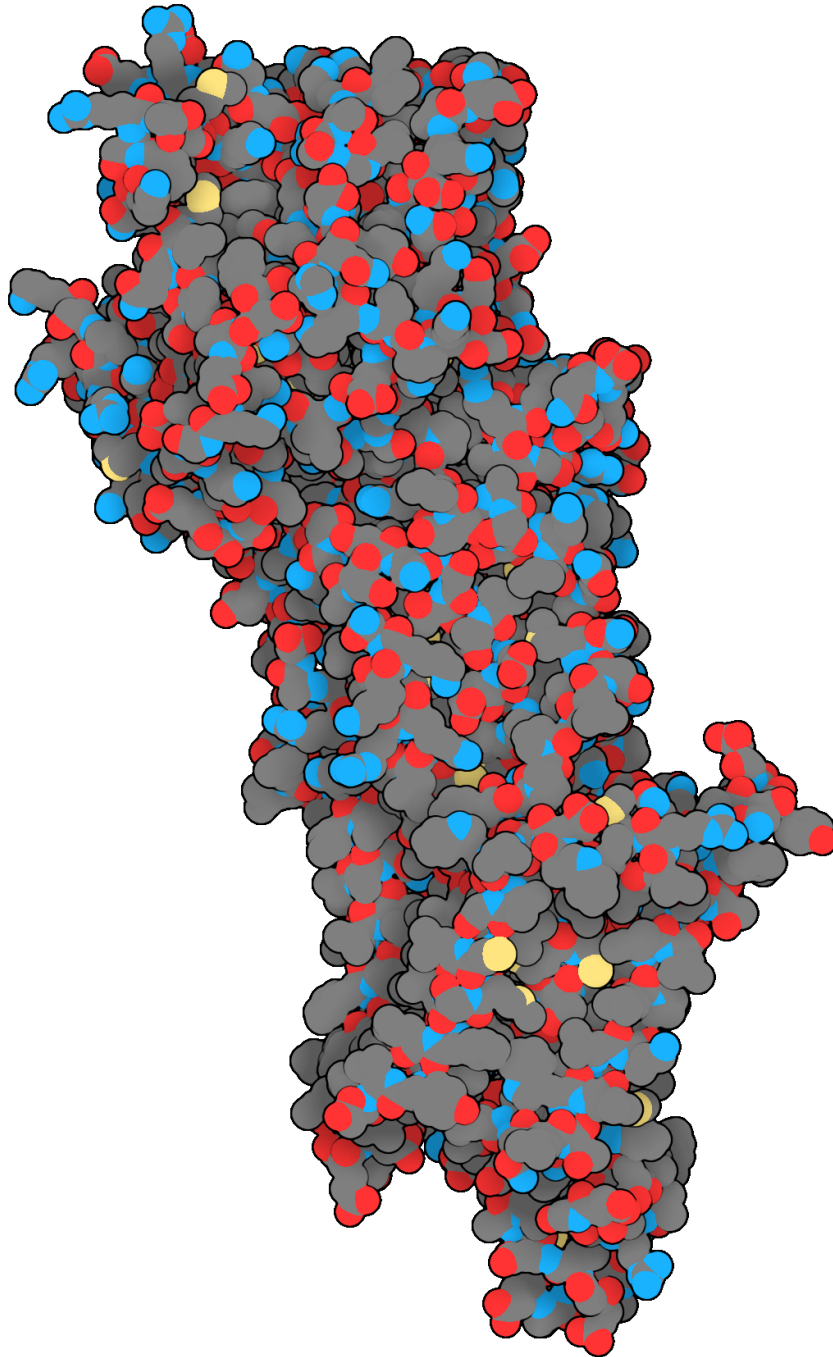
Stylized crystal structure of SERCA 2A (PDB: 5MPM)

Preface

This chapter represents the culmination of a work in progress. JOP performed the research, analyzed data, and wrote the manuscript. GPA provided initial secondary structure determination and mutagenesis. HSY advised the research, analyzed the data, and edited the manuscript. **Title page figure generated using *Illustrate: Non-photorealistic Biomolecular Illustration* (1).**

5.1 – Introduction

The majority of structures in the Protein Data Bank were determined by the major structural biology techniques X-ray crystallography and NMR spectroscopy. While these techniques can be slow and challenging, they have provided stunning atomic-level structures of biological macromolecules. Both techniques require large amounts of protein, with NMR being mostly limited to smaller proteins ($\leq$30 kDa) and X-ray crystallography requiring large crystals of the target protein. However, for many biological macromolecules, well-ordered crystals of large proteins, complexes, integral membrane proteins, or highly dynamic proteins has proven problematic. What if we could avoid these constraints and look directly at a single molecule, in a native environment, in multiple conformations, as a multimeric complex, and at near-atomic resolution? Up until ten years ago, this was unthinkable.

Jacques Dubochet, Joachim Frank, and Richard Henderson were pioneers in establishing modern cryoelectron microscopy (CryoEM) in the 1980s (2, 3), and they received the 2017 Nobel Prize in Chemistry for their efforts. Cryo-EM involves the vitrification of a target protein in a thin layer of amorphous ice, allowing for direct viewing of macromolecules in a hydrated environment, free of any heavy-metal stain or embedding plastics. This technique is suitable for membrane protein structural analysis, a field of structural biology that has traditionally been considered a difficult undertaking. Membrane proteins can be stabilized in detergent micelles, lipid bicelles, co-reconstituted lipid membranes, and other synthetic model membrane systems, offering reasonable substitutes for the native-membrane embedded environment. Favourable environments such as these provide an opportunity to view large macromolecular complexes usually not possible with other techniques. Structural insights gleaned from CryoEM analysis of multi-protein complexes offer a unique understanding of protein-protein interactions, or lipid-dependent protein-protein interactions, that are typically not amenable by X-ray crystallography or NMR spectroscopy.

Technological advances in cryo-EM, such as improved freezing techniques (4), direct electron detectors (5), phase plates (6), subframe alignments (7), *et cetera*, have led to a surge in near atomic-level resolution macromolecular structures (8–14). These structures have become of great interest not only because of the fundamental biology they reveal but also for drug and pharmaceutical development, ushering in a new era of high-resolution structures that some have dubbed as the *resolution revolution*. The application of this technique to the analysis of single-molecules involves recording thousands of images of randomly orientated single particles, which are used to generate a high-resolution structure. However, if the target protein is not stable in solution (like most membrane proteins) or requires an unusually large detergent micelle for stabilization, two-dimensional crystals

and electron crystallography provide an alternative to single-particle analysis to address these prior concerns. First established in the '70s, electron crystallography has been used to determine a handful of unique crystal structures (15). By imaging single-layered, regular array of membrane proteins in a native membrane environment, one can produce medium to high-resolution structures of membrane protein complexes. Two-dimensional crystals (2D crystals) of SERCA have been analyzed for many years (16–21), providing remarkable insight into SERCA structural studies complementary to X-ray crystallography.

5.1.1 SERCA and phospholamban 2D crystals

As previously described in the literature (19, 22, 23) and the body of this thesis (*see* **Chapters 2 and 3**), 2D crystals of SERCA and PLN or SLN indicate that PLN/SLN form an oligomeric interaction with membrane-embedded SERCA at an interface independent of the inhibitory groove. Previous work by Dr. John Paul Glaves also investigated the effect of phospholamban mutations on 2D crystal formation, finding that mutations to PLN such as Lys^{27}-to-Ala (gain of function) and Asn^{34}-to-Ala (loss of function) have a profound impact on PLN function and 2D crystal formation. These mutations had significant effects on PLN function as a SERCA regulator, notably by altering both K_{Ca} and V_{max} of SERCA, which aligns with the central message of this thesis.

By noting that mutations to PLN can have substantial effects on the formation of 2D crystals, our lab has been investigating more 'interesting' human variations in PLN and evaluating their impact on 2D crystal formation and structure. One such mutation, Pro^{21}-to-Thr (24) found in patients with dilated cardiomyopathy (DCM), was deemed a member of the 'interesting human mutation' cohort. Pro^{21}, located in PLN's flexible linker domain (**Figure 5.1**) has been identified as an essential residue for PLN regulation of SERCA activity (25). Li et al. determined that mutating Pro^{21} to an alanine residue increased α-helical characteristics of the peptide, as well as altered PLN's ability to regulate SERCA calcium transport properties (likely by altering PLN cytoplasmic interaction with SERCA (26)). Unpublished work performed by Gareth Armanious determined that mutating Pro^{21}-to-Thr also increases α-helical characteristics of PLN based on CD spectroscopy when compared to wild-type PLN. Pro^{21}-to-Thr was also found to depress the V_{max} of SERCA (2.1 ± 0.1 μmol/mg/min for SERCA in the presence of Pro^{21}-to-Thr PLN versus 6.3 ± 0.1 μmol/mg/min for SERCA in the absence of PLN) and increase the K_{Ca} (1.5 ± 0.1 μmol/L versus 0.88 ± 0.03 μmol/L, respectively). These data suggest that this mutation results in a gain of inhibitory properties of PLN (compared to wild-type PLN). Because this mutation has proven to be structurally and functionally different from

wild-type PLN, it became a definite candidate for further structural studies by cryo-EM of 2D crystals. The obvious question was, "does a Pro[21]-to-Thr PLN mutation alter the structure of the pentameric interface with SERCA". The significant effect on V_{max} suggests that this mutation is affecting the pentamer interaction with the calcium access funnel of SERCA, likely due to altered PLN cytoplasmic domain dynamics. In turn, by combining the Lys[27]-to-Ala (gain-of-function pentameric form of PLN) and Pro[21]-to-Thr (entirely α-helical form of PLN) mutations, we have an ideal candidate to investigate how PLN pentamer structure alters SERCA regulation and 2D crystals of PLN and SERCA, ultimately leading to a better understanding of the role of this mutation in DCM.
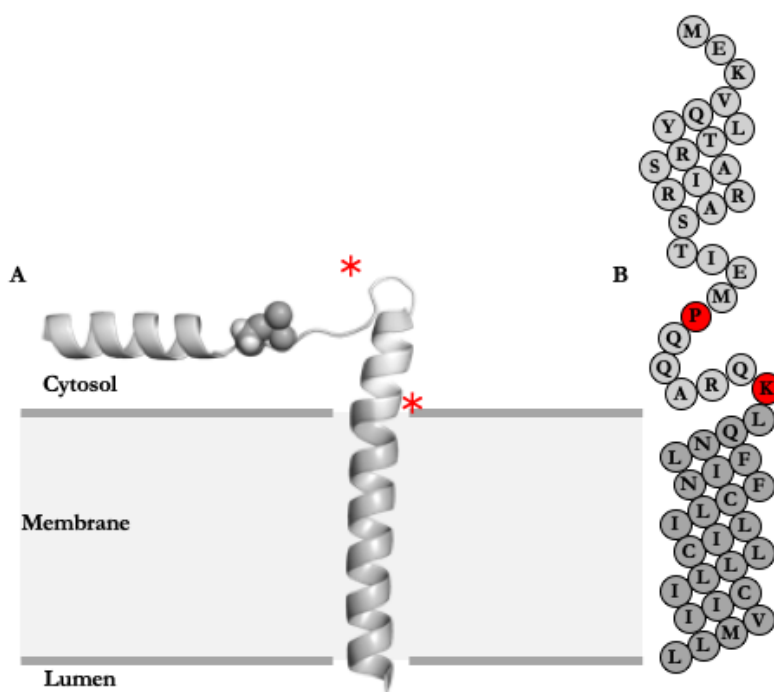
Figure 5.1: Pro[21] and Lys[27] are located in the linker region of phospholamban. (A) A solution and solid-state NMR ensemble structure of Ser[16] phosphorylated PLN (PDB: 2M3B) and a topology diagram (B) indicating the primary sequence. The highlighted residues indicate the relative positions of Pro[21] and Lys[27] (red, red asterix) on the phospholamban molecule.

5.2 – Results

5.2.1 – Pro[21]-to-Thr and Lys[27]-to-Ala mutations alter PLN regulatory function

As stated previously, mutations to PLN can have significant effects on its regulatory capabilities. We can assess the impact of mutations on PLN by measuring the calcium-dependent ATPase activity of SERCA co-reconstituted in membrane vesicle with PLN mutants of our choice.

By fitting the resultant ATPase activity data to the Hill equation, we determine kinetic parameters such as apparent calcium affinity (K_{Ca}) and maximal activity (V_{max}) of SERCA. As previously noted, the effects of PLN on K_{Ca} saturate at a molar ratio of 1:1 PLN:SERCA (27, 28) and the PLN monomer is thought to be responsible for the shift in calcium affinity when interacting with the inhibitory groove (19). As such, alterations to the calcium affinity of SERCA in the presence of PLN can be interpreted as a change in the inhibitory SERCA-PLN complex. The oligomeric state of PLN and association with M3 of SERCA (19) influences the turnover rate of SERCA. In this case, substantial changes in the V_{max} of SERCA in the presence of PLN can be interpreted as changes in the oligomer interaction with the accessory site of SERCA.

We have established that SERCA ATPase activity and kinetic parameters can be used to estimate how PLN interacts with SERCA. The effects of Pro[21]-to-Thr and Ly[27]-to-Ala mutations in PLN (PLN P21T K27A) on calcium-dependent ATPase activity measurements of co-reconstituted proteoliposomes were compared to SERCA alone (negative control) and SERCA in the presence of wild-type PLN (positive control) (**Figure 5.2**). The P21T K27A mutant of PLN flipped PLN's V_{max} stimulatory effect to an inhibitory effect (4.09 ± 0.01 μmol/min/mg for SERCA alone, 6.1 ± 0.2 μmol/min/mg with wild-type PLN, and 3.6 ± 0.1 μmol/min/mg for SERCA with PLN P21T K27A). The effect of these mutations is such that it reduces SERCA K_{Ca} when compared to wild-type PLN (0.87 ± 0.05 μmol/L for SERCA with wild-type PLN and 0.66 ± 0.07 μmol/L for SERCA with PLN P21T K27A). This represents a partial loss of function for the P21T K27A form of PLN. The significant change in V_{max}, compared to the more subtle K_{Ca} effect, suggests that these mutations modulate the interaction with the M3 accessory site more than the inhibitory groove interaction. These results are intriguing as the PLN pentamer is required for to facilitate modulation of SERCA V_{max}. SDS-PAGE of co-reconstituted proteoliposomes containing SERCA alone, SERCA in the presence of wild-type PLN, and SERCA in the presence of P21T K27A PLN (**Figure 5.2**-*inset*) reveals the stability of the pentameric form of P21T K27A PLN (intensity of the pentamer band is 1.8 ± 0.3 times higher than that of wild-type PLN). The evidence suggests that the tandem effects of these mutations increase pentamer stability even though SERCA V_{max} is depressed. If the mutants are considered separately, the Lys[27]-to-Ala mutation remains a pentamer and is a super-inhibitor of SERCA (22), while the Pro[21]-to-Ala mutant lowers the Vmax of SERCA and has no effect on calcium affinity (unpublished). Thus, the combined effects of the mutants in P21T K27A PLN is surprising.

	SERCA	PLN	P21T K27A PLN
K_{Ca}	0.46 ± 0.01	0.87 ± 0.05	0.66 ± 0.07
V_{max}	4.10 ± 0.05	6.1 ± 0.2	3.6 ± 0.1
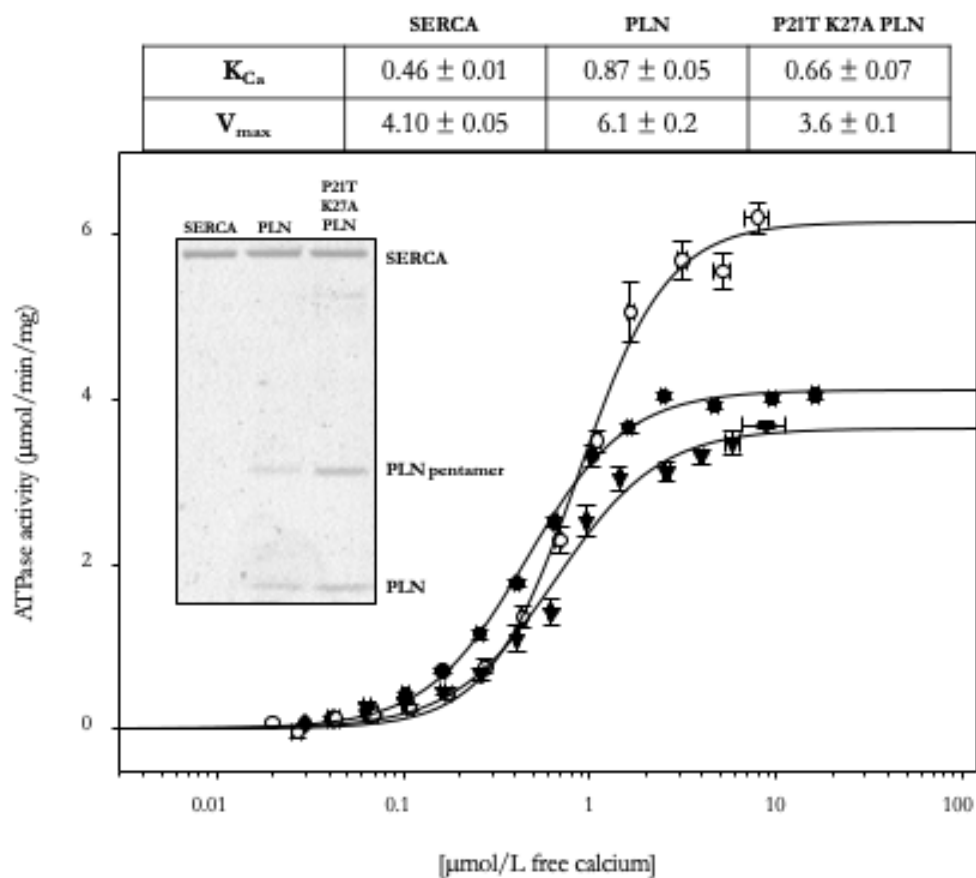
Figure 5.2: ATPase activity as a function of calcium concentration for SERCA proteoliposomes containing SERCA alone, SERCA with PLN, and SERCA with Pro[21]-to-Thr Lys[27]-to-Ala PLN. Experimental data of proteoliposomes containing SERCA alone (filled circles), proteoliposomes containing SERCA and PLN (open circles), and proteoliposomes containing SERCA and P21T K27A PLN (filled triangles, gray line) are fit to the Hill equation. Values of V_{max} (maximal activity) and K_{Ca} (apparent calcium affinity) are indicated in the inset table. Each data point is the mean $\pm$ standard error (n$\geq$3). The inset shows 10% sodium dodecyl sulphate polyacrylamide gel electrophoresis gel of the reconstituted proteoliposomes of SERCA in the absence and presence of PLN or P21T K27A PLN with bands corresponding to SERCA and the PLN pentamer and monomer identified

5.2.2 – PLN Pro²¹-to-Thr Lys²⁷-to-Ala forms 2D crystals with SERCA

Previous studies of helical and wide 2D crystals of SERCA with PLN (18, 19, 22) identified that the natural association of PLN with M3 of SERCA is functionally significant for regulation of SERCA calcium transport. The evidence presented in this thesis indicates that this interaction is essential for the regulatory capabilities of PLN on SERCA. Thus, determining the effect of deleterious PLN mutations on this interaction can provide insight into how particularly adverse mutations can affect overall heart health. The formation and analysis of two-dimensional crystals of SERCA and P21T K27A PLN was preformed under two crystallization conditions (see *methods* (19)). However, a concentration of 0.5 mmol/L Na_3VO_4 converted to decavanadate was used, as well as the absence of thapsigargin (TG)). The conditions differed only in the magnesium concentration used for crystal formation, with 15mmol/L $MgCl_2$ promoting helical crystal formation and 35mmol/L $MgCl_2$ promoting the formation of wide 2D crystals. Initial experiments with this construct indicate that P21T K27A PLN can form helical and wide 2D crystals (**Figure 5.3**). Previous studies have shown that wide 2D crystals do not form in the absence of PLN, and as such, we can infer that P21T K27A PLN similarly stabilizes wide 2D crystals as seen wild-type, Ile⁴⁰-to-Ala, and Lys²⁷-to-Ala PLN (22). It is reasonable to assume that P21T K27A PLN associates with M3 of SERCA, as the crystals are morphologically similar, which is also in agreement with functional data indicating that the mutant PLN is altering the V_{max} of SERCA. Unfortunately, the number of wide 2D crystals found (so far) has been inconsistent and not suitable for cryo-EM analysis (at least not yet). Thin helical crystals also appear to be morphologically similar to crystals analyzed in previous studies (~70nm in diameter and several μm in length (20, 29, 30)) As these crystals were found in high abundance, they are a prime candidate for cryo-EM studies (**Figure 5.4**). Thus far, approximately 100 micrographs have been collected (and more are being collected) for future analysis.
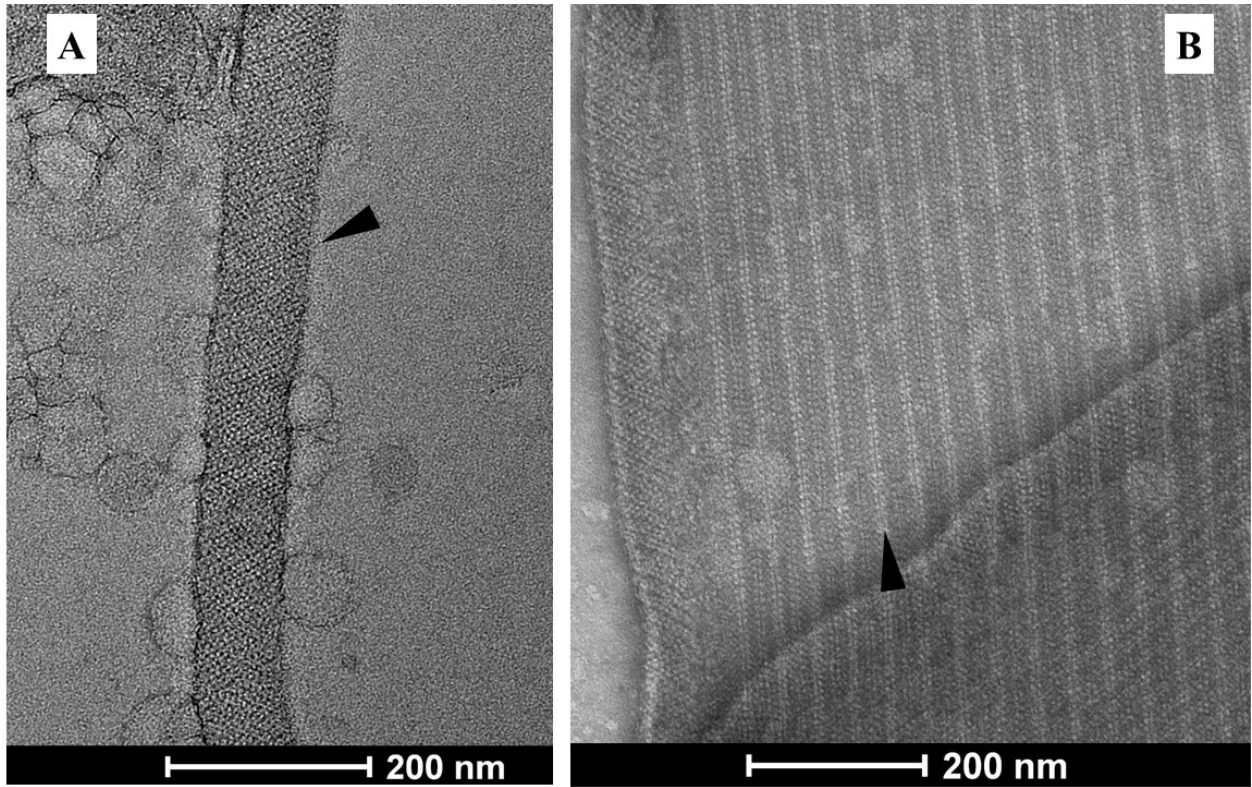
Figure 5.3: Example micrographs of negatively-stained helical and wide two-dimensional crystals containing SERCA and Pro²¹-to-Thr Lys²⁷-to-Ala PLN. Proteoliposomes containing SERCA and P21T K27A PLN form helical (A) and wide 2D (B) crystals. In both crystal morphologies, SERCA is seen aligning in anti-parallel dimer ribbons (arrows). Helical crystals can be described as tubular and have dimensions of ~70nm in width and several μm in length. Alternatively, wide 2D crystals have a different packing morphology than helical crystals (which is evident in spacing between dimer ribbons) and form flattened tubes approximately 500nm in width and several μm in length.

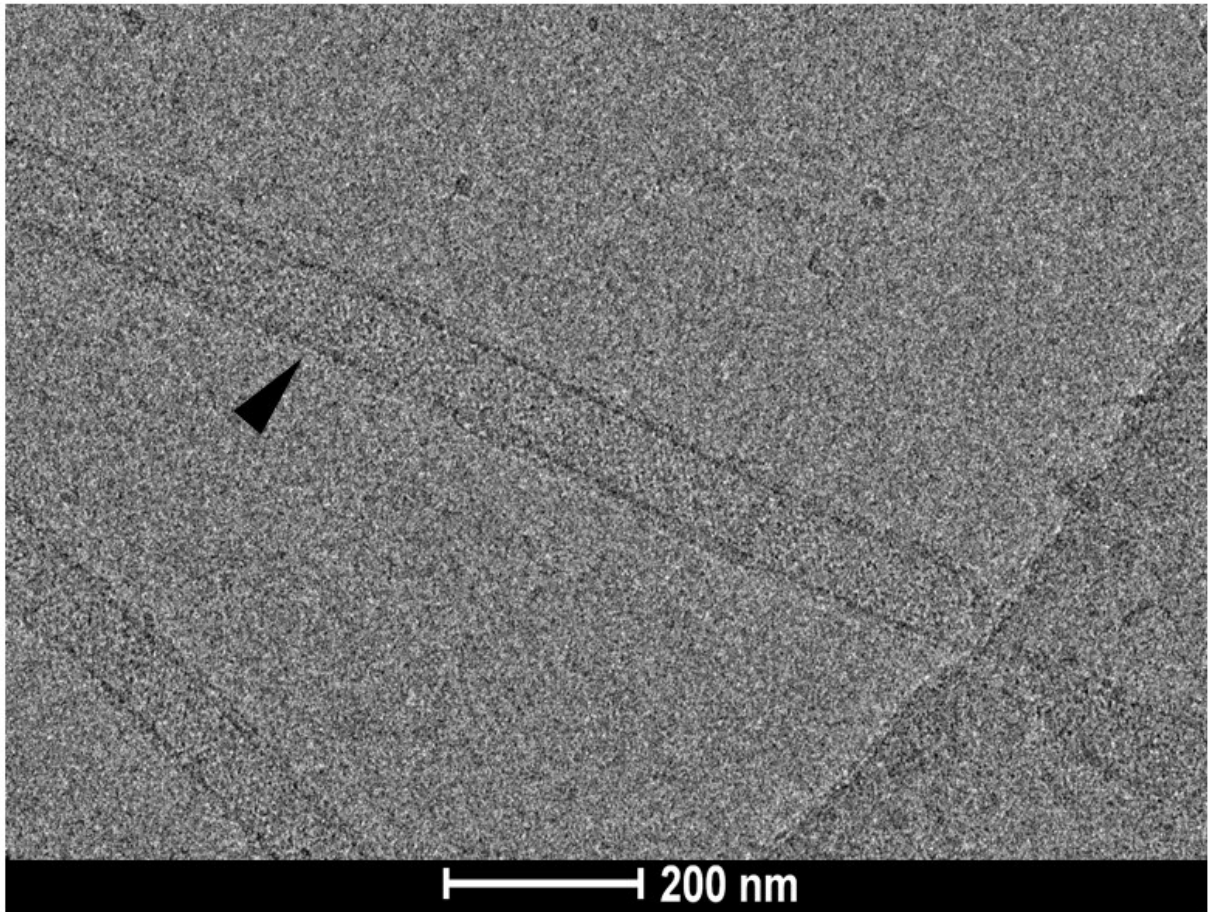**Figure 5.4: Example micrographs of frozen-hydrated helical two-dimensional crystals containing SERCA and Pro²¹-to-Thr Lys²⁷-to-Ala PLN.** Frozen hydrated helical 2D crystals containing SERCA and P21T K27A PLN embedded in vitrified crystallization buffer. Note the reduced contrast compared to negatively stained crystals (**Figure 5.3**). Arrow indicates the location of SERCA dimer ribbons in the tubular helical crystal.

5.3 – Discussion

As noted in previous studies, the effect of PLN on the V_{max} and K_{Ca} of SERCA is sensitive to PLN mutation (31–33). N-terminal residues (Val^4 and Gln^5) and C-terminal residues (Met^{50} and Leu^{51}) of PLN are critical for the V_{max} effect, indicating that a coordination of the cytoplasmic and transmembrane domains plays a role in influencing the turnover rate of SERCA. Additionally, alanine-scanning mutagenesis of PLN (32) reveals that the N- and C-termini of the transmembrane domain, laying near the membrane surfaces, were critical for influencing the V_{max} of SERCA. Mutation of pentamer stabilizing residues such as Leu^{37} and Ile^{40} impact the effect of PLN on the V_{max} of SERCA. These observations suggest that the interaction requires a PLN pentamer in conjunction with molecular interactions with M3 of SERCA to facilitate an increased turnover rate for SERCA. The coordinated positioning of cytoplasmic and transmembrane domains of PLN and the positioning of the cytoplasmic domains of PLN on the surface of the membrane (19), cause membrane perturbation near the calcium access funnel as the mechanism for increasing SERCA's turnover rate. An interesting point to consider is that previous work performed by Gustavsson et al. (26) has highlighted the importance of the conformational equilibrium between PLN's cytoplasmic and transmembrane domains. Based on their work, the conformation of PLN is in equilibrium between a ground-state (T-state) where the helical cytoplasmic domain of PLN rests on the membrane surface and an excited, conformationally dynamic state (R-state) where the helix becomes unwound, dissociates from the membrane and can interact with SERCA (B-state). The T-state of PLN is the most populated conformation (~80%) while the dynamic R-state is less populated, and the B-state is sparsely populated. They assert that the T-state interaction of PLN with the inhibitory groove of SERCA is inhibitory, while the excited R and B-states are non-inhibitory. We find a very similar T-state orientation of PLN in the pentamer interaction with the M3 accessory site of SERCA.

The effect of Pro^{21}-to-Thr in conjunction with Lys^{27}-to-Ala mutation facilitates two-dimensional crystal formation, amenable for cryoEM studies. Based on previous CD spectroscopy data, the Pro^{21}-to-Thr mutation renders PLN entirely α-helical, creating a continuous helix structure of PLN. This change in secondary structure could alter how the PLN pentamer packs and associates with SERCA. There are three aspects to consider here, the interaction with M3 of SERCA, the positioning of the cytoplasmic domains of PLN on the membrane surface, and the requirement for a pentameric (oligomeric) form of PLN. The Pro^{21}-to-Thr Lys^{27}-to-Ala form of PLN remains pentameric. It is reasonable to assume that this mutation, in combination with the Lys^{27}-to-Ala mutation, would facilitate interactions with SERCA at the accessory site and the inhibitory groove.

The effect of the double mutant on the K_{Ca} and V_{max} of SERCA supports this assertion. Thus, the mutations promote a complex with SERCA, which involves a stable pentamer, an interaction with M3 (22), and a helical structure of PLN that lifts the cytoplasmic domain off the membrane surface. Functionally, we can observe the effects of these mutations as changes to pentamer propensity, V_{max}, and K_{Ca}. Based on the results, P21T K27A PLN nearly doubles pentamer stability in SDS when compared to wild-type PLN. This element of P21T K27A PLN, however, appears to be the only aspect consistent with the two separate individual mutants. Pro[21]-to-Ala PLN decreases the V_{max} of SERCA and has a partial loss-of-function effect on K_{Ca}. In stark contrast, Lys[27]-to-Ala PLN increases the V_{max} of SERCA and has a gain-of-function (super-inhibitory) effect on K_{Ca}.

As established previously, PLN and SLN modulation of SERCA V_{max} and K_{Ca} reflects different regulatory site interactions, with changes to SERCA V_{max} mediated by the M3 accessory site and changes to K_{Ca} mediated by inhibitory groove association. Both PLN and SLN alter SERCA's K_{Ca} to a similar extent, and the mode of interaction with the inhibitory groove is similar (34–36). However, PLN increases the V_{max} of SERCA (19, 31, 32, 37), while SLN decreases the V_{max} of SERCA (38). SLN also interacts with the M3 accessory site of SERCA, though the interaction involves an SLN monomer and the consequence is a decrease in SERCA's turnover rate. In our previous work (19, 39, 40), we concluded that the interaction with M3 alone, whether by PLN or SLN, decreases the V_{max} of SERCA. For PLN, this is overcome by the placement of PLN's cytoplasmic domains at the surface of the membrane near the calcium access funnel of SERCA. The membrane perturbation caused by the cytoplasmic domains of PLN increases the turnover rate of SERCA. With this interpretation in mind, the effects of the P21T K27A double mutant are such that SERCA's V_{max} is decreased, which is an SLN-like characteristic. The P21T K27A form of PLN retains PLN molecules in an oligomer with their cytoplasmic domains lifted off the membrane surface (**Figure 5.5**), eliminating the membrane perturbation proximal to the calcium access funnel of SERCA. Since the mutant form of PLN can still associate with M3 of SECRA, the net effect is a decrease in the turnover rate. As such, these results are similar to what we have observed with SLN pentamers (39), which associate with SERCA through an indirect interaction with M3 and act to lower the V_{max} of SERCA. Our observations indicate that if you lift the PLN's cytoplasmic domain off the membrane interface, we no longer see a stimulatory effect on SERCA V_{max}, but we see a V_{max} depression similar to what we observe with the SLN interaction. Membrane fluidity is no longer perturbed, resulting in a net inhibitory interaction with M3, akin to the SLN interaction. This interesting double mutation aligns with our current understanding of the SERCA-Regulin regulatory axis, where an association with M3

of SERCA is fundamentally inhibitory by nature, but secondary effects such as modifying the local lipid environment can cause an increase in SERCA turnover.
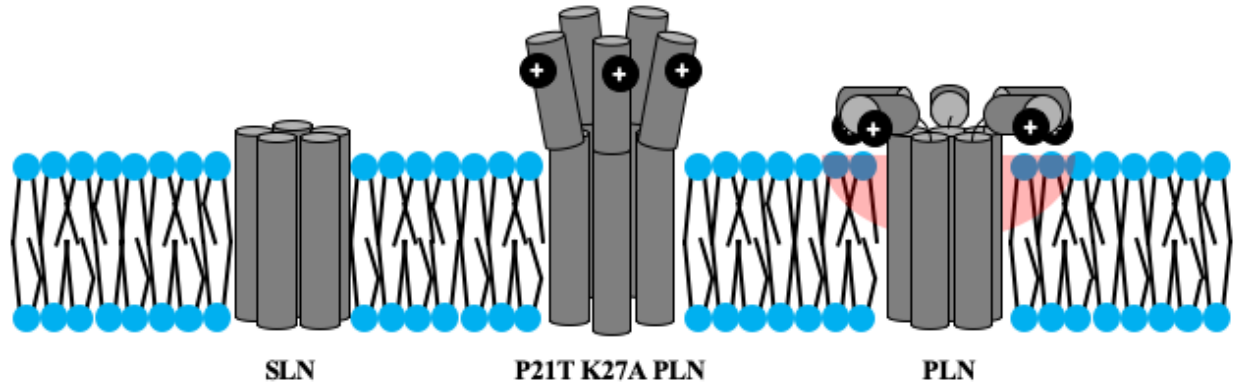
Figure 5.5: A schematic representation of Pro[21]-to-Thr Lys[27]-to-Ala PLN pentamers in a membrane. Based on the pinwheel structural model of a PLN pentamer, wild-type PLN (right) cytoplasmic domains lie on the membrane surface where charged amino acid residues destabilize membrane fluidity by interacting with phospholipid headgroups. In comparison, P21T K27A PLN (middle) lifts the cytoplasmic domain away from the membrane interface, removing the destabilizing effect on the phospholipid membrane, akin to SLN (left) pentamers.

If we now focus on PLN-mediated modulation of SERCA calcium affinity, we see that the effects of the P21T K27A PLN mutation on SERCA K_{Ca} is not as prominent as the K27A mutant alone (i.e. partial loss of function versus super-inhibition, respectively). As noted earlier, Gustavsson et al. demonstrated that PLN exists in a conformational equilibrium between and 'ordered' (T) and 'disordered' (R) states to facilitate PLN's regulatory interaction with SERCA (26). Lys[27] resides in the linker region of PLN between the N-terminal cytoplasmic helix and the transmembrane domain helix. The linker region of PLN modulates the interaction with the inhibitory groove of SERCA, fine-tuning the interaction such that it is reversible at physiological calcium concentrations. Lys[27] is thought to be proximal to positively charged residues of SERCA such that charge repulsion modulates the affinity of PLN, and mutation of this residue to alanine (i.e. Lys[27]-to-Ala) allows tighter binding and super-inhibition of SERCA. The Pro[21]-to-Thr mutation converts the linker region to an α-helix, which alters the interaction of the linker region of PLN with SERCA and has a deleterious effect on PLN alignment within the inhibitory groove. Based on the partial loss-of-function to K_{Ca} modulation observed for P21T K27A PLN, we can conclude that this mutation is indeed affecting the ability of PLN to associate with SERCA's inhibitory groove. What this does tell us is that the secondary structure of

PLN is critical for optimal interaction with SERCA, bridging our understanding of how structural modifications to PLN can affect its function and also highlights the homologous regulatory functions of PLN and SLN. By forming a continuous helix in PLN with the mutation of a single residue (Pro[21]-to-Thr), we can make PLN act more like SLN. These results beg the question, do the regulatory functions of the other discovered SERCA regulators agree with these observations? Further research will shed light on this mystery.

5.4 – Experimental procedures

5.4.1 – Materials

All reagents were of the highest purity available: octaethylene glycol monododecyl ether ($C_{12}E_8$; Barnet Products, Englewood Cliff, NJ); egg yolk phosphatidylcholine, egg yolk phosphatidylethanolamine (PE), and egg yolk phosphatidic acid (PA) (Avanti Polar Lipids, Alabaster, AL); all reagents used for crystallization and the coupled-enzyme assay including sodium orthovanadate, NADH, ATP, phosphoenolpyruvate, lactate dehydrogenase, and pyruvate kinase (Sigma-Aldrich, Oakville, ON, Canada).

5.4.2 – Co-reconstitution of PLN mutants and SERCA

Recombinant Pro[21]-to-Thr Lys[27]-to-Ala PLN mutant (human PLN sequence (22)) was expressed and purified as previously described (41). SERCA1a was purified from rabbit skeletal muscle SR (42, 43). Lyophilized Pro[21]-to-Thr Lys[27]-to-Ala PLN mutant (100 µg) was suspended in a 100-µL mixture of water-trifluoroethanol (1:5) and mixed with lipids (400 µg egg yolk phosphatidylcholine (PC), 50 µg egg yolk PE, and 50 µg egg yolk PA) from stock chloroform solutions. The peptide-lipid mixture was dried to a thin film under nitrogen gas and desiccated under vacuum overnight. The peptide-lipid mixture was hydrated in buffer (20 mmol/L imidazole (pH 7.0); 100 mmol/L KCl; 0.02% NaN$_3$) at 37°C for 10 min, cooled to room temperature, and detergent-solubilized by the addition of $C_{12}E_8$ (0.2% final concentration) with vigorous vortexing. Detergent-solubilized SERCA1a was added (500 µg in a total volume of 500 µL), and the reconstitution was stirred gently at room temperature. Detergent was slowly removed by the addition of SM-2 Bio-Beads (Bio-Rad, Hercules, CA) over a 4-h time course (final weight ratio of 25 Bio-Beads to 1 detergent). After detergent removal, the reconstitution was centrifuged over a sucrose gradient for 1 h at 100,000 x RCF. The resultant layer of reconstituted proteoliposomes was removed, flash-frozen in liquid N$_2$, and stored at -80°C.

5.4.3 – Calcium-dependent ATPase activity measurements

ATPase activity of co-reconstituted proteoliposomes was determined by a coupled-enzyme reaction over a calcium concentration range (0.1 – 10 μmol/L) (31, 44, 45). The assay used has been adjusted to fit a 96-well format for use in a Synergy 4 (Biotek Instruments, Winooski, VT) or SpectraMax M3 (Molecular Devices, San Jose, CA) microplate reader. Proteoliposomes containing SERCA1a alone (negative control) and SERCA1a with PLN P21T K27A (experimental) were utilized in the coupled-enzyme reaction (~10-20nmol/L SERCA1a at 30°C). Absorbance measurements at 340nm were collected every ~30 seconds for 30 minutes, and slopes were determined for each [Ca^{2+}] interval. These slopes were then used to determine the specific ATPase activity as each respective [Ca^{2+}] interval. Assays were performed in assay mix buffer (50mmol/L imidazole pH 7.0, 100mmol/L KCl, 5mmol/L $MgCl_2$, 0.5mmol/L EGTA pH 8.0, 4mmol/L ATP, 0.18mmol/L NADH, 0.5mmol/L PEP, 9.6U/mL LDH, 9.6U/mL PK). Enzymatic parameters V_{max} (maximal activity), K_{Ca} (apparent calcium affinity) and nH (co-operativity) were determined by nonlinear least-squares fitting of the activity data to the Hill equation (46) (Sigma Plot software, SPSS, Chicago, IL). Errors were determined using S.E.M for a minimum of three independent reconstitutions.

5.4.4 – Crystallization conditions

The methods used to generate helical and wide-two dimensional crystals have been described in great detail (22, 30, 47, 48) but will be reiterated here. Co-reconstituted proteoliposomes were collected by centrifugation in crystallization buffer (20 mmol/L imidazole (pH 7.4), 100 mmol/L KCl, 15 or 35 mmol/L $MgCl_2$, 0.5 mmol/L EGTA, and 0.5 mmol/L Na_3VO_4, with or without 30 mmol/L thapsigargin). The 0.5 mmol/L Na_3VO_4 was converted to decavanadate form by lowering the pH to 2 on ice, then slowly raising the pH to ~7 and immediately using the solution for crystallization. The pellet was subjected to two freeze-thaw cycles, resuspended with a micropipette, followed by two additional freeze-thaw cycles. The samples were incubated at 4°C for three to five days. The use of 15 mmol/L $MgCl_2$ in the crystallization buffer promoted the formation of helical crystals, whereas the use of 15 or 35 mmol/L $MgCl_2$ promoted the formation of large 2D crystals. The large 2D crystals were formed from SERCA in the presence of a Pro[21]-to-Thr Lys[27]-to-Ala PLN mutant (human PLN sequence (22)).

5.4.5 – Negative-stain TEM analysis of Pro²¹-to-Thr Lys²⁷-to-Ala PLN two-dimensional crystals

Two-dimensional crystals (prepared as previously described *5.3.4*) were applied to home-made carbon-coated 400-mesh Maxtaform Rh-flashed Cu grids (Ted Pella, Redding, CA, USA) and stained with 2% uranyl acetate. Imaging was conducted with a Tecnai F20 200 KV TEM outfitted with a Falcon II Direct Electron Detector (FEI/ThermoFisher Scientific, Hillsboro, OR, USA) and a Hitachi H-7650 60 KV TEM outfitted with an EMCCD (Hitachi Ltd, Chiyoda-ku, Tokyo, JAP).

5.4.6 – CryoEM analysis of Pro²¹-to-Thr Lys²⁷-to-Ala PLN two-dimensional crystals

Two-dimensional crystals (prepared as previously described *5.3.4*) were diluted in their respective crystallization buffers and applied to R 2/2 Quantifoil support-film coated, 300-mesh, Cu grids (Quantifoil Micro Tools, Großlöbichau, Germany) and vitrified in liquid ethane with a Vitrobot (FEI/ThermoFisher Scientific, Hillsboro, OR, USA) and imaged with a Tecnai F20 200 KV TEM outfitted with a Falcon II Direct Electron Detector (FEI/ThermoFisher Scientific, Hillsboro, OR, USA). Images were collected under low-dose conditions and automated with EPU for high-throughput data collection.

5.5 – Acknowledgements

5.6 – Conflict of interest

There is no conflict of interest in the work reported in this chapter.

5.7 – References

1. Goodsell, D. S., Autin, L., and Olson, A. J. (2019) Illustrate: Software for Biomolecular Illustration. *Structure*. 10.1016/j.str.2019.08.011

2. Adrian, M., Dubochet, J., Lepault, J., and McDowall, A. W. (1984) Cryo-electron microscopy of viruses. *Nature*. **308**, 32–36

3. Dubochet, J., Adrian, M., Chang, J.-J., Homo, J.-C., Lepault, J., McDowall, A. W., and Schultz, P. (1988) Cryo-electron microscopy of vitrified specimens. *Q. Rev. Biophys*. **21**, 129–228

4. Noble, A. J., Wei, H., Dandey, V. P., Zhang, Z., Tan, Y. Z., Potter, C. S., and Carragher, B. (2018) Reducing effects of particle adsorption to the air–water interface in cryo-EM. *Nat. Methods*. **15**, 793–795

5. Song, B., Lenhart, J., Flegler, V. J., Makbul, C., Rasmussen, T., and Böttcher, B. (2019) Capabilities of the Falcon III detector for single-particle structure determination. *Ultramicroscopy*. **203**, 145–154

6. von Loeffelholz, O., Papai, G., Danev, R., Myasnikov, A. G., Natchiar, S. K., Hazemann, I., Ménétret, J. F., and Klaholz, B. P. (2018) Volta phase plate data collection facilitates image processing and cryo-EM structure determination. *J. Struct. Biol*. **202**, 191–199

7. Bai, X. chen, McMullan, G., and Scheres, S. H. W. (2014) How cryo-EM is revolutionizing structural biology. *Trends Biochem. Sci*. **40**, 49–57

8. Yang, G., Zhou, R., Zhou, Q., Guo, X., Yan, C., Ke, M., Lei, J., and Shi, Y. (2019) Structural basis of Notch recognition by human γ-secretase. *Nature*. **565**, 192–197

9. Timcenko, M., Lyons, J. A., Januliene, D., Ulstrup, J. J., Dieudonné, T., Montigny, C., Ash, M.-R., Karlsen, J. L., Boesen, T., Kühlbrandt, W., Lenoir, G., Moeller, A., and Nissen, P. (2019) Structure and autoregulation of a P4-ATPase lipid flippase. *Nature*. 10.1038/s41586-019-1344-7

10. Bartesaghi, A., Aguerrebere, C., Falconieri, V., Banerjee, S., Earl, L. A., Zhu, X., Grigorieff, N., Milne, J. L. S., Sapiro, G., Wu, X., and Subramaniam, S. (2018) Atomic Resolution Cryo-EM Structure of β-Galactosidase. *Structure*. **26**, 848-856.e3

11. Merk, A., Bartesaghi, A., Banerjee, S., Falconieri, V., Rao, P., Davis, M. I., Pragani, R., Boxer, M. B., Earl, L. A., Milne, J. L. S., and Subramaniam, S. (2016) Breaking Cryo-EM Resolution Barriers to Facilitate Drug Discovery. *Cell*. **165**, 1698–1707

12. Murphy, B. J., Klusch, N., Langer, J., Mills, D. J., Yildiz, Ö., and Kühlbrandt, W. (2019) Rotary substates of mitochondrial ATP synthase reveal the basis of flexible F1-Fo coupling. *Science (80-*

. *).* 10.1126/science.aaw9128

13. Hofmann, S., Januliene, D., Mehdipour, A. R., Thomas, C., Stefan, E., Brüchert, S., Kuhn, B. T., Geertsma, E. R., Hummer, G., Tampé, R., and Moeller, A. (2019) Conformation space of a heterodimeric ABC exporter under turnover conditions. *Nature.* **571**, 580–583

14. Banerjee, S., Bartesaghi, A., Merk, A., Rao, P., Bulfer, S. L., Yan, Y., Green, N., Mroczkowski, B., Neitz, R. J., Wipf, P., Falconieri, V., Deshaies, R. J., Milne, J. L. S., Huryn, D., Arkin, M., and Subramaniam, S. (2016) 2.3 Å resolution cryo-EM structure of human p97 and mechanism of allosteric inhibition. *Science (80-.).* **351**, 871–875

15. Henderson, R., and Unwin, P. N. T. (1975) Three-dimensional model of purple membrane obtained by electron microscopy. *Nature.* **257**, 28–32

16. Young, H. S., Jones, L. R., and Stokes, D. L. (2001) Locating Phospholamban in Co-Crystals with Ca2+-ATPase by Cryoelectron Microscopy. *Biophys. J.* **81**, 884–894

17. Glaves, J. P., Fisher, L., Ward, A., and Young, H. S. (2010) *Helical Crystallization of Two Example Membrane Proteins. MsbA and the Ca2+-ATPase*, 1st Ed., Elsevier Inc., 10.1016/S0076-6879(10)83007-1

18. Stokes, D. L., Pomfret, A. J., Rice, W. J., Glaves, J. P., and Young, H. S. (2006) Interactions between Ca2+-ATPase and the pentameric form of phospholamban in two-dimensional co-crystals. *Biophys. J.* **90**, 4213–4223

19. Glaves, J. P., Primeau, J. O., Espinoza-Fonseca, L. M., Lemieux, M. J., and Young, H. S. (2019) The Phospholamban Pentamer Alters Function of the Sarcoplasmic Reticulum Calcium Pump SERCA. *Biophys. J.* **116**, 633–647

20. Young, H. S., Rigaud, J. L., Lacapère, J. J., Reddy, L. G., and Stokes, D. L. (1997) How to make tubular crystals by reconstitution of detergent-solubilized Ca2(+)-ATPase. *Biophys. J.* **72**, 2545–2558

21. Martonosi, A. N., and Pikula, S. (2003) The structure of the Ca 2 + -ATPase of sarcoplasmic reticulum . *Rev. Lit. Arts Am.* **50**, 337–365

22. Glaves, J. P., Trieber, C. a., Ceholski, D. K., Stokes, D. L., and Young, H. S. (2011) Phosphorylation and mutation of phospholamban alter physical interactions with the sarcoplasmic reticulum calcium pump. *J. Mol. Biol.* **405**, 707–723

23. Stokes, D. L., Pomfret, A. J., Rice, W. J., Glaves, J. P., and Young, H. S. (2006) Interactions between Ca2+-ATPase and the Pentameric Form of Phospholamban in Two-Dimensional Co-Crystals. *Biophys. J.* **90**, 4213–4223

24. Pugh, T. J., Kelly, M. A., Gowrisankar, S., Hynes, E., Seidman, M. A., Baxter, S. M., Bowser, M., Harrison, B., Aaron, D., Mahanta, L. M., Lakdawala, N. K., McDermott, G., White, E. T., Rehm, H. L., Lebo, M., and Funke, B. H. (2014) The landscape of genetic variation in dilated cardiomyopathy as surveyed by clinical DNA sequencing. *Genet. Med.* **16**, 601–608

25. Li, J., Boschek, C. B., Xiong, Y., Sacksteder, C. A., Squier, T. C., and Bigelow, D. J. (2005) Essential role for Pro21 in phospholamban for optimal inhibition of the Ca-ATPase. *Biochemistry.* **44**, 16181–16191

26. Gustavsson, M., Verardi, R., Mullen, D. G., Mote, K. R., Traaseth, N. J., Gopinath, T., and Veglia, G. (2013) Allosteric regulation of SERCA by phosphorylation-mediated conformational shift of phospholamban. *Proc. Natl. Acad. Sci. U. S. A.* **110**, 17338–43

27. Ferrington, D. A., Yao, Q., Squier, T. C., and Bigelow, D. J. (2002) Comparable Levels of Ca-ATPase Inhibition by Phospholamban in Slow-Twitch Skeletal and Cardiac Sarcoplasmic Reticulum. *Biochemistry.* **41**, 13289–13296

28. Waggoner, J. R., Huffman, J., Griffith, B. N., Jones, L. R., and Mahaney, J. E. (2004) Improved expression and characterization of Ca2+-ATPase and phospholamban in High-Five cells. *Protein Expr. Purif.* **34**, 56–67

29. Young, H. S., Reddy, L. G., Jones, L. R., and Stokes, D. L. (1998) Co-reconstitution and Co-crystallization of Phospholamban and Ca2+-ATPase a. *Ann. N. Y. Acad. Sci.* **853**, 103–115

30. Young, H. S., Jones, L. R., and Stokes, D. L. (2001) Locating phospholamban in co-crystals with Ca(2+)-ATPase by cryoelectron microscopy. *Biophys. J.* **81**, 884–894

31. Trieber, C. A., Douglas, J. L., Afara, M., and Young, H. S. (2005) The Effects of Mutation on the Regulatory Properties of Phospholamban in Co-Reconstituted Membranes†. *Biochemistry.* **44**, 3289–3297

32. Trieber, C. A., Afara, M., and Young, H. S. (2009) Effects of Phospholamban Transmembrane Mutants on the Calcium Affinity, Maximal Activity, and Cooperativity of the Sarcoplasmic Reticulum Calcium Pump. *Biochemistry.* **48**, 9287–9296

33. Ceholski, D. K., Trieber, C. a., and Young, H. S. (2012) Hydrophobic imbalance in the cytoplasmic domain of phospholamban is a determinant for lethal dilated cardiomyopathy. *J. Biol. Chem.* **287**, 16521–16529

34. Akin, B. L., Hurley, T. D., Chen, Z., and Jones, L. R. (2013) The structural basis for phospholamban inhibition of the calcium pump in sarcoplasmic reticulum. *J. Biol. Chem.* **288**, 30181–30191

35. Toyoshima, C., Iwasawa, S., Ogawa, H., Hirata, A., Tsueda, J., and Inesi, G. (2013) Crystal structures of the calcium pump and sarcolipin in the Mg2+-bound E1 state. *Nature.* **495**, 260

36. Winther, A.-M. L., Bublitz, M., Karlsen, J. L., Møller, J. V, Hansen, J. B., Nissen, P., and Buch-Pedersen, M. J. (2013) The sarcolipin-bound calcium pump stabilizes calcium sites exposed to the cytoplasm. *Nature.* **495**, 265

37. Ceholski, D. K., Trieber, C. a., Holmes, C. F. B., and Young, H. S. (2012) Lethal, hereditary mutants of phospholamban elude phosphorylation by protein kinase A. *J. Biol. Chem.* **287**, 26596–26605

38. Gorski, P. A., Glaves, J. P., Vangheluwe, P., and Young, H. S. (2013) Sarco(endo)plasmic Reticulum Calcium ATPase (SERCA) Inhibition by Sarcolipin Is Encoded in Its Luminal Tail. *J. Biol. Chem. .* **288**, 8456–8467

39. Glaves, J. P., Primeau, J. O., Gorski, P. A., Espinoza-Fonseca, L. M., Lemieux, M. J., and Young, H. S. (2019) Interaction of a sarcolipin pentamer and monomer with the sarcoplasmic reticulum calcium pump, SERCA. Running Title: A novel complex of sarcolipin and SERCA. *Biophysj.* **118**, 518–531

40. Young, H. S., and Stokes, D. L. (2004) The mechanics of calcium transport. *J. Membr. Biol.* **198**, 55–63

41. Douglas, J. L., Trieber, C. a., Afara, M., and Young, H. S. (2005) Rapid, high-yield expression and purification of Ca2+-ATPase regulatory proteins for high-resolution structural studies. *Protein Expr. Purif.* **40**, 118–125

42. Eletr, S., and Inesi, G. (1972) Phospholipid orientation in sacroplasmic membranes: Spin-label ESR and proton NMR studies. *Biochim. Biophys. Acta - Biomembr.* **282**, 174–179

43. Stokes, D. L., and Green, N. M. (1990) Three-dimensional crystals of CaATPase from sarcoplasmic reticulum. Symmetry and molecular packing. *Biophys. J.* **57**, 1–14

44. Smeazzetto, S., Armanious, G. P., Moncelli, M. R., Bak, J. J., Lemieux, M. J., Young, H. S., and Tadini-Buoninsegni, F. (2017) Conformational memory in the association of the transmembrane protein phospholamban with the sarcoplasmic reticulum calcium pump SERCA. *J. Biol. Chem.* **292**, 21330–21339

45. Warren, G. B., Toon, P. A., Birdsall, N. J., Lee, A. G., and Metcalfe, J. C. (1974) Reconstitution of a calcium pump using defined membrane components. *Proc. Natl. Acad. Sci. U. S. A.* **71**, 622–626

46. Weiss, J. N. (1997) The Hill equation revisited: uses and misuses. *FASEB J. Off. Publ. Fed. Am.*

Soc. Exp. Biol. **11**, 835–841

47. Xu, C., Rice, W. J., He, W., and Stokes, D. L. (2002) A structural model for the catalytic cycle of Ca2+-ATPase11Edited by W. Baumeister. *J. Mol. Biol.* **316**, 201–211

48. Glaves, J. P., Primeau, J. O., and Young, H. S. (2016) Two-Dimensional Crystallization of the Ca2+-ATPase for Electron Crystallography BT - P-Type ATPases: Methods and Protocols (Bublitz, M. ed), pp. 421–441, Springer New York, New York, NY, 10.1007/978-1-4939-3179-8_38

"If I have seen further it is by standing on ye sholders of Giants."

I. Newton – 1676

Chapter 6

Conclusion and future directions

6.1 – Conclusions and future directions

Conclusions in science are transient, reflecting the knowledge available at the time. Before the findings raised from the Michelson-Morley experiment in 1887 (1), the idea of light travelling through luminiferous ether explained the properties of light at the time. These experiments reevaluated the understanding of the physics of optics on earth and opened a new avenue for investigation. In a similar vein, one of the most significant shifts in the understanding of molecular biology and genetic transferred occurred with the formation of the Central Dogma (2). Crick, himself, remarked that his explanation would prove to be a "considerable over-simplification." Reflecting on the conclusions reached by prevailing theories in the past is not to highlight that they were 'incorrect,' but demonstrates that science is ever-evolving and provides support for the next major endeavour. With this said, the conclusions of the observations supported in this thesis are useful for addressing the current state of understanding in P-type ATPase regulation. However, perhaps the legitimate value of the work herein described is not just the evidence-based conclusions but how these conclusions provide the foundation for future endeavours in the field of calcium-ATPase mediated calcium re-uptake.

Although the conclusions for each chapter of the thesis have been provided within the text, there is merit in restating the findings to gain a broader perspective on the effects of SERCA regulation on the organism as a whole. The conclusions found can be summed up in 3 points.

1. The phospholamban pentamer naturally associates with SERCA

Previous 2D crystal analysis in our lab established that PLN pentamers interact with SERCA at a site near M3, although at the time, we lacked an explanation as to the functional significance of this interaction. Evidence of this interaction observed by cryoEM (3) had support from functional studies of mutations to PLN residues essential to pentamer formation. These mutations to PLN were subsequently found to have effects on SERCA's calcium transport properties and 2D crystal formation. The study outlined in Chapter 2 sought to explain the observed pentameric interaction of PLN with SERCA. By re-examining previous analyses of helical 2D crystals containing SERCA and PLN, we determined that, like the wide crystal morphology, PLN interacts with M3 of SERCA as an oligomer. What is significant about the SERCA-PLN interaction in helical crystals is that SERCA and PLN pack differently than in the wide 2D crystals. In the wide 2D crystals, the PLN pentamer participates in a crystal contact, though the same interaction in the helical crystals would not involve a crystals contact. Nonetheless, we observed an oligomeric form of PLN interacting with M3 of

SERCA in the helical crystals. The M3-PLN interaction in the helical crystals competes with a crystal contact between SERCA molecules; thus, a somewhat distorted PLN oligomer was observed. Co-reconstituted proteoliposomes containing SERCA and PLN were functionally analyzed at molar ratios targeting the monomeric and pentameric PLN interaction with SERCA, and these data revealed a functional role for the interaction observed in 2D crystals. We found that the modulation of SERCA's calcium affinity by PLN saturates at lower molar ratios of PLN to SERCA (<2:1). However, as the membrane concentration of PLN increases to a molar ratio of 5:1 PLN to SERCA (1 pentamer per SERCA), we observed an increase in the maximal activity of SERCA. We concluded that the PLN pentamer is responsible for the observed increase in SERCA turnover rate. MD simulations and molecular modelling of the interaction between PLN pentamer and SERCA showed that this interaction is stable and mediates its action by positioning two PLN molecules in contact with M3 and the calcium access funnel of SERCA. The SERCA-PLN interface includes an acyl chain, which offers an explanation for the lipid dependence of the interaction. In other words, the SERCA-PLN pentamer complex only forms at the low lipid-to-protein ratios found in SR membranes. The interaction of the pentamer places the cytoplasmic domains at the membrane surface, which leads us to conclude that the increased in SERCA's turnover rate is related to a local membrane perturbation caused by charged residues in PLN's cytoplasmic domain laying near the calcium access funnel.

This mechanism is exciting in the context of the regulation of calcium flux in the heart. It provides a mechanism to modulate SERCA activity to a variety of stimuli. For example, at low to medium cytosolic calcium concentrations (0.05 to 1.0 μmol/L), we observe a net inhibitory effect on SERCA calcium reuptake. The outlined mechanism of calcium reuptake provides adequate control of cardiac contractility at baseline levels. However, under conditions of heavy cardiac load, where cytosolic calcium concentrations become consistently elevated (1 to 10 μmol/L), the heart utilizes another arm of this same mechanism that maximizes SERCA activity to refill the SR for the next subsequent contraction quickly. For the organism as a whole, this allows rapid adaptation of the heart rate and cardiac output in response to multiple stimuli. However, this is only one part of an immensely complicated regulatory axis of cardiac contractility and cardiomyocyte relaxation.

These results provide the groundwork for future endeavours in elucidating the molecular details of this interaction. In particular, the effect of PLN phosphorylation on the natural association of PLN pentamers with SERCA requires attention. Phosphorylation is an essential part of the PLN-SERCA regulatory axis that likely plays an enormous role in regulatory modulation. Additionally, with

the identification of essential PLN residues for pentamer mediated V_{max} stimulation, one can now predict potentially deleterious SERCA residues and mutations in the region near the pentameric interface. By utilizing mutagenesis to move charged residues closer to and further from the calcium access funnel, we could further elaborate on the effects of the charge interaction between PLN, SERCA, and the lipid membrane.

2. The sarcolipin pentamer persistently and naturally associates with SERCA

While SLN was not initially thought to form a pentamer, evidence for oligomerization has been published (4–6). Given the similarity of SLN to PLN, we hypothesized that SLN would form a functional pentamer that interacts with M3, as SLN also uses a similar mechanism for SERCA regulation. Analysis of 2D crystals containing SERCA and SLN revealed that, indeed, SLN forms a higher-order oligomer that indirectly interacts with M3 of SERCA, but the interaction is distinct in that an additional SLN monomer mediates it. As outlined in Chapter 3, the evidence collected suggested that SERCA's V_{max} is sensitive to the concentration of SLN in the membrane. Based on our results, we found that SLN's ability to shift SERCA's calcium affinity saturates at lower molar ratios SLN to SERCA (>2:1), implying that the SLN monomer is sufficient to occupy the inhibitory groove of SERCA. Further analysis of SLN's effect on SERCA at a molar ratio of 5:1 SLN to SERCA revealed that as the membrane concentration of SLN increases, SERCA's maximal activity decreases, opposite to what we see with PLN. Molecular models, generated using protein docking and MD simulations of the SERCA-SLN monomer complex and the SLN pentamer, were investigated to probe the finer molecular details of the mechanism of interaction. MD simulations revealed that the structure of the SLN pentamer deviated from the expected symmetrical pentameric architecture expected. The SLN pentamer appeared to be an asymmetric combination of an SLN dimer and an SLN trimer. MD simulations of the interaction between SLN and transmembrane segment M3 of SERCA revealed that a stable interaction occurs via hydrophobic interactions between SLN's opposite face (to that utilized in pentamer formation) and the exposed face of M3. Distinct from the interaction of PLN with SERCA (Chapter 2), a lipid straddles the interaction between SLN and transmembrane segment M3 of SERCA and the lipid headgroup impinges on the M3-M4 loop of SERCA. We postulated that the position of SLN interacts with the lipid headgroup, which in turn restricts the movement of the M3-M4 loop involved in calcium transport.

We have identified that SLN elicits a membrane concentration-dependent effect on SERCA's calcium transport properties. Cross-linking and crystallographic evidence has identified that PLN and

SLN occupy SERCA's inhibitory groove. While the inhibitory culprit has been the monomer, a dimer of PLN was found in the crystal structure (7). The specific inhibitory groove interaction has only been observed in a distinct SERCA conformational state during calcium transport, a point between E2 and E1 with magnesium ions bound near the calcium-binding sites. Previous work has established that SERCA can undergo substrate-dependent conformational memory (8), where it has been identified that PLN has a continued regulatory effect on SERCA throughout the calcium transport cycle, not just on a single conformational state. By testing the substrate-dependence of SERCA's ATPase activity, we could demonstrate 'conformational memory.' We set to identify if SLN also has a persistent effect on SERCA's calcium transport properties throughout the E1-E2 conformational transitions during calcium translocation. We found that SLN's regulatory function is dependent on the conformation of SERCA, suggesting that there are multiple modes of SERCA-SLN interaction that persist throughout SERCA's calcium transport pathway and multiple turnover events. We can conclude that SLN remains associated with SERCA and depending on the starting conformation of SERCA, it can involve one or both interaction sites. This conclusion provides an exciting new complication to the already complicated regulatory arc of calcium transport. A modal SERCA-SLN complex can quickly compensate its regulatory functions to a fluctuating myocyte environment, particularly in the atria of the heart and in skeletal muscle during high activity.

To further explore the functional relevance of the SLN oligomeric interaction, there are a few avenues we can take. As the 2D crystal data suggests, there is an additional density consistent with an SLN monomer bridging the interaction between SERCA and an SLN pentamer. To provide a more precise explanation as to this additional density, we could explore the functional effects of a 6:1 molar ratio of SLN to SERCA on the calcium transport properties of SERCA. In addition, there is a lack of understanding of how these observations fit into the concept of SLN mediated thermogenesis in skeletal muscle as well as the physiological relevance of an SLN oligomer.

3. Regulatory interaction with M3 is modulatory and dependent on local micro-environments

As established in Chapter 5, PLN's regulatory capabilities are sensitive to mutation. Some human mutations to PLN have been linked to heart disease, and as such, we investigated one such mutation at the Pro[21] position, a Pro[21]-to-Thr mutation originally found in a 60-year-old female with clinical diagnoses and a family history of heart failure (9). The Pro[21]-to-Thr mutation to PLN has been found to alter PLN's secondary structure by increasing the α-helical characteristics of PLN. By linking this mutation to another mutation strongly associated with SERCA inhibition, we set to establish the effect

of this mutation in the context of a pentamer association with SERCA. What we found is that the effects of the mutation were consistent with a PLN pentamer with the cytoplasmic domain lifted off the lipid membrane interface, causing PLN to exhibit more 'SLN-like' pentameric characteristic. The effect of this mutation aligns with the central thesis of this document, in that regulatory modulation of SERCA is sensitive to the lipid-protein microenvironment near transmembrane segment M3. This conclusion supports our hypothesis and provides insight into the deleterious nature of the Pro^{21}-to-Thr mutation with respect to its association with DCM. Of course, a structure of the complex from 2D crystals with SERCA would provide valuable additional support for our hypothesis.

Where do we go from here? It would be interesting to test a permanently stabilized PLN pentamer in the absence of PLN monomers. The effect of such a construct on 2D crystals and on SERCA function would be very informative. One such peptide has been published (10) consisting of the transmembrane domain of PLN with a series of mutations that promote a very stable pentamer. We are in the process of testing this PL5 peptide for 2D crystallization and functional analyses.

6.2 – Take home message

When the whole is taken into consideration, regulation of a portion of SERCA's calcium transport properties occur at interfaces shared by both PLN and SLN. In cardiac tissue, these structures can explain modulatory modes of regulation in a tissue where there is a substantial variation in calcium movement, accompanying the relaxation and contraction of the heart. As mentioned in this thesis, there has been a sort of 'regulin-revolution' in the last few years with the discovery of more tissue-specific, small-peptide SERCA regulators (and there are likely more to be discovered). The conclusions of this thesis lay the groundwork for future investigations into the effects of these new 'regulins' on calcium regulation in the cell. It is exciting to consider that an oligomeric interaction between SERCA and its tissue/isoform-specific regulins could be part of the new dogma on the regulation of SERCA-based calcium reuptake.

"If I have seen further it is by standing on ye sholders of Giants" – Isaac Newton.

6.3 – References

1.   Michelson, A. A., and Morley, E. W. (1887) On the relative motion of the Earth and the luminiferous ether. *Am. J. Sci.* . **Series 3 V**, 333–345

2.   Crick, F. (1970) Central dogma of molecular biology. *Nature.* **227**, 561–563

3.   Glaves, J. P., Trieber, C. a., Ceholski, D. K., Stokes, D. L., and Young, H. S. (2011) Phosphorylation and mutation of phospholamban alter physical interactions with the sarcoplasmic reticulum calcium pump. *J. Mol. Biol.* **405**, 707–723

4.   Cao, Y., Wu, X., Yang, R., Wang, X., Sun, H., and Lee, I. (2017) Self-assembling study of sarcolipin and its mutants in multiple molecular dynamic simulations. *Proteins Struct. Funct. Bioinforma.* **85**, 1065–1077

5.   Autry, J. M., Rubin, J. E., Pietrini, S. D., Winters, D. L., Robia, S. L., and Thomas, D. D. (2011) Oligomeric Interactions of Sarcolipin and the Ca-ATPase. *J. Biol. Chem.* . **286**, 31697–31706

6.   Hellstern, S., Pegoraro, S., Karim, C. B., Lustig, A., Thomas, D. D., Moroder, L., and Engel, J. (2001) Sarcolipin, the Shorter Homologue of Phospholamban, Forms Oligomeric Structures in Detergent Micelles and in Liposomes. *J. Biol. Chem.* **276**, 30845–30852

7.   Akin, B. L., Hurley, T. D., Chen, Z., and Jones, L. R. (2013) The structural basis for phospholamban inhibition of the calcium pump in sarcoplasmic reticulum. *J. Biol. Chem.* **288**, 30181–30191

8.   Smeazzetto, S., Armanious, G. P., Moncelli, M. R., Bak, J. J., Lemieux, M. J., Young, H. S., and Tadini-Buoninsegni, F. (2017) Conformational memory in the association of the transmembrane protein phospholamban with the sarcoplasmic reticulum calcium pump SERCA. *J. Biol. Chem.* **292**, 21330–21339

9.   Pugh, T. J., Kelly, M. A., Gowrisankar, S., Hynes, E., Seidman, M. A., Baxter, S. M., Bowser, M., Harrison, B., Aaron, D., Mahanta, L. M., Lakdawala, N. K., McDermott, G., White, E. T., Rehm, H. L., Lebo, M., and Funke, B. H. (2014) The landscape of genetic variation in dilated cardiomyopathy as surveyed by clinical DNA sequencing. *Genet. Med.* **16**, 601–608

10.   Mravic, M., Thomaston, J. L., Tucker, M., Solomon, P. E., Liu, L., and DeGrado, W. F. (2019) Packing of apolar side chains enables accurate design of highly stable membrane proteins.

Science (80-.). **363**, 1418 LP – 1423

Works cited

Chapter 1: The SarcoEndoplasmic Reticulum Calcium ATPase

1.   Goodsell, D. S., Autin, L., and Olson, A. J. (2019) Illustrate: Software for Biomolecular Illustration. *Structure*. 10.1016/j.str.2019.08.011

2.   Izawa, M. R. M., Nesbitt, H. W., MacRae, N. D., and Hoffman, E. L. (2010) Composition and evolution of the early oceans: Evidence from the Tagish Lake meteorite. *Earth Planet. Sci. Lett.* **298**, 443–449

3.   Kazmierczak, J., and Kempe, S. (2004) Calcium build-up in the Precambrian Sea: A major promoter in the evolution of eukaryotic life, pp. 329–345

4.   Plattner, H., and Verkhratsky, A. (2013) Ca2+ signalling early in evolution – all but primitive. *J. Cell Sci.* **126**, 2141 LP – 2150

5.   Berkelman, T., Garret-Engele, P., and Hoffman, N. E. (1994) The pacL gene of Synechococcus sp. strain PCC 7942 encodes a Ca2+- transporting ATPase. *J. Bacteriol.* **176**, 4430–4436

6.   Case, R. M., Eisner, D., Gurney, A., Jones, O., Muallem, S., and Verkhratsky, A. (2007) Evolution of calcium homeostasis: From birth of the first cell to an omnipresent signalling system. *Cell Calcium.* **42**, 345–350

7.   Shemarova, I. V., and Nesterov, V. P. (2005) Evolution of mechanisms of Ca2+-signaling: Role of calcium ions in signal transduction in prokaryotes. *J. Evol. Biochem. Physiol.* **41**, 12–19

8.   López-García, P., and Moreira, D. (2019) Eukaryogenesis, a syntrophy affair. *Nat. Microbiol.* **4**, 1068–1070

9.   Plattner, H., and Verkhratsky, A. (2015) Evolution of calcium signalling. *Cell Calcium.* **57**, 121–122

10.   Verkhratsky, A., and Parpura, V. (2014) Calcium signalling and calcium channels: Evolution and general principles. *Eur. J. Pharmacol.* **739**, 1–3

11.   Cai, X., Wang, X., Patel, S., and Clapham, D. E. (2015) Insights into the early evolution of animal calcium signaling machinery: A unicellular point of view. *Cell Calcium.* **57**, 166–173

12.   Blackstone, N. W. (2015) The impact of mitochondrial endosymbiosis on the evolution of calcium signaling. *Cell Calcium.* **57**, 133–139

13.   Snavely, M. D., Florer, J. B., Miller, C. G., and Maguire, M. E. (1989) Magnesium transport in Salmonella typhimurium: Expression of cloned genes for three distinct Mg2+ transport systems. *J. Bacteriol.* **171**, 4752–4760

14.   Argüello, J. M., González-Guerrero, M., and Raimunda, D. (2011) Bacterial transition metal P 1B-ATPases: Transport mechanism and roles in virulence. *Biochemistry.* **50**, 9940–9949

15. Timcenko, M., Lyons, J. A., Januliene, D., Ulstrup, J. J., Dieudonné, T., Montigny, C., Ash, M.-R., Karlsen, J. L., Boesen, T., Kühlbrandt, W., Lenoir, G., Moeller, A., and Nissen, P. (2019) Structure and autoregulation of a P4-ATPase lipid flippase. *Nature*. 10.1038/s41586-019-1344-7

16. Skou, J. C. (1957) The influence of some cations on an adenosine triphosphatase from peripheral nerves. *Biochim. Biophys. Acta*. **23**, 394–401

17. Berridge, M. J., Bootman, M. D., and Roderick, H. L. (2003) Calcium signalling: dynamics, homeostasis and remodelling. *Nat. Rev. Mol. Cell Biol.* **4**, 517–529

18. Carafoli, E., and Krebs, J. (2016) Why Calcium? How Calcium Became the Best Communicator. *J. Biol. Chem.* . **291**, 20849–20857

19. Lieber, R. L., Roberts, T. J., Blemker, S. S., Lee, S. S. M., and Herzog, W. (2017) Skeletal muscle mechanics, energetics and plasticity. *J. Neuroeng. Rehabil.* **14**, 1–16

20. Doroudgar, S., and Glembotski, C. C. (2013) New concepts of endoplasmic reticulum function in the heart: Programmed to conserve. *J. Mol. Cell. Cardiol.* **55**, 85–91

21. Bers, D. M. (2008) Calcium Cycling and Signaling in Cardiac Myocytes. *Annu. Rev. Physiol.* **70**, 23–49

22. Møller, J. V., Olesen, C., Winther, A.-M. L., and Nissen, P. (2010) The sarcoplasmic Ca2+-ATPase: design of a perfect chemi-osmotic pump. *Q. Rev. Biophys.* **43**, 501–566

23. Brini, M., Calì, T., Ottolini, D., and Carafoli, E. (2012) Calcium Pumps: Why So Many? *Compr. Physiol.* doi:10.1002/cphy.c110034

24. Wuytack, F., Raeymaekers, L., and Missiaen, L. (2002) Molecular physiology of the SERCA and SPCA pumps. *Cell Calcium*. **32**, 279–305

25. Dally, S., Corvazier, E., Bredoux, R., Bobe, R., and Enouf, J. (2010) Multiple and diverse coexpression, location, and regulation of additional SERCA2 and SERCA3 isoforms in nonfailing and failing human heart. *J. Mol. Cell. Cardiol.* **48**, 633–644

26. Kósa, M., Brinyiczki, K., van Damme, P., Goemans, N., Hancsák, K., Mendler, L., and Zádor, E. (2015) The neonatal sarcoplasmic reticulum Ca2+-ATPase gives a clue to development and pathology in human muscles. *J. Muscle Res. Cell Motil.* **36**, 195–203

27. Toustrup-Jensen, M. S., Holm, R., Einholm, A. P., Schack, V. R., Morth, J. P., Nissen, P., Andersen, J. P., and Vilsen, B. (2009) The C Terminus of Na+,K+-ATPase Controls Na+ Affinity on Both Sides of the Membrane through Arg935. *J. Biol. Chem.* . **284**, 18715–18725

28. Vangheluwe, P., Raeymaekers, L., Dode, L., and Wuytack, F. (2005) Modulating

sarco(endo)plasmic reticulum Ca2+ ATPase 2 (SERCA2) activity: Cell biological implications. *Cell Calcium.* **38**, 291–302

29. Gorski, P. a., Trieber, C. a., Larivière, E., Schuermans, M., Wuytack, F., Young, H. S., and Vangheluwe, P. (2012) Transmembrane helix 11 is a genuine regulator of the endoplasmic reticulum Ca2+ pump and acts as a functional parallel of β-subunit on α-Na+,K+-ATPase. *J. Biol. Chem.* **287**, 19876–19885

30. Vandecaetsbeek, I., Trekels, M., De Maeyer, M., Ceulemans, H., Lescrinier, E., Raeymaekers, L., Wuytack, F., and Vangheluwe, P. (2009) Structural basis for the high Ca2+ affinity of the ubiquitous SERCA2b Ca2+ pump. *Proc. Natl. Acad. Sci. U. S. A.* **106**, 18533–18538

31. Gélébart, P., Martin, V., Enouf, J., and Papp, B. (2003) Identification of a new SERCA2 splice variant regulated during monocytic differentiation. *Biochem. Biophys. Res. Commun.* **303**, 676–684

32. Regis Bobe, E. R. C. (2013) Sarco (Endo) Plasmic Reticulum Calcium Atpases (SERCA) Isoforms in the Normal and Diseased Cardiac, Vascular and Skeletal Muscle. *J. Cardiovasc. Dis. Diagnosis.* **01**, 1–6

33. Sagara, Y., Fernandez-Belda, F., de Meis, L., and Inesi, G. (1992) Characterization of the inhibition of intracellular Ca2+ transport ATPases by thapsigargin. *J. Biol. Chem. .* **267**, 12606–12613

34. Reddy, L. G., Jones, L. R., Pace, R. C., and Stokes, D. L. (1996) Purified, Reconstituted Cardiac Ca2+-ATPase Is Regulated by Phospholamban but Not by Direct Phosphorylation with Ca2+/Calmodulin-dependent Protein Kinase. *J. Biol. Chem. .* **271**, 14964–14970

35. Lipskaia, L., Keuylian, Z., Blirando, K., Mougenot, N., Jacquet, A., Rouxel, C., Sghairi, H., Elaib, Z., Blaise, R., Adnot, S., Hajjar, R. J., Chemaly, E. R., Limon, I., and Bobe, R. (2014) Expression of sarco (endo) plasmic reticulum calcium ATPase (SERCA) system in normal mouse cardiovascular tissues, heart failure and atherosclerosis. *Biochim. Biophys. Acta - Mol. Cell Res.* **1843**, 2705–2718

36. Toyoshima, C., Nakasako, M., Nomura, H., and Ogawa, H. (2000) Crystal structure of the calcium pump of sarcoplasmic reticulum at 2.6 A resolution. *Nature.* **405**, 647–655

37. Laursen, M., Bublitz, M., Moncoq, K., Olesen, C., Møller, J. V., Young, H. S., Nissen, P., and Morth, J. P. (2009) Cyclopiazonic Acid Is Complexed to a Divalent Metal Ion When Bound to the Sarcoplasmic Reticulum Ca2+-ATPase. *J. Biol. Chem. .* **284**, 13513–13518

38. Moncoq, K., Trieber, C. A., and Young, H. S. (2007) The Molecular Basis for Cyclopiazonic Acid Inhibition of the Sarcoplasmic Reticulum Calcium Pump. *J. Biol. Chem. .* **282**, 9748–9757

39. MacLennan, D. H., Brandl, C. J., Korczak, B., and Green, N. M. (1985) Amino-acid sequence of a Ca2+ + Mg2+ -dependent ATPase from rabbit muscle sarcoplasmic reticulum, deduced from its complementary DNA sequence. *Nature.* **316**, 696–700

40. de Meis, L., and Vianna, A. L. (1979) Energy interconversion by the Ca2+-dependent ATPase of the sarcoplasmic reticulum. *Annu. Rev. Biochem.* **48**, 275–292

41. Yokokawa, M., and Takeyasu, K. (2011) Motion of the Ca2+-pump captured. *FEBS J.* **278**, 3025–3031

42. Toyoshima, C. (2008) Structural aspects of ion pumping by Ca2+-ATPase of sarcoplasmic reticulum. *Arch. Biochem. Biophys.* **476**, 3–11

43. Toyoshima, C. (2009) How Ca2+-ATPase pumps ions across the sarcoplasmic reticulum membrane. *Biochim. Biophys. Acta - Mol. Cell Res.* **1793**, 941–946

44. Sørensen, T. L.-M., Møller, J. V., and Nissen, P. (2004) Phosphoryl Transfer and Calcium Ion Occlusion in the Calcium Pump. *Science (80-.).* **304**, 1672 LP – 1675

45. Winther, A.-M. L., Bublitz, M., Karlsen, J. L., Møller, J. V, Hansen, J. B., Nissen, P., and Buch-Pedersen, M. J. (2013) The sarcolipin-bound calcium pump stabilizes calcium sites exposed to the cytoplasm. *Nature.* **495**, 265

46. Toyoshima, C., Iwasawa, S., Ogawa, H., Hirata, A., Tsueda, J., and Inesi, G. (2013) Crystal structures of the calcium pump and sarcolipin in the Mg2+-bound E1 state. *Nature.* **495**, 260

47. Akin, B. L., Hurley, T. D., Chen, Z., and Jones, L. R. (2013) The Structural Basis for Phospholamban Inhibition of the Calcium Pump in Sarcoplasmic Reticulum. *J. Biol. Chem. .* **288**, 30181–30191

48. Henderson, I. M., Starling, A. P., Wictome, M., East, J. M., and Lee, A. G. (1994) Binding of Ca2+ to the Ca2+-ATPase of sarcoplasmic reticulum: kinetic studies. *Biochem. J.* **297**, 625 LP – 636

49. Peinelt, C., and Apell, H.-J. (2002) Kinetics of the Ca2+, H+, and Mg2+ Interaction with the Ion-Binding Sites of the SR Ca-ATPase. *Biophys. J.* **82**, 170–181

50. Kirchberger, M. A., Tada, M., and Katz, A. M. (1975) Phospholamban: a regulatory protein of the cardiac sarcoplasmic reticulum. *Recent Adv. Stud. Cardiac Struct. Metab.* **5**, 103–115

51. Wawrzynow, A., Theibert, J. L., Murphy, C., Jona, I., Martonosi, A., and Collins, J. H. (1992) Sarcolipin, the "proteolipid" of skeletal muscle sarcoplasmic reticulum, is a unique, amphipathic, 31-residue peptide. *Arch. Biochem. Biophys.* **298**, 620–623

52. Odermatt, A, Becker, S., Khanna, V. K., Kurzydlowski, K., Leisner, E., Pette, D., and

MacLennan, D. H. (1998) Sarcolipin regulates the activity of SERCA1, the fast-twitch skeletal muscle sarcoplasmic reticulum Ca2+-ATPase. *J. Biol. Chem.* **273**, 12360–12369

53. Odermatt, a, Taschner, P. E., Scherer, S. W., Beatty, B., Khanna, V. K., Cornblath, D. R., Chaudhry, V., Yee, W. C., Schrank, B., Karpati, G., Breuning, M. H., Knoers, N., and MacLennan, D. H. (1997) Characterization of the gene encoding human sarcolipin (SLN), a proteolipid associated with SERCA1: absence of structural mutations in five patients with Brody disease. *Genomics.* **45**, 541–553

54. Simmerman, H. K. B., Collins, J. H., Theibert, J. L., Wegener, a. D., and Jones, L. R. (1986) Sequence analysis of phospholamban. Identification of phosphorylation sites and two major structural domains. *J. Biol. Chem.* **261**, 13333–13341

55. Stokes, D. L. (1997) Keeping Calcium in its Place: Ca2+ ATPase and Phospholamban. *Curr. Opin. Struct. Biol.* **7**, 550–556

56. Glaves, J. P., Primeau, J. O., Espinoza-Fonseca, L. M., Lemieux, M. J., and Young, H. S. (2019) The Phospholamban Pentamer Alters Function of the Sarcoplasmic Reticulum Calcium Pump SERCA. *Biophys. J.* **116**, 633–647

57. KATZ, A. M. (1998) Discovery of Phospholamban: A Personal History. *Ann. N. Y. Acad. Sci.* **853**, 9–19

58. Tada, M., Kirchberger, M. A., Repke, D. I., and Katz, A. M. (1974) The Stimulation of Calcium Transport in Cardiac Sarcoplasmic Reticulum by Adenosine 3':5'-Monophosphate-dependent Protein Kinase. *J. Biol. Chem.* . **249**, 6174–6180

59. MacLennan, D. H., and Kranias, E. G. (2003) Phospholamban: a crucial regulator of cardiac contractility. *Nat. Rev. Mol. Cell Biol.* **4**, 566–577

60. Asahi, M., Mckenna, E., Kurzydlowski, K., Tada, M., and Maclennan, D. H. (2000) Physical Interactions between Phospholamban and Sarco (endo) plasmic Reticulum Ca 2+-ATPases Are Dissociated by Elevated Ca 2+, but Not by Phospholamban Phosphorylation, Vanadate, or Thapsigargin, and Are Enhanced by ATP *. **275**, 15034–15038

61. Tada, M., Kirchberger, M. A., and Katz, A. M. (1976) Regulation of calcium transport in cardiac sarcoplasmic reticulum by cyclic AMP-dependent protein kinase. *Recent Adv. Stud. Cardiac Struct. Metab.* **9**, 225–239

62. Tada, M., Inui, M., Yamada, M., Kadoma, M., Kuzuya, T., Abe, H., and Kakiuchi, S. (1983) Effects of phospholamban phosphorylation catalyzed by adenosine 3':5'-monophosphate- and calmodulin-dependent protein kinases on calcium transport ATPase of cardiac sarcoplasmic

reticulum. *J. Mol. Cell. Cardiol.* **15**, 335–346

63. Cornea, R. L., Jones, L. R., Autry, J. M., and Thomas, D. D. (1997) Mutation and Phosphorylation Change the Oligomeric Structure of Phospholamban in Lipid Bilayers. *Biochemistry.* **36**, 2960–2967

64. Chu, G., Li, L., Sato, Y., Harrer, J. M., Kadambi, V. J., Hoit, B. D., Bers, D. M., and Kranias, E. G. (1998) Pentameric Assembly of Phospholamban Facilitates Inhibition of Cardiac Function in Vivo . *J. Biol. Chem. .* **273**, 33674–33680

65. Glaves, J. P., Trieber, C. a., Ceholski, D. K., Stokes, D. L., and Young, H. S. (2011) Phosphorylation and mutation of phospholamban alter physical interactions with the sarcoplasmic reticulum calcium pump. *J. Mol. Biol.* **405**, 707–723

66. Stokes, D. L., Pomfret, A. J., Rice, W. J., Glaves, J. P., and Young, H. S. (2006) Interactions between Ca2+-ATPase and the Pentameric Form of Phospholamban in Two-Dimensional Co-Crystals. *Biophys. J.* **90**, 4213–4223

67. Rasmussen, S. G. F., Devree, B. T., Zou, Y., Kruse, A. C., Chung, K. Y., Kobilka, T. S., Thian, F. S., Chae, P. S., Pardon, E., Calinski, D., Mathiesen, J. M., Shah, S. T. A., Lyons, J. A., Caffrey, M., Gellman, S. H., Steyaert, J., Skiniotis, G., Weis, W. I., Sunahara, R. K., and Kobilka, B. K. (2011) Crystal structure of the β 2 adrenergic receptor-Gs protein complex. *Nature.* **477**, 549–557

68. Hilger, D., Masureel, M., and Kobilka, B. K. (2018) Structure and dynamics of GPCR signaling complexes. *Nat. Struct. Mol. Biol.* **25**, 4–12

69. Kimura, Y., Kurzydlowski, K., Tada, M., and MacLennan, D. H. (1997) Phospholamban Inhibitory Function Is Activated by Depolymerization. *J. Biol. Chem. .* **272**, 15061–15064

70. Catalucci, D., Latronico, M. V. G., Ceci, M., Rusconi, F., Young, H. S., Gallo, P., Santonastasi, M., Bellacosa, A., Brown, J. H., and Condorelli, G. (2009) Akt Increases Sarcoplasmic Reticulum Ca2+ Cycling by Direct Phosphorylation of Phospholamban at Thr17. *J. Biol. Chem. .* **284**, 28180–28187

71. Bartel, S., Vetter, D., Schlegel, W.-P., Wallukat, G., Krause, E.-G., and Karczewski, P. (2000) Phosphorylation of Phospholamban at Threonine-17 in the Absence and Presence of β - Adrenergic Stimulation in Neonatal Rat Cardiomyocytes. *J. Mol. Cell. Cardiol.* **32**, 2173–2185

72. Mattiazzi, A., and Kranias, E. (2014) The role of CaMKII regulation of phospholamban activity in heart disease. *Front. Pharmacol. .* **5**, 5

73. Haghighi, K., Kolokathis, F., Pater, L., Lynch, R. A., Asahi, M., Gramolini, A. O., Fan, G.-C.,

Tsiapras, D., Hahn, H. S., Adamopoulos, S., Liggett, S. B., Dorn II, G. W., MacLennan, D. H., Kremastinos, D. T., and Kranias, E. G. (2003) Human phospholamban null results in lethal dilated cardiomyopathy revealing a critical difference between mouse and human. *J. Clin. Invest.* **111**, 869–876

74. Landstrom, A. P., Adekola, B. A., Bos, J. M., Ommen, S. R., and Ackerman, M. J. (2011) PLN-encoded phospholamban mutation in a large cohort of hypertrophic cardiomyopathy cases: Summary of the literature and implications for genetic testing. *Am. Heart J.* **161**, 165–171

75. Schmitt, J. P., Kamisago, M., Asahi, M., Li, G. H., Ahmad, F., Mende, U., Kranias, E. G., MacLennan, D. H., Seidman, J. G., and Seidman, C. E. (2003) Dilated cardiomyopathy and heart failure caused by a mutation in phospholamban. *Science.* **299**, 1410–1413

76. P., S. J., Ferhaan, A., Kristina, L., Lutz, H., Stefan, S., Michio, A., H., M. D., E., S. C., J.G., S., and J., L. M. (2009) Alterations of Phospholamban Function Can Exhibit Cardiotoxic Effects Independent of Excessive Sarcoplasmic Reticulum Ca2+-ATPase Inhibition. *Circulation.* **119**, 436–444

77. DeWitt, M. M., MacLeod, H. M., Soliven, B., and McNally, E. M. (2006) Phospholamban R14 Deletion Results in Late-Onset, Mild, Hereditary Dilated Cardiomyopathy. *J. Am. Coll. Cardiol.* **48**, 1396–1398

78. Haghighi, K., Kolokathis, F., Gramolini, A. O., Waggoner, J. R., Pater, L., Lynch, R. A., Fan, G.-C., Tsiapras, D., Parekh, R. R., Dorn, G. W., MacLennan, D. H., Kremastinos, D. T., and Kranias, E. G. (2006) A mutation in the human phospholamban gene, deleting arginine 14, results in lethal, hereditary cardiomyopathy. *Proc. Natl. Acad. Sci.* **103**, 1388 LP – 1393

79. Toyofuku, T., Kurzydlowski, K., Tada, M., and MacLennan, D. H. (1994) Amino acids Glu2 to Ile18 in the cytoplasmic domain of phospholamban are essential for functional association with the Ca(2+)-ATPase of sarcoplasmic reticulum. *J. Biol. Chem.* . **269**, 3088–3094

80. Fajardo, V. a., Bombardier, E., Vigna, C., Devji, T., Bloemberg, D., Gamu, D., Gramolini, A. O., Quadrilatero, J., and Tupling, a. R. (2013) Co-Expression of SERCA isoforms, phospholamban and sarcolipin in human skeletal muscle fibers. *PLoS One.* **8**, 1–13

81. Trieber, C. A., Afara, M., and Young, H. S. (2009) Effects of Phospholamban Transmembrane Mutants on the Calcium Affinity, Maximal Activity, and Cooperativity of the Sarcoplasmic Reticulum Calcium Pump. *Biochemistry.* **48**, 9287–9296

82. Autry, J. M., and Jones, L. R. (1997) Functional Co-expression of the Canine Cardiac Ca2+Pump and Phospholamban in Spodoptera frugiperda (Sf21) Cells Reveals New Insights

on ATPase Regulation . *J. Biol. Chem.* . **272**, 15872–15880

83. Simmerman, H. K. B., Kobayashi, Y. M., Autry, J. M., and Jones, L. R. (1996) A leucine zipper stabilizes the pentameric membrane domain of phospholamban and forms a coiled-coil pore structure. *J. Biol. Chem.* **271**, 5941–5946

84. Sugita, Y., Miyashita, N., Yoda, T., Ikeguchi, M., and Toyoshima, C. (2006) Structural Changes in the Cytoplasmic Domain of Phospholamban by Phosphorylation at Ser16: A Molecular Dynamics Study. *Biochemistry.* **45**, 11752–11761

85. Gustavsson, M., Verardi, R., Mullen, D. G., Mote, K. R., Traaseth, N. J., Gopinath, T., and Veglia, G. (2013) Allosteric regulation of SERCA by phosphorylation-mediated conformational shift of phospholamban. *Proc. Natl. Acad. Sci. U. S. A.* **110**, 17338–43

86. Karim, C. B., Zhang, Z., Howard, E. C., Torgersen, K. D., and Thomas, D. D. (2006) Phosphorylation-dependent conformational switch in spin-labeled phospholamban bound to SERCA. *J. Mol. Biol.* **358**, 1032–40

87. Ceholski, D. K., Trieber, C. A., Holmes, C. F. B., and Young, H. S. (2012) Lethal, Hereditary Mutants of Phospholamban Elude Phosphorylation by Protein Kinase A. *J. Biol. Chem.* . **287**, 26596–26605

88. Wittmann, T., Lohse, M. J., and Schmitt, J. P. (2015) Phospholamban pentamers attenuate PKA-dependent phosphorylation of monomers. *J. Mol. Cell. Cardiol.* **80C**, 90–97

89. Masterson, L. R., Cheng, C., Yu, T., Tonelli, M., Kornev, A., Taylor, S. S., and Veglia, G. (2010) Dynamics connect substrate recognition to catalysis in protein kinase A. *Nat. Chem. Biol.* **6**, 821

90. Kemp, B. E., Bylund, D. B., Huang, T. S., and Krebs, E. G. (1975) Substrate specificity of the cyclic AMP-dependent protein kinase. *Proc. Natl. Acad. Sci. U. S. A.* **72**, 3448–3452

91. Macdougall, L. K., Jones, L. R., and Cohen, P. (1991) Identification of the major protein phosphatases in mammalian cardiac muscle which dephosphorylate phospholamban. *Eur. J. Biochem.* **196**, 725–734

92. Steenaart, N. A. E., Ganim, J. R., Di Salvo, J., and Kranias, E. G. (1992) The phospholamban phosphatase associated with cardiac sarcoplasmic reticulum is a type 1 enzyme. *Arch. Biochem. Biophys.* **293**, 17–24

93. Blackwell, D. J., Zak, T. J., and Robia, S. L. (2016) Cardiac Calcium ATPase Dimerization Measured by Cross-Linking and Fluorescence Energy Transfer. *Biophys. J.* **111**, 1192–1202

94. Haghighi, K., Bidwell, P., and Kranias, E. G. (2014) Phospholamban interactome in cardiac contractility and survival: A new vision of an old friend. *J. Mol. Cell. Cardiol.* **77**, 160–167

95. Kovacs, R. J., Nelson, M. T., Simmerman, H. K., and Jones, L. R. (1988) Phospholamban forms Ca2+-selective channels in lipid bilayers. *J. Biol. Chem. .* **263**, 18364–18368

96. Smeazzetto, S., Schröder, I., Thiel, G., and Moncelli, M. R. (2011) Phospholamban generates cation selective ion channels. *Phys. Chem. Chem. Phys.* **13**, 12935–12939

97. Smeazzetto, S., Saponaro, A., Young, H. S., Moncelli, M. R., and Thiel, G. (2013) Structure-Function Relation of Phospholamban: Modulation of Channel Activity as a Potential Regulator of SERCA Activity. *PLoS One.* **8**, e52744

98. Trieber, C. A., Douglas, J. L., Afara, M., and Young, H. S. (2005) The Effects of Mutation on the Regulatory Properties of Phospholamban in Co-Reconstituted Membranes†. *Biochemistry.* **44**, 3289–3297

99. Autry, J. M., Thomas, D. D., and Espinoza-Fonseca, L. M. (2016) Sarcolipin Promotes Uncoupling of the SERCA Ca2+ Pump by Inducing a Structural Rearrangement in the Energy-Transduction Domain. *Biochemistry.* **55**, 6083–6086

100. Gorski, P. A., Glaves, J. P., Vangheluwe, P., and Young, H. S. (2013) Sarco(endo)plasmic Reticulum Calcium ATPase (SERCA) Inhibition by Sarcolipin Is Encoded in Its Luminal Tail. *J. Biol. Chem. .* **288**, 8456–8467

101. Winther, A.-M. L., Bublitz, M., Karlsen, J. L., Møller, J. V, Hansen, J. B., Nissen, P., and Buch-Pedersen, M. J. (2013) The sarcolipin-bound calcium pump stabilizes calcium sites exposed to the cytoplasm. *Nature.* **495**, 265–9

102. Sahoo, S. K., Shaikh, S. A., Sopariwala, D. H., Bal, N. C., Bruhn, D. S., Kopec, W., Khandelia, H., and Periasamy, M. (2015) The N Terminus of Sarcolipin Plays an Important Role in Uncoupling Sarco-endoplasmic Reticulum Ca2+-ATPase (SERCA) ATP Hydrolysis from Ca2+ Transport. *J. Biol. Chem.* **290**, 14057–14067

103. Sahoo, S. K., Shaikh, S. A., Sopariwala, D. H., Bal, N. C., and Periasamy, M. (2013) Sarcolipin protein interaction with sarco(endo)plasmic reticulum Ca2+ ATPase (SERCA) is distinct from phospholamban protein, and only sarcolipin can promote uncoupling of the SERCA pump. *J. Biol. Chem.* **288**, 6881–6889

104. Reddy, L. G., Cornea, R. L., Winters, D. L., McKenna, E., and Thomas, D. D. (2003) Defining the Molecular Components of Calcium Transport Regulation in a Reconstituted Membrane System. *Biochemistry.* **42**, 4585–4592

105. Hughes, E., Clayton, J. C., Kitmitto, A., Esmann, M., and Middleton, D. A. (2007) Solid-state NMR and functional measurements indicate that the conserved tyrosine residues of sarcolipin

are involved directly in the inhibition of SERCA1. *J. Biol. Chem.* **282**, 26603–26613

106. Tupling, A. R., Asahi, M., and MacLennan, D. H. (2002) Sarcolipin Overexpression in Rat Slow Twitch Muscle Inhibits Sarcoplasmic Reticulum Ca2+ Uptake and Impairs Contractile Function . *J. Biol. Chem. .* **277**, 44740–44746

107. Babu, G. J., Bhupathy, P., Petrashevskaya, N. N., Wang, H., Raman, S., Wheeler, D., Jagatheesan, G., Wieczorek, D., Schwartz, A., Janssen, P. M. L., Ziolo, M. T., and Periasamy, M. (2006) Targeted Overexpression of Sarcolipin in the Mouse Heart Decreases Sarcoplasmic Reticulum Calcium Transport and Cardiac Contractility. *J. Biol. Chem. .* **281**, 3972–3979

108. Bal, N. C., Maurya, S. K., Sopariwala, D. H., Sahoo, S. K., Gupta, S. C., Shaikh, S. a, Pant, M., Rowland, L. a, Goonasekera, S. a, Molkentin, J. D., and Periasamy, M. (2012) Sarcolipin is a newly identified regulator of muscle-based thermogenesis in mammals. *Nat. Med.* **18**, 1575–1579

109. Smith, W. S., Broadbridge, R., East, J. M., and Lee, A. G. (2002) Sarcolipin uncouples hydrolysis of ATP from accumulation of Ca2+ by the Ca2+-ATPase of skeletal-muscle sarcoplasmic reticulum. *Biochem. J.* **361**, 277–286

110. Bhupathy, P., Babu, G. J., Ito, M., and Periasamy, M. (2009) Threonine-5 at the N-terminus can modulate sarcolipin function in cardiac myocytes. *J. Mol. Cell. Cardiol.* **47**, 723–729

111. Gamu, D., Bombardier, E., Smith, I. C., Fajardo, V. A., and Tupling, A. R. (2014) Sarcolipin Provides a Novel Muscle-Based Mechanism for Adaptive Thermogenesis. *Exerc. Sport Sci. Rev.* **42**, 136–142

112. Pant, M., Bal, N. C., and Periasamy, M. (2016) Sarcolipin: A Key Thermogenic and Metabolic Regulator in Skeletal Muscle. *Trends Endocrinol. Metab.* 10.1016/j.tem.2016.08.006

113. Bal, N. C., Singh, S., Reis, F. C. G., Maurya, S. K., Pani, S., Rowland, L. A., and Periasamy, M. (2017) Both brown adipose tissue and skeletal muscle thermogenesis processes are activated during mild to severe cold adaptation in mice. *J. Biol. Chem.* **292**, 16616–16625

114. Campbell, K. L., and Dicke, A. A. (2018) Sarcolipin Makes Heat, but Is It Adaptive Thermogenesis? *Front. Physiol.* **9**, 714

115. Rowland, L. A., Bal, N. C., Kozak, L. P., and Periasamy, M. (2015) Uncoupling protein 1 and sarcolipin are required to maintain optimal thermogenesis, and loss of both systems compromises survival of mice under cold stress. *J. Biol. Chem.* **290**, 12282–12289

116. MacLennan, D. H., Asahi, M., and Tupling, A. R. (2003) The regulation of SERCA-type pumps by phospholamban and sarcolipin. *Ann. N. Y. Acad. Sci.* **986**, 472–480

117. Zheng, J., Yancey, D. M., Ahmed, M. I., Wei, C. C., Powell, P. C., Shanmugam, M., Gupta, H., Lloyd, S. G., McGiffin, D. C., Schiros, C. G., Denney, T. S., Babu, G. J., and Dell'Italia, L. J. (2014) Increased sarcolipin expression and adrenergic drive in humans with preserved left ventricular ejection fraction and chronic isolated mitral regurgitation. *Circ. Hear. Fail.* **7**, 194–202

118. Gramolini, A. O., Trivieri, M. G., Oudit, G. Y., Kislinger, T., Li, W., Patel, M. M., Emili, A., Kranias, E. G., Backx, P. H., and MacLennan, D. H. (2006) Cardiac-specific overexpression of sarcolipin in phospholamban null mice impairs myocyte function that is restored by phosphorylation. *Proc. Natl. Acad. Sci.* **103**, 2446 LP – 2451

119. Cornea, R. L., Autry, J. M., Jones, L. R., and Chen, Z. (2000) Membrane Transport Structure Function and Biogenesis : Reexamination of the Role of the Leucine / Isoleucine Zipper Residues of Phospholamban in Inhibition of the Ca 2+ Pump of Cardiac Sarcoplasmic Reticulum Reexamination of the Role of the Leucine / Iso. *J. Biol. Chem.* **275**, 41487–41494

120. Cao, Y., Wu, X., Yang, R., Wang, X., Sun, H., and Lee, I. (2017) Self-assembling study of sarcolipin and its mutants in multiple molecular dynamic simulations. *Proteins Struct. Funct. Bioinforma.* **85**, 1065–1077

121. Hellstern, S., Pegoraro, S., Karim, C. B., Lustig, A., Thomas, D. D., Moroder, L., and Engel, J. (2001) Sarcolipin, the Shorter Homologue of Phospholamban, Forms Oligomeric Structures in Detergent Micelles and in Liposomes. *J. Biol. Chem.* **276**, 30845–30852

122. Autry, J. M., Rubin, J. E., Pietrini, S. D., Winters, D. L., Robia, S. L., and Thomas, D. D. (2011) Oligomeric interactions of sarcolipin and the Ca-ATPase. *J. Biol. Chem.* **286**, 31697–31706

123. Anderson, D. M., Anderson, K. M., Chang, C.-L., Makarewich, C. A., Nelson, B. R., McAnally, J. R., Kasaragod, P., Shelton, J. M., Liou, J., Bassel-Duby, R., and Olson, E. N. (2015) A Micropeptide Encoded by a Putative Long Noncoding RNA Regulates Muscle Performance. *Cell.* **160**, 595–606

124. Nelson, B. R., Catherine A. Makarewich, Douglas M. Anderson, Benjamin R. Winders, Constantine D. Troupes, F. W., Reese, A. L., McAnally, J. R., Chen, X., Kavalali, E. T., Cannon, S. C., Houser, S. R., Bassel-Duby, R., and Olson, E. N. (2016) A peptide encoded by a transcript annotated as long noncoding RNA enhances SERCA activity in muscle. *Science (80-.).*

125. Anderson, D. M., Makarewich, C. A., Anderson, K. M., Shelton, J. M., Bezprozvannaya, S., Bassel-Duby, R., and Olson, E. N. (2016) Widespread control of calcium signaling by a family of SERCA-inhibiting micropeptides. *Sci. Signal.* **9**, ra119 LP-ra119

126. Afara, M. R., Trieber, C. A., Glaves, J. P., and Young, H. S. (2006) Rational Design of Peptide Inhibitors of the Sarcoplasmic Reticulum Calcium Pump. *Biochemistry*. **45**, 8617–8627

127. Afara, M. R., Trieber, C. a., Ceholski, D. K., and Young, H. S. (2008) Peptide inhibitors use two related mechanisms to alter the apparent calcium affinity of the sarcoplasmic reticulum calcium pump. *Biochemistry*. **47**, 9522–9530

128. Desmond, P. F., Muriel, J., Markwardt, M. L., Rizzo, M. A., and Bloch, R. J. (2015) Identification of small ankyrin 1 as a novel sarco(endo)plasmic reticulum Ca2+-ATPase 1 (SERCA1) regulatory protein in skeletal muscle. *J. Biol. Chem.* **290**, 27854–27867

Chapter 2: The phospholamban pentamer alters function of the sarcoplasmic reticulum calcium pump SERCA

1. Goodsell, D. S., Autin, L., and Olson, A. J. (2019) Illustrate: Software for Biomolecular Illustration. *Structure*. 10.1016/j.str.2019.08.011

2. Toyoshima, C. (2009) How Ca2+-ATPase pumps ions across the sarcoplasmic reticulum membrane. *Biochim. Biophys. Acta - Mol. Cell Res.* **1793**, 941–946

3. Toyoshima, C., and Cornelius, F. (2013) New crystal structures of PII-type ATPases: Excitement continues. *Curr. Opin. Struct. Biol.* **23**, 507–514

4. Møller, J. V., Olesen, C., Winther, A.-M. L., and Nissen, P. (2010) The sarcoplasmic Ca2+-ATPase: design of a perfect chemi-osmotic pump. *Q. Rev. Biophys.* **43**, 501–566

5. Fajardo, V. a., Bombardier, E., Vigna, C., Devji, T., Bloemberg, D., Gamu, D., Gramolini, A. O., Quadrilatero, J., and Tupling, a. R. (2013) Co-Expression of SERCA isoforms, phospholamban and sarcolipin in human skeletal muscle fibers. *PLoS One*. **8**, 1–13

6. Stokes, D. L. (1997) Keeping Calcium in its Place: Ca2+ ATPase and Phospholamban. *Curr. Opin. Struct. Biol.* **7**, 550–556

7. Kimura, Y., Kurzydlowski, K., Tada, M., and MacLennan, D. H. (1997) Phospholamban Inhibitory Function Is Activated by Depolymerization. *J. Biol. Chem.* . **272**, 15061–15064

8. Autry, J. M., and Jones, L. R. (1997) Functional Co-expression of the Canine Cardiac Ca2+Pump and Phospholamban in Spodoptera frugiperda (Sf21) Cells Reveals New Insights on ATPase Regulation . *J. Biol. Chem.* . **272**, 15872–15880

9. Jones, L. R., Cornea, R. L., and Chen, Z. (2002) Close proximity between residue 30 of phospholamban and cysteine 318 of the cardiac Ca2+ pump revealed by intermolecular thiol cross-linking. *J. Biol. Chem.* **277**, 28319–28329

10.   Asahi, M., Mckenna, E., Kurzydlowski, K., Tada, M., and Maclennan, D. H. (2000) Physical Interactions between Phospholamban and Sarco (endo) plasmic Reticulum Ca 2 $^{/.}$ -ATPases Are Dissociated by Elevated Ca 2 $^{/.}$, but Not by Phospholamban Phosphorylation , Vanadate , or Thapsigargin , and Are Enhanced by ATP *. **275**, 15034–15038

11.   Cornea, R. L., Jones, L. R., Autry, J. M., and Thomas, D. D. (1997) Mutation and Phosphorylation Change the Oligomeric Structure of Phospholamban in Lipid Bilayers. *Biochemistry.* **36**, 2960–2967

12.   Becucci, L., Cembran, A., Karim, C. B., Thomas, D. D., Guidelli, R., Gao, J., and Veglia, G. (2009) On the Function of Pentameric Phospholamban: Ion Channel or Storage Form? *Biophys. J.* **96**, L60–L62

13.   Negash, S., Yao, Q., Sun, H., LI, J., Bigelow, D. J., and Squier, T. C. (2000) Phospholamban remains associated with the Ca2+- and Mg2+-dependent ATPase following phosphorylation by cAMP-dependent protein kinase. *Biochem. J.* **351**, 195 LP – 205

14.   Mueller, B., Karim, C. B., Negrashov, I. V, Kutchai, H., and Thomas, D. D. (2004) Direct Detection of Phospholamban and Sarcoplasmic Reticulum Ca-ATPase Interaction in Membranes Using Fluorescence Resonance Energy Transfer. *Biochemistry.* **43**, 8754–8765

15.   Li, J., Bigelow, D. J., and Squier, T. C. (2004) Conformational Changes within the Cytosolic Portion of Phospholamban upon Release of Ca-ATPase Inhibition. *Biochemistry.* **43**, 3870–3879

16.   Bidwell, P., Blackwell, D. J., Hou, Z., Zima, A. V, and Robia, S. L. (2011) Phospholamban Binds with Differential Affinity to Calcium Pump Conformers. *J. Biol. Chem. .* **286**, 35044–35050

17.   James, Z. M., McCaffrey, J. E., Torgersen, K. D., Karim, C. B., and Thomas, D. D. (2012) Protein-Protein Interactions in Calcium Transport Regulation Probed by Saturation Transfer Electron Paramagnetic Resonance. *Biophys. J.* **103**, 1370–1378

18.   Martin, P. D., James, Z. M., and Thomas, D. D. (2018) Effect of Phosphorylation on Interactions between Transmembrane Domains of SERCA and Phospholamban. *Biophys. J.* **114**, 2573–2583

19.   Gustavsson, M., Verardi, R., Mullen, D. G., Mote, K. R., Traaseth, N. J., Gopinath, T., and Veglia, G. (2013) Allosteric regulation of SERCA by phosphorylation-mediated conformational shift of phospholamban. *Proc. Natl. Acad. Sci. U. S. A.* **110**, 17338–43

20.   Chu, G., Li, L., Sato, Y., Harrer, J. M., Kadambi, V. J., Hoit, B. D., Bers, D. M., and Kranias, E. G. (1998) Pentameric assembly of phospholamban facilitates inhibition of cardiac function

in vivo. *J. Biol. Chem.* **273**, 33674–33680

21. Kovacs, R. J., Nelson, M. T., Simmerman, H. K., and Jones, L. R. (1988) Phospholamban forms Ca2+-selective channels in lipid bilayers. *J. Biol. Chem.* . **263**, 18364–18368

22. Smeazzetto, S., Schröder, I., Thiel, G., and Moncelli, M. R. (2011) Phospholamban generates cation selective ion channels. *Phys. Chem. Chem. Phys.* **13**, 12935–12939

23. Wittmann, T., Lohse, M. J., and Schmitt, J. P. (2015) Phospholamban pentamers attenuate PKA-dependent phosphorylation of monomers. *J. Mol. Cell. Cardiol.* **80C**, 90–97

24. Ceholski, D. K., Trieber, C. A., Holmes, C. F. B., and Young, H. S. (2012) Lethal, Hereditary Mutants of Phospholamban Elude Phosphorylation by Protein Kinase A. *J. Biol. Chem.* . **287**, 26596–26605

25. Stokes, D. L., Pomfret, A. J., Rice, W. J., Glaves, J. P., and Young, H. S. (2006) Interactions between Ca2+-ATPase and the pentameric form of phospholamban in two-dimensional co-crystals. *Biophys. J.* **90**, 4213–4223

26. Glaves, J. P., Trieber, C. a., Ceholski, D. K., Stokes, D. L., and Young, H. S. (2011) Phosphorylation and mutation of phospholamban alter physical interactions with the sarcoplasmic reticulum calcium pump. *J. Mol. Biol.* **405**, 707–723

27. Akin, B. L., Hurley, T. D., Chen, Z., and Jones, L. R. (2013) The Structural Basis for Phospholamban Inhibition of the Calcium Pump in Sarcoplasmic Reticulum. *J. Biol. Chem.* . **288**, 30181–30191

28. Toyoshima, C., Iwasawa, S., Ogawa, H., Hirata, A., Tsueda, J., and Inesi, G. (2013) Crystal structures of the calcium pump and sarcolipin in the Mg2+-bound E1 state. *Nature.* **495**, 260

29. Winther, A.-M. L., Bublitz, M., Karlsen, J. L., Møller, J. V, Hansen, J. B., Nissen, P., and Buch-Pedersen, M. J. (2013) The sarcolipin-bound calcium pump stabilizes calcium sites exposed to the cytoplasm. *Nature.* **495**, 265

30. Gorski, P. A., Trieber, C. A., Ashrafi, G., and Young, H. S. (2015) Regulation of the Sarcoplasmic Reticulum Calcium Pump by Divergent Phospholamban Isoforms in Zebrafish. *J. Biol. Chem.* . **290**, 6777–6788

31. Verboomen, H., Wuytack, F., De Smedt, H., Himpens, B., and Casteels, R. (1992) Functional difference between SERCA2a and SERCA2b Ca<sup>2+</sup> pumps and their modulation by phospholamban. *Biochem. J.* **286**, 591 LP – 595

32. Akin, B. L., and Jones, L. R. (2012) Characterizing Phospholamban to Sarco(endo)plasmic Reticulum Ca2+-ATPase 2a (SERCA2a) Protein Binding Interactions in Human Cardiac

Sarcoplasmic Reticulum Vesicles Using Chemical Cross-linking. *J. Biol. Chem.* **287**, 7582–7593

33. Ferrington, D. A., Yao, Q., Squier, T. C., and Bigelow, D. J. (2002) Comparable Levels of Ca-ATPase Inhibition by Phospholamban in Slow-Twitch Skeletal and Cardiac Sarcoplasmic Reticulum. *Biochemistry.* **41**, 13289–13296

34. Negash, S., Chen, L. T., Bigelow, D. J., and Squier, T. C. (1996) Phosphorylation of Phospholamban by cAMP-Dependent Protein Kinase Enhances Interactions between Ca-ATPase Polypeptide Chains in Cardiac Sarcoplasmic Reticulum Membranes. *Biochemistry.* **35**, 11247–11259

35. Ceholski, D. K., Trieber, C. a., and Young, H. S. (2012) Hydrophobic imbalance in the cytoplasmic domain of phospholamban is a determinant for lethal dilated cardiomyopathy. *J. Biol. Chem.* **287**, 16521–16529

36. Waggoner, J. R., Huffman, J., Griffith, B. N., Jones, L. R., and Mahaney, J. E. (2004) Improved expression and characterization of Ca2+-ATPase and phospholamban in High-Five cells. *Protein Expr. Purif.* **34**, 56–67

37. Trieber, C. A., Douglas, J. L., Afara, M., and Young, H. S. (2005) The Effects of Mutation on the Regulatory Properties of Phospholamban in Co-Reconstituted Membranes†. *Biochemistry.* **44**, 3289–3297

38. Trieber, C. A., Afara, M., and Young, H. S. (2009) Effects of Phospholamban Transmembrane Mutants on the Calcium Affinity, Maximal Activity, and Cooperativity of the Sarcoplasmic Reticulum Calcium Pump. *Biochemistry.* **48**, 9287–9296

39. Reddy, L. G., Cornea, R. L., Winters, D. L., McKenna, E., and Thomas, D. D. (2003) Defining the Molecular Components of Calcium Transport Regulation in a Reconstituted Membrane System. *Biochemistry.* **42**, 4585–4592

40. Young, H. S., Xu, C., Zhang, P., and Stokes, D. L. (2001) Locating the thapsigargin-binding site on Ca(2+)-ATPase by cryoelectron microscopy. *J. Mol. Biol.* **308**, 231–240

41. Xu, C., Rice, W. J., He, W., and Stokes, D. L. (2002) A structural model for the catalytic cycle of Ca2+-ATPase11Edited by W. Baumeister. *J. Mol. Biol.* **316**, 201–211

42. Young, H. S., Rigaud, J. L., Lacapère, J. J., Reddy, L. G., and Stokes, D. L. (1997) How to make tubular crystals by reconstitution of detergent-solubilized Ca2(+)-ATPase. *Biophys. J.* **72**, 2545–2558

43. Dux, L., and Martonosi, A. (1983) Two-dimensional arrays of proteins in sarcoplasmic reticulum and purified Ca2+-ATPase vesicles treated with vanadate. *J. Biol. Chem. .* **258**, 2599–

2603

44. Maurer, A., and Fleischer, S. (1984) Decavanadate is responsible for vanadate-induced two-dimensional crystals in sarcoplasmic reticulum. *J. Bioenerg. Biomembr.* **16**, 491–505

45. Young, H. S., Jones, L. R., and Stokes, D. L. (2001) Locating phospholamban in co-crystals with Ca(2+)-ATPase by cryoelectron microscopy. *Biophys. J.* **81**, 884–894

46. Robia, S. L., Campbell, K. S., Kelly, E. M., Hou, Z., Winters, D. L., and Thomas, D. D. (2007) Förster Transfer Recovery Reveals That Phospholamban Exchanges Slowly From Pentamers but Rapidly From the SERCA Regulatory Complex. *Circ. Res.* **101**, 1123–1129

47. Toyoshima, C., Asahi, M., Sugita, Y., Khanna, R., Tsuda, T., and MacLennan, D. H. (2003) Modeling of the inhibitory interaction of phospholamban with the Ca2+ ATPase. *Proc. Natl. Acad. Sci. U. S. A.* **100**, 467–472

48. Seidel, K., Andronesi, O. C., Krebs, J., Griesinger, C., Young, H. S., Becker, S., and Baldus, M. (2008) Structural Characterization of Ca2+-ATPase-Bound Phospholamban in Lipid Bilayers by Solid-State Nuclear Magnetic Resonance (NMR) Spectroscopy,. *Biochemistry.* **47**, 4369–4376

49. Li, M., Reddy, L. G., Bennett, R., Silva, N. D., Jones, L. R., and Thomas, D. D. (1999) A Fluorescence Energy Transfer Method for Analyzing Protein Oligomeric Structure: Application to Phospholamban. *Biophys. J.* **76**, 2587–2599

50. Reddy, L. G., Jones, L. R., and Thomas, D. D. (1999) Depolymerization of Phospholamban in the Presence of Calcium Pump: A Fluorescence Energy Transfer Study [†]. *Biochemistry.* **38**, 3954–3962

51. Stokes, D. L., Delavoie, F., Rice, W. J., Champeil, P., McIntosh, D. B., and Lacapère, J.-J. (2005) Structural Studies of a Stabilized Phosphoenzyme Intermediate of Ca2+-ATPase. *J. Biol. Chem.* . **280**, 18063–18072

52. Traaseth, N. J., Shi, L., Verardi, R., Mullen, D. G., Barany, G., and Veglia, G. (2009) Structure and topology of monomeric phospholamban in lipid membranes determined by a hybrid solution and solid-state NMR approach. *Proc. Natl. Acad. Sci. U. S. A.* **106**, 10165–10170

53. Stokes, D. L., and Green, N. M. (1990) Three-dimensional crystals of CaATPase from sarcoplasmic reticulum. Symmetry and molecular packing. *Biophys. J.* **57**, 1–14

54. Afara, M. R., Trieber, C. A., Glaves, J. P., and Young, H. S. (2006) Rational Design of Peptide Inhibitors of the Sarcoplasmic Reticulum Calcium Pump. *Biochemistry.* **45**, 8617–8627

55. YOUNG, H. S., REDDY, L. G., JONES, L. R., and STOKES, D. L. (1998) Co-reconstitution and Co-crystallization of Phospholamban and Ca2+-ATPase a. *Ann. N. Y. Acad. Sci.* **853**, 103–

56. Douglas, J. L., Trieber, C. a., Afara, M., and Young, H. S. (2005) Rapid, high-yield expression and purification of Ca2+-ATPase regulatory proteins for high-resolution structural studies. *Protein Expr. Purif.* **40**, 118–125

57. Eletr, S., and Inesi, G. (1972) Phospholipid orientation in sacroplasmic membranes: Spin-label ESR and proton NMR studies. *Biochim. Biophys. Acta - Biomembr.* **282**, 174–179

58. Warren, G. B., Toon, P. A., Birdsall, N. J., Lee, A. G., and Metcalfe, J. C. (1974) Reconstitution of a calcium pump using defined membrane components. *Proc. Natl. Acad. Sci. U. S. A.* **71**, 622–626

59. Smeazzetto, S., Armanious, G. P., Moncelli, M. R., Bak, J. J., Lemieux, M. J., Young, H. S., and Tadini-Buoninsegni, F. (2017) Conformational memory in the association of the transmembrane protein phospholamban with the sarcoplasmic reticulum calcium pump SERCA. *J. Biol. Chem.* **292**, 21330–21339

60. Kozakov, D., Hall, D. R., Xia, B., Porter, K. A., Padhorny, D., Yueh, C., Beglov, D., and Vajda, S. (2017) The ClusPro web server for protein–protein docking. *Nat. Protoc.* **12**, 255

61. Espinoza-Fonseca, L. M., Autry, J. M., Ramírez-Salinas, G. L., and Thomas, D. D. (2015) Atomic-Level Mechanisms for Phospholamban Regulation of the Calcium Pump. *Biophys. J.* **108**, 1697–1708

62. Phillips, J. C., Braun, R., Wang, W., Gumbart, J., Tajkhorshid, E., Villa, E., Chipot, C., Skeel, R. D., Kalé, L., and Schulten, K. (2005) Scalable molecular dynamics with NAMD. *J. Comput. Chem.* **26**, 1781–1802

63. Weber, W., Hünenberger, P. H., and McCammon, J. A. (2000) Molecular Dynamics Simulations of a Polyalanine Octapeptide under Ewald Boundary Conditions: Influence of Artificial Periodicity on Peptide Conformation. *J. Phys. Chem. B.* **104**, 3668–3675

64. Darden, T., York, D., and Pedersen, L. (1993) Particle mesh Ewald: An N·log(N) method for Ewald sums in large systems. *J. Chem. Phys.* **98**, 10089–10092

65. Essmann, U., Perera, L., Berkowitz, M. L., Darden, T., Lee, H., and Pedersen, L. G. (1995) A smooth particle mesh Ewald method. *J. Chem. Phys.* **103**, 8577–8593

66. Best, R. B., Zhu, X., Shim, J., Lopes, P. E. M., Mittal, J., Feig, M., and MacKerell, A. D. (2012) Optimization of the Additive CHARMM All-Atom Protein Force Field Targeting Improved Sampling of the Backbone ϕ, ψ and Side-Chain $\chi1$ and $\chi2$ Dihedral Angles. *J. Chem. Theory Comput.* **8**, 3257–3273

67.   Klauda, J. B., Venable, R. M., Freites, J. A., O'Connor, J. W., Tobias, D. J., Mondragon-Ramirez, C., Vorobyov, I., MacKerell, A. D., and Pastor, R. W. (2010) Update of the CHARMM All-Atom Additive Force Field for Lipids: Validation on Six Lipid Types. *J. Phys. Chem. B.* **114**, 7830–7843

Chapter 3: Interaction of a sarcolipin pentamer and monomer with the sarcoplasmic reticulum calcium pump, SERCA

1.   Goodsell, D. S., Autin, L., and Olson, A. J. (2019) Illustrate: Software for Biomolecular Illustration. *Structure.* 10.1016/j.str.2019.08.011

2.   Anderson, D. M., Anderson, K. M., Chang, C.-L., Makarewich, C. A., Nelson, B. R., McAnally, J. R., Kasaragod, P., Shelton, J. M., Liou, J., Bassel-Duby, R., and Olson, E. N. (2015) A Micropeptide Encoded by a Putative Long Noncoding RNA Regulates Muscle Performance. *Cell.* **160**, 595–606

3.   Anderson, D. M., Makarewich, C. A., Anderson, K. M., Shelton, J. M., Bezprozvannaya, S., Bassel-Duby, R., and Olson, E. N. (2016) Widespread control of calcium signaling by a family of SERCA-inhibiting micropeptides. *Sci. Signal.* **9**, ra119 LP-ra119

4.   Nelson, B. R., Catherine A. Makarewich, Douglas M. Anderson, Benjamin R. Winders, Constantine D. Troupes, F. W., Reese, A. L., McAnally, J. R., Chen, X., Kavalali, E. T., Cannon, S. C., Houser, S. R., Bassel-Duby, R., and Olson, E. N. (2016) A peptide encoded by a transcript annotated as long noncoding RNA enhances SERCA activity in muscle. *Science (80-.).*

5.   Bal, N. C., Maurya, S. K., Sopariwala, D. H., Sahoo, S. K., Gupta, S. C., Shaikh, S. A., Pant, M., Rowland, L. A., Bombardier, E., Goonasekera, S. A., Tupling, A. R., Molkentin, J. D., and Periasamy, M. (2012) Sarcolipin is a newly identified regulator of muscle-based thermogenesis in mammals. *Nat. Med.* **18**, 1575

6.   Gorski, P. A., Glaves, J. P., Vangheluwe, P., and Young, H. S. (2013) Sarco(endo)plasmic Reticulum Calcium ATPase (SERCA) Inhibition by Sarcolipin Is Encoded in Its Luminal Tail. *J. Biol. Chem. .* **288**, 8456–8467

7.   Sahoo, S. K., Shaikh, S. a., Sopariwala, D. H., Bal, N. C., and Periasamy, M. (2013) Sarcolipin protein interaction with Sarco(endo)plasmic reticulum CA 2+ ATPase (SERCA) Is distinct from phospholamban protein,and only sarcolipin can promote uncoupling of the serca pump. *J. Biol. Chem.* **288**, 6881–6889

8. Winther, A.-M. L., Bublitz, M., Karlsen, J. L., Møller, J. V, Hansen, J. B., Nissen, P., and Buch-Pedersen, M. J. (2013) The sarcolipin-bound calcium pump stabilizes calcium sites exposed to the cytoplasm. *Nature.* **495**, 265

9. Toyoshima, C., Iwasawa, S., Ogawa, H., Hirata, A., Tsueda, J., and Inesi, G. (2013) Crystal structures of the calcium pump and sarcolipin in the Mg2+-bound E1 state. *Nature.* **495**, 260

10. Glaves, J. P., Trieber, C. a., Ceholski, D. K., Stokes, D. L., and Young, H. S. (2011) Phosphorylation and mutation of phospholamban alter physical interactions with the sarcoplasmic reticulum calcium pump. *J. Mol. Biol.* **405**, 707–723

11. Stokes, D. L., Pomfret, A. J., Rice, W. J., Glaves, J. P., and Young, H. S. (2006) Interactions between Ca2+-ATPase and the Pentameric Form of Phospholamban in Two-Dimensional Co-Crystals. *Biophys. J.* **90**, 4213–4223

12. Glaves, J. P., Primeau, J. O., Espinoza-Fonseca, L. M., Lemieux, M. J., and Young, H. S. (2019) The Phospholamban Pentamer Alters Function of the Sarcoplasmic Reticulum Calcium Pump SERCA. *Biophys. J.* **116**, 633–647

13. Hellstern, S., Pegoraro, S., Karim, C. B., Lustig, A., Thomas, D. D., Moroder, L., and Engel, J. (2001) Sarcolipin, the Shorter Homologue of Phospholamban, Forms Oligomeric Structures in Detergent Micelles and in Liposomes. *J. Biol. Chem.* **276**, 30845–30852

14. Autry, J. M., Rubin, J. E., Pietrini, S. D., Winters, D. L., Robia, S. L., and Thomas, D. D. (2011) Oligomeric interactions of sarcolipin and the Ca-ATPase. *J. Biol. Chem.* **286**, 31697–31706

15. Douglas, J. L., Trieber, C. a., Afara, M., and Young, H. S. (2005) Rapid, high-yield expression and purification of Ca2+-ATPase regulatory proteins for high-resolution structural studies. *Protein Expr. Purif.* **40**, 118–125

16. Trieber, C. A., Douglas, J. L., Afara, M., and Young, H. S. (2005) The Effects of Mutation on the Regulatory Properties of Phospholamban in Co-Reconstituted Membranes†. *Biochemistry.* **44**, 3289–3297

17. Trieber, C. A., Afara, M., and Young, H. S. (2009) Effects of Phospholamban Transmembrane Mutants on the Calcium Affinity, Maximal Activity, and Cooperativity of the Sarcoplasmic Reticulum Calcium Pump. *Biochemistry.* **48**, 9287–9296

18. Buck, B., Zamoon, J., Kirby, T. L., DeSilva, T. M., Karim, C., Thomas, D., and Veglia, G. (2003) Overexpression, purification, and characterization of recombinant Ca-ATPase regulators for high-resolution solution and solid-state NMR studies. *Protein Expr. Purif.* **30**,

253–261

19. Odermatt, A., Becker, S., Khanna, V. K., Kurzydlowski, K., Leisner, E., Pette, D., and MacLennan, D. H. (1998) Sarcolipin Regulates the Activity of SERCA1, the Fast-twitch Skeletal Muscle Sarcoplasmic Reticulum Ca2+-ATPase . *J. Biol. Chem.* . **273**, 12360–12369

20. Kimura, Y., Asahi, M., Kurzydlowski, K., Tada, M., and MacLennan, D. H. (1998) Phospholamban Domain Ib Mutations Influence Functional Interactions with the Ca2+-ATPase Isoform of Cardiac Sarcoplasmic Reticulum . *J. Biol. Chem.* . **273**, 14238–14241

21. Toyofuku, T., Kurzydlowski, K., Tada, M., and MacLennan, D. H. (1994) Amino acids Glu2 to Ile18 in the cytoplasmic domain of phospholamban are essential for functional association with the Ca(2+)-ATPase of sarcoplasmic reticulum. *J. Biol. Chem.* . **269**, 3088–3094

22. Ferrington, D. A., Yao, Q., Squier, T. C., and Bigelow, D. J. (2002) Comparable Levels of Ca-ATPase Inhibition by Phospholamban in Slow-Twitch Skeletal and Cardiac Sarcoplasmic Reticulum. *Biochemistry.* **41**, 13289–13296

23. Waggoner, J. R., Huffman, J., Griffith, B. N., Jones, L. R., and Mahaney, J. E. (2004) Improved expression and characterization of Ca2+-ATPase and phospholamban in High-Five cells. *Protein Expr. Purif.* **34**, 56–67

24. Maurer, A., and Fleischer, S. (1984) Decavanadate is responsible for vanadate-induced two-dimensional crystals in sarcoplasmic reticulum. *J. Bioenerg. Biomembr.* **16**, 491–505

25. Dux, L., and Martonosi, A. (1983) Two-dimensional arrays of proteins in sarcoplasmic reticulum and purified Ca2+-ATPase vesicles treated with vanadate. *J. Biol. Chem.* . **258**, 2599–2603

26. Verardi, R., Shi, L., Traaseth, N. J., Walsh, N., and Veglia, G. (2011) Structural topology of phospholamban pentamer in lipid bilayers by a hybrid solution and solid-state NMR method. *Proc. Natl. Acad. Sci.* **108**, 9101 LP – 9106

27. Kimura, Y., Kurzydlowski, K., Tada, M., and MacLennan, D. H. (1997) Phospholamban Inhibitory Function Is Activated by Depolymerization. *J. Biol. Chem.* . **272**, 15061–15064

28. Smeazzetto, S., Tadini-Buoninsegni, F., Thiel, G., Berti, D., and Montis, C. (2016) Phospholamban spontaneously reconstitutes into giant unilamellar vesicles where it generates a cation selective channel. *Phys. Chem. Chem. Phys.* **18**, 1629–1636

29. Wittmann, T., Lohse, M. J., and Schmitt, J. P. (2015) Phospholamban pentamers attenuate PKA-dependent phosphorylation of monomers. *J. Mol. Cell. Cardiol.* **80C**, 90–97

30. Ceholski, D. K., Trieber, C. a., Holmes, C. F. B., and Young, H. S. (2012) Lethal, hereditary

mutants of phospholamban elude phosphorylation by protein kinase A. *J. Biol. Chem.* **287**, 26596–26605

31.   Reddy, L. G., Cornea, R. L., Winters, D. L., McKenna, E., and Thomas, D. D. (2003) Defining the Molecular Components of Calcium Transport Regulation in a Reconstituted Membrane System. *Biochemistry*. **42**, 4585–4592

32.   Afara, M. R., Trieber, C. A., Glaves, J. P., and Young, H. S. (2006) Rational Design of Peptide Inhibitors of the Sarcoplasmic Reticulum Calcium Pump. *Biochemistry*. **45**, 8617–8627

33.   Ceholski, D. K., Trieber, C. a., and Young, H. S. (2012) Hydrophobic imbalance in the cytoplasmic domain of phospholamban is a determinant for lethal dilated cardiomyopathy. *J. Biol. Chem.* **287**, 16521–16529

34.   Akin, B. L., Hurley, T. D., Chen, Z., and Jones, L. R. (2013) The structural basis for phospholamban inhibition of the calcium pump in sarcoplasmic reticulum. *J. Biol. Chem.* **288**, 30181–30191

35.   Gaudry, M. J., Jastroch, M., Treberg, J. R., Hofreiter, M., Paijmans, J. L. A., Starrett, J., Wales, N., Signore, A. V, Springer, M. S., and Campbell, K. L. (2017) Inactivation of thermogenic UCP1 as a historical contingency in multiple placental mammal clades. *Sci. Adv.* **3**, e1602878–e1602878

36.   Becucci, L., Guidelli, R., Karim, C. B., Thomas, D. D., and Veglia, G. (2007) An Electrochemical Investigation of Sarcolipin Reconstituted into a Mercury-Supported Lipid Bilayer. *Biophys. J.* **93**, 2678–2687

37.   Becucci, L., Guidelli, R., Karim, C. B., Thomas, D. D., and Veglia, G. (2009) The role of sarcolipin and ATP in the transport of phosphate ion into the sarcoplasmic reticulum. *Biophys. J.* **97**, 2693–2699

38.   Smeazzetto, S., Schröder, I., Thiel, G., and Moncelli, M. R. (2011) Phospholamban generates cation selective ion channels. *Phys. Chem. Chem. Phys.* **13**, 12935–12939

39.   Negash, S., Chen, L. T., Bigelow, D. J., and Squier, T. C. (1996) Phosphorylation of Phospholamban by cAMP-Dependent Protein Kinase Enhances Interactions between Ca-ATPase Polypeptide Chains in Cardiac Sarcoplasmic Reticulum Membranes. *Biochemistry*. **35**, 11247–11259

40.   Colyer, J., and Wang, J. H. (1991) Dependence of cardiac sarcoplasmic reticulum calcium pump activity on the phosphorylation status of phospholamban. *J. Biol. Chem.* . **266**, 17486–17493

41.   Brittsan, A. G., Carr, A. N., Schmidt, A. G., and Kranias, E. G. (2000) Maximal Inhibition of SERCA2 Ca2+ Affinity by Phospholamban in Transgenic Hearts Overexpressing a Non-phosphorylatable Form of Phospholamban . *J. Biol. Chem. .* **275**, 12129–12135

42.   Mishra, S., Gupta, R. C., Tiwari, N., Sharov, V. G., and Sabbah, H. N. (2002) Molecular mechanisms of reduced sarcoplasmic reticulum Ca2+ uptake in human failing left ventricular myocardium. *J. Hear. Lung Transplant.* **21**, 366–373

43.   Henderson, R., and Unwin, P. N. T. (1975) Three-dimensional model of purple membrane obtained by electron microscopy. *Nature.* **257**, 28–32

44.   Warren, G. B., Toon, P. a, Birdsall, N. J., Lee, a G., and Metcalfe, J. C. (1974) Reconstitution of a calcium pump using defined membrane components. *Proc. Natl. Acad. Sci. U. S. A.* **71**, 622–626

45.   Young, H. S., Jones, L. R., and Stokes, D. L. (2001) Locating Phospholamban in Co-Crystals with Ca2+-ATPase by Cryoelectron Microscopy. *Biophys. J.* **81**, 884–894

46.   Young, H. S., Rigaud, J. L., Lacapère, J. J., Reddy, L. G., and Stokes, D. L. (1997) How to make tubular crystals by reconstitution of detergent-solubilized Ca2(+)-ATPase. *Biophys. J.* **72**, 2545–2558

47.   Crowther, R. A., Henderson, R., and Smith, J. M. (1996) MRC Image Processing Programs. *J. Struct. Biol.* **116**, 9–16

48.   Toyoshima, C., Yonekura, K., and Sasabe, H. (1993) Contrast transfer for frozen-hydrated specimens II. Amplitude contrast at very low frequencies. *Ultramicroscopy.* **48**, 165–176

49.   Potterton, E., McNicholas, S., Krissinel, E., Cowtan, K., and Noble, M. (2002) The CCP4 molecular-graphics project. *Acta Crystallogr. Sect. D.* **58**, 1955–1957

50.   Kozakov, D., Hall, D. R., Xia, B., Porter, K. A., Padhorny, D., Yueh, C., Beglov, D., and Vajda, S. (2017) The ClusPro web server for protein–protein docking. *Nat. Protoc.* **12**, 255

51.   Espinoza-Fonseca, L. M., Autry, J. M., Ramírez-Salinas, G. L., and Thomas, D. D. (2015) Atomic-Level Mechanisms for Phospholamban Regulation of the Calcium Pump. *Biophys. J.* **108**, 1697–1708

52.   Phillips, J. C., Braun, R., Wang, W., Gumbart, J., Tajkhorshid, E., Villa, E., Chipot, C., Skeel, R. D., Kalé, L., and Schulten, K. (2005) Scalable molecular dynamics with NAMD. *J. Comput. Chem.* **26**, 1781–1802

53.   Weber, W., Hünenberger, P. H., and McCammon, J. A. (2000) Molecular Dynamics Simulations of a Polyalanine Octapeptide under Ewald Boundary Conditions: Influence of

Artificial Periodicity on Peptide Conformation. *J. Phys. Chem. B.* **104**, 3668–3675

54. Darden, T., York, D., and Pedersen, L. (1993) Particle mesh Ewald: An N·log(N) method for Ewald sums in large systems. *J. Chem. Phys.* **98**, 10089–10092

55. Essmann, U., Perera, L., Berkowitz, M. L., Darden, T., Lee, H., and Pedersen, L. G. (1995) A smooth particle mesh Ewald method. *J. Chem. Phys.* **103**, 8577–8593

56. Best, R. B., Zhu, X., Shim, J., Lopes, P. E. M., Mittal, J., Feig, M., and MacKerell, A. D. (2012) Optimization of the Additive CHARMM All-Atom Protein Force Field Targeting Improved Sampling of the Backbone ϕ, ψ and Side-Chain χ1 and χ2 Dihedral Angles. *J. Chem. Theory Comput.* **8**, 3257–3273

57. Klauda, J. B., Venable, R. M., Freites, J. A., O'Connor, J. W., Tobias, D. J., Mondragon-Ramirez, C., Vorobyov, I., MacKerell, A. D., and Pastor, R. W. (2010) Update of the CHARMM All-Atom Additive Force Field for Lipids: Validation on Six Lipid Types. *J. Phys. Chem. B.* **114**, 7830–7843

Chapter 4: Conformational diversity and memory in the interaction of sarcolipin with the sarcoplasmic reticulum calcium pump SERCA

1. Ebashi, S., and Lipmann, F. (1962) Adenosine triphosphate-linked concentration of calcium ions in a particulate fraction of rabbit muscle. *J. Cell Biol.* **14**, 389–400

2. Kühlbrandt, W. (2004) Biology, structure and mechanism of P-type ATPases. *Nat. Rev. Mol. Cell Biol.* **5**, 282–295

3. Toyoshima, C., and Mizutani, T. (2004) Crystal structure of the calcium pump with a bound ATP analogue. *Nature.* **430**, 529–535

4. Toyoshima, C., and Cornelius, F. (2013) New crystal structures of PII-type ATPases: Excitement continues. *Curr. Opin. Struct. Biol.* **23**, 507–514

5. Drachmann, N. D., Olesen, C., Møller, J. V., Guo, Z., Nissen, P., and Bublitz, M. (2014) Comparing crystal structures of Ca(2+) -ATPase in the presence of different lipids. *FEBS J.* **281**, 4249–4262

6. Toyoshima, C. (2009) How Ca2+-ATPase pumps ions across the sarcoplasmic reticulum membrane. *Biochim. Biophys. Acta - Mol. Cell Res.* **1793**, 941–946

7. Primeau, J. O., Armanious, G. P., Fisher, M. E., and Young, H. S. (2018) The SarcoEndoplasmic Reticulum Calcium ATPase BT - Membrane Protein Complexes: Structure and Function (Harris, J. R., and Boekema, E. J. eds), pp. 229–258, Springer

Singapore, Singapore, 10.1007/978-981-10-7757-9_8

8. Anderson, D. M., Makarewich, C. A., Anderson, K. M., Shelton, J. M., Bezprozvannaya, S., Bassel-Duby, R., and Olson, E. N. (2016) Widespread control of calcium signaling by a family of SERCA-inhibiting micropeptides. *Sci. Signal.* **9**, ra119 LP-ra119

9. Kirchberber, M. A., Tada, M., and Katz, A. M. (1975) Phospholamban: a regulatory protein of the cardiac sarcoplasmic reticulum. *Recent Adv. Stud. Cardiac Struct. Metab.* **5**, 103–115

10. Anderson, D. M., Anderson, K. M., Chang, C.-L., Makarewich, C. A., Nelson, B. R., McAnally, J. R., Kasaragod, P., Shelton, J. M., Liou, J., Bassel-Duby, R., and Olson, E. N. (2015) A Micropeptide Encoded by a Putative Long Noncoding RNA Regulates Muscle Performance. *Cell.* **160**, 595–606

11. Odermatt, a, Becker, S., Khanna, V. K., Kurzydlowski, K., Leisner, E., Pette, D., and MacLennan, D. H. (1998) Sarcolipin regulates the activity of SERCA1, the fast-twitch skeletal muscle sarcoplasmic reticulum Ca2+-ATPase. *J. Biol. Chem.* **273**, 12360–12369

12. Odermatt, a, Taschner, P. E., Scherer, S. W., Beatty, B., Khanna, V. K., Cornblath, D. R., Chaudhry, V., Yee, W. C., Schrank, B., Karpati, G., Breuning, M. H., Knoers, N., and MacLennan, D. H. (1997) Characterization of the gene encoding human sarcolipin (SLN), a proteolipid associated with SERCA1: absence of structural mutations in five patients with Brody disease. *Genomics.* **45**, 541–553

13. Asahi, M., Sugita, Y., Kurzydlowski, K., De Leon, S., Tada, M., Toyoshima, C., and MacLennan, D. H. (2003) Sarcolipin regulates sarco(endo)plasmic reticulum Ca2+-ATPase (SERCA) by binding to transmembrane helices alone or in association with phospholamban. *Proc. Natl. Acad. Sci. U. S. A.* **100**, 5040–5045

14. Toyoshima, C., Iwasawa, S., Ogawa, H., Hirata, A., Tsueda, J., and Inesi, G. (2013) Crystal structures of the calcium pump and sarcolipin in the Mg2+-bound E1 state. *Nature.* **495**, 260

15. Winther, A.-M. L., Bublitz, M., Karlsen, J. L., Møller, J. V, Hansen, J. B., Nissen, P., and Buch-Pedersen, M. J. (2013) The sarcolipin-bound calcium pump stabilizes calcium sites exposed to the cytoplasm. *Nature.* **495**, 265–9

16. Chen, Z., Akin, B. L., Stokes, D. L., and Jones, L. R. (2006) Cross-linking of C-terminal residues of phospholamban to the Ca 2+ pump of cardiac sarcoplasmic reticulum to probe spatial and functional interactions within the transmembrane domain. *J. Biol. Chem.* **281**, 14163–14172

17. Akin, B. L., Hurley, T. D., Chen, Z., and Jones, L. R. (2013) The structural basis for

phospholamban inhibition of the calcium pump in sarcoplasmic reticulum. *J. Biol. Chem.* **288**, 30181–30191

18.   Stammers, A. N., Susser, S. E., Hamm, N. C., Hlynsky, M. W., Kimber, D. E., Kehler, D. S., and Duhamel, T. A. (2015) The regulation of sarco(endo)plasmic reticulum calcium-ATPases (SERCA). *Can. J. Physiol. Pharmacol.* **93**, 843–854

19.   Glaves, J. P., Primeau, J. O., Espinoza-Fonseca, L. M., Lemieux, M. J., and Young, H. S. (2019) The Phospholamban Pentamer Alters Function of the Sarcoplasmic Reticulum Calcium Pump SERCA. *Biophys. J.* **116**, 633–647

20.   Chen, Z., Akin, B. L., and Jones, L. R. (2007) Mechanism of reversal of phospholamban inhibition of the cardiac Ca 2+-ATPase by protein kinase A and by anti-phospholamban monoclonal antibody 2D12. *J. Biol. Chem.* **282**, 20968–20976

21.   Shaikh, S. A., Sahoo, S. K., and Periasamy, M. (2016) Phospholamban and sarcolipin: Are they functionally redundant or distinct regulators of the Sarco(Endo)Plasmic Reticulum Calcium ATPase? *J. Mol. Cell. Cardiol.* **91**, 81–91

22.   Gorski, P. A., Glaves, J. P., Vangheluwe, P., and Young, H. S. (2013) Sarco(endo)plasmic Reticulum Calcium ATPase (SERCA) Inhibition by Sarcolipin Is Encoded in Its Luminal Tail. *J. Biol. Chem.* **288**, 8456–8467

23.   Bal, N. C., Maurya, S. K., Sopariwala, D. H., Sahoo, S. K., Gupta, S. C., Shaikh, S. a, Pant, M., Rowland, L. a, Goonasekera, S. a, Molkentin, J. D., and Periasamy, M. (2012) Sarcolipin is a newly identified regulator of muscle-based thermogenesis in mammals. *Nat. Med.* **18**, 1575–1579

24.   Sahoo, S. K., Shaikh, S. A., Sopariwala, D. H., Bal, N. C., and Periasamy, M. (2013) Sarcolipin protein interaction with sarco(endo)plasmic reticulum Ca2+ ATPase (SERCA) is distinct from phospholamban protein, and only sarcolipin can promote uncoupling of the SERCA pump. *J. Biol. Chem.* **288**, 6881–6889

25.   Bal, N. C., Sahoo, S. K., Maurya, S. K., and Periasamy, M. (2018) The Role of Sarcolipin in Muscle Non-shivering Thermogenesis   . *Front. Physiol.*   . **9**, 1217

26.   Pant, M., Bal, N. C., and Periasamy, M. (2016) Sarcolipin: A Key Thermogenic and Metabolic Regulator in Skeletal Muscle. *Trends Endocrinol. Metab.* **27**, 881–892

27.   Smith, W. S., Broadbridge, R., East, J. M., and Lee, A. G. (2002) Sarcolipin uncouples hydrolysis of ATP from accumulation of Ca2+ by the Ca2+-ATPase of skeletal-muscle sarcoplasmic reticulum. *Biochem. J.* **361**, 277–286

28. Sahoo, S. K., Shaikh, S. a., Sopariwala, D. H., Bal, N. C., Bruhn, D. S., Kopec, W., Khandelia, H., and Periasamy, M. (2015) The N-Terminus of Sarcolipin plays an important role in uncoupling Sarco-endoplasmic Reticulum Ca 2+ ATPase (SERCA) ATP hydrolysis from Ca 2+transport. *J. Biol. Chem.* 10.1074/jbc.M115.636738

29. Cypess, A. M., Lehman, S., Williams, G., Tal, I., Rodman, D., Goldfine, A. B., Kuo, F. C., Palmer, E. L., Tseng, Y.-H., Doria, A., Kolodny, G. M., and Kahn, C. R. (2009) Identification and importance of brown adipose tissue in adult humans. *N. Engl. J. Med.* **360**, 1509–1517

30. Smeazzetto, S., Armanious, G. P., Moncelli, M. R., Bak, J. J., Lemieux, M. J., Young, H. S., and Tadini-Buoninsegni, F. (2017) Conformational memory in the association of the transmembrane protein phospholamban with the sarcoplasmic reticulum calcium pump SERCA. *J. Biol. Chem.* **292**, 21330–21339

31. Schörner, M., Beyer, S. R., Southall, J., Cogdell, R. J., and Köhler, J. (2015) Conformational Memory of a Protein Revealed by Single-Molecule Spectroscopy. *J. Phys. Chem. B.* **119**, 13964–13970

32. Anderson, D. M., Anderson, K. M., Bassel-duby, R., Olson, E. N., Mcanally, J. R., Kasaragod, P., Shelton, J. M., Liou, J., Bassel-duby, R., and Olson, E. N. (2015) A Micropeptide Encoded by a Putative Long Noncoding RNA Regulates Muscle Performance Article A Micropeptide Encoded by a Putative Long Noncoding RNA Regulates Muscle Performance. *Cell.* **160**, 1–12

33. Tonkin, J., and Rosenthal, N. (2015) One small step for muscle: a new micropeptide regulates performance. *Cell Metab.* **21**, 515–6

34. Nelson, B. R., Catherine A. Makarewich, Douglas M. Anderson, Benjamin R. Winders, Constantine D. Troupes, F. W., Reese, A. L., McAnally, J. R., Chen, X., Kavalali, E. T., Cannon, S. C., Houser, S. R., Bassel-Duby, R., and Olson, E. N. (2016) A peptide encoded by a transcript annotated as long noncoding RNA enhances SERCA activity in muscle. *Science (80-.).*

35. Schoenmakers, T. J., Visser, G. J., Flik, G., and Theuvenet, A. P. (1992) CHELATOR: an improved method for computing metal ion concentrations in physiological solutions. *Biotechniques.* **12**, 870-874,876-879

36. Lolkema, J. S., and Slotboom, D.-J. (2015) The Hill analysis and co-ion-driven transporter kinetics. *J. Gen. Physiol.* **145**, 565–574

37. Trieber, C. A., Douglas, J. L., Afara, M., and Young, H. S. (2005) The Effects of Mutation on the Regulatory Properties of Phospholamban in Co-Reconstituted Membranes†. *Biochemistry.*

44, 3289–3297

38.   Toyoshima, C., Nakasako, M., Nomura, H., and Ogawa, H. (2000) Crystal structure of the calcium pump of sarcoplasmic reticulum at 2.6 A resolution. *Nature*. **405**, 647–655

39.   Clausen, J. D., Bublitz, M., Arnou, B., Montigny, C., Jaxel, C., Møller, J. V., Nissen, P., Andersen, J. P., and le Maire, M. (2013) SERCA mutant E309Q binds two Ca(2+) ions but adopts a catalytically incompetent conformation. *EMBO J*. **32**, 3231–3243

40.   Toyoshima, C., and Nomura, H. (2002) Structural changes in the calcium pump accompanying the dissociation of calcium. *Nature*. **418**, 605–611

41.   Glaves, J. P., Primeau, J. O., Gorski, P. A., Espinoza-Fonseca, L. M., Lemieux, M. J., and Young, H. S. (2019) Interaction of a sarcolipin pentamer and monomer with the sarcoplasmic reticulum calcium pump, SERCA. Running Title: A novel complex of sarcolipin and SERCA. *Biophysj*. **118**, 518–531

42.   Toyoshima, C., Yonekura, S.-I., Tsueda, J., and Iwasawa, S. (2011) Trinitrophenyl derivatives bind differently from parent adenine nucleotides to Ca2+-ATPase in the absence of Ca2+. *Proc. Natl. Acad. Sci. U. S. A.* **108**, 1833–1838

43.   Autry, J. M., Rubin, J. E., Svensson, B., Li, J., and Thomas, D. D. (2012) Nucleotide activation of the Ca-ATPase. *J. Biol. Chem.* **287**, 39070–39082

44.   Akin, B. L., and Jones, L. R. (2012) Characterizing Phospholamban to Sarco(endo)plasmic Reticulum Ca2+-ATPase 2a (SERCA2a) Protein Binding Interactions in Human Cardiac Sarcoplasmic Reticulum Vesicles Using Chemical Cross-linking. *J. Biol. Chem.* **287**, 7582–7593

45.   James, P., Inui, M., Tada, M., Chiesi, M., and Carafoli, E. (1989) Nature and site of phospholamban regulation of the Ca2+ pump of sarcoplasmic reticulum. *Nature*. **342**, 90–92

46.   Jones, L. R., Cornea, R. L., and Chen, Z. (2002) Close proximity between residue 30 of phospholamban and cysteine 318 of the cardiac Ca2+ pump revealed by intermolecular thiol cross-linking. *J. Biol. Chem.* **277**, 28319–28329

47.   Campbell, K. L., and Dicke, A. A. (2018) Sarcolipin Makes Heat, but Is It Adaptive Thermogenesis? *Front. Physiol.* **9**, 714

48.   Inesi, G., Kurzmack, M., Coan, C., and Lewis, D. E. (1980) Cooperative calcium binding and ATPase activation in sarcoplasmic reticulum vesicles. *J. Biol. Chem.* **255**, 3025–3031

49.   Stokes, D. L., and Green, N. M. (1990) Three-dimensional crystals of CaATPase from sarcoplasmic reticulum. Symmetry and molecular packing. *Biophys. J.* **57**, 1–14

50.   Eletr, S., and Inesi, G. (1972) Phospholipid orientation in sarcoplasmic membranes: spin-label

ESR and proton MNR studies. *Biochim. Biophys. Acta.* **282**, 174–179

51. Warren, G. B., Toon, P. A., Birdsall, N. J., Lee, A. G., and Metcalfe, J. C. (1974) Reconstitution of a calcium pump using defined membrane components. *Proc. Natl. Acad. Sci. U. S. A.* **71**, 622–626

52. Young, H. S., Jones, L. R., and Stokes, D. L. (2001) Locating phospholamban in co-crystals with Ca(2+)-ATPase by cryoelectron microscopy. *Biophys. J.* **81**, 884–894

53. Weiss, J. N. (1997) The Hill equation revisited: uses and misuses. *FASEB J. Off. Publ. Fed. Am. Soc. Exp. Biol.* **11**, 835–841

Chapter 5: CryoEM of two-dimensional crystals of SERCA and PLN

1. Goodsell, D. S., Autin, L., and Olson, A. J. (2019) Illustrate: Software for Biomolecular Illustration. *Structure.* 10.1016/j.str.2019.08.011

2. Adrian, M., Dubochet, J., Lepault, J., and McDowall, A. W. (1984) Cryo-electron microscopy of viruses. *Nature.* **308**, 32–36

3. Dubochet, J., Adrian, M., Chang, J.-J., Homo, J.-C., Lepault, J., McDowall, A. W., and Schultz, P. (1988) Cryo-electron microscopy of vitrified specimens. *Q. Rev. Biophys.* **21**, 129–228

4. Noble, A. J., Wei, H., Dandey, V. P., Zhang, Z., Tan, Y. Z., Potter, C. S., and Carragher, B. (2018) Reducing effects of particle adsorption to the air–water interface in cryo-EM. *Nat. Methods.* **15**, 793–795

5. Song, B., Lenhart, J., Flegler, V. J., Makbul, C., Rasmussen, T., and Böttcher, B. (2019) Capabilities of the Falcon III detector for single-particle structure determination. *Ultramicroscopy.* **203**, 145–154

6. von Loeffelholz, O., Papai, G., Danev, R., Myasnikov, A. G., Natchiar, S. K., Hazemann, I., Ménétret, J. F., and Klaholz, B. P. (2018) Volta phase plate data collection facilitates image processing and cryo-EM structure determination. *J. Struct. Biol.* **202**, 191–199

7. Bai, X. chen, McMullan, G., and Scheres, S. H. W. (2014) How cryo-EM is revolutionizing structural biology. *Trends Biochem. Sci.* **40**, 49–57

8. Yang, G., Zhou, R., Zhou, Q., Guo, X., Yan, C., Ke, M., Lei, J., and Shi, Y. (2019) Structural basis of Notch recognition by human γ-secretase. *Nature.* **565**, 192–197

9. Timcenko, M., Lyons, J. A., Januliene, D., Ulstrup, J. J., Dieudonné, T., Montigny, C., Ash, M.-R., Karlsen, J. L., Boesen, T., Kühlbrandt, W., Lenoir, G., Moeller, A., and Nissen, P. (2019) Structure and autoregulation of a P4-ATPase lipid flippase. *Nature.* 10.1038/s41586-019-1344-

10. Bartesaghi, A., Aguerrebere, C., Falconieri, V., Banerjee, S., Earl, L. A., Zhu, X., Grigorieff, N., Milne, J. L. S., Sapiro, G., Wu, X., and Subramaniam, S. (2018) Atomic Resolution Cryo-EM Structure of β-Galactosidase. *Structure.* **26**, 848-856.e3

11. Merk, A., Bartesaghi, A., Banerjee, S., Falconieri, V., Rao, P., Davis, M. I., Pragani, R., Boxer, M. B., Earl, L. A., Milne, J. L. S., and Subramaniam, S. (2016) Breaking Cryo-EM Resolution Barriers to Facilitate Drug Discovery. *Cell.* **165**, 1698–1707

12. Murphy, B. J., Klusch, N., Langer, J., Mills, D. J., Yildiz, Ö., and Kühlbrandt, W. (2019) Rotary substates of mitochondrial ATP synthase reveal the basis of flexible F1-Fo coupling. *Science (80-.).* 10.1126/science.aaw9128

13. Hofmann, S., Januliene, D., Mehdipour, A. R., Thomas, C., Stefan, E., Brüchert, S., Kuhn, B. T., Geertsma, E. R., Hummer, G., Tampé, R., and Moeller, A. (2019) Conformation space of a heterodimeric ABC exporter under turnover conditions. *Nature.* **571**, 580–583

14. Banerjee, S., Bartesaghi, A., Merk, A., Rao, P., Bulfer, S. L., Yan, Y., Green, N., Mroczkowski, B., Neitz, R. J., Wipf, P., Falconieri, V., Deshaies, R. J., Milne, J. L. S., Huryn, D., Arkin, M., and Subramaniam, S. (2016) 2.3 Å resolution cryo-EM structure of human p97 and mechanism of allosteric inhibition. *Science (80-.).* **351**, 871–875

15. Henderson, R., and Unwin, P. N. T. (1975) Three-dimensional model of purple membrane obtained by electron microscopy. *Nature.* **257**, 28–32

16. Young, H. S., Jones, L. R., and Stokes, D. L. (2001) Locating Phospholamban in Co-Crystals with Ca2+-ATPase by Cryoelectron Microscopy. *Biophys. J.* **81**, 884–894

17. Glaves, J. P., Fisher, L., Ward, A., and Young, H. S. (2010) *Helical Crystallization of Two Example Membrane Proteins. MsbA and the Ca2+-ATPase*, 1st Ed., Elsevier Inc., 10.1016/S0076-6879(10)83007-1

18. Stokes, D. L., Pomfret, A. J., Rice, W. J., Glaves, J. P., and Young, H. S. (2006) Interactions between Ca2+-ATPase and the pentameric form of phospholamban in two-dimensional co-crystals. *Biophys. J.* **90**, 4213–4223

19. Glaves, J. P., Primeau, J. O., Espinoza-Fonseca, L. M., Lemieux, M. J., and Young, H. S. (2019) The Phospholamban Pentamer Alters Function of the Sarcoplasmic Reticulum Calcium Pump SERCA. *Biophys. J.* **116**, 633–647

20. Young, H. S., Rigaud, J. L., Lacapère, J. J., Reddy, L. G., and Stokes, D. L. (1997) How to make tubular crystals by reconstitution of detergent-solubilized Ca2(+)-ATPase. *Biophys. J.* **72**, 2545–

2558

21. Martonosi, A. N., and Pikula, S. (2003) The structure of the Ca 2 + -ATPase of sarcoplasmic reticulum . *Rev. Lit. Arts Am.* **50**, 337–365

22. Glaves, J. P., Trieber, C. a., Ceholski, D. K., Stokes, D. L., and Young, H. S. (2011) Phosphorylation and mutation of phospholamban alter physical interactions with the sarcoplasmic reticulum calcium pump. *J. Mol. Biol.* **405**, 707–723

23. Stokes, D. L., Pomfret, A. J., Rice, W. J., Glaves, J. P., and Young, H. S. (2006) Interactions between Ca2+-ATPase and the Pentameric Form of Phospholamban in Two-Dimensional Co-Crystals. *Biophys. J.* **90**, 4213–4223

24. Pugh, T. J., Kelly, M. A., Gowrisankar, S., Hynes, E., Seidman, M. A., Baxter, S. M., Bowser, M., Harrison, B., Aaron, D., Mahanta, L. M., Lakdawala, N. K., McDermott, G., White, E. T., Rehm, H. L., Lebo, M., and Funke, B. H. (2014) The landscape of genetic variation in dilated cardiomyopathy as surveyed by clinical DNA sequencing. *Genet. Med.* **16**, 601–608

25. Li, J., Boschek, C. B., Xiong, Y., Sacksteder, C. A., Squier, T. C., and Bigelow, D. J. (2005) Essential role for Pro21 in phospholamban for optimal inhibition of the Ca-ATPase. *Biochemistry.* **44**, 16181–16191

26. Gustavsson, M., Verardi, R., Mullen, D. G., Mote, K. R., Traaseth, N. J., Gopinath, T., and Veglia, G. (2013) Allosteric regulation of SERCA by phosphorylation-mediated conformational shift of phospholamban. *Proc. Natl. Acad. Sci. U. S. A.* **110**, 17338–43

27. Ferrington, D. A., Yao, Q., Squier, T. C., and Bigelow, D. J. (2002) Comparable Levels of Ca-ATPase Inhibition by Phospholamban in Slow-Twitch Skeletal and Cardiac Sarcoplasmic Reticulum. *Biochemistry.* **41**, 13289–13296

28. Waggoner, J. R., Huffman, J., Griffith, B. N., Jones, L. R., and Mahaney, J. E. (2004) Improved expression and characterization of Ca2+-ATPase and phospholamban in High-Five cells. *Protein Expr. Purif.* **34**, 56–67

29. Young, H. S., Reddy, L. G., Jones, L. R., and Stokes, D. L. (1998) Co-reconstitution and Co-crystallization of Phospholamban and Ca2+-ATPase a. *Ann. N. Y. Acad. Sci.* **853**, 103–115

30. Young, H. S., Jones, L. R., and Stokes, D. L. (2001) Locating phospholamban in co-crystals with Ca(2+)-ATPase by cryoelectron microscopy. *Biophys. J.* **81**, 884–894

31. Trieber, C. A., Douglas, J. L., Afara, M., and Young, H. S. (2005) The Effects of Mutation on the Regulatory Properties of Phospholamban in Co-Reconstituted Membranes†. *Biochemistry.* **44**, 3289–3297

32. Trieber, C. A., Afara, M., and Young, H. S. (2009) Effects of Phospholamban Transmembrane Mutants on the Calcium Affinity, Maximal Activity, and Cooperativity of the Sarcoplasmic Reticulum Calcium Pump. *Biochemistry.* **48**, 9287–9296

33. Ceholski, D. K., Trieber, C. a., and Young, H. S. (2012) Hydrophobic imbalance in the cytoplasmic domain of phospholamban is a determinant for lethal dilated cardiomyopathy. *J. Biol. Chem.* **287**, 16521–16529

34. Akin, B. L., Hurley, T. D., Chen, Z., and Jones, L. R. (2013) The structural basis for phospholamban inhibition of the calcium pump in sarcoplasmic reticulum. *J. Biol. Chem.* **288**, 30181–30191

35. Toyoshima, C., Iwasawa, S., Ogawa, H., Hirata, A., Tsueda, J., and Inesi, G. (2013) Crystal structures of the calcium pump and sarcolipin in the Mg2+-bound E1 state. *Nature.* **495**, 260

36. Winther, A.-M. L., Bublitz, M., Karlsen, J. L., Møller, J. V, Hansen, J. B., Nissen, P., and Buch-Pedersen, M. J. (2013) The sarcolipin-bound calcium pump stabilizes calcium sites exposed to the cytoplasm. *Nature.* **495**, 265

37. Ceholski, D. K., Trieber, C. a., Holmes, C. F. B., and Young, H. S. (2012) Lethal, hereditary mutants of phospholamban elude phosphorylation by protein kinase A. *J. Biol. Chem.* **287**, 26596–26605

38. Gorski, P. A., Glaves, J. P., Vangheluwe, P., and Young, H. S. (2013) Sarco(endo)plasmic Reticulum Calcium ATPase (SERCA) Inhibition by Sarcolipin Is Encoded in Its Luminal Tail. *J. Biol. Chem.* . **288**, 8456–8467

39. Glaves, J. P., Primeau, J. O., Gorski, P. A., Espinoza-Fonseca, L. M., Lemieux, M. J., and Young, H. S. (2019) Interaction of a sarcolipin pentamer and monomer with the sarcoplasmic reticulum calcium pump, SERCA. Running Title: A novel complex of sarcolipin and SERCA. *Biophysj.* **118**, 518–531

40. Young, H. S., and Stokes, D. L. (2004) The mechanics of calcium transport. *J. Membr. Biol.* **198**, 55–63

41. Douglas, J. L., Trieber, C. a., Afara, M., and Young, H. S. (2005) Rapid, high-yield expression and purification of Ca2+-ATPase regulatory proteins for high-resolution structural studies. *Protein Expr. Purif.* **40**, 118–125

42. Eletr, S., and Inesi, G. (1972) Phospholipid orientation in sacroplasmic membranes: Spin-label ESR and proton NMR studies. *Biochim. Biophys. Acta - Biomembr.* **282**, 174–179

43. Stokes, D. L., and Green, N. M. (1990) Three-dimensional crystals of CaATPase from

sarcoplasmic reticulum. Symmetry and molecular packing. *Biophys. J.* **57**, 1–14

44.   Smeazzetto, S., Armanious, G. P., Moncelli, M. R., Bak, J. J., Lemieux, M. J., Young, H. S., and Tadini-Buoninsegni, F. (2017) Conformational memory in the association of the transmembrane protein phospholamban with the sarcoplasmic reticulum calcium pump SERCA. *J. Biol. Chem.* **292**, 21330–21339

45.   Warren, G. B., Toon, P. A., Birdsall, N. J., Lee, A. G., and Metcalfe, J. C. (1974) Reconstitution of a calcium pump using defined membrane components. *Proc. Natl. Acad. Sci. U. S. A.* **71**, 622–626

46.   Weiss, J. N. (1997) The Hill equation revisited: uses and misuses. *FASEB J. Off. Publ. Fed. Am. Soc. Exp. Biol.* **11**, 835–841

47.   Xu, C., Rice, W. J., He, W., and Stokes, D. L. (2002) A structural model for the catalytic cycle of Ca2+-ATPase11Edited by W. Baumeister. *J. Mol. Biol.* **316**, 201–211

48.   Glaves, J. P., Primeau, J. O., and Young, H. S. (2016) Two-Dimensional Crystallization of the Ca2+-ATPase for Electron Crystallography BT - P-Type ATPases: Methods and Protocols (Bublitz, M. ed), pp. 421–441, Springer New York, New York, NY, 10.1007/978-1-4939-3179-8_38

Chapter 6: Conclusions and future directions

1.   Michelson, A. A., and Morley, E. W. (1887) On the relative motion of the Earth and the luminiferous ether. *Am. J. Sci.* . **Series 3 V**, 333–345

2.   Crick, F. (1970) Central dogma of molecular biology. *Nature.* **227**, 561–563

3.   Glaves, J. P., Trieber, C. a., Ceholski, D. K., Stokes, D. L., and Young, H. S. (2011) Phosphorylation and mutation of phospholamban alter physical interactions with the sarcoplasmic reticulum calcium pump. *J. Mol. Biol.* **405**, 707–723

4.   Cao, Y., Wu, X., Yang, R., Wang, X., Sun, H., and Lee, I. (2017) Self-assembling study of sarcolipin and its mutants in multiple molecular dynamic simulations. *Proteins Struct. Funct. Bioinforma.* **85**, 1065–1077

5.   Autry, J. M., Rubin, J. E., Pietrini, S. D., Winters, D. L., Robia, S. L., and Thomas, D. D. (2011) Oligomeric Interactions of Sarcolipin and the Ca-ATPase. *J. Biol. Chem.* . **286**, 31697–31706

6. Hellstern, S., Pegoraro, S., Karim, C. B., Lustig, A., Thomas, D. D., Moroder, L., and Engel, J. (2001) Sarcolipin, the Shorter Homologue of Phospholamban, Forms Oligomeric Structures in Detergent Micelles and in Liposomes. *J. Biol. Chem.* **276**, 30845–30852

7. Akin, B. L., Hurley, T. D., Chen, Z., and Jones, L. R. (2013) The structural basis for phospholamban inhibition of the calcium pump in sarcoplasmic reticulum. *J. Biol. Chem.* **288**, 30181–30191

8. Smeazzetto, S., Armanious, G. P., Moncelli, M. R., Bak, J. J., Lemieux, M. J., Young, H. S., and Tadini-Buoninsegni, F. (2017) Conformational memory in the association of the transmembrane protein phospholamban with the sarcoplasmic reticulum calcium pump SERCA. *J. Biol. Chem.* **292**, 21330–21339

9. Pugh, T. J., Kelly, M. A., Gowrisankar, S., Hynes, E., Seidman, M. A., Baxter, S. M., Bowser, M., Harrison, B., Aaron, D., Mahanta, L. M., Lakdawala, N. K., McDermott, G., White, E. T., Rehm, H. L., Lebo, M., and Funke, B. H. (2014) The landscape of genetic variation in dilated cardiomyopathy as surveyed by clinical DNA sequencing. *Genet. Med.* **16**, 601–608

10. Mravic, M., Thomaston, J. L., Tucker, M., Solomon, P. E., Liu, L., and DeGrado, W. F. (2019) Packing of apolar side chains enables accurate design of highly stable membrane proteins. *Science (80-.).* **363**, 1418 LP – 1423

fin